

**Chemoenzymatic Assembly of Macrolactones: Merging Synthetic
Chemistry with Biocatalysis to Afford Diverse Compound Libraries**

by

Jennifer J. Schmidt

A dissertation submitted in partial fulfillment
of the requirements for the degree of
Doctor of Philosophy
(Medicinal Chemistry)
in the University of Michigan
2018

Doctoral Committee:

Professor David H. Sherman, Chair
Professor Scott D. Larsen
Professor John Montgomery
Professor Nouri Neamati

Jennifer J. Schmidt

jejschmi@umich.edu

ORCID ID: 0000-0002-1795-1756

© Jennifer J. Schmidt 2018

Acknowledgements

Graduate school is an exciting and stressful adventure that would not have been possible without the support of not only my advisor and the exemplary scientists I have had the pleasure of working with, but the friends and family whose kind words, constructive criticism, great adventures, and lively discussions have made the last six years a productive and enjoyable experience. I began my journey through science by working as an undergraduate for Dr. Phil Crews at the University of California Santa Cruz, who I will forever be indebted to for inspiring me to apply to graduate school, and ultimately leading me to the world of natural product biosynthesis. Despite graduate school not having been on my initial life plan, I embraced the process whole heartedly and continued my studies in the laboratory of Dr. David Sherman. Thinking about the past 5.5 years, I can honestly say I consider myself lucky to have had the privilege to not only work for, but learn from such a fantastic scientist. Despite his hands-off mentoring style, David has been a wonderful advisor and a solid pillar of support for each step of this process. His willingness for discussions and unwavering excitement for all facets of science has continued to inspire me to work through the rough patches and helped me to become the independent researcher I am today.

I would be remiss if I didn't also thank David for the laboratory environment he has fostered. The wealth of knowledge and good heartedness of each of the talented scientists I have had the pleasure of working with, is as far as I can tell unmatched and I am thankful every day to have had the opportunity to work with each and every one of you. In particular, I can not imagine graduate school without my bench/desk mate Dr. Andrew Lowell, who took me under his wing as a new graduate student and somewhere along the way I was able to call you not only my colleagues but one of my best friends. The debt of gratitude I owe you can not be expressed in words, not just for teaching me the skills I needed to succeed in graduate school, but for all of our in-depth discussions (science and otherwise), inside jokes, lab dance parties, and your increscent belief that I will succeed if I just try one more time. Additionally, I would like to thank Dr. Stela Romminger, Dr. Shasha Lee, and Amy Fraley who have been with me for (most)

of graduate school and not only helped me learn molecular biology as a fourth year graduate student, but who have been some of the best friends I could ask for. I wouldn't change a single minute I have spent laughing, commiserating, and being goofy with you. As we all continue to go our separate ways, I am constantly reminded that parting is such sweet sorrow, but I look forward to new adventures in new places with all of you in the future. I would also like to extend my gratitude to others in the lab specifically including, but not limited to Dr. Ashu Tripathi, Dr. Andrew Robertson, Dr. Aaron Koch, Dr. Michael Kaufman-Schofield, Dr. Kinshuk Srivastava, Lyanne Gomez-Rodriguez, and Rosa Vasquez Espinoza who have helped both in my scientific endeavors and made coming to work fun each and every day. Lastly I need to thank Pam Schultz, Debbie Lounds, and Shamilya Williams, whose hard work and dedication over the years have made the lab run as efficiently and effectively as possible.

Outside of the lab I have been very fortunate to have a great cohort and group of friends who have been a constant vein of support and source of entertainment. Helen Waldschmidt, Taylor Johnson, Max Stefan, Mike Agius, Eric Lachacz, Sameer Phadke, and Katie Beasley you are all amazing people who have helped me unwind at the end of long weeks and I have enjoyed getting to know each and every one of you. Our late night conversations on all facets of life, love, science, and pursuit of happiness kept me going and I cherish the memories we have made and look forward to those of the future.

Lastly, I would like to thank my family who despite living three time zones away have been there for me every step of the way. I have always believed in the phrase your friends are the family you choose, but I am lucky enough to have both friends I choose as family, and family that I choose as friends. The love and support that I have seen from my mom, dad, sister, and brother continues to inspire me. Even though none of them quite understand where my love for science and research comes from or exactly what I do, they are always immensely proud of my accomplishments and there to celebrate each one, despite often residing far away from each other. I am fortunate enough to not only be surrounded by the members of my immediate family, but my Aunt Lynne, Uncle Heinz, Jeannette and Ron who have been through every walk of life with me. You have always treated me like your own daughter and I could not imagine my life without you. I can not express how much the love, support, and encouragement my entire family has shown me has influenced my life. I can say with absolute certainty that I would not be who or where I am today without you and I am more than honored to be a part of all of your lives.

Table of Contents

Acknowledgments	ii
List of Figures	viii
List of Tables	x
List of Schemes	xi
Abstract	xii
Chapter 1: Introduction and Background	1
1.1 Natural Products as Therapeutic agents	1
<i>1.1.1 History of Natural Products in Medicine</i>	1
<i>1.1.2 Natural Products in Clinical Drug Discovery and Development</i>	1
1.2 Polyketide Synthase and Non-Ribosomal Peptide Natural Products	3
<i>1.2.1 General Biosynthetic Machinery of Polyketide Synthases</i>	3
<i>1.2.2 General Biosynthetic Machinery of Non-Ribosomal Peptides</i>	5
<i>1.2.3 Tailoring enzymes in PKS and NRPS systems</i>	6
1.3 Strategies for Synthesis of Natural Products	6
1.4 Combinatorial Biosynthesis and its uses in Drug Discovery	8
1.5 Thesis Overview	10
1.6 References	13
Chapter 2: Chemoenzymatic Synthesis of Cryptophycin Anti-Cancer Agents	18
2.1 Introduction to the Cryptophycin Family of Natural Products	18
<i>2.1.1 Cryptophycin Discovery</i>	18
<i>2.1.2 Mechanism of Action for Cryptophycin Anticancer Agents</i>	19
<i>2.1.3 Structure Activity Relationship of Cryptophycin Anticancer Agents</i>	20
<i>2.1.4 Cryptophycins as Antibody Drug Conjugate Warheads</i>	22
<i>2.1.5 Biosynthetic Assembly of Cryptophycins</i>	22
2.2 Synthesis of <i>seco</i> cryptophycin analogues	25
<i>2.2.1 Synthesis of Cryptophycin Unit AB Fragment</i>	26

2.2.2	<i>Formulation of Unit CD Fragment</i>	27
2.2.3	<i>Assembly of Seco Cryptophycin Chain Elongation intermediates</i>	27
2.3	Optimization and Evaluation of Seco Cryptophycin Analogues	29
2.3.1	<i>Analytical Scale Evaluation of the CrpTE with Seco Analogues</i>	29
2.3.2	<i>Semi-Preparative Scale Reactions and Biological Evaluation</i>	32
2.3.3	<i>Formation of Geminal Dimethyl Variants of Unit A Analogues</i>	33
2.4	Evaluation of Cryptophycin P450 with Unit A Analogues	34
2.4.1	<i>Cytochrome P450 Background</i>	34
2.4.2	<i>Evaluation of P450 with Unit A Heterocyclic Analogues</i>	36
2.5	References	38
Chapter 3:	Structural and Mechanistic Insights into the Crp TE	43
3.1	Introduction and Background on Thioesterase Structure and Function	43
3.1.1	<i>Overall Structural Features of Thioesterases</i>	43
3.1.2	<i>Structural Insights into PKS Derived TEs</i>	44
3.1.3	<i>Structural Insights into NRPS Derived TEs</i>	44
3.2	Optimization of the Crp TE for Structural Characterization	45
3.2.1	<i>Rational Construct Design of Variant Crp TEs</i>	45
3.2.2	<i>Variant Crp TE Protein Expression and Purification</i>	46
3.2.3	<i>Engineering the Crp TE from a Hydrolase to an Acyl Transferase</i>	49
3.3	Evaluation of the Crp TE as a Candidate for Solution Phase Structure	51
3.3.1	<i>Background on Solution Phase (NMR) Structural Determination</i>	51
3.3.2	<i>Formulation of Crp TE for NMR Experiments</i>	53
3.4	References	55
Chapter 4:	Molecular Interrogation of Polyketide Synthase Modules in the Pikromycin System Using Unnatural Pentaketides	57
4.1	Background on the Macrolide Antibiotic Pikromycin	57
4.1.1	<i>Macrolides as Antibiotics</i>	57
4.1.2	<i>Biosynthesis of Pikromycin</i>	58
4.1.3	<i>Structural Investigations of Polyketide Synthase Modules</i>	60
4.1.4	<i>Biochemical Characterization of Pik AIIITE and Pik AIII/AIV</i>	61
4.2	Synthesis of Alternate Pentaketide Chain Elongation Intermediates	63

4.2.1 <i>Synthesis of Ester and Amide Containing Pentaketides</i>	64
4.2.2 <i>Synthesis of Pentaketides Containing Varied Alkyl Substituents</i>	64
4.2.3 <i>Synthesis of Extended Chain Pentaketides</i>	67
4.3 Biochemical Evaluation of Synthesized Pentaketides	67
4.3.1 <i>Evaluation of Pentaketide Analogues with Pik AIIITE</i>	68
4.3.2 <i>Evaluation of Pentaketide Analogues with Pik AIII/AIV</i>	70
4.3.3 <i>Evaluation of Pentaketides with Engineered Pik AIIITES148C</i>	72
4.4 References	74
Chapter 5: Summary, Discussion, and Future Directions	76
5.1 Biocatalytic Synthesis of Cryptophycin Anticancer Agents	76
5.1.1 <i>Summary and Discussion of Work Completed</i>	76
5.1.2 <i>Future Directions</i>	78
5.2 Structural and Mechanistic Insights into the Crp TE	79
5.2.1 <i>Summary and Discussion of Work Completed</i>	79
5.2.2 <i>Future Directions</i>	79
5.3 Molecular Interrogation of Polyketide Synthase Modules in the Pikromycin System Using Unnatural Pentaketides	80
5.3.1 <i>Summary and Discussion of Work Completed</i>	80
5.3.2 <i>Future Directions</i>	81
5.4 Contributions to the Understanding of PKS/NRPS Pathways for use Combinatorial biosynthesis	82
5.5 References	84
Chapter 6: Cryptophycin Experimentals	85
6.1 Chemical Synthesis of <i>Seco</i> Cryptophycin Analogues	85
6.1.1 <i>Unit A Synthetic Procedures and Characterization</i>	85
6.1.2 <i>Unit AB Synthetic Procedures and Characterization</i>	90
6.1.3 <i>Heterocyclic Unit AB Analogue Characterization</i>	92
6.1.4 <i>Unit CD Synthetic Procedures and Characterization</i>	97
6.1.5 <i>Heterocyclic <i>Seco</i> Analogue Characterization</i>	98
6.2 Crp TE Mediated Cyclization Experimentals and Characterization	108
6.3 Construct Design and Protein Expression Experimentals (Chapter 3)	116
6.3.1 <i>Generation of Mutant Crp TEs</i>	116

6.3.2 <i>Crp TE Expression and Purification for Enzymatic Reactions and Crystallography</i>	117
6.3.3 <i>Crp TE Protein Expression and Purification for NMR</i>	119
6.4 References	122
Chapter 7: Pikromycin Synthesis and Biocatalytic Conversion Experimentals	123
7.1 Pentaketide Synthetic Procedures and Experimentals	123
7.2 PKS Expression and Purification Protocols	141
7.2.1 <i>Enzymatic Reaction Experimental Procedures</i>	142
7.3 Macrolactone Characterization	144
7.4 References	147

List of Figures

Figure 1.1 Natural Products as Drug Leads	2
Figure 1.2 Schematic of a generic PKS module	4
Figure 1.3 Schematic of a generic NRPS module	5
Figure 1.4 Schematic of the strategies used in combinatorial biosynthesis	9
Figure 2.1 Select cryptophycin analogues produced by the Lichen symbiont Nostoc	18
Figure 2.2 Common microtubule binding agents	20
Figure 2.3 Generalized schematic of Cryptophycin SAR	21
Figure 2.4 Biosynthetic Pathway of the mixed PKS/NRPS natural product cryptophycin	23
Figure 2.5 Generalized schematic of thioesterase mechanism	24
Figure 2.6 Retrosynthetic analysis of <i>seco</i> cryptophycin chain elongation intermediate	25
Figure 2.7 Analysis of substrate concentration on % conversion	29
Figure 2.8 QTOF-LCMS analysis of <i>seco</i> cryptophycin analogues with the CrpTE	30
Figure 2.9 P450 catalytic cycle	35
Figure 2.10 Analysis of CrpE P450 with styrene cryptophycin analogues	36
Figure 3.1 General thioesterase structure diagrams	43
Figure 3.2 Gel of initial expression tests for mutant CrpTEs	47
Figure 3.3 Size exclusion results for the different CrpTE constructs	48
Figure 3.4 General schematic of the workflow involved in assigning carbon and hydrogen signals using standard triple resonance NMR experiments	51
Figure 3.5 Magnetization transfer pathways seen in three-dimensional NMR experiments necessary for the assignment of large proteins	52
Figure 3.6 $^{15}\text{N}/^2\text{H}$ HSQC spectrum of CrpTE as observed in SPARKY NMR program	54
Figure 4.1 Antibiotic generations and their binding site on the ribosome	58
Figure 4.2 Pikromycin biosynthetic pathway for the formation of aglycones 10- Deoxymethynolide (10-DML) and Narbonolide	59

Figure 4.3 Cryo-EM reconstruction of PikAIII	60
Figure 4.4 Reconstitution of PikAIII-TE and PikAIII/AIV modules pentaketides	61
Figure 4.5 Initial right half pentaketides analogues assayed with PikAIII-TE	62
Figure 4.6 Potential unnatural pentaketide analogues	63
Figure 4.7 Analytical reaction traces with new pentaketides utilizing the PikAIII-TE fusion protein	68
Figure 4.8 Mechanism of hydrolytic byproduct production in PikAIII-TE	69
Figure 4.9 Analytical reaction traces with new pentaketides utilizing the Pik AIII/AIV fusion protein	70
Figure 4.10 Semi-preparative Pik AIII/AIV scale ups of select pentaketides	71
Figure 4.11 Potential isoberic macrolactone products produced by the Pik AIII/AIV system ...	72
Figure 4.12 Comparison of analytical reactions with Ester, Amide, and Desmethyl Pentaketides against wildtype Pik AIIIITE and Pik AIII-TE S148C	73
Figure 7.1 HMBC correlations for amide narbonolide as blue arrows	144
Figure 7.2 HMBC correlations for ester narbonolide as blue arrows	145
Figure 7.3 Desmethyl narbonolide structure	146

List of Tables

Table 2.1 Comparison of cryptophycin analogues 2.29 a-m percent conversion, isolation yields, and cyclization to hydrolysis ratio	31
Table 2.2 IC ₅₀ values for unit A heterocyclic analogues in HCT 116 cells	33
Table 3.1 Schematic and table of mutant constructs of Crp TE generated	46
Table 6.1 Primers utilized for generation of CrpTE mutants	117
Table 7.1 Amide narbonolide assignments and correlations	144
Table 7.2 Ester narbonolide assignments and correlations	145
Table 7.3 Desmethyl narbonolide assignments and correlations	145

List of Schemes

Scheme 2.1 Synthesis of unit A	26
Scheme 2.2 Synthesis of unit AB	27
Scheme 2.3 Synthesis of unit CD	27
Scheme 2.4 Assembly of <i>seco</i> cryptophycin analogues.....	28
Scheme 3.1 Synthesis of thiophenol containing substrate	50
Scheme 4.1 Synthesis of ester and amide containing pentaketides	65
Scheme 4.2 Vinyl magnesium bromide ring opening strategy for analogue formation	65
Scheme 4.3 Synthesis of desmethyl, dimethyl and cyclohexyl pentaketide analogues	66
Scheme 4.4 Synthetic scheme for the formulation of homologated pentaketides	67

Abstract

Complex secondary metabolites display a wealth of biological activities and, together with their derivatives, have provided over 60% of new pharmaceutical agents over the past 40 years. Despite their clinical success, limitations in isolation yields as well as the synthetic challenges posed by these scaffolds often hinders the medicinal chemistry efforts necessary to overcome suboptimal pharmacological properties, highlighting the need for alternative methods. A promising strategy for generating libraries of natural product analogues is through the use of biosynthetic enzymes. These systems have long been hypothesized to be capable of producing almost unlimited structural diversity, due to their modular nature, however to date, efforts towards PKS engineering have mostly met with failure. Despite notable successes, decreased product yields and/or failure to produce the desired structures entirely have stymied these efforts. Recent studies focusing on the interrogation of single modules or module domains via biochemical analysis coupled with structural determination have begun to shed light on these complex systems and give us insight into the reasons for the initial failures.

The studies presented in this thesis focus on investigations into the structural and mechanistic parameters that govern selectivity in the biosynthetic enzymes of interest from two key natural products, the PKS/NRPS derived cryptophycin family of anticancer agents, and the PKS antibiotic Pikromycin. In the cryptophycin system, synthetic chain elongation intermediates have been coupled with the Crp TE macrocyclizing catalyst to produce a library of heterocyclic unit A analogues. This was met with remarkable success as all the analogues were processed by the TE with similar or greater efficiency than that seen with the native substrate. Current efforts are focused on gaining an NMR structure of this TE with hopes of shedding light on the underlying catalytic mechanism that makes this enzyme so versatile. This facilitated the biological evaluation of these analogues, allowing us to identify one that displays remarkable activity without the presence of an epoxide group that was previously thought to be necessary for maximum efficacy.

Utilizing the same strategy in the Pikromycin system, five new pentaketides analogues were generated that could be used with three separate intact PKS modules, the PikAIII-TE and the

coupled PikAIII/AIV system. These synthetic intermediates have continued to lend credence to the hypothesis that in PKS systems, the TE tends to be the deciding factor on whether hydrolytic byproducts are formed or macrocycles. Utilizing our biocatalytic platform we have been able to show that the TE can more effectively produce 14 membered macrolactones containing unnatural functionality than 12, leading to the isolation of three new macrolactone products. Altered alkyl chain substituents on these pentaketides substrates have also shed light on the likelihood of a size restriction for the loading of these substrates onto the KS domain of the initial module. The continued investigation of these substrates as well as others continues to build the groundwork for future engineering campaigns aimed at generating more flexible catalysts for the production of novel natural product analogues.

Chapter 1

Introduction and Background

1.1 Natural Products as Therapeutic Agents

1.1.1 History of Natural Products in Medicine

Natural products, or secondary metabolites, are chemical compounds derived from all kingdoms of life, that are not required for primary survival (i.e. growth, reproduction, or metabolism), but confer a selective advantage to a given organism within their niche.¹ These compounds have been used in the treatment of human illnesses since before the advent of modern medicine and continue to play a vital role in combating major diseases.² The first recorded reports of natural product usage stem from ancient civilizations including Mesopotamia (2600 BC) and the ancient Egyptians (1550 BC) who used plant derived medicines to formulate oils, ointments, pills, and gargles to treat a variety of ailments including colds and inflammation.²⁻⁴ The early 1800's saw a renaissance of drug development and natural product exploration with the isolation of morphine and other alkaloids (including quinine and nicotine) from a variety of plant sources⁵ and by 1853 salicylic acid, the active metabolite in aspirin, became the first natural product to be made by chemical synthesis with the advent of the Kolbe-Schmitt reaction.⁶ In 1928, natural product medicines were again a sensation as one of the most profound medical discoveries came when Alexander Flemming discovered a molecule, penicillin, with antibacterial activity from a fungus, *Penicillium chrysogenum*, changing the course of modern medicine.²

1.1.2 Natural Products in Clinical Drug Discovery and Development

The field of natural product drug discovery continued to expand through the early 1900s and with the onset of the “golden age of antibiotics”, all major pharmaceutical companies initiated natural products discovery teams, looking for not only antimicrobials, but anti-fungals and anti-cancer agents.³ The wide variety of chemical diversity seen in these molecules makes them effective agents in all areas of clinical medicine, with over 60% of all drugs approved from 1981

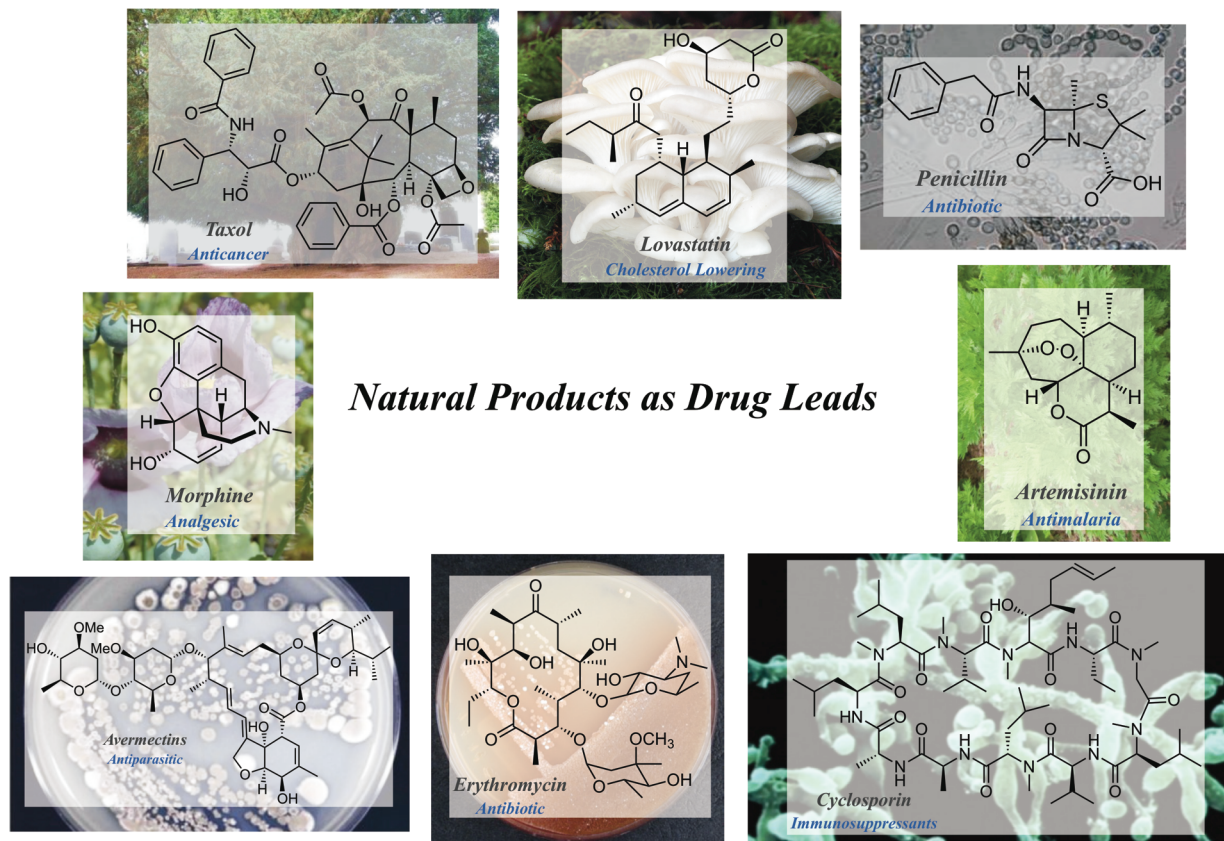


Figure 1.1 Natural Products as Drug Leads. Examples of well-known natural products with clinical significance, demonstrating the vast array of scaffolds and assorted therapeutic applications of these types of compounds.

to 2014 being direct natural products or natural product derivatives. The significance of these molecules is even more pronounced in the area of antibiotics and anticancer agents, with the number of compounds being derived from natural sources being above 70% for these classes of drugs.¹ Some examples of clinically used natural products are antibiotics like penicillin and erythromycin A, anti-cancer agents like Taxol, antiparasitics like avermectin, analgesics like morphine, cholesterol lowering agents like lovostatin, insecticidal agents like spinosyn A, and immunosuppressant's like cyclosporine (**Figure 1.1**).⁷

Despite the clinical success of natural products, the early 2000's saw a decline in pharmaceutical company involvement. With the advent of combinatorial synthesis and high throughput screening (HTS) technology, large libraries of compounds could be chemically synthesized and screened for activity over a variety of targets. These initial hit identifications could then be translated into promising leads through structure activity relationship (SAR) campaigns,

circumventing the need to pursue natural products which historically have been plagued with lengthy, complex chemical syntheses and high production costs.⁸ In recent years however, interest in natural products has been reinvigorated as combinatorial synthesis, despite many successes, cannot compete with the chemical diversity found in nature. These “privileged scaffolds” have developed over thousands of years to interact specifically with a variety of biological targets,⁹ making their structural diversity an unavoidable necessity, and thus providing an advantage over traditional synthetic libraries.

1.2 Polyketide Synthase and Non-Ribosomal Peptide Natural Products

Polyketides (PKs), non-ribosomal peptides (NRPs), and their hybrids (PK/NRP) are a large sub-class of natural products which historically possess a wealth of pharmacological activities, specifically in the areas of anticancer and antibiotics.¹⁰⁻¹² These molecules are formulated in an analogous manner by megasynthase enzymes that are organized into biosynthetic pathways. Polyketides are comprised of multiple, two carbon ketide units, that are joined together to form the growing polyketide chain. Non-ribosomal peptides are also formulated by multidomain proteins, except these are responsible for the joining of amino acids or amino acid derivatives via peptide bond formation to produce the complex structures seen in nature (e.g. **Figure 1.1**). A subset of these PK and NRP natural products contain a macrocyclic core, formulated via an intramolecular ester or amide bond, which serves to lock these otherwise flexible molecules into their precise, biologically relevant, conformation. The biosynthesis of these is terminated by a thioesterase, the enzyme responsible for effecting, regio- and stereo- specific macrocyclization.¹³

1.2.1 General Biosynthetic Machinery of Polyketide Synthases

The enzymatic systems responsible for the production of polyketide natural products are termed Polyketide Synthases (PKS) and utilize a similar mechanistic strategy as Fatty Acid Synthases (FAS) found in primary metabolism. Based on their architecture, PKSs can be classified into three different types, Type I, Type II,¹⁴ and Type III,¹⁵ with Type I being covered here. Type I PKS, like FAS, select for two carbon units in the form of malonyl Coenzyme A (CoA) derivatives that are then joined together through a series of Claisen Condensation reactions. Each module of a polyketide synthase is comprised of three necessary domains, the ketosynthase (KS), the acyl

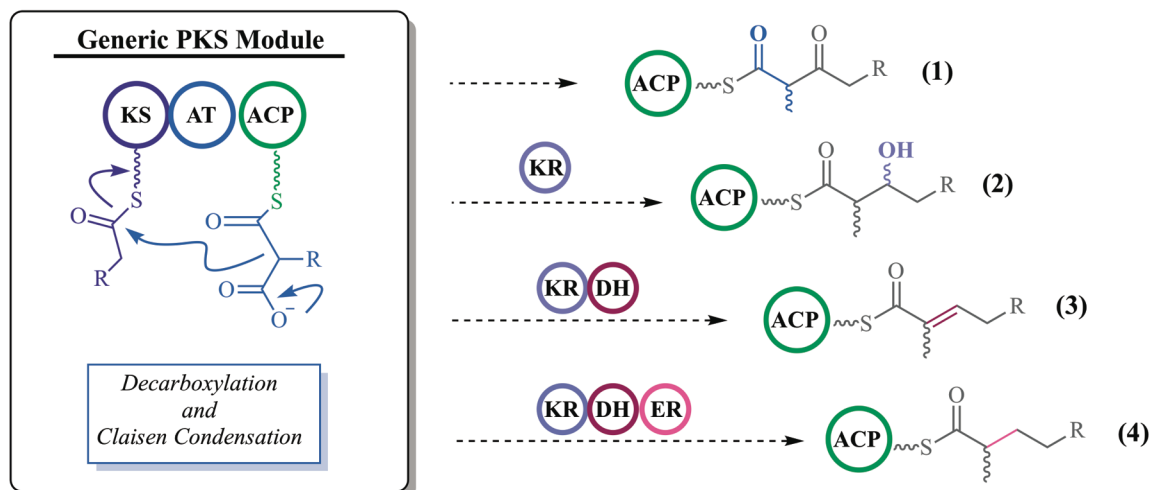


Figure 1.2 Schematic of a generic PKS module. The cycle starts when the **AT** selects an appropriate extender unit and loads it to the **ACP**. Decarboxylation and subsequently Claisen Condensation is catalyzed by the **KS** which produces the β keto substrate **1**. Optional domains present in the different modules can then act upon the newly extended product. These include the **KR** which performs a keto reduction (**2**), **DH** which performs dehydration (**3**), and the **ER** which reduces the double bond to a saturated alkane (**4**).

transferase (AT), and the acyl carrier protein (ACP) seen in **Figure 1.2**.¹⁶⁻¹⁷ During elongation, the AT selects an appropriate malonyl derivative and loads it onto the ACP. The KS, containing the growing polyketide chain from the previous module, catalyzes decarboxylation of the ACP bound malonyl derivative. This generates a transient nucleophile that reacts with the growing chain in a Claisen Condensation type reaction, increasing the backbone length by two carbons with each cycle.

In addition to the necessary domains, there are three “optional” domains, the ketoreductase (KR), dehydratase (DH), and enoyl reductase (ER) which are responsible for reductions of the 3-keto group to either a hydroxyl, alkene, or alkane functionality (**Figure 1.2: 2, 3, and 4**). In FAS there are a single copy of all six of these which iteratively act upon each ketide unit, producing the relatively simple, unsaturated chains seen in these systems. In PKS systems, the necessary domains are organized into modules, each capable of accepting potentially different extension units (malonyl, methyl malonyl, and ethyl malonyl, etc.). Each module will contain all three necessary domains and can be complemented with one, two, or all three optional domains, producing the vast diversity seen in polyketide chains (**Figure 1.2**).¹⁰

Once a single module has completed its extension, the growing polyketide chain is then passed off to the downstream module via protein-protein interactions. These are modulated by a non-

covalent association of “docking domains”, short helical segments that are fused to the C-terminus of the upstream module and the N-terminus of the downstream.¹⁸ The interaction of these two dimerization elements facilitates effective and specific transfer of growing polyketide chain.

1.2.2 General Biosynthetic Machinery of Non-Ribosomal Peptide Synthetases

Non-ribosomal peptides are formulated by a separate set of multi-modular enzymes termed Non-Ribosomal Peptide Synthetases (NRPS). These systems utilize amino acids or amino acid derivatives, instead of malonyl derivatives, and join them together via peptide bond formation in a ribosome-independent fashion. These proteins also contain three necessary domains: the adenylation domain (A) which selects the appropriate amino acid, the condensation domain (C) which catalyzes peptide bond formation, and a peptidyl carrier protein (PCP) that shuttles the growing chain from module to module (**Figure 1.3**).¹⁹⁻²⁰ These systems have a variety of optional domains as well, that can act upon the growing chain in a non-iterative fashion. An epimerization domain can take the L-amino acids, manufactured during primary metabolism, and invert the stereochemistry to produce the much rarer, D variant (**6**). N-methylation is another optional domain that is accomplished through a s-adenosyl methionine (SAM) methyl transferase (**7**) and

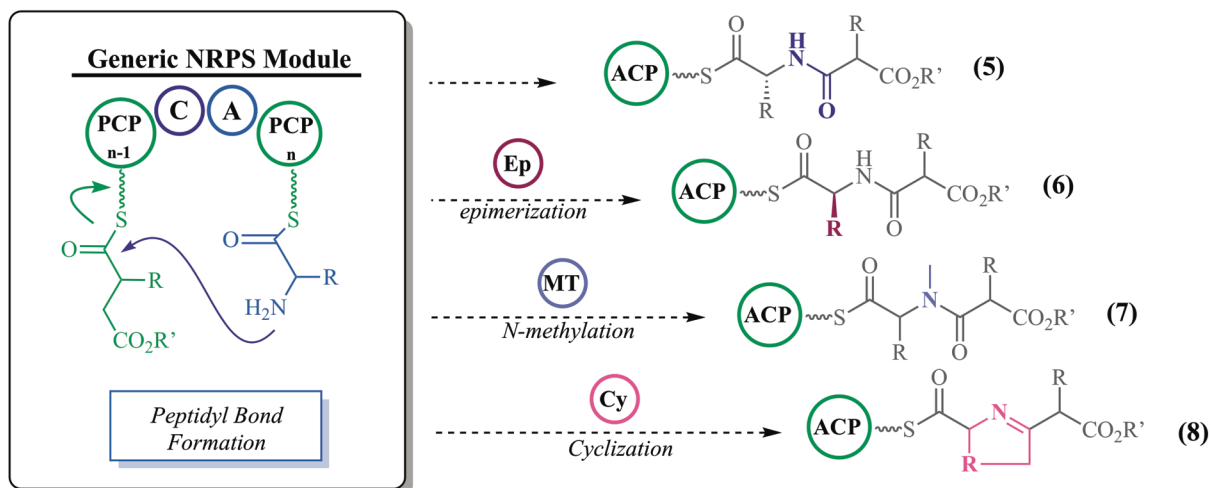


Figure 1.3 Schematic of a generic NRPS mechanism. The catalytic cycle begins when the **A** domain selects an appropriate amino acid and loads it to the cognate **PCP**. Peptide bond formation is then catalyzed by the **C** domain to produce substrate **1**. Optional domains present in the modules include the **Ep** domain, responsible for epimerization of the α stereocenter (**6**), the **MT** domain which catalyzes N-methylation (**7**), and the **Cy** domain that cyclizes nucleophilic sidechains to form the corresponding oxazole/thiazole rings (**8**).

lastly, cyclization of amino acids containing nucleophile sidechains (serine, threonine and cysteines) to form oxazoline and thiazoline rings (8). These rings can also undergo redox reactions to change their unsaturation state. Although many of these natural products are exclusively biosynthesized by PKS or NRPS systems, hybrid biosynthetic systems that combine both PKS and NRPS modules also exist and formulate molecules containing both polyketide portions and peptide portions, exponentially increasing the possible diversity that nature is able to make with these systems.

The final step in the biosynthesis of macrocyclic PK and NRP natural products is offloading which, in the case of macrocycles, is catalyzed by a thioesterase that is appended to the terminal module of these biosynthetic systems. These enzymes are broadly classified as serine hydrolases and utilize a serine, histidine, aspartic acid catalytic triad to either hydrolyze off the growing linear chain or facilitate intramolecular cyclization to form the core macrocycle.

1.2.3 Tailoring Enzymes in PKS and NRPS Systems

Polyketide/Non-ribosomal peptide cores are often modified by late stage tailoring enzymes, which can further increase the diversity seen in these systems. The common post-PKS and NRPS modifications seen are produced by a plethora of different enzymes, including oxidoreductases, group transferases, halogenases, cyclases, and deoxysugar biosynthetic cassettes.²¹⁻²² Often these enzymes are responsible for the production of functional groups that are imperative for biological function. The very nature of macrolide (macrolactone glycoside)²³ antibiotics relies upon glycotransferases that append a variety of sugars to hydroxyls on macrocycles, whose cores are not active without this moiety. These hydroxyls can come from PKS KRs or from oxygenases, specifically P450s or flaven dependent oxygenases, that are able to install hydroxyl, aldehyde, and/or epoxide groups to often otherwise unactivated C-H bonds.

1.3 Strategies for Synthesis of Natural Products

Since the modern era of natural product total synthesis began, it has continued to expand exponentially, making complex scaffolds such as ciguatoxin CTX3C, a polyether containing 12 rings and 30 stereogenic centers, synthetically tractable.²⁴ The continued development of organometallics,²⁵ chiral auxiliary chemistry, and asymmetric aldol reactions²⁶ have been instrumental in natural product drug discovery as they facilitate access to analogues that are

unattainable by other methods including semi-synthesis and fermentation.²⁷ Despite the formulation of these molecules usually being constrained to academic endeavors, complex total synthesis has also found practicality in industrial settings when low isolation yields cause “bottlenecks” that hinder development. This is best exemplified by Halaven (Eribulin mesylate), a drug approved in 2010 for the treatment of metastatic breast cancer.²⁸⁻²⁹ This molecule is considered the most structurally complex therapeutic formulated by total synthesis for clinical use. This molecule is a truncated, synthetic version of the halichondrin B isolated from a marine sponge. Low isolation yields, and the unculturable nature of sponges made access to this molecule for clinical development a major hurdle.³⁰ The complexity seen, with its 19 stereocenters, would frequently make it out of reach for industrial scale total synthesis however, a herculean effort to formulate convergent synthesis led to a 62 step route, with the longest linear sequence being 30 steps. The critical discovery, that changed the fate of this molecule in the clinic was the crystallinity of multiple late stage fragments, which facilitated easy access, with minimal chromatography, to the appropriate diastereomer needed to formulate this complicated scaffold.³⁰⁻³³

Supply issues and medicinal chemistry efforts towards natural products are not limited to synthetic chemistry, but are also solved through fermentation, precursor directed biosynthesis (**Figure 1.4**), and/or semi synthesis.³⁴ This is especially prevalent in antibiotic discovery. Erythromycin, the first clinically used antibiotic, has a single published total synthesis which requires 77 steps,³⁵⁻³⁷ illustrating the need for alternative methods. Fermentation has largely overcome this hurdle by providing rapid access to kilograms of this macrolide. The ease at which this can be produced allowed for further medicinal chemistry efforts to this scaffold which have identified second, third and even fourth generation antibiotics.³⁸ These relatives are made by semi-synthesis from the fermented erythromycin scaffold and include Azithromycin (Zithromax) one of the highest grossing drugs on the market today, which is synthesized through a Beckman rearrangement ring expansion. Other clinical natural products, like the anticancer agent taxol, are formulated for clinical use through semi-synthesis as well. In this case, isolation of the natural product faced insurmountable challenges as it is only produced in the bark of the pacific yew tree. In order to obtain it for clinical trials, the bark of a single tree had to be striped (effectively killing it) for each dose.³⁹ Despite this, the clinical success of this drug later led to the discovery of a taxol precursor, 10-deacetyl-baccatin III made by the needles of the pacific yew tree, that could be extracted and synthetically converted to the anticancer agent without killing old growth trees.

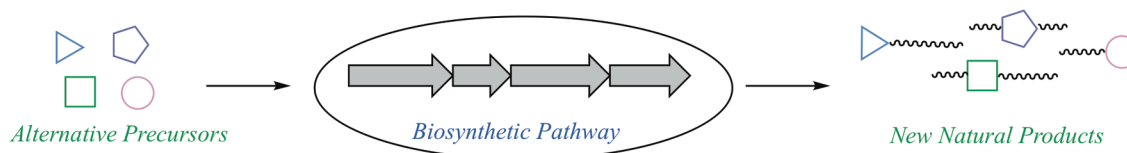
Taking advantage of the efficiency and selectivity of the biosynthetic machinery in these organisms to formulate the full natural product or advanced intermediates cuts production time and costs significantly, lending credence to the effectiveness of this strategy.

Although both methods are viable and have their advantages, each has their disadvantages: synthetic chemistry is able to produce almost unlimited structural variations, however the cost and time necessary is often debilitating, whereas fermentation and semi-synthesis is frequently more time and cost effective, but it is constrained by activated functional groups for manipulation, and low isolation yields. The ability to merge these two fields and explore chemoenzymatic syntheses could bridge the current gaps left by both disciplines and provide rapid access to previously inaccessible compound analogues. Despite the notable enzymatic transformations that are widely used in synthetic chemistry (esterases, lipases),⁴⁰ the use of multienzyme systems such as PKS and NRPS modules has yet to gain widespread interest, presumably due to the specificity seen in these systems and the expertise necessary to overcome these hurdles. Continued research in this area is required to gain a more detailed understanding of the catalytic systems used by these enzymes as well as their selectivity profiles in order to reach our ultimate goal of engineering broad scope catalysts capable of processing large libraries of “unnatural” natural products with the same enzyme variant.

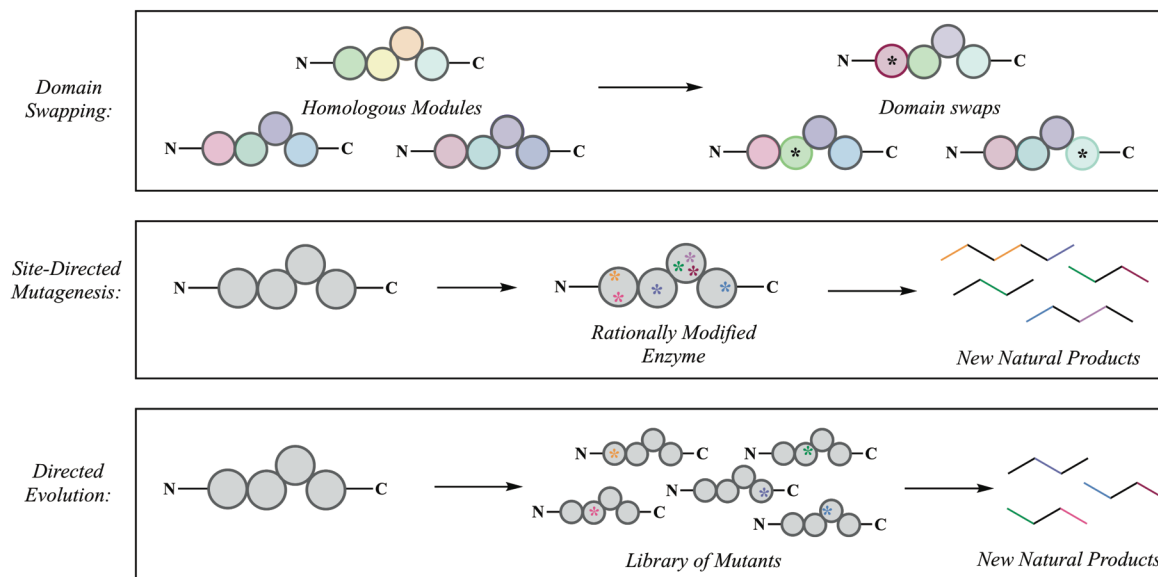
1.4 Combinatorial Biosynthesis in Drug Discovery

Utilizing PKS and NRPS systems to formulate natural product libraries has met with great enthusiasm in academics over the past two decades due to the almost limitless structural variation that could be imparted to scaffolds of interest. These systems have the capability to produce hundreds of millions of compounds by exploiting substrate promiscuity through protein and pathway engineering. Diversity can be introduced in these systems in three main ways: precursor directed biosynthesis, modification of discrete enzymes within a pathway, and recombinant pathway construction (**Figure 1.4: 1, 2, and 3**).⁴¹⁻⁴⁴ Feeding of alternate precursors has been used extensively to modify natural products as it takes advantage of inherent flexibility in the biosynthetic systems to incorporate new extender units without the need for genetic engineering (**Figure 1.4: 1**).⁴⁵⁻⁵⁰ This is exemplified by the polyether antibiotic monensin, which contains a leaky AT and has been shown to accept synthetic propargyl malonyl when cultures are supplemented with it.⁵¹ Augmenting with larger synthetic intermediates has also shown some

1. Precursor Directed Biosynthesis



2. Module Level Modifications



3. Pathway Recombination

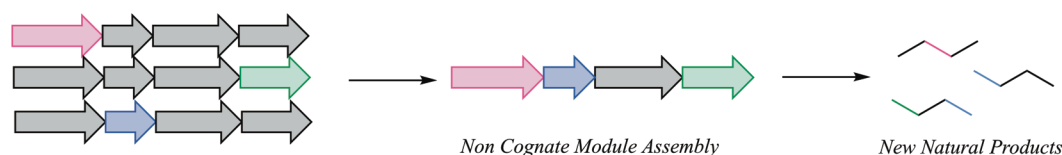


Figure 1.4 Schematic of the strategies used in combinatorial biosynthesis: **1** Precursor Directed Biosynthesis which takes advantage of the inherent flexibility of the system and synthetic precursors to formulate unnatural analogues, **2** Module level modifications which include moving parts of one module into a homologous one termed “domain swapping”, as well as site-directed mutagenesis and directed evolution which take advantage of mutations throughout the biosynthetic cluster to produce new molecules, and finally **3** Pathway recombination which takes entire genes from multiple pathways to formulate chimeric ones.

success as in the 6-deoxyerythronolide B (DEBS) system. In this study, synthetic diketides were fed to *E. coli* containing plasmids encoding the remaining PKS modules as well as the enzymes responsible for glycosylation/oxidation. This system was effectively able process these substrates into novel macrolides.⁵²

The second two facets of combinatorial biosynthesis rely heavily on genetic engineering to produce structural variations. Modifications to discrete enzymes within a pathway frequently focuses on swapping of domains within modules. Diversity can be introduced in a number of ways by changing the selectivity and optional processing of an overall module including choice of malonyl or amino acid extender units (selected for by the AT or A domains), degree of unsaturation in both products (controlled by optional domains in PKS and NRPS systems), as well as altered stereochemistry.⁵³⁻⁵⁴ This strategy has led to impressive libraries in the both the DEBS pathway and the NRPS derived daptomycin pathway. Both of these studies swapped analogous domains in related systems to form novel molecules with the same scaffold, but altered redox states and side chain incorporation.⁵⁵⁻⁵⁸ Other methods of modifying discrete enzymes within a pathway take advantage of site directed mutagenesis or directed evolution to increase promiscuity for non-native extender units,⁵⁹⁻⁶² fluorine atom incorporation,⁶³ and redox state changes.⁶⁴ Lastly, pathway level changes can produce hybrid molecules through the formulation of chimeric biosynthetic systems. This has met with success especially in the case of sugar containing natural products. The ability to append non-cognate sugars to macrolactones using genetic systems has produced altered biological activities, including modulating toxicity and potency.⁶⁵⁻⁷¹

Despite the successful examples discussed above, this strategy often meets with failure as alterations to biosynthetic enzymes frequently causes abysmal isolation yields, when products can be detected with many more expected products being elusive. Unraveling the molecular mechanism responsible for this diminished activity has garnered minimal traction as many of these manipulations have targeted early genes, making it impossible to determine what portions of the downstream modules are incompatible with the desired structural modifications. More detailed investigations into discrete enzymes within these systems will shed light on the selectivity of each step in the biosynthesis and can guide rational engineering endeavors in the future.

1.5 Thesis overview

My doctoral research has focused on two projects aimed at merging synthetic chemistry with *in vitro* biocatalysis in order to leverage chemoenzymatic platforms for the discovery of “unnatural” natural products of biological significance. Combining this biochemical information with current and future structural endeavors will hopefully continue to shed light on the complex processes used by biosynthetic enzymes to effect synthetic transformations. This will enable us

to achieve our ultimate goal of engineering more general biocatalysts for medicinal chemistry exploration.

The first of the two projects focused on the use of discrete biosynthetic enzymes in the cryptophycin anticancer agent's biosynthetic pathway to produce heterocyclic analogues for medicinal chemistry exploration. This work had four main themes, the first of which focused on the development of a scalable synthesis of *seco* cryptophycin chain elongation intermediates as the N-acetyl cysteamine (SNAC) thioesters, that could be diversified at a late stage. The second utilized these intermediates to interrogate the cryptophycin thioesterase (CrpTE) to effect macrocyclization. The *in vitro* evaluation produced all the desired macrocycles which could be isolated and tested for activity in HCT-116 human colorectal cancer cells. This strategy facilitated the discovery of one of the most potent analogues of this family seen to date with single digit picomolar IC₅₀ values. In addition, this analogue does not contain a β epoxy functionality that had previously been thought necessary for maximum potency, as all other analogues lacking it show activities in the low nM range.

The second facet of the cryptophycin project, described in **Chapter 3** has focused on gaining structural information on the CrpTE. Over the past decade countless crystal trays have been set in the hopes of identifying conditions that would promote crystal growth. With the continued failures our efforts turned to designing new constructs and taking advantage of a strategy like Surface Entropy Reduction (SER) in hopes of engineering better crystal packing interfaces. We in collaboration with Dr. John Lutz at Eli Lilly designed and formulated a number of constructs that hoped to eliminate some of the potential issues identified in a more thorough examination of the primary structure.

Although these efforts have yet to produce any significant breakthroughs in crystal formation, they have identified constructs that are predominantly monomeric allowing us to consider alternative structural pursuits. In collaboration with Dr. Vivekanandan Subramanian in biophysics, we screened the CrpTE for potential NMR characterization. Finding that it had ideal folding and tumbling properties, structural characterization utilizing multiple labeling strategies and triple resonance NMR experiments are possible. We are currently completing the assignments of each residue in the NMR spectra and will be moving forward with three-dimensional analysis shortly.

The last subset of my doctoral thesis, focuses on a second system, the pikromycin family of macrolide antibiotics. Previous efforts in our lab have focused on reconstituting the last two modules of the biosynthetic system for use in the production of the pikromycin macrocyclic core. From here these can be glycosylated and oxidized to form the fully functionalized macrolide antibiotics. Utilizing this platform, we hoped to explore the ability of these enzymes to accept unnatural chain elongation intermediates. It has been hypothesized that the TE may be the most selective enzyme in these pathways and may hold the key to successful processing of unnatural substrates. Although this work is ongoing, it has indicated that the TE does play a large role in selectivity of substrates, but that it has some flexibility. We have been able to formulate macrolactones on milligram scale that contain unnatural ester, amide, and di desmethyl functional groups, the details of which can be found in **Chapter 4**. It has also shown that the KS in these systems may also play a large role in selecting substrates and that it is sensitive to larger groups closer to the site of transthioesterification.

1.6 References

1. Newman, D. J.; Cragg, G. M., Natural Products as Sources of New Drugs from 1981 to 2014. *Journal of natural products* **2016**, *79* (3), 629-661.
2. Bernardini, S.; Tiezzi, A.; Laghezza Masci, V.; Ovidi, E., Natural products for human health: an historical overview of the drug discovery approaches. *Nat Prod Res* **2017**, 1-25.
3. Dias, D. A.; Urban, S.; Roessner, U., A historical overview of natural products in drug discovery. *Metabolites* **2012**, *2* (2), 303-36.
4. Cragg, G. M.; Newman, D. J., Biodiversity: A continuing source of novel drug leads. *Pure Appl Chem* **2005**, *77* (1), 7-24.
5. Hosztafi, S., The discovery of alkaloids. *Pharmazie* **1997**, *52* (7), 546-550.
6. Lindsey, A. S.; Jeskey, H., The Kolbe-Schmitt Reaction. *Chem Rev* **1957**, *57* (4), 583-620.
7. Clardy, J.; Walsh, C., Lessons from natural molecules. *Nature* **2004**, *432* (7019), 829-837.
8. Ortholand, J. Y.; Ganesan, A., Natural products and combinatorial chemistry: back to the future. *Curr Opin Chem Biol* **2004**, *8* (3), 271-280.
9. Evans, B. E.; Rittle, K. E.; Bock, M. G.; Dipardo, R. M.; Freidinger, R. M.; Whitter, W. L.; Lundell, G. F.; Veber, D. F.; Anderson, P. S.; Chang, R. S. L.; Lotti, V. J.; Cerino, D. J.; Chen, T. B.; Kling, P. J.; Kunkel, K. A.; Springer, J. P.; Hirshfield, J., Methods for Drug Discovery - Development of Potent, Selective, Orally Effective Cholecystokinin Antagonists. *Journal of medicinal chemistry* **1988**, *31* (12), 2235-2246.
10. Hertweck, C., The Biosynthetic Logic of Polyketide Diversity. *Angew Chem Int Edit* **2009**, *48* (26), 4688-4716.
11. Chan, Y. A.; Podevels, A. M.; Kevany, B. M.; Thomas, M. G., Biosynthesis of polyketide synthase extender units. *Natural Product Reports* **2009**, *26* (1), 90-114.
12. Staunton, J.; Weissman, K. J., Polyketide biosynthesis: a millennium review. *Natural Product Reports* **2001**, *18* (4), 380-416.
13. Horsman, M. E.; Hari, T. P.; Boddy, C. N., Polyketide synthase and non-ribosomal peptide synthetase thioesterase selectivity: logic gate or a victim of fate? *Nat Prod Rep* **2016**, *33* (2), 183-202.
14. Hertweck, C.; Luzhetskyy, A.; Rebets, Y.; Bechthold, A., Type II polyketide synthases: gaining a deeper insight into enzymatic teamwork. *Natural Product Reports* **2007**, *24* (1), 162-190.
15. Shimizu, Y.; Ogata, H.; Goto, S., Type III Polyketide Synthases: Functional Classification and Phylogenomics. *Chembiochem* **2017**, *18* (1), 50-65.
16. Weissman, K. J., Uncovering the structures of modular polyketide synthases. *Natural Product Reports* **2015**, *32* (3), 436-453.
17. Weissman, K. J., The structural biology of biosynthetic megaenzymes. *Nature Chemical Biology* **2015**, *11* (9), 660-670.
18. Buchholz, T. J.; Geders, T. W.; Bartley, F. L.; Reynolds, K. A.; Smith, J. L.; Sherman, D. H., Structural Basis for Binding Specificity between Subclasses of Modular Polyketide Synthase Docking Domains. *ACS chemical biology* **2009**, *4* (1), 41-52.
19. Walsh, C. T., Insights into the chemical logic and enzymatic machinery of NRPS assembly lines. *Nat Prod Rep* **2016**, *33* (2), 127-35.
20. Cane, D. E.; Walsh, C. T., The parallel and convergent universes of polyketide synthases and nonribosomal peptide synthetases. *Chem Biol* **1999**, *6* (12), R319-R325.

21. Olano, C.; Mendez, C.; Salas, J. A., Post-PKS tailoring steps in natural product-producing actinomycetes from the perspective of combinatorial biosynthesis. *Natural Product Reports* **2010**, *27* (4), 571-616.
22. Rix, U.; Fischer, C.; Remsing, L. L.; Rohr, J., Modification of post-PKS tailoring steps through combinatorial biosynthesis. *Natural Product Reports* **2002**, *19* (5), 542-580.
23. Katz, L.; Ashley, G. W., Translation and protein synthesis: Macrolides. *Chem Rev* **2005**, *105* (2), 499-527.
24. Hirama, M.; Oishi, T.; Uehara, H.; Inoue, M.; Maruyama, M.; Guri, H.; Satake, M., Total synthesis of ciguatoxin CTX3C. *Science* **2001**, *294* (5548), 1904-1907.
25. Zweig, J. E.; Kim, D. E.; Newhouse, T. R., Methods Utilizing First-Row Transition Metals in Natural Product Total Synthesis. *Chem Rev* **2017**, *117* (18), 11680-11752.
26. Andrushko, V.; Andrushko, N.; ProQuest (Firm), Stereoselective synthesis of drugs and natural products. Wiley: Hoboken, N.J., 2013; p. 2 v. in 1. <https://ebookcentral.proquest.com/lib/umichigan/detail.action?docID=1435995>.
27. Wender, P. A., Toward the ideal synthesis and molecular function through synthesis-informed design. *Natural Product Reports* **2014**, *31* (4), 433-440.
28. Twelves, C.; Cortes, J.; Vahdat, L. T.; Wanders, J.; Akerele, C.; Kaufman, P. A., Phase III Trials of Eribulin Mesylate (E7389) in Extensively Pretreated Patients With Locally Recurrent or Metastatic Breast Cancer. *Clin Breast Cancer* **2010**, *10* (2), 160-163.
29. Cortes, J.; Vahdat, L.; Blum, J. L.; Twelves, C.; Campone, M.; Roche, H.; Bachelot, T.; Awada, A.; Paridaens, R.; Goncalves, A.; Shuster, D. E.; Wanders, J.; Fang, F.; Gurnani, R.; Richmond, E.; Cole, P. E.; Ashworth, S.; Allison, M. A., Phase II Study of the Halichondrin B Analog Eribulin Mesylate in Patients With Locally Advanced or Metastatic Breast Cancer Previously Treated With an Anthracycline, a Taxane, and Capecitabine. *J Clin Oncol* **2010**, *28* (25), 3922-3928.
30. Yu, M. J.; Zheng, W. J.; Seletsky, B. M., From micrograms to grams: scale-up synthesis of eribulin mesylate. *Natural Product Reports* **2013**, *30* (9), 1158-1164.
31. Chase, C. E.; Fang, F. G.; Lewis, B. M.; Wilkie, G. D.; Schnaderbeck, M. J.; Zhu, X. J., Process Development of Halaven (R): Synthesis of the C1-C13 Fragment from D-(-)-Gulono-1,4-lactone. *Synlett* **2013**, *24* (3), 323-326.
32. Austad, B. C.; Calkins, T. L.; Chase, C. E.; Fang, F. G.; Horstmann, T. E.; Hu, Y. B.; Lewis, B. M.; Niu, X.; Noland, T. A.; Orr, J. D.; Schnaderbeck, M. J.; Zhang, H. M.; Asakawa, N.; Asai, N.; Chiba, H.; Hasebe, T.; Hoshino, Y.; Ishizuka, H.; Kajima, T.; Kayano, A.; Komatsu, Y.; Kubota, M.; Kuroda, H.; Miyazawa, M.; Tagami, K.; Watanabe, T., Commercial Manufacture of Halaven (R): Chemoselective Transformations En Route to Structurally Complex Macrocyclic Ketones. *Synlett* **2013**, *24* (3), 333-337.
33. Austad, B. C.; Benayoud, F.; Calkins, T. L.; Campagna, S.; Chase, C. E.; Choi, H. W.; Christ, W.; Costanzo, R.; Cutter, J.; Endo, A.; Fang, F. G.; Hu, Y. B.; Lewis, B. M.; Lewis, M. D.; McKenna, S.; Noland, T. A.; Orr, J. D.; Pesant, M.; Schnaderbeck, M. J.; Wilkie, G. D.; Abe, T.; Asai, N.; Asai, Y.; Kayano, A.; Kimoto, Y.; Komatsu, Y.; Kubota, M.; Kuroda, H.; Mizuno, M.; Nakamura, T.; Omae, T.; Ozeki, N.; Suzuki, T.; Takigawa, T.; Watanabe, T.; Yoshizawa, K., Process Development of Halaven (R): Synthesis of the C14-C35 Fragment via Iterative Nozaki-Hiyama-Kishi Reaction-Williamson Ether Cyclization. *Synlett* **2013**, *24* (3), 327-332.
34. Newman, D. J., Developing natural product drugs: Supply problems and how they have been overcome. *Pharmacol Therapeut* **2016**, *162*, 1-9.

35. Woodward, R. B.; Logusch, E.; Nambiar, K. P.; Sakan, K.; Ward, D. E.; Auyeung, B. W.; Balaram, P.; Browne, L. J.; Card, P. J.; Chen, C. H.; Chenevert, R. B.; Fliri, A.; Frobels, K.; Gais, H. J.; Garratt, D. G.; Hayakawa, K.; Heggie, W.; Hesson, D. P.; Hoppe, D.; Hoppe, I.; Hyatt, J. A.; Ikeda, D.; Jacobi, P. A.; Kim, K. S.; Kobuke, Y.; Kojima, K.; Krowicki, K.; Lee, V. J.; Leutert, T.; Malchenko, S.; Martens, J.; Matthews, R. S.; Ong, B. S.; Press, J. B.; Rajanbabu, T. V.; Rousseau, G.; Sauter, H. M.; Suzuki, M.; Tatsuta, K.; Tolbert, L. M.; Truesdale, E. A.; Uchida, I.; Ueda, Y.; Uyehara, T.; Vasella, A. T.; Vladuchick, W. C.; Wade, P. A.; Williams, R. M.; Wong, H. N. C., Asymmetric Total Synthesis of Erythromycin .3. Total Synthesis of Erythromycin. *J Am Chem Soc* **1981**, *103* (11), 3215-3217.
36. Woodward, R. B.; Logusch, E.; Nambiar, K. P.; Sakan, K.; Ward, D. E.; Auyeung, B. W.; Balaram, P.; Browne, L. J.; Card, P. J.; Chen, C. H.; Chenevert, R. B.; Fliri, A.; Frobels, K.; Gais, H. J.; Garratt, D. G.; Hayakawa, K.; Heggie, W.; Hesson, D. P.; Hoppe, D.; Hoppe, I.; Hyatt, J. A.; Ikeda, D.; Jacobi, P. A.; Kim, K. S.; Kobuke, Y.; Kojima, K.; Krowicki, K.; Lee, V. J.; Leutert, T.; Malchenko, S.; Martens, J.; Matthews, R. S.; Ong, B. S.; Press, J. B.; Rajanbabu, T. V.; Rousseau, G.; Sauter, H. M.; Suzuki, M.; Tatsuta, K.; Tolbert, L. M.; Truesdale, E. A.; Uchida, I.; Ueda, Y.; Uyehara, T.; Vasella, A. T.; Vladuchick, W. C.; Wade, P. A.; Williams, R. M.; Wong, H. N. C., Asymmetric Total Synthesis of Erythromycin .2. Synthesis of an Erythronolide a Lactone System. *J Am Chem Soc* **1981**, *103* (11), 3213-3215.
37. Woodward, R. B.; Logusch, E.; Nambiar, K. P.; Sakan, K.; Ward, D. E.; Auyeung, B. W.; Balaram, P.; Browne, L. J.; Card, P. J.; Chen, C. H.; Chenevert, R. B.; Fliri, A.; Frobels, K.; Gais, H. J.; Garratt, D. G.; Hayakawa, K.; Heggie, W.; Hesson, D. P.; Hoppe, D.; Hoppe, I.; Hyatt, J. A.; Ikeda, D.; Jacobi, P. A.; Kim, K. S.; Kobuke, Y.; Kojima, K.; Krowicki, K.; Lee, V. J.; Leutert, T.; Malchenko, S.; Martens, J.; Matthews, R. S.; Ong, B. S.; Press, J. B.; Rajanbabu, T. V.; Rousseau, G.; Sauter, H. M.; Suzuki, M.; Tatsuta, K.; Tolbert, L. M.; Truesdale, E. A.; Uchida, I.; Ueda, Y.; Uyehara, T.; Vasella, A. T.; Vladuchick, W. C.; Wade, P. A.; Williams, R. M.; Wong, H. N. C., Asymmetric Total Synthesis of Erythromycin .1. Synthesis of an Erythronolide a Seco Acid-Derivative Via Asymmetric Induction. *J Am Chem Soc* **1981**, *103* (11), 3210-3213.
38. Fernandes, P.; Martens, E.; Pereira, D., Nature nurtures the design of new semi-synthetic macrolide antibiotics. *J Antibiot* **2017**, *70* (5), 527-533.
39. Wani, M. C.; Horwitz, S. B., Nature as a remarkable chemist: a personal story of the discovery and development of Taxol. *Anti-Cancer Drug* **2014**, *25* (5), 482-487.
40. Clouthier, C. M.; Pelletier, J. N., Expanding the organic toolbox: a guide to integrating biocatalysis in synthesis. *Chem Soc Rev* **2012**, *41* (4), 1585-1605.
41. Donadio, S.; Sosio, M., Strategies for combinatorial biosynthesis with modular polyketide synthases. *Comb Chem High Throughput Screen* **2003**, *6* (6), 489-500.
42. Floss, H. G., Combinatorial biosynthesis - Potential and problems. *J Biotechnol* **2006**, *124* (1), 242-257.
43. Sun, H. H.; Liu, Z. H.; Zhao, H. M.; Ang, E. L., Recent advances in combinatorial biosynthesis for drug discovery. *Drug Des Dev Ther* **2015**, *9*, 823-833.
44. Weissman, K. J., Genetic engineering of modular PKSs: from combinatorial biosynthesis to synthetic biology. *Nat Prod Rep* **2016**, *33* (2), 203-30.
45. Kreutzer, M. F.; Kage, H.; Herrmann, J.; Pauly, J.; Hermenau, R.; Muller, R.; Hoffmeister, D.; Nett, M., Precursor-directed biosynthesis of micacocidin derivatives with activity against *Mycoplasma pneumoniae*. *Organic & Biomolecular Chemistry* **2014**, *12* (1), 113-118.
46. Sheehan, L. S.; Lill, R. E.; Wilkinson, B.; Sheridan, R. M.; Vousden, W. A.; Kaja, A. L.; Crouse, G. D.; Gifford, J.; Graupner, P. R.; Karr, L.; Lewer, P.; Sparks, T. C.; Leadlay, P. F.;

- Waldron, C.; Martin, C. J., Engineering of the spinosyn PKS: Directing starter unit incorporation. *Journal of natural products* **2006**, *69* (12), 1702-1710.
47. Boddy, C. N.; Hotta, K.; Tse, M. L.; Watts, R. E.; Khosla, C., Precursor-directed biosynthesis of epothilone in *Escherichia coli*. *J Am Chem Soc* **2004**, *126* (24), 7436-7437.
48. Cane, D. E.; Kudo, F.; Kinoshita, K.; Khosla, C., Precursor-directed biosynthesis: Biochemical basis of the remarkable selectivity of the erythromycin polyketide synthase toward unsaturated triketides. *Chem Biol* **2002**, *9* (1), 131-142.
49. Donadio, S.; Mcalpine, J. B.; Sheldon, P. J.; Jackson, M.; Katz, L., An Erythromycin Analog Produced by Reprogramming of Polyketide Synthesis. *P Natl Acad Sci USA* **1993**, *90* (15), 7119-7123.
50. Leaf, T.; Cadapan, L.; Carreras, C.; Regentin, R.; Ou, S.; Woo, E.; Ashley, G.; Licari, P., Precursor-directed biosynthesis of 6-deoxyerythronolide B analogs in *Streptomyces coelicolor*: understanding precursor effects. *Biotechnol Prog* **2000**, *16* (4), 553-6.
51. Bravo-Rodriguez, K.; Ismail-Ali, A. F.; Klopries, S.; Kushnir, S.; Ismail, S.; Fansa, E. K.; Wittinghofer, A.; Schulz, F.; Sanchez-Garcia, E., Predicted Incorporation of Non-native Substrates by a Polyketide Synthase Yields Bioactive Natural Product Derivatives. *Chembiochem* **2014**, *15* (13), 1991-1997.
52. Harvey, C. J. B.; Puglisi, J. D.; Pande, V. S.; Cane, D. E.; Khosla, C., Precursor Directed Biosynthesis of an Orthogonally Functional Erythromycin Analogue: Selectivity in the Ribosome Macrolide Binding Pocket. *J Am Chem Soc* **2012**, *134* (29), 12259-12265.
53. Hertweck, C., Decoding and reprogramming complex polyketide assembly lines: prospects for synthetic biology. *Trends Biochem Sci* **2015**, *40* (4), 189-199.
54. Winn, M.; Fyans, J. K.; Zhuo, Y.; Micklefield, J., Recent advances in engineering nonribosomal peptide assembly lines. *Natural Product Reports* **2016**, *33* (2), 317-347.
55. McDaniel, R.; Thamchaipenet, A.; Gustafsson, C.; Fu, H.; Betlach, M.; Betlach, M.; Ashley, G., Multiple genetic modifications of the erythromycin polyketide synthase to produce a library of novel "unnatural" natural products. *P Natl Acad Sci USA* **1999**, *96* (5), 1846-1851.
56. Nguyen, K. T.; He, X. W.; Alexander, D. C.; Li, C.; Gu, J. Q.; Mascio, C.; Van Praagh, A.; Mortin, L.; Chu, M.; Silverman, J. A.; Brian, P.; Baltz, R. H., Genetically Engineered Lipopeptide Antibiotics Related to A54145 and Daptomycin with Improved Properties. *Antimicrob Agents Ch* **2010**, *54* (4), 1404-1413.
57. Doekel, S.; Gal, M. F. C. L.; Gu, J. Q.; Chu, M.; Baltz, R. H.; Brian, P., Non-ribosomal peptide synthetase module fusions to produce derivatives of daptomycin in *Streptomyces roseosporus*. *Microbiol-Sgm* **2008**, *154*, 2872-2880.
58. Baltz, R. H.; Miao, V.; Wrigley, S. K., Natural products to drugs: daptomycin and related lipopeptide antibiotics. *Natural Product Reports* **2005**, *22* (6), 717-741.
59. Zhang, K.; Nelson, K. M.; Bhuripanyo, K.; Grimes, K. D.; Zhao, B.; Aldrich, C. C.; Yin, J., Engineering the Substrate Specificity of the DhbE Adenylation Domain by Yeast Cell Surface Display. *Chem Biol* **2013**, *20* (1), 92-101.
60. Thirlway, J.; Lewis, R.; Nunns, L.; Al Nakeeb, M.; Styles, M.; Struck, A. W.; Smith, C. P.; Micklefield, J., Introduction of a Non-Natural Amino Acid into a Nonribosomal Peptide Antibiotic by Modification of Adenylation Domain Specificity. *Angew Chem Int Edit* **2012**, *51* (29), 7181-7184.
61. Evans, B. S.; Chen, Y. Q.; Metcalf, W. W.; Zhao, H. M.; Kelleher, N. L., Directed Evolution of the Nonribosomal Peptide Synthetase AdmK Generates New Andrimid Derivatives In Vivo. *Chem Biol* **2011**, *18* (5), 601-607.

62. Fischbach, M. A.; Lai, J. R.; Roche, E. D.; Walsh, C. T.; Liu, D. R., Directed evolution can rapidly improve the activity of chimeric assembly-line enzymes. *P Natl Acad Sci USA* **2007**, *104* (29), 11951-11956.
63. Walker, M. C.; Thuronyi, B. W.; Charkoudian, L. K.; Lowry, B.; Khosla, C.; Chang, M. C. Y., Expanding the Fluorine Chemistry of Living Systems Using Engineered Polyketide Synthase Pathways. *Science* **2013**, *341* (6150), 1089-1094.
64. Kushnir, S.; Sundermann, U.; Yahiaoui, S.; Brockmeyer, A.; Janning, P.; Schulz, F., Minimally Invasive Mutagenesis Gives Rise to a Biosynthetic Polyketide Library. *Angew Chem Int Edit* **2012**, *51* (42), 10664-10669.
65. Shinde, P. B.; Han, A. R.; Cho, J.; Lee, S. R.; Ban, Y. H.; Yoo, Y. J.; Kim, E. J.; Kim, E.; Song, M. C.; Park, J. W.; Lee, D. G.; Yoon, Y. J., Combinatorial biosynthesis and antibacterial evaluation of glycosylated derivatives of 12-membered macrolide antibiotic YC-17. *J Biotechnol* **2013**, *168* (2), 142-148.
66. Nunez, L. E.; Nybo, S. E.; Gonzalez-Sabin, J.; Perez, M.; Menendez, N.; Brana, A. F.; Shaaban, K. A.; He, M.; Moris, F.; Salas, J. A.; Rohr, J.; Mendez, C., A Novel Mithramycin Analogue with High Antitumor Activity and Less Toxicity Generated by Combinatorial Biosynthesis. *Journal of medicinal chemistry* **2012**, *55* (12), 5813-5825.
67. Han, A. R.; Shinde, P. B.; Park, J. W.; Cho, J.; Lee, S. R.; Ban, Y. H.; Yoo, Y. J.; Kim, E. J.; Kim, E.; Park, S. R.; Kim, B. G.; Lee, D. G.; Yoon, Y. J., Engineered biosynthesis of glycosylated derivatives of narbomycin and evaluation of their antibacterial activities. *Appl Microbiol Biot* **2012**, *93* (3), 1147-1156.
68. Shepherd, M. D.; Liu, T.; Mendez, C.; Salas, J. A.; Rohr, J., Engineered Biosynthesis of Gilvocarcin Analogues with Altered Deoxyhexopyranose Moieties. *Appl Environ Microb* **2011**, *77* (2), 435-441.
69. Han, A. R.; Park, J. W.; Lee, M. K.; Ban, Y. H.; Yoo, Y. J.; Kim, E. J.; Kim, E.; Kim, B. G.; Sohng, J. K.; Yoon, Y. J., Development of a *Streptomyces venezuelae*-Based Combinatorial Biosynthetic System for the Production of Glycosylated Derivatives of Doxorubicin and Its Biosynthetic Intermediates. *Appl Environ Microb* **2011**, *77* (14), 4912-4923.
70. Jung, W. S.; Han, A. R.; Hong, J. S. J.; Park, S. R.; Choi, C. Y.; Park, J. W.; Yoon, Y. J., Bioconversion of 12-, 14-, and 16-membered ring aglycones to glycosylated macrolides in an engineered strain of *Streptomyces venezuelae*. *Appl Microbiol Biot* **2007**, *76* (6), 1373-1381.
71. Jung, W. S.; Lee, S. K.; Hong, J. S. J.; Park, S. R.; Jeong, S. J.; Han, A. R.; Sohng, J. K.; Kim, B. G.; Choi, C. Y.; Sherman, D. H.; Yoon, Y. J., Heterologous expression of tylosin polyketide synthase and production of a hybrid bioactive macrolide in *Streptomyces venezuelae*. *Appl Microbiol Biot* **2006**, *72* (4), 763-769.

Chapter 2

Chemoenzymatic Synthesis of Cryptophycin Anti-Cancer Agents

2.1 Introduction to the Cryptophycin Family of Natural Products

2.1.1 Cryptophycin Discovery

The cryptophycins are a family of macrocyclic natural products produced by a lichen symbiotic cyanobacteria of the genus *Nostoc sp* ATCC 53789. These compounds were originally isolated in 1990 by researchers at Merck as a part of their algae screening program.¹ The main isolate, later termed cryptophycin 1 (**Figure 2.1**), was determined to have exceptionally potent antifungal properties, specifically against its namesake *Cryptococcus* fungi, but was not pursued as a potential lead due to systemic toxicity seen in mice. In 1992, cryptophycin 1 was rediscovered in a related cyanobacteria *Nostoc sp* GSV 224 by Moore et al. as a potent antiproliferative agent.² A close analogue of cryptophycin 1, arenastatin A (later renamed cryptophycin 24) was also discovered in the same year from an Okinowan marine sponge *Dysidea arenaria* and is proposed to be biosynthesized by a cyanobacterial symbiont.³ Over the next 10 years, over 25 naturally occurring analogues of cryptophycin were isolated from GSV 224 including different chlorination

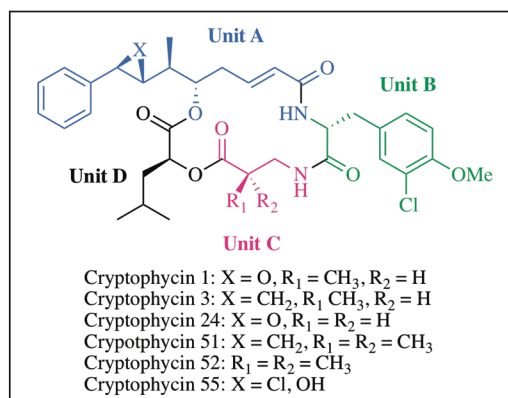


Figure 2.1: Select cryptophycin analogues produced by the Lichen symbiont *Nostoc*.

events, altered amino acids, as well as some variability in the PKS produced α/β unsaturated amide.⁴⁻⁶ All naturally occurring cryptophycins are described by subdividing them into 4 units that form the 16-membered core macrolactone; **unit A** a hydroxy-phenyloctenoic acid moiety, **unit B** a 3-chloro-O-methyl tyrosine, **unit C** a methyl- β -alanine, and **unit D** a leucic acid seen in **Figure 2.1**.

2.1. Introduction to the Cryptophycin Family of Natural Products

2.1.2 Mechanism of Action for Cryptophycin Anticancer Agents

Many of the isolated cryptophycins display potent antiproliferative activity with the major isolate, cryptophycin 1 containing low picomolar activity. More exciting was the marked potency seen against drug resistant cancers including p-glycoprotein (PGP) and multiple drug resistant protein (MRP) expressing cell lines.⁶⁻⁷ More in-depth studies into the mechanism of action of the cryptophycin has shown that it is an antimetabolic, which specifically bind β tubulin leading to apoptosis and cell death. Tubulin is a hetero-dimeric protein comprised of 2 subunits, α and β (**Figure 2.2, B**), which associate and polymerize to formulate microtubules.⁸ The majority of antimetabolic agents bind to the β subunit of tubulin including the taxanes, vinca alkaloids, colchicine, and epothilone anticancer agents (**Figure 2.2, A**).⁹ The vinca alkaloids and colchicine bind in distinctive sites named after these specific agents (the vinca site and the colchicine site shown in green and purple in **Figure 2.2 C**)¹⁰⁻¹¹ and prevent the polymerization of tubulin. The taxanes and epothilone natural products also bind distinct site on β tubulin (the taxane site, shown in blue and yellow, **Figure 2.2 C**)¹²⁻¹³ and are known to operate by the opposite mechanism, promoting microtubule polymerization and further stabilizing them.¹⁴ Ultimately both modes of action cause altered microtubule dynamics which results in an inability to undergo effective mitosis and ultimately cell death.

Despite the interest in cryptophycins as antimetabolic, there are no crystal structures of β tubulin with cryptophycin bound leaving the exact site and mode of binding unclear. Biochemical assays along with computational methods have shed light on both the likely binding site as well as the orientation. Cryptophycins were determined to bind β tubulin and have a similar mechanism of action as the vinca alkaloids and colchicine in that they destabilize microtubules.¹⁵⁻¹⁷ Competition assays with the afore mentioned microtubule binding agents taxol, colchicine, and

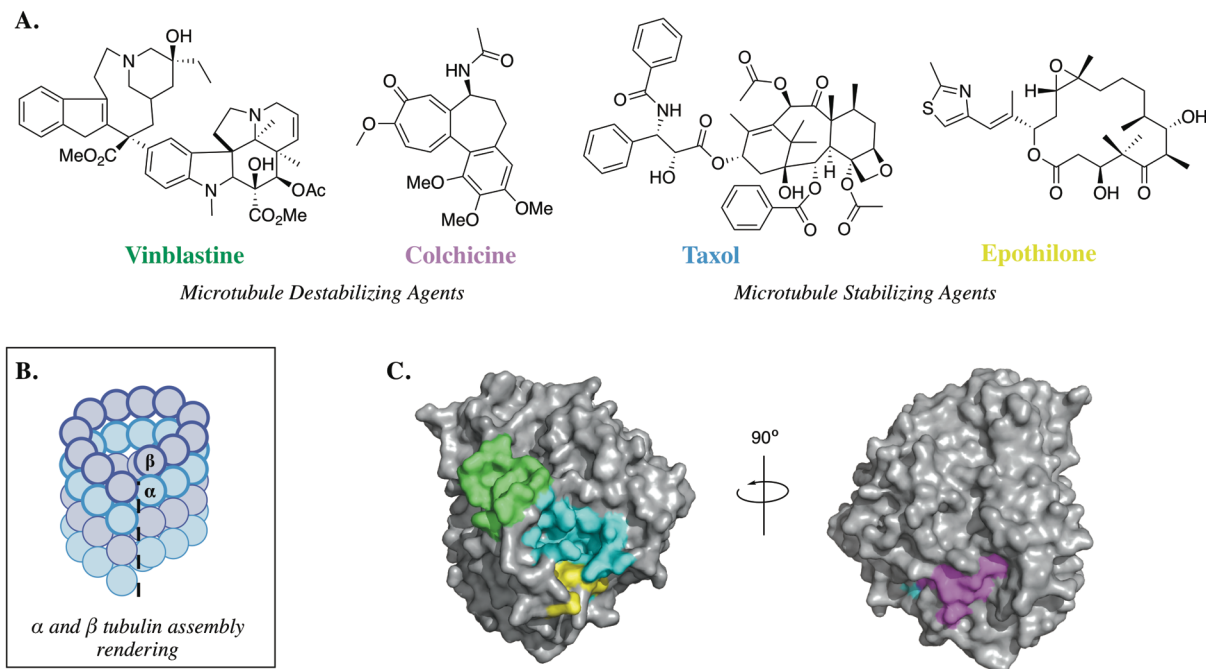


Figure 2.2 Common microtubule binding agents: **(A)** subdivided by mechanism of action. **B** Cartoon of tubulin assembly by the association of the α/β tubulin dimers. **C** The binding sites of **A** on β tubulin (**C**). The binding sites of Taxol and Epothilone somewhat overlap and stabilize microtubules whereas Vinblastine and Colchicine bind distinct sites and act by the opposite mechanism, destabilizing the microtubules.

vinblastine show non-competitive inhibition with only vinblastine indicating the binding site overlaps with the vinca site.¹⁸⁻²¹ This is further supported by molecular dynamics and molecular docking experiments that identified a common binding site of multiple known depsipeptides natural products including the cryptophycins, termed the “peptide site”.²² Early hypotheses on the mode of binding included a covalent linkage through the epoxide group seen on unit A. A combination of synthetic analogues and biochemical assays have mostly disproven this theory. Cryptophycins containing other acceptor functionalities including enones, ynones and allylic electrophiles were all not active.²³ Additionally, biochemical work that shows intact cryptophycin could be recovered from its tubulin complex upon denaturation.²⁴ All of these experiments indicate that most likely, the epoxide does not undergo a covalent modification upon binding to β tubulin and is likely a mixture of hydrophobic and electrostatic interactions.

2.1.3 Structure Activity Relationship of Cryptophycin Anticancer Agents

Aside from the many natural analogues of cryptophycin that were isolated, hundreds of synthetic analogues have been reported the majority of which were synthesized by Eli Lilly.²⁵⁻⁴³

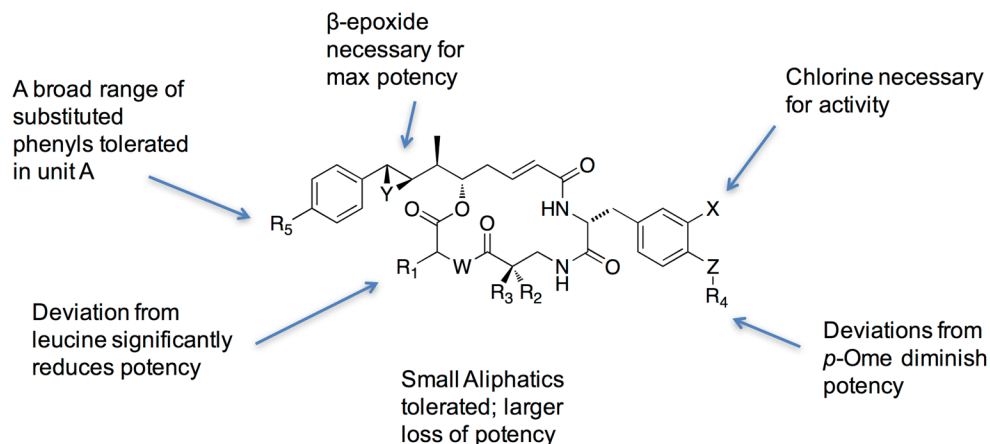


Figure 2.3 Generalized schematic of Cryptophycin SAR.

These analogues have given a distinct understanding of the functional groups that are important for biological activity, a summary of which can be seen in **Figure 2.3**. The unit A aryl group tolerates methyl group substituents as well as some larger amine containing groups in the para position, although substituting the benzene ring with a thiophene or a furan ring showed a 1000-fold decrease in potency.^{14, 44} The *R,R* configuration of the unit A epoxide group is far superior to that of the *S,S* as well as the styrene, again showing 1000 fold decrease in potency.⁴⁵⁻⁴⁶ Replacing the epoxide with a chlorhydrin, cryptophycin 55 (**Figure 2.1**) was equally as potent as the native β epoxide as it spontaneously reforms this moiety in water. Many substitution patterns have been investigated in unit B, however without exception all caused a decrease in potency, including the necessity for the uncommon D-tyrosine stereochemistry.^{6, 45, 47} The β amino acid seen in unit C was necessary for the active conformation and larger substitutions off either the α or β position of this unit were detrimental to activity.³⁰⁻³¹ A geminal dimethyl group introduced at the α position was tolerated fairly well and was later termed cryptophycin 52 (**Figure 2.1**), and used for the subsequent clinical trials. This small change imparted more stability to the ester bond between unit's C and D as well as removed a stereocenter that was costly to generate synthetically. Unit D, which has some flexibility within the biosynthesis, tolerates changes to *sec*-butyl and *n*-propyl groups from the isobutyl without deleterious effects to potency.⁶ Interestingly, the stereochemistry may not be important in this region as an analogue with the inverted (*R*) stereochemistry appears to be equipotent as its (*S*) counterpart.⁴¹

Out of all the synthetic analogues generated, one that contained a geminal dimethyl in unit C (cryptophycin 52, LY355703) was determined to be the best candidate for clinical trials by Eli Lilly.³⁰ This modification protected the ester bond between unit's C and D from degradation as well as simplified the synthesis. Cryptophycin 52 (LY355703) entered into clinical trials for non-small cell lung cancer as well as platinum resistant ovarian cancer, but failed out of phase 2 due to reversible dose limiting peripheral neuropathy as well as only modest *in vivo* efficacy with the dosing schedule utilized.⁴⁸⁻⁵⁰ Despite these failures, both studies indicated that alternative analogues or dosing schedules could greatly affect the outcomes and should be further investigated especially for difficult to treat, resistant cancers.

2.1.4 Cryptophycins as Antibody Drug Conjugate Warheads

Recently, the incredible potency of cryptophycins has generated interest in them as antibody drug conjugate (ADC) warheads. Sanofi was the first to investigate these using both cleavable and non-cleavable linkers to connect the benzyl amine containing cryptophycin with an hu2H11 antibody.⁵¹⁻⁵² Genentech has also utilized a similar strategy to conjugate cryptophycin to their antibody that targets HER2 and CD22 receptors.⁵³ These have shown some promise for target antigen expressing cells.

2.1.5 Biosynthetic Assembly of Cryptophycins

The continued interest in cryptophycins as well as the complexity of this molecule and the difficulties formulating it, led to investigations into its biosynthesis, and potentially the use of discrete enzymes as biocatalysts for the production of novel analogues. The cryptophycins are biosynthesized by a mixed PKS/NRPS system (**Figure 2.4**). Unit A is believed to be initiated by an unusual NRPS loading domain that incorporates a phenylalanine which is then deaminated to produce a cinnamyl group.⁵⁴ Feeding experiments previously reported by Magarvey et al. indicate that this is not the starter unit picked up by the first PKS module in the cryptophycin pathway, as there is a lack of deuterium present when the organism is supplemented with [²H₈]phenylalanine.⁵⁵ It likely undergoes a single carbon truncation to give the phenyl acetyl group, which is then loaded and processed by the rest of the cryptophycin biosynthetic pathway.⁵⁴ From here the full length unit A is extended via the condensation of three malonyl extender units by the Crp A and B PKS modules,⁵⁵ with an s-adenosyl methionine (SAM) dependent methylation at C6,⁵⁴ completing the unit A biosynthesis.

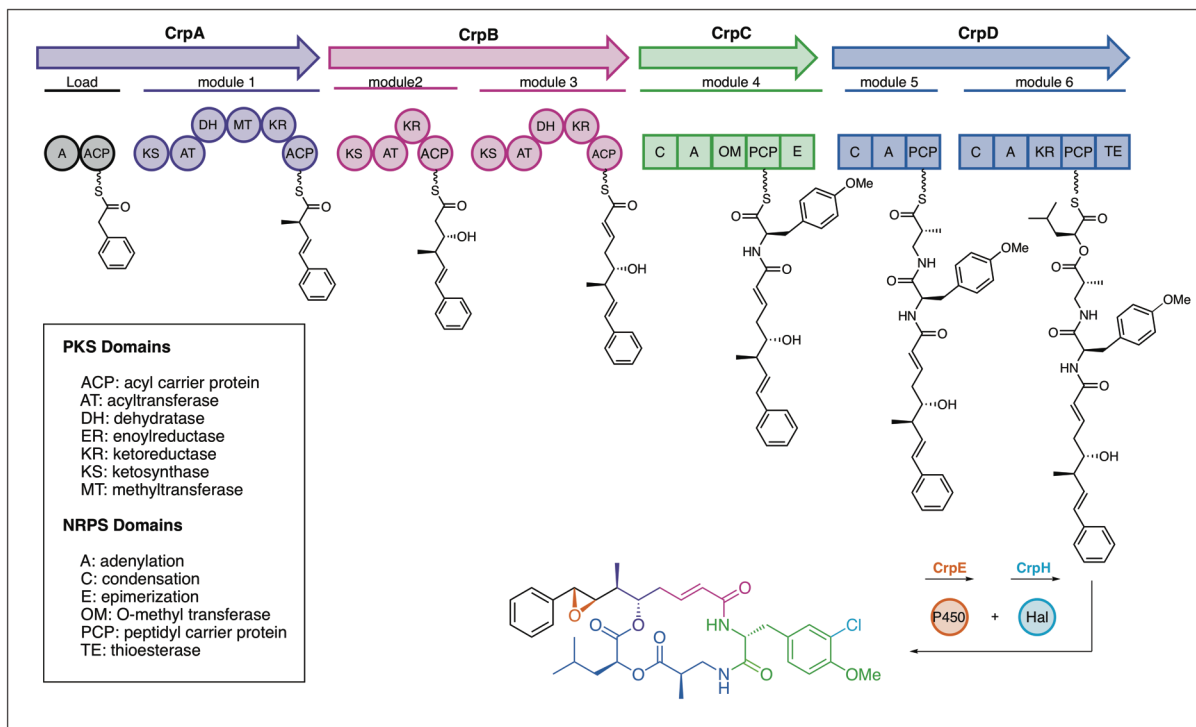


Figure 2.4 Biosynthetic Pathway of the mixed PKS/NRPS natural product cryptophycin.

Once the PKS intermediate is formulated, it is passed off to the NRPS portion of the biosynthetic pathway, CrpC and CrpD. CrpC is a monomodular NRPS domain that contains an O-methyl transferase which is capable of methylating the tyrosine residue. This tyrosine residue is further modified by CrpH, a Flavin dependent halogenase, that is responsible for the chlorination event, however it is unclear if this enzyme acts on the full length substrate or the tyrosine prior to incorporation. Next it is passed to the bimodular CrpD which first incorporates a methyl- β -alanine, derived from aspartate. Finally, CrpD module 2 incorporates an α -hydroxyisocaproic acid moiety derived from leucine to produce the full length chain elongation intermediate. This is then passed to the third portion of CrpD, the thioesterase which is responsible for the formulation of the macrocyclic core by facilitating intramolecular attack of the unit A hydroxyl.⁵⁵ This is further tailored by the CrpE, a heme containing P450 responsible for the installation of the β epoxy group on unit A from molecular oxygen.⁵⁶ Each of the above modules has been shown to contain some inherent flexibility for unnatural substrates as is evident by the large size of this family (over 25 members). This feature presents a unique opportunity to leverage some of the enzymes within this

pathway for use in a biocatalytic syntheses of not only the native molecules, but structural analogues that could combat some of the shortcomings seen in clinical trials.

Thioesterases contain a serine, histidine, and aspartic acid catalytic triad that are able to accept upstream intermediates and effect macrocyclization. The linear chain elongation intermediate is passed from the upstream PKS or NRPS module via the peptidyl or acyl carrier protein by a prosthetic group known as the phosphopantetheine (Ppant) arm (**Figure 2.5**).⁵⁷ Nucleophilic attack by the serine hydroxyl on substrate bound Ppant arm, creates a tetrahedral intermediate stabilized by the area of the TE known as the oxanion hole. Loss of the Ppant arm then generates the acyl-TE intermediate and a free carrier protein. Within the TE active site the intramolecular hydroxyl is folded back in towards the ester bond, and nucleophilic attack causes macrocyclic offloading of the product (**Figure 2.5**).⁵⁸

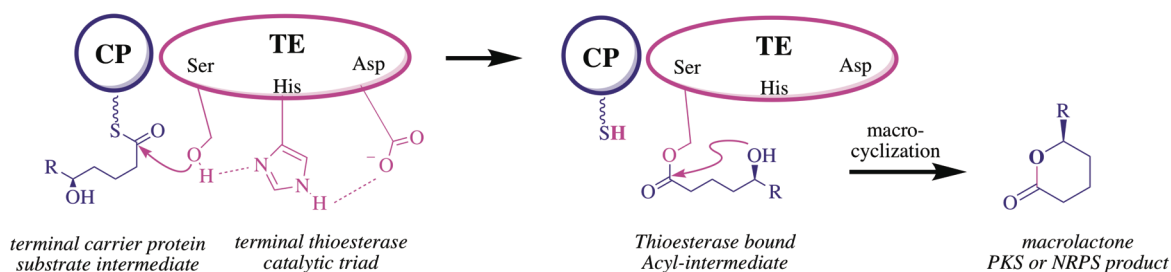


Figure 2.5 Generalized schematic of a Thioesterase mechanism. The upstream carrier protein (CP) delivers the growing chain to the active site serine of the thioesterase. A deprotonation event, facilitated by the histidine and aspartic acid (catalytic triad) allows for nucleophilic transfer of the chain elongation intermediate. The histidine is then responsible for coordinating the intramolecular hydroxyl and facilitating cyclization

In a previous study, we demonstrated that excised CrpTE is able to catalyze facile cyclization of native and modified substrates to formulate cryptophycin 3, 51 (**Figure 2.1**) and an unnatural cryptophycin containing a terminal olefin in unit A, originally synthesized as LY404291 at Eli Lilly.⁵⁹ This work indicated that the CrpTE's inherent flexibility may render it an effective biocatalyst for the production of novel cryptophycin analogues. This was further supported by investigations into the Crp D-M2 NRPS module which further showed the ability of the CrpTE to accept unnatural amino acids for unit D, an unusual result as often the site of ring closure is very sensitive to amino acid changes.⁶⁰ In order to continue to interrogate the CrpTE as well as explore some under-represented areas of cryptophycin SAR, we embarked on an effort to synthesize a series of novel cryptophycin chain elongation intermediates. Heterocyclic unit A analogues were designed to probe the CrpTE substrate tolerance, as well as produce analogues that may address

some of major shortcomings identified in clinical trials, including dose limiting peripheral neuropathy and broad *in vivo* efficacy.^{48, 50}

2.2 Synthesis of *seco* cryptophycin analogues

In order to test the flexibility of the CrpTE towards unnatural unit A aryl groups, we needed to devise a scalable synthesis of the *seco* cryptophycin intermediate containing an N-acetyl cysteamine (NAc) on unit D that is used as a recognition element by the TE. A synthesis of the native chain and the unit C gem dimethyl chain elongation intermediates had been reported previously⁵⁹ as well as a diversifiable unit A synthesis⁶¹ that took advantage of crotylation chemistry to set the stereocenters seen in unit A. Initial analogues made use of this strategy unfortunately, low yields and scalability issues prompted us to investigate alternative strategies that would be more amenable to the larger scale formulation.

Retrosynthetically, the linear chain elongation intermediate can be disconnected through the ester and amide bonds present between units A, B, C, and D as well as through the double bond of the α/β unsaturated amide present in unit A. In order to avoid peptide coupling between unit A and unit B that has been plagued with difficulties, analogues were synthesized using two key intermediates, a boronic ester containing unit AB and unit CD-NAc (**Figure 2.6**). Further disjoining units AB can be accomplished with a Horner Wadsworth Emmons olefination (HWE) olefination between the modified tyrosine (unit B) and a boronic ester containing unit A in order to take advantage of a late stage Suzuki coupling strategy reported by Bolduc et al.⁶¹ to diversify the aryl group. Unit A can be further disconnected by a single aldol reaction which set the (2*R*, 3*S*)

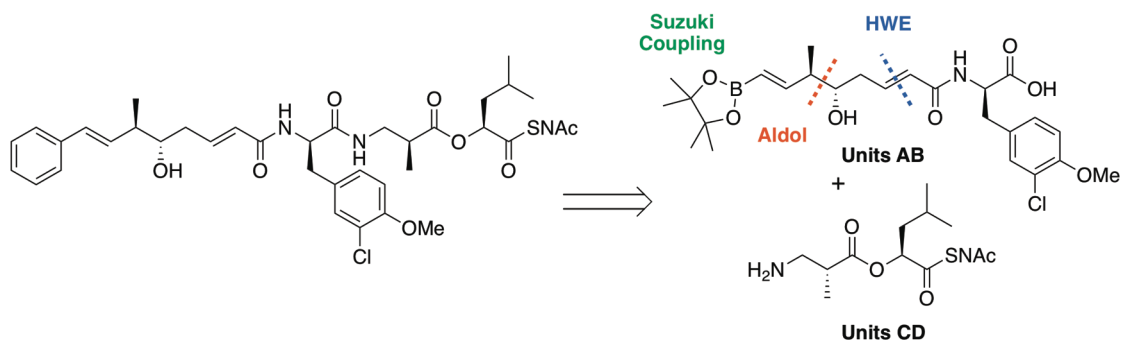
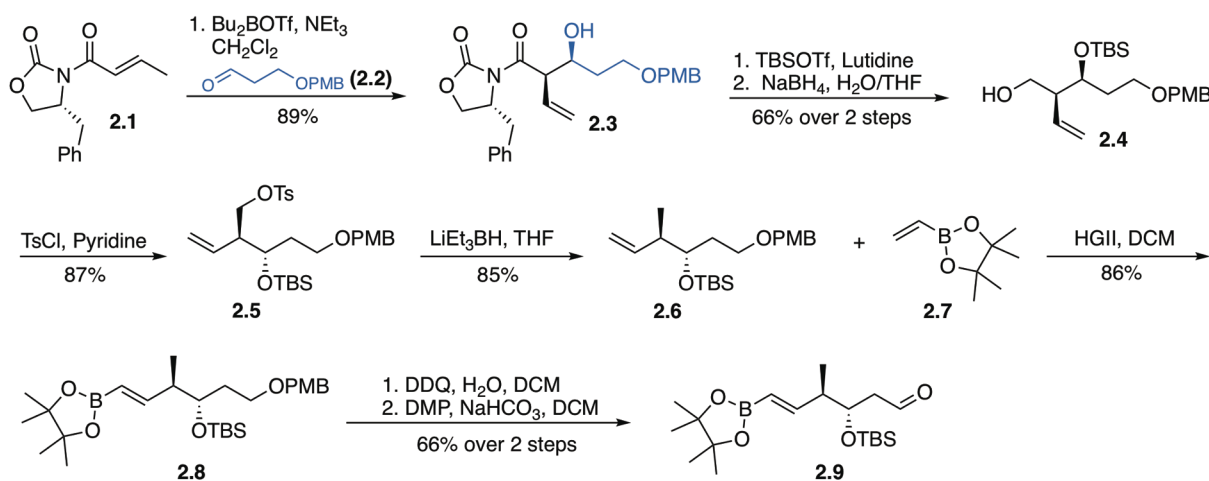


Figure 2.6 Retrosynthetic analysis of *seco* cryptophycin chain elongation intermediate. This highlights the main disconnections including final peptide coupling between Units AB and Units CD, Suzuki coupling for aryl ring diversification, HWE for formulation of Unit AB, and an aldol responsible for setting the C6 and C7 stereocenters.

stereochemistry seen. Units' CD-NAC can be formulated via peptide coupling of commercially available starting materials (**Figure 2.5**).

2.2.1 Synthesis of Cryptophycin Unit AB Fragment

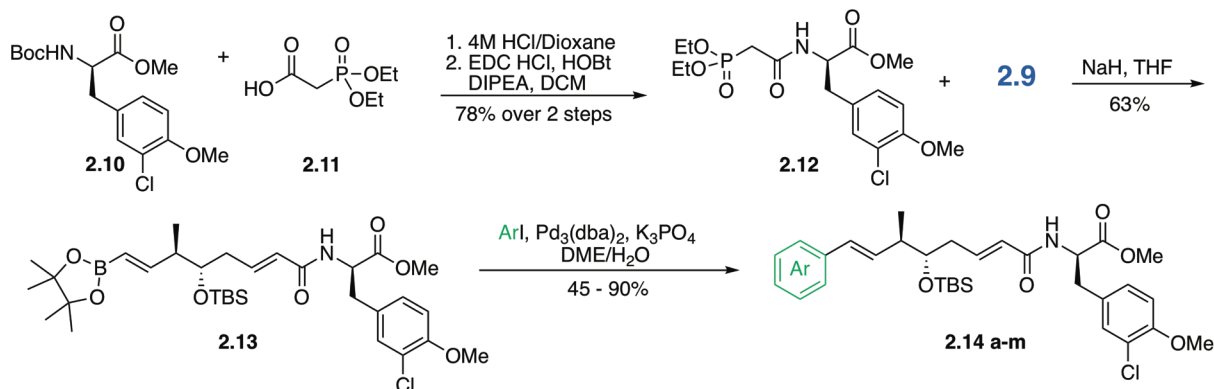
Towards that end, unit A was synthesized using an Evans asymmetric aldol with *N*-crotonyl oxazolidinone **2.1** and aldehyde **2.2**, which proceeded in excellent yields with a high dr (>20:1) to afford the desired (*2R*, *3S*) adduct **2.3**. Subsequent silylation with TBS trifluoromethanesulfonate and reductive cleavage of the chiral auxiliary afforded alcohol **2.4**.³⁹ Tosylation and consecutive reductive deoxygenation was next investigated. Reduction of the corresponding tosylate proved difficult, however a screen of reducing reagents saw the best results with lithium triethylborohydride which produced the desired intermediate **2.6** in 85% yield.⁶² At



Scheme 2.1 Synthesis of unit A. Formation of unit A **18** from crotonyl alkylated Evans auxiliary **9**, incorporating the use of a pinacol boronic ester for use as a Suzuki handle in late stage diversification.

this stage a pinacol boronic ester (**2.7**) was introduced via Hoveyda-Grubbs cross metathesis for use as a Suzuki handle for later diversification.⁶¹ Removal of the PMB protecting group of **2.8** with DDQ and subsequent Des Martin Periodinane (DMP) oxidation to **2.9** furnished the unit A aldehyde fragment necessary for the HWE olefination (**Scheme 2.1**).⁶³

The phosphonate partner **2.12** (**Scheme 2.2**) was synthesized via Boc deprotection of previously described **2.10** with 4 M HCl/Dioxane and subsequent coupling with diethylphosphonoacetic acid (**2.11**) and EDC. From here conditions for the HWE olefination were explored. The best results were seen with sodium hydride in THF, which yielded diversifiable unit



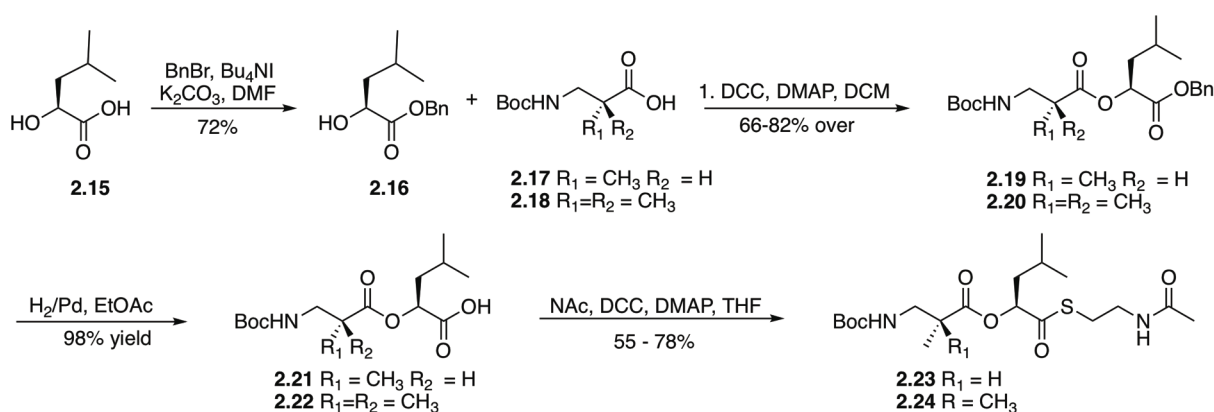
Scheme 2.2 Synthesis of unit AB. Formation of diversifiable units AB **22** from unit A (**18**) and unit B phosphonate adduct (**21**) mediated by a Horner Wadsworth Emmons (HWE) reaction. Successive Suzuki coupling produced the desired unit AB analogues **2.14 a-m**.

AB fragment **2.13** in a 63% yield of the correct isomer (80% overall yield, with ~ 5:1 E:Z product dispersion).

2.2.2 Formulation of Unit CD Fragment

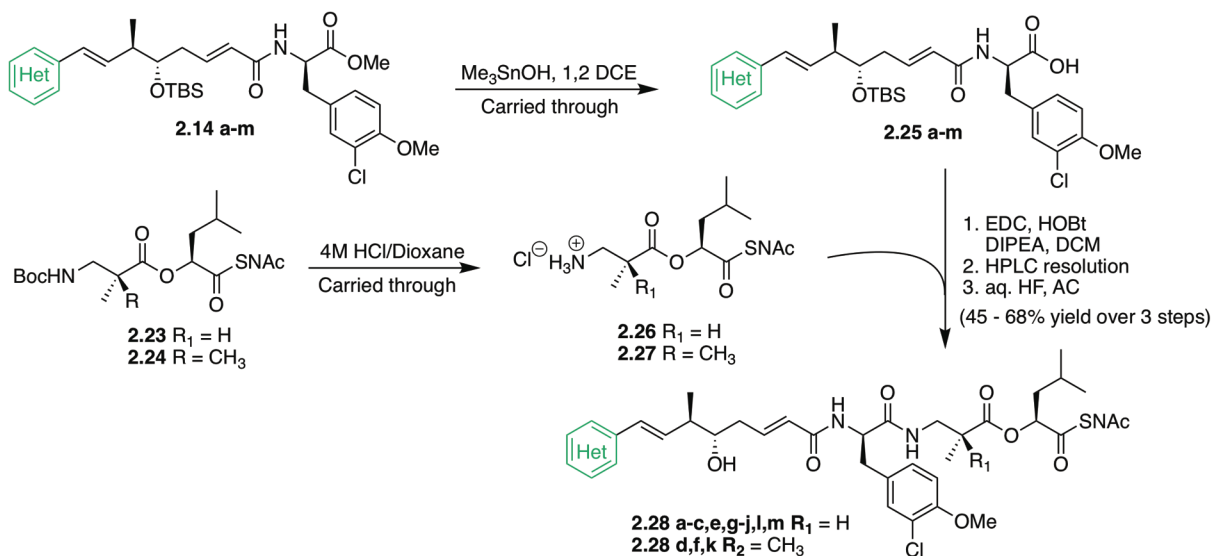
Unit CD-NAc was readily synthesized from commercially available leucic acid **2.15** and methyl- β -alanine **2.17** (Dimethyl unit C **2.18**, see section 2.3.3, Scheme **2.3**). Initial benzyl protection of leucic acid and subsequent coupling with β -amino acids **15** or **16** produced the desired ester, which could be readily deprotected via hydrogenolysis to furnish the desired acids **2.21** or **2.22**.⁶⁴ These were coupled with NAc to yield Units CD.

2.2.3 Assembly of Seco-Cryptophycin Chain Elongation Intermediate and Suzuki Diversification



Scheme 2.3 Synthesis of unit CD. Formation of native unit CD fragment and dimethyl version from leucic acid and either β -homo-alanine or the dimethyl variant **2.18**

With diversifiable substrates **2.13** in hand, coupling with **2.23** and successive Suzuki diversification were investigated. A screen of palladium catalysts as well as bases and solvents yielded no conditions that successfully produced cross coupling in moderate to high yields without racemization or degradation of the NAc thioester. With these results, Suzuki coupling prior to the final peptide coupling was investigated. Another screen of palladium catalysts and solvents yielded Pd₂(dba)₃ with K₃PO₄ in dimethoxy ethane and water at reflux as the highest yielding, however racemization was still observed. By running this at room temperature for 12 hours, racemization was completely abolished and we were able to produce a suite of novel unit AB cryptophycin analogues **2.14 a-m** (**Scheme 2.2**), in moderate to excellent yields (45 – 92%). Successive saponification of the methyl ester to produce **2.25 a-m** (**Scheme 2.4**) also proved to be susceptible to racemization and a screen of different hydrolysis procedures yielded trimethyl tin hydroxide that provided the desired acids in good yield with no detectable racemization. Subsequent peptide coupling on ice produced the TBS protected intermediates with an 8:1 dr (**Scheme 2.4**).⁶⁵⁻⁶⁶ Diastereomers were resolved using reverse phase HPLC in order to obtain CrpTE data for the native diastereomer only. Finally, deprotection of the silyl group using aqueous HF furnished the desired *seco* cryptophycin NAc analogues (**Scheme 2.4, 2.28 a-m**).



Scheme 2.4 Assembly of the *seco* cryptophycin analogues. unit AB fragments (**2.14 a-m**) and unit CD fragment (**2.23** or **2.24**) fragments were simultaneously deprotected and carried through to EDC coupling without purification. Diastereomers were separated by reverse phase HPLC prior to deprotection with HF.

2.3 Optimization and Evaluation of *seco* cryptophycin analogues with CrpTE biocatalyst

2.3.1 Analytical Scale Evaluation of the CrpTE with *Seco* Analogues

With a diversifiable synthesis in hand we began exploring the flexibility of CrpTE against the heterocyclic unit A chain elongation intermediates (**Scheme 2.4**, **2.28 a-m**). Initially, enzymatic conditions were optimized using the native, benzyl containing intermediate. Initial screens utilized the standard 5% DMSO to look at different concentrations of substrate and using an arbitrary 0.5 μM of CrpTE catalyst. Screening conditions from 10 μM to 500 μM substrate concentration at 3 different temperatures showed that these enzymes are much more efficient at elevated temperatures (30 $^{\circ}\text{C}$ or 37 $^{\circ}\text{C}$) and need to be at lower concentrations. This is likely because of the inherent insolubility of the substrates in the reaction media, leading to enzyme inaccessibility. In order to keep reaction volumes to the minimum, and to minimize the variability seen in the 37 $^{\circ}\text{C}$ reactions, 30 $^{\circ}\text{C}$ and 50 μM was chosen as the optimal substrate concentration for analysis (**Figure 2.7**).

The initial set of CrpTE analogues contained six membered ring heterocycles in place of the native benzene ring (**Figure 2.8**, **2.28 b-g**) were run using the previously optimized conditions. Initial analytical scale reactions revealed remarkable turnover to product compared to the native benzyl substrate (**Figure 2.7, a**). The 2-, 3-, 4-pyridyl and pyrazine (**2.28 b, c, e, g**) substrates

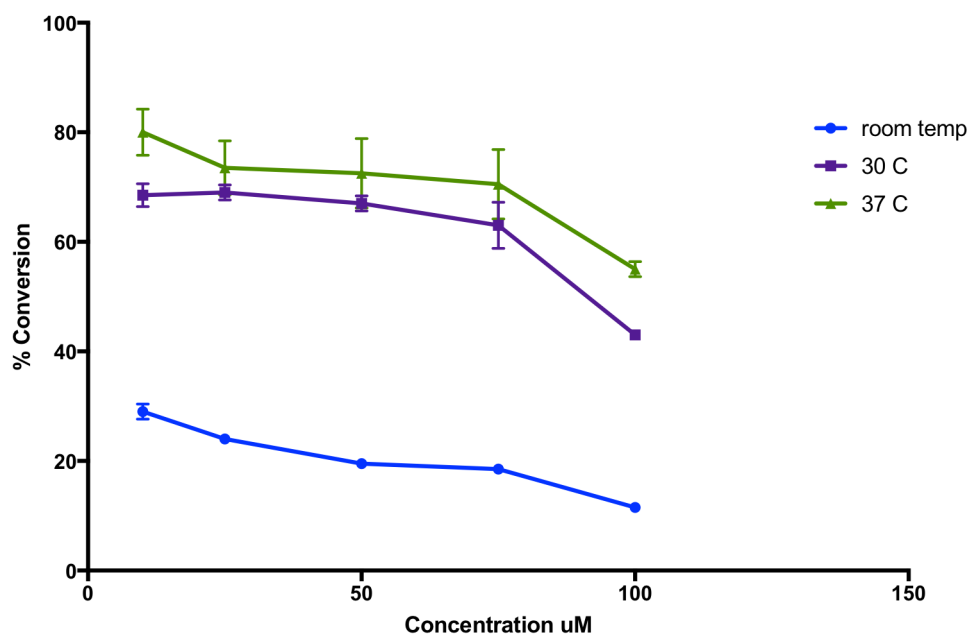


Figure 2.7 Analysis of substrate concentration on % conversion. Conditions include 5% DMSO and 0.5 μM CrpTE.

showed complete turnover of starting material and nearly undetectable levels of hydrolytic bi-products (**Figure 2.8**) in contrast to **2.28a**, which shows incomplete consumption of starting material for an overall conversion of $\sim 68\%$. This is reflected in the % conversion as well as cyclization to hydrolysis ratios (**Table 2.1**), all of which are significantly greater (91 – 96% conversion, $>10:1$ cyclization:hydrolysis ratio) when compared to the native substrate (68% conversion, 9:1 cyclization: hydrolysis). It is unclear if this is due to more favorable interactions in the binding pocket of the CrpTE, reflecting more productive catalysis or if these heterocyclic groups impart improved solubility in the reaction medium making these substrates more accessible to the enzyme.

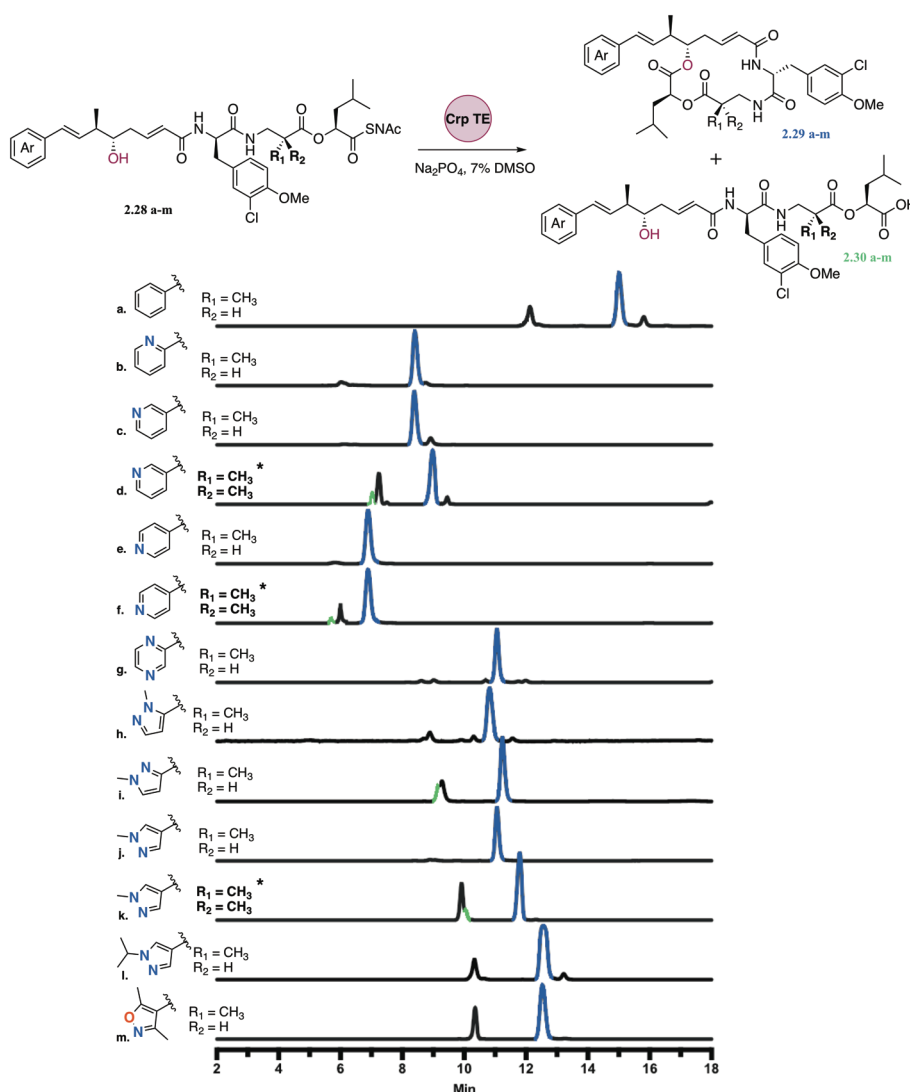


Figure 2.8 QTOF-LCMS analysis of *seco* cryptophycin analogues with the CrpTE, product peaks are denoted in blue color and hydrolysis peaks in green.

The set of unnatural unit A analogues was expanded to include five membered ring aromatic heterocycles with varying alkyl chains. 2-, 3-, and 4-methyl pyrazole (**2.28 h-j**) were formulated and tested in the same analytical assay as previously discussed, utilizing the benzyl substrate as standard. The 2-methyl pyrazole (**2.28 h**) and 3-methyl pyrazole (**2.28 i**) groups showed slightly lower % conversion than the previous six membered rings at 85% and 84% (**Table 2.1**). This decrease in conversion was not attributed to nonproductive catalysis (as the hydrolysis to cyclization ratios are still above those of the native substrate), but to a lack in substrate consumption. Despite these substrates being processed less efficiently than the six membered ring

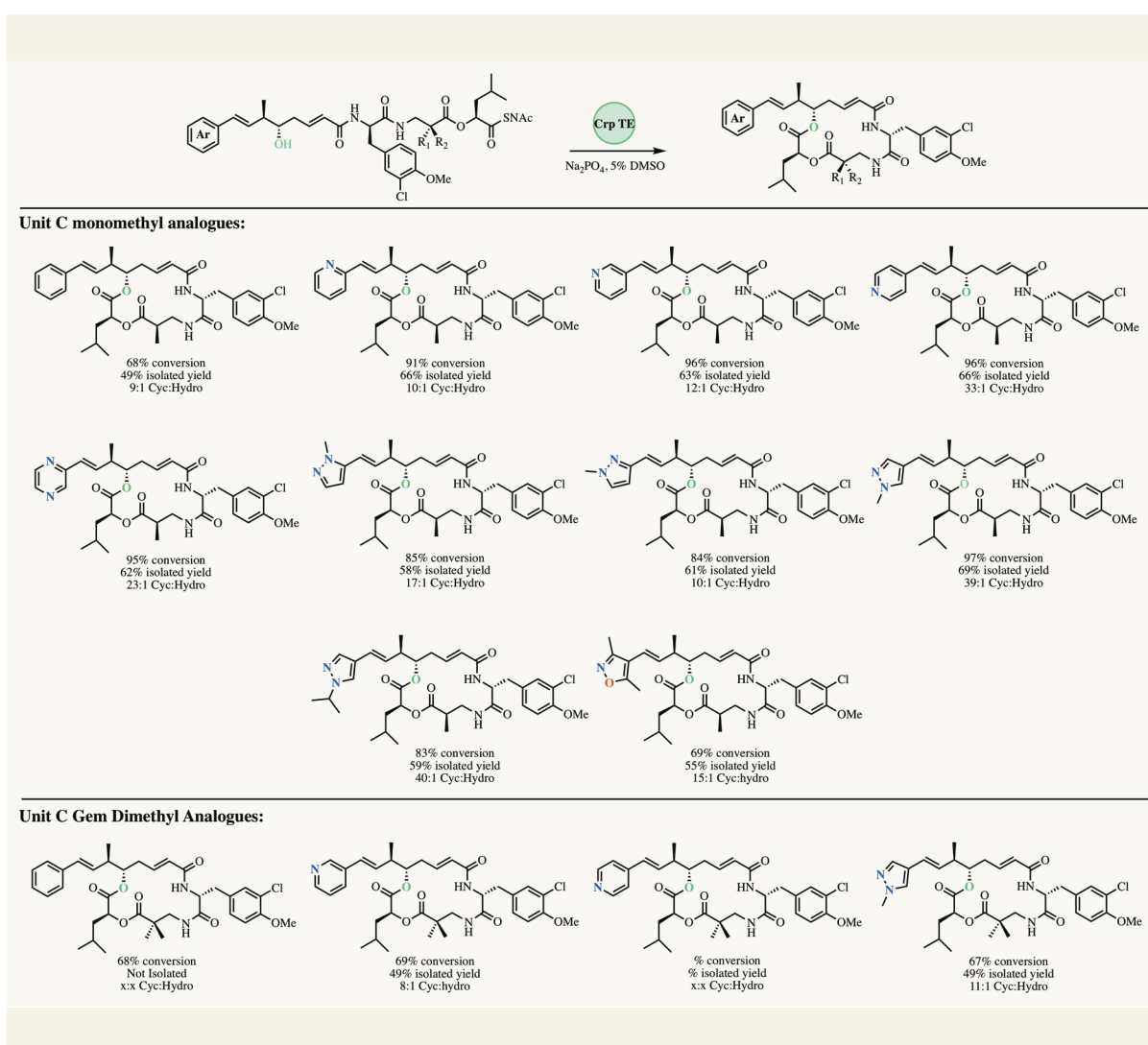


Table 2.1 Comparison of cryptophycin analogues **2.29 a-m** percent conversion, isolation yields, and cyclization to hydrolysis ratio.

analogues, they retain % conversion to product comparable to native substrate reaction catalyzed by wild type CrpTE. Interestingly, the 4-methyl pyrazole (**2.28 j**) showed nearly complete conversion to product with essentially no remaining starting material and no hydrolytic byproducts.

Testing a larger alkyl chain, the 4-isopropyl pyrazole (**2.28 l**) provided important insight into potential size restrictions of the CrpTE binding pocket. Although there is again a very high cyclization:hydrolysis ratio (40:1), starting material remained after conclusion of the reaction (83% conversion), indicating possible steric constraints within the enzyme. Finally, a dimethyl isoxazole substrate was investigated. This substrate showed similar % conversion in comparison with the native substrate (**Figure 2.8**) with a significant amount of starting material remaining.

2.3.2 Semi-Preparative Scale Enzymatic Reactions, Isolation, and Subsequent Biological Evaluation

All reactions were conducted on semi-preparative scale (using the same conditions as the analytical reactions) of 10 mg in order to obtain isolated yields, full structural characterization, and biological evaluation. These results corresponded closely with percent conversions observed in the analytical reactions. The six membered heterocycles **2.29 b, c, e, and f** were isolated in good yields from 62 – 66% (**Table 1**). The five membered rings **2.29 h - 12j, 12i and 12m** were also isolated in yields that span from 55% for the isoxazole analogue to 69% for the 4-methyl pyrazole analogue (**Table 1**). All novel cryptophycin analogues generated from these chemoenzymatic reactions were confirmed by HRMS, ¹HNMR, and ¹³CNMR and subsequently tested for biological activity.

Each of the cryptophycin analogs were assessed for IC₅₀ in HCT-116 human colorectal cancer cell line. Previous studies on synthetic cryptophycin analogues containing a thiophene and a furan in place of the benzyl ring on unit A showed a marked decrease in activity.⁶⁷ Our results (**Table 2**) showed significant differences in activities depending on the heterocyclic ring present. For the six membered rings, the IC₅₀ values spanned a wide range even within the pyridyl set of analogues, varying by three orders of magnitude from the **2.29 c** and **2.29 e** (0.860 nM and 0.51 nM, **Table 2**) to the **2.29 b** (102 nM, **Table 2**). The five membered rings show even larger differences in IC₅₀ values spanning almost six orders of magnitude. The inclusion of an isoxazole ring (**2.29 m**) greatly diminished activity, however, the introduction of a 4-methyl pyrazole ring

(**2.29 j**) provided a low pico-molar IC_{50} , making it one of the most potent cryptophycin analogues observed to date. The potency observed in the 4-methyl pyrazole cryptophycin derivative has only been observed in previously described β -epoxy cryptophycin analogues, which had previously demonstrated the requirement of the epoxide functionality to achieve maximum activity. Here, we have shown that a similar single digit picomolar potency is achievable in the absence of the β -epoxy group. This could have crucial effects on the neurotoxicity observed with these compounds during clinical trials as this moiety has been considered the likely cause of this side-effect.

2.3.3 Formulation of Geminal Dimethyl Unit C variants of Unit A Analogues

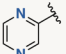
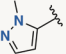
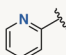
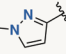
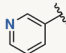
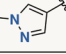
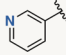
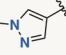
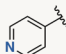
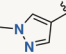
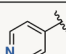
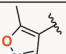
Cryptophycin Analogue IC_{50} Values in HCT-116					
Unit A	Unit C	IC_{50} [nM] HCT - 116	Unit A	Unit C	IC_{50} [nM] HCT - 116
	Crp 52	0.033	g.	 $R_1 = CH_3$ $R_2 = H$	10.2
	Crp 55	0.067	h.	 $R_1 = CH_3$ $R_2 = H$	6.3
b.	 $R_1 = CH_3$ $R_2 = H$	102	i.	 $R_1 = CH_3$ $R_2 = H$	84
c.	 $R_1 = CH_3$ $R_2 = H$	0.86	j.	 $R_1 = CH_3$ $R_2 = H$	0.010
d.	 $R_1 = CH_3$ $R_2 = CH_3$	2.06	k.	 $R_1 = CH_3$ $R_2 = CH_3$	0.94
e.	 $R_1 = CH_3$ $R_2 = H$	0.50	l.	 $R_1 = CH_3$ $R_2 = H$	6.3
f.	 $R_1 = CH_3$ $R_2 = CH_3$	1.16	m.	 $R_1 = CH_3$ $R_2 = H$	1400

Table 2.2 IC_{50} values for unit A heterocyclic analogues in HCT 116 cells.

Utilizing the above data to guide our design of analogues to test with the CrpTE biocatalyst, the geminal dimethyl unit C analogues were synthesized utilizing the same chemistry as above for our top three analogues, the 3- and 4- pyridyl as well as the 4-methyl pyrazole, substituting the dimethyl unit C (**2.18**). The ester linkage between units C and D is thought to be somewhat metabolically labile and addition of a second methyl group adjacent to this labile position is known to improve drug half-lives as well as remove a stereocenter which simplifies the synthesis.^{6, 68} In our previous work we showed an increase in hydrolytic byproducts (6:1 cyclization to hydrolysis versus 10:1) when including the gem dimethyl in the benzyl containing unit A.⁵⁹ Our new

analogues (**2.28 d, f, and k**) were first tested on an analytical scale for a direct comparison of hydrolysis to cyclization ratios as well as % conversion to their monomethyl counterparts. All three showed an increase in hydrolytic activity when incubated with CrpTE (**Table 2.1** and **Figure 2.8**) as well as a higher percentage of unreacted starting material, consistent with our previous findings. Despite the lower overall processing to macrocycle, the corresponding chain elongation intermediates were processed with almost the same efficiency as the native substrate, further demonstrating the remarkable flexibility of CrpTE against substrates containing non-native functional groups in both the PKS and NRPS derived portions of the molecule.

2.4 Evaluation of Cryptophycin P450 with Unit A Analogues

2.4.1 Cytochrome P450 Background

Cytochromes P450 have been used extensively in the pharmaceutical industry for the production of drug molecules as they are capable of regio- and stereo-selectively installing oxidative functionality often replacing otherwise inactivated C-H bonds. P450s are iron-heme containing enzymes capable of utilizing molecular oxygen to formulate the oxygenated organic compound and water via a two electron transfer mechanism mediated by NAD(P)H. The catalytic mechanism, which has been reviewed extensively,⁶⁹⁻⁷⁰ starts with ferrous iron (Fe^{II}), generated by a single electron transfer, and the binding of O_2 . A second electron transfer event generates the peroxy intermediate which can then be protonated to generate compound 0 (**Figure 2.9**). Compound 0 then rapidly undergoes heterolytic cleavage to produce compound 1, water, and an Fe^{IV} radical species known as compound 1. This is then able to abstract a hydrogen atom from the correctly oriented substrate, leading to a radical rebound that produces the hydroxylated species (**Figure 2.9**). In this catalytic process, there are three separate possible shunt pathways including autoxidation shunt, the peroxide shunt, and the oxidase shunt pathway all of which cause ineffective catalysis.

The cryptophycin pathway contains a late stage P450 that is responsible for the installation of the β epoxy functionality that imparts 100 to 1000 times greater potency to the styrene counterparts. Historically, this has been incredibly difficult to install both regio- and stereo-selectively as only a couple of catalytic systems exist to execute this transformation, many of which having only modest selectivity for the β epoxide over the α . Initial synthetic methods utilized *m*-

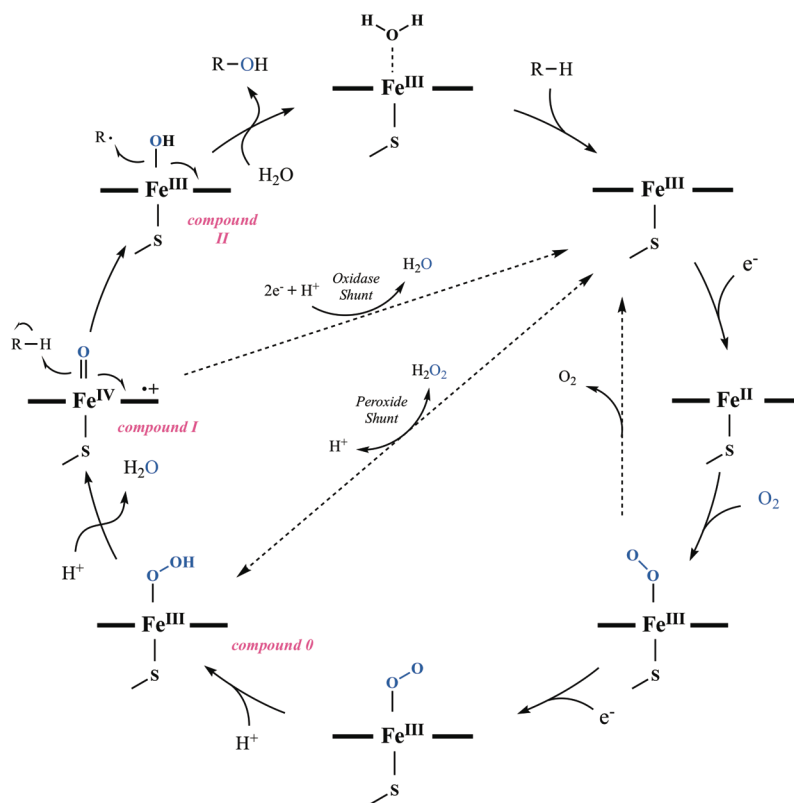


Figure 2.9 P450 catalytic cycle; O₂ is utilized along with a two electron transfer, mediated by NAD(P)H to produce the desired hydroxylated species.

Chloroperoxybenzoic acid however the yields were only moderate as the selectivity seen with this method was at most 2.5:1 β : α isomer.⁷¹ Other strategies have utilized dimethyldioxirane (DMDO)⁴⁶ however these usually didn't increase the diastereomeric ratio or Shi conditions⁷² which only produced a 17% conversion due to low solubility in the aqueous reaction conditions. Diol epoxidations have also been utilized and took advantage of a modified sharpless epoxidation strategy that gave the desired β epoxide from the diol in 3 steps with a 38% overall yield.⁷³ Despite some success installing this functionality, the use of a P450 to facilitate this process could have profound implications for the formulation of the most active compounds.

Previously, Dr. Yousong Ding cloned and expressed the MBP fusion of CrpE as soluble protein. As the native redox partners for this protein was unknown, spinach ferredoxin (Fdx) and ferredoxin NADP⁺ reductase (Fdr) along with the glucose-6-phosphate NADPH regeneration system were utilized to recapitulate the P450 activity and show ~45% conversion of cryptophycin 3 to cryptophycin 1. This was further extended to show that the P450 was tolerant of structural

variations on unit B and C indicating this P450 could be used as a biocatalyst for the production of epoxidized cryptophycin analogues.⁵⁶

2.4.2 Evaluation of P450 with unit A heterocyclic analogues

With successful implementation of the CrpTE as a biocatalyst for the production of novel cryptophycin analogues, we turned to investigating the use of the CrpE P450 to generate fully functionalized, β epoxy cryptophycins. With the help of Dr. Yogan Khatri, the CrpE was re-cloned into His tag containing pET-17b as the MBP fusion was not ideal due to its large size. This was then expressed in TB media, with extensive oxygenation. Purification yielded bright red protein which, when combined with the Fdx/Fdr NADPH system, again showed $\sim 45\%$ turnover of styrene

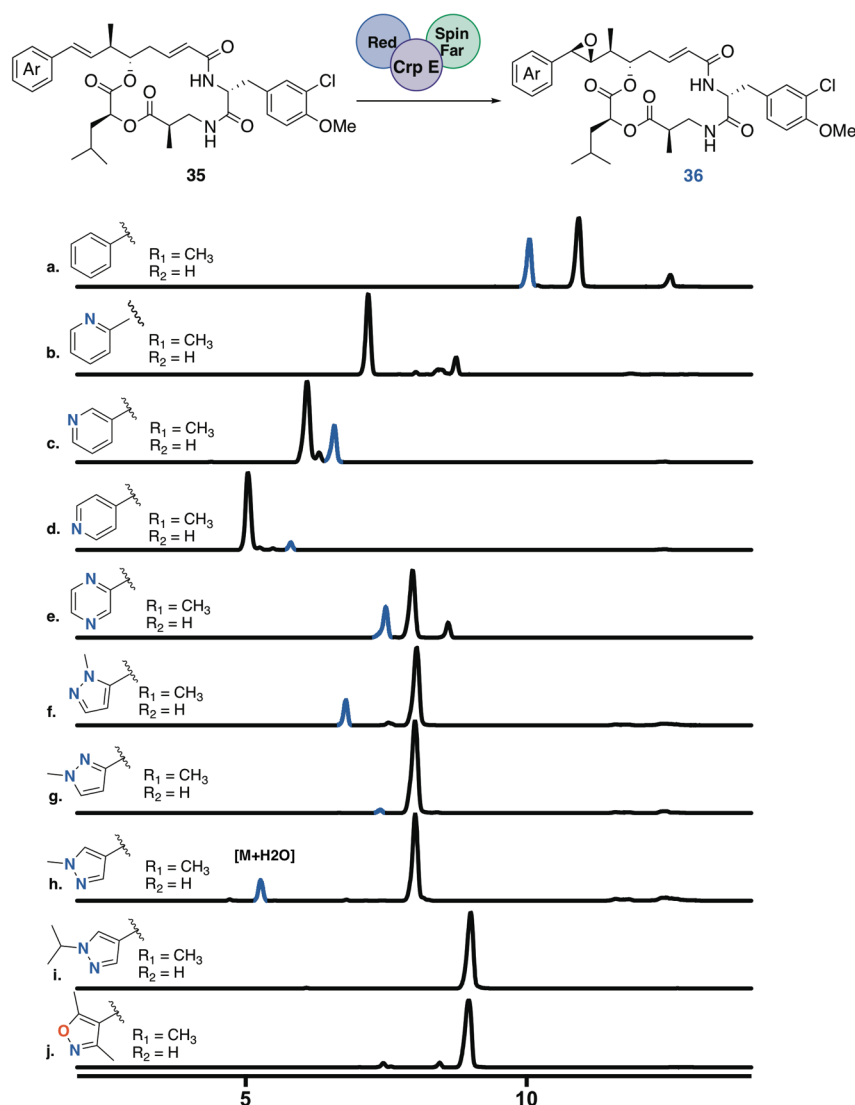


Figure 2.10 Analysis of CrpE P450 with styrene cryptophycin analogues. Epoxidized products observed by mass are in blue.

cryptophycin 3 to epoxidated cryptophycin 1 (**Figure 2.10**). Interestingly, experimentation with another redox partner commonly used in the lab, RhFRED produced no turnover to product indicating the importance of an appropriate redox partner. With the CrpE activity reconfirmed, the newly generated, unit A analogues were assayed with the CrpE.

Initial analytical tests were run and analyzed by TOF-MS, showing varying results. Turnover to a product that corresponds to the epoxidized mass is observed with the 3-pyridyl, 4 pyridyl, pyrazine, and 2 methyl pyrazole cryptophycins (**Figure 2.10**, peaks corresponding to product by MS in blue). The most potent analogue from the previous section, the 4 methyl pyrazole shows a mass indicative of the dihydroxylated species which has been seen before with extremely electron withdrawing aryl substituents. The rest of the analogues produced no detectable product formation. Although the initial results are not as exciting as with the CrpTE, seeing turnover to epoxidized products on these was surprising, as aryl ring modifications are conjugated into the double bond, causing the electronics of it to change significantly from analogue to analogue, likely causing the decrease or lack of product production.

In order to utilize this enzyme along with our CrpTE for the effective production of epoxidized cryptophycins, continued optimization and exploration of reaction conditions needs to be examined. The native substrate only shows ~45% turnover to product which isn't optimal. It is currently unclear if this is caused by instability in the protein or another factor. This protein begins to precipitate out of the reaction mixture within a few hours which may not be enough time to effect total turnover of substrate indicating dosing schedules should be investigated for better consumption of starting material. Another potential problem is that spinach ferredoxin is being used as a surrogate redox partner, because the native one is currently unknown. This system may not be as adept at electron transfer as the native partners would be causing decreases in turnover. Continued exploration of surrogate redox partners or a screening campaign of the seven potential redox partners found within the producing organism's genome may lead to better turnover and more effective production of products.

2.5 References

1. Schwartz, R. E.; Hirsch, C. F.; Sesin, D. F.; Flor, J. E.; Chartrain, M.; Fromtling, R. E.; Harris, G. H.; Salvatore, M. J.; Liesch, J. M.; Yudin, K., Pharmaceuticals from Cultured Algae. *J Ind Microbiol* **1990**, *5* (2-3), 113-123.
2. Smith, C. D.; Zhang, X. Q.; Mooberry, S. L.; Patterson, G. M. L.; Moore, R. E., Cryptophycin - a New Antimicrotubule Agent Active against Drug-Resistant Cells. *Cancer Res* **1994**, *54* (14), 3779-3784.
3. Burja, A. M.; Banaigs, B.; Abou-Mansour, E.; Burgess, J. G.; Wright, P. C., Marine cyanobacteria - a prolific source of natural products. *Tetrahedron* **2001**, *57* (46), 9347-9377.
4. Chaganty, S.; Golakoti, T.; Heltzel, C.; Moore, R. E.; Yoshida, W. Y., Isolation and structure determination of cryptophycins 38, 326, and 327 from the terrestrial cyanobacterium *Nostoc* sp GSV 224. *Journal of natural products* **2004**, *67* (8), 1403-1406.
5. Subbaraju, G. V.; Golakoti, T.; Patterson, G. M. L.; Moore, R. E., Three new cryptophycins from *Nostoc* sp. GSV 224. *Journal of natural products* **1997**, *60* (3), 302-305.
6. Golakoti, T.; Ogino, J.; Heltzel, C. E.; LeHusebo, T.; Jensen, C. M.; Larsen, L. K.; Patterson, G. M. L.; Moore, R. E.; Mooberry, S. L.; Corbett, T. H.; Valeriote, F. A., Structure determination, conformational analysis, chemical stability studies, and antitumor evaluation of the cryptophycins. Isolation of 18 new analogs from *Nostoc* sp strain GSV 224 (vol 117, pg 12030, 1995). *J Am Chem Soc* **1996**, *118* (13), 3323-3323.
7. Corbett, T. H.; Valeriote, F. A.; Demchik, L.; Lowichik, N.; Polin, L.; Panchapor, C.; Pugh, S.; White, K.; Kushner, J.; Rake, J.; Wentland, M.; Golakoti, T.; Hetzel, C.; Ogino, J.; Patterson, G.; Moore, R., Discovery of cryptophycin-1 and BCN-183577: Examples of strategies and problems in the detection of antitumor activity in mice. *Investigational new drugs* **1997**, *15* (3), 207-218.
8. Jordan, A.; Hadfield, J. A.; Lawrence, N. J.; McGown, A. T., Tubulin as a target for anticancer drugs: Agents which interact with the mitotic spindle. *Medicinal research reviews* **1998**, *18* (4), 259-296.
9. Jordan, M. A.; Wilson, L., Microtubules as a target for anticancer drugs. *Nat Rev Cancer* **2004**, *4* (4), 253-265.
10. Prota, A. E.; Danel, F.; Bachmann, F.; Bargsten, K.; Buey, R. M.; Pohlmann, J.; Reinelt, S.; Lane, H.; Steinmetz, M. O., The Novel Microtubule-Destabilizing Drug BAL27862 Binds to the Colchicine Site of Tubulin with Distinct Effects on Microtubule Organization. *J Mol Biol* **2014**, *426* (8), 1848-1860.
11. Gigant, B.; Wang, C. G.; Ravelli, R. B. G.; Roussi, F.; Steinmetz, M. O.; Curmi, P. A.; Sobel, A.; Knossow, M., Structural basis for the regulation of tubulin by vinblastine. *Nature* **2005**, *435* (7041), 519-522.
12. Nettles, J. H.; Li, H. L.; Cornett, B.; Krahn, J. M.; Snyder, J. P.; Downing, K. H., The binding mode of epothilone A on alpha,beta-tubulin by electron crystallography. *Science* **2004**, *305* (5685), 866-869.
13. Nogales, E.; Wolf, S. G.; Downing, K. H., Structure of the alpha beta tubulin dimer by electron crystallography. *Nature* **1998**, *391* (6663), 199-203.
14. Eissler, S.; Stoncius, A.; Nahrwold, M.; Sewald, N., The synthesis of cryptophycins. *Synthesis-Stuttgart* **2006**, (22), 3747-3789.

15. Panda, D.; DeLuca, K.; Williams, D.; Jordan, M. A.; Wilson, L., Antiproliferative mechanism of action of cryptophycin-52: Kinetic stabilization of microtubule dynamics by high-affinity binding to microtubule ends. *P Natl Acad Sci USA* **1998**, *95* (16), 9313-9318.
16. Panda, D.; Himes, R. H.; Moore, R. E.; Wilson, L.; Jordan, M. A., Mechanism of action of the unusually potent microtubule inhibitor cryptophycin 1. *Biochemistry-Us* **1997**, *36* (42), 12948-12953.
17. Mooberry, S. L.; Busquets, L.; Tien, G., Induction of apoptosis by cryptophycin 1, a new antimicrotubule agent. *Int J Cancer* **1997**, *73* (3), 440-448.
18. Smith, C. D.; Zhang, X. Q., Mechanism of action of cryptophycin - Interaction with the Vinca alkaloid domain of tubulin. *Journal of Biological Chemistry* **1996**, *271* (11), 6192-6198.
19. Mooberry, S. L.; Taoka, C. R.; Busquets, L., Cryptophycin 1 binds to tubulin at a site distinct from the colchicine binding site and at a site that may overlap the vinca binding site. *Cancer Lett* **1996**, *107* (1), 53-57.
20. Kerksiek, K.; Mejillano, M. R.; Schwartz, R. E.; George, G. I.; Himes, R. H., Interaction of cryptophycin 1 with tubulin and microtubules. *Febs Lett* **1995**, *377* (1), 59-61.
21. Bai, R. L.; Schwartz, R. E.; Kepler, J. A.; Pettit, G. R.; Hamel, E., Characterization of the interaction of cryptophycin 1 with tubulin: Binding in the Vinca domain, competitive inhibition of dolastatin 10 binding, and an unusual aggregation reaction. *Cancer Res* **1996**, *56* (19), 4398-4406.
22. Mitra, A.; Sept, D., Localization of the antimitotic peptide and depsipeptide binding site on beta-tubulin. *Biochemistry-Us* **2004**, *43* (44), 13955-62.
23. deMuys, J. M.; Rej, R.; Nguyen, D.; Go, B.; Fortin, S.; Lavallee, J. F., Synthesis and in vitro cytotoxicity of cryptophycins and related analogs. *Bioorg Med Chem Lett* **1996**, *6* (10), 1111-1116.
24. Panda, D.; Ananthnarayan, V.; Larson, G.; Shih, C.; Jordan, M. A.; Wilson, L., Interaction of the antitumor compound cryptophycin-52 with tubulin. *Biochemistry-Us* **2000**, *39* (46), 14121-7.
25. Norman, B. H.; Hemscheidt, T.; Schultz, R. M.; Andis, S. L., Total synthesis of cryptophycin analogues. Isosteric replacement of the C-D ester. *J Org Chem* **1998**, *63* (15), 5288-5294.
26. Dhokte, U. P.; Khau, V. V.; Hutchison, D. R.; Martinelli, M. J., A novel approach for total synthesis of cryptophycins via asymmetric crotylboration protocol. *Tetrahedron Lett* **1998**, *39* (48), 8771-8774.
27. Ali, S. M.; Himes, R. H.; Stella, V. J.; Georg, G. I., Cryptophycin halohydrins: Synthesis, biological evaluation, and stability studies. *Abstr Pap Am Chem S* **1998**, *215*, U913-U913.
28. Al-Awar, R. S.; Shih, C.; Ray, J. E.; Gossett, L. S.; Gruber, J. M.; Grossman, C. S.; Schultz, R.; Andis, S.; Worzalla, J.; Kennedy, J.; Corbett, T., The synthesis and evaluation of novel cryptophycin analogues. *Ann Oncol* **1998**, *9*, 90-90.
29. Barrow, R. A.; Moore, R. E.; Li, L. H.; Tius, M. A., Synthesis of 1-aza-cryptophycin 1, an unstable cryptophycin. An unusual skeletal rearrangement. *Tetrahedron* **2000**, *56* (21), 3339-3351.
30. Varie, D. L.; Shih, C.; Hay, D. A.; Andis, S. L.; Corbett, T. H.; Gossett, L. S.; Janisse, S. K.; Martinelli, M. J.; Moher, E. D.; Schultz, R. M.; Toth, J. E., Synthesis and biological evaluation of cryptophycin analogs with substitution at C-6 (fragment C region). *Bioorg Med Chem Lett* **1999**, *9* (3), 369-374.
31. Shih, C.; Gossett, L. S.; Gruber, J. M.; Grossman, C. S.; Andis, S. L.; Schultz, R. M.; Worzalla, J. F.; Corbett, T. H.; Metz, J. T., Synthesis and biological evaluation of novel

- cryptophycin analogs with modification in the beta-alanine region. *Bioorg Med Chem Lett* **1999**, *9* (1), 69-74.
32. Leahy, J. W.; Gardinier, K. M., Synthesis of potent new analogs of cryptophycin. *Abstr Pap Am Chem S* **1999**, 218, U53-U53.
33. Mezrai, A.; Drici, W.; Lesur, D.; Mulengi, J. K.; Wadouachi, A.; Pilard, F., The Synthesis of an Aziridinyl Analogue of Unit A of Cryptophycin-1. *Lett Org Chem* **2014**, *11* (4), 259-267.
34. Weiss, C.; Bogner, T.; Sammet, B.; Sewald, N., Total synthesis and biological evaluation of fluorinated cryptophycins. *Beilstein journal of organic chemistry* **2012**, *8*, 2060-6.
35. Sammet, B.; Bogner, T.; Nahrwold, M.; Weiss, C.; Sewald, N., Approaches for the Synthesis of Functionalized Cryptophycins. *J Org Chem* **2010**, *75* (20), 6953-6960.
36. Liu, W. L.; Zhang, J. C.; Jiang, F. Q.; Fu, L., Synthesis and cytotoxicity studies of new cryptophycin analogues. *Archiv der Pharmazie* **2009**, *342* (10), 577-83.
37. Eissler, S.; Neumann, B.; Stammeler, H. G.; Sewald, N., Synthetic routes towards cryptophycin unit A diastereomers. *Synlett* **2008**, (2), 273-277.
38. White, J. D.; Smits, H.; Hamel, E., Synthesis of cryptothilone 1, the first cryptophycin-epothilone hybrid. *Org Lett* **2006**, *8* (18), 3947-50.
39. Kotoku, N.; Kato, T.; Narumi, F.; Ohtani, E.; Kamada, S.; Aoki, S.; Okada, N.; Nakagawa, S.; Kobayashi, M., Synthesis of 15,20-triamide analogue with polar substituent on the phenyl ring of arenastatin A, an extremely potent cytotoxic spongean depsipeptide. *Bioorgan Med Chem* **2006**, *14* (22), 7446-7457.
40. Murakami, N.; Tamura, S.; Koyama, K.; Sugimoto, M.; Maekawa, R.; Kobayashi, M., New analogue of arenastatin A, a potent cytotoxic spongean depsipeptide, with anti-tumor activity. *Bioorg Med Chem Lett* **2004**, *14* (10), 2597-2601.
41. Buck, S. B.; Huff, J. K.; Himes, R. H.; Georg, G. I., Total synthesis and anti-tubulin activity of epi-c3 analogues of cryptophycin-24. *Journal of medicinal chemistry* **2004**, *47* (14), 3697-9.
42. Buck, S. B.; Huff, J. K.; Himes, R. H.; Georg, G. I., Total synthesis and antitubulin activity of c10 analogues of cryptophycin-24. *Journal of medicinal chemistry* **2004**, *47* (3), 696-702.
43. Li, Q.; Woods, K. W.; Claiborne, A.; Gwaltney, S. L.; Barr, K. J.; Liu, G.; Gehrke, L.; Credo, R. B.; Hui, Y. H.; Lee, J.; Warner, R. B.; Kovar, P.; Nukkala, M. A.; Zielinski, N. A.; Tahir, S. K.; Fitzgerald, M.; Kim, K. H.; Marsh, K.; Frost, D.; Ng, S. C.; Rosenberg, S.; Sham, H. L., Synthesis and biological evaluation of 2-indolyloxazolines as a new class of tubulin polymerization inhibitors. Discovery of A-289099 as an orally active antitumor agent. *Bioorg Med Chem Lett* **2002**, *12* (3), 465-469.
44. Eggen, M.; Georg, G. I., The cryptophycins: their synthesis and anticancer activity. *Medicinal research reviews* **2002**, *22* (2), 85-101.
45. Patel, V. F.; Andis, S. L.; Kennedy, J. H.; Ray, J. E.; Schultz, R. M., Novel cryptophycin antitumor agents: Synthesis and cytotoxicity of fragment "B" analogues. *Journal of medicinal chemistry* **1999**, *42* (14), 2588-2603.
46. Kobayashi, M.; Wang, W. Q.; Ohyabu, N.; Kurosu, M.; Kitagawa, I., Improved Total Synthesis and Structure-Activity Relationship of Arenastatin-a, a Potent Cytotoxic Spongean Depsipeptide. *Chem Pharm Bull* **1995**, *43* (9), 1598-1600.
47. Kobayashi, M.; Kurosu, M.; Ohyabu, N.; Wang, W. Q.; Fujii, S.; Kitagawa, I., The Absolute Stereostructure of Arenastatin-a, a Potent Cytotoxic Depsipeptide from the Okinawan Marine Sponge Dysidea-Arenaria. *Chem Pharm Bull* **1994**, *42* (10), 2196-2198.

48. Edelman, M. J.; Gandara, D. R.; Hausner, P.; Israel, V.; Thornton, D.; DeSanto, J.; Doyle, L. A., Phase 2 study of cryptophycin 52 (LY355703) in patients previously treated with platinum based chemotherapy for advanced non-small cell lung cancer. *Lung cancer* **2003**, *39* (2), 197-9.
49. Sessa, C.; Weigang-Kohler, K.; Pagani, O.; Greim, G.; Mora, O.; De Pas, T.; Burgess, M.; Weimer, I.; Johnson, R., Phase I and pharmacological studies of the cryptophycin analogue LY355703 administered on a single intermittent or weekly schedule. *European journal of cancer* **2002**, *38* (18), 2388-2396.
50. D'Agostino, G.; del Campo, J.; Mellado, B.; Izquierdo, M. A.; Minarik, T.; Cirri, L.; Marini, L.; Perez-Gracia, J. L.; Scambia, G., A multicenter phase II study of the cryptophycin analog LY355703 in patients with platinum-resistant ovarian cancer. *International journal of gynecological cancer : official journal of the International Gynecological Cancer Society* **2006**, *16* (1), 71-6.
51. Bigot, A.; Bouchard, H.; Brun, M.-P.; Clerc, F.; Zhang, J. Novel Cryptophycin Compounds and Conjugates, Their Preparation and Their Therapeutic Use. WO2017076998 (A1), 2017/05/11/, 2017.
52. Bouchard, H.; Brun, M.-P.; Commercon, A.; Zhang, J. Novel Conjugates, Preparation Thereof, and Therapeutic Use Thereof. WO2011001052 (A1), 2011/01/06/, 2011.
53. Verma, V. A.; Pillow, T. H.; DePalatis, L.; Li, G.; Phillips, G. L.; Polson, A. G.; Raab, H. E.; Spencer, S.; Zheng, B., The cryptophycins as potent payloads for antibody drug conjugates. *Bioorg Med Chem Lett* **2015**, *25* (4), 864-868.
54. Jones, A. C.; Monroe, E. A.; Eisman, E. B.; Gerwick, L.; Sherman, D. H.; Gerwick, W. H., The unique mechanistic transformations involved in the biosynthesis of modular natural products from marine cyanobacteria. *Natural Product Reports* **2010**, *27* (7), 1048-1065.
55. Magarvey, N. A.; Beck, Z. Q.; Golakoti, T.; Ding, Y.; Huber, U.; Hemscheidt, T. K.; Abelson, D.; Moore, R. E.; Sherman, D. H., Biosynthetic characterization and chemoenzymatic assembly of the cryptophycins. Potent anticancer agents from cyanobionts. *ACS chemical biology* **2006**, *1* (12), 766-79.
56. Ding, Y.; Seufert, W. H.; Beck, Z. Q.; Sherman, D. H., Analysis of the cryptophycin P450 epoxidase reveals substrate tolerance and cooperativity. *J Am Chem Soc* **2008**, *130* (16), 5492-5498.
57. Kohli, R. M.; Walsh, C. T., Enzymology of acyl chain macrocyclization in natural product biosynthesis. *Chem Commun (Camb)* **2003**, (3), 297-307.
58. Horsman, M. E.; Hari, T. P.; Boddy, C. N., Polyketide synthase and non-ribosomal peptide synthetase thioesterase selectivity: logic gate or a victim of fate? *Nat Prod Rep* **2016**, *33* (2), 183-202.
59. Beck, Z. Q.; Aldrich, C. C.; Magarvey, N. A.; Georg, G. I.; Sherman, D. H., Chemoenzymatic synthesis of cryptophycin/arenastatin natural products. *Biochemistry-Us* **2005**, *44* (41), 13457-13466.
60. Ding, Y.; Rath, C. M.; Bolduc, K. L.; Hakansson, K.; Sherman, D. H., Chemoenzymatic synthesis of cryptophycin anticancer agents by an ester bond-forming non-ribosomal peptide synthetase module. *J Am Chem Soc* **2011**, *133* (37), 14492-5.
61. Bolduc, K. L.; Larsen, S. D.; Sherman, D. H., Efficient, divergent synthesis of cryptophycin unit A analogues. *Chem Commun (Camb)* **2012**.
62. Krishnamurthy, S., Rapid Reduction of Alkyl Tosylates with Lithium Triethylborohydride - Convenient and Advantageous Procedure for Deoxygenation of Simple and Hindered Alcohols - Comparison of Various Hydride Reagents. *J Organomet Chem* **1978**, *156* (1), 171-181.

63. Ghosh, A. K.; Swanson, L., Enantioselective synthesis of (+)-cryptophycin 52 (LY355703), a potent antimitotic antitumor agent. *J Org Chem* **2003**, *68* (25), 9823-6.
64. Mast, C. A.; Eissler, S.; Stoncius, A.; Stammler, H. G.; Neumann, B.; Sewald, N., Efficient and versatile stereoselective synthesis of cryptophycins. *Chemistry* **2005**, *11* (16), 4667-77.
65. Ramu, V. G.; Bardaji, E.; Heras, M., DEPBT as Coupling Reagent To Avoid Racemization in a Solution-Phase Synthesis of a Kyotorphin Derivative. *Synthesis-Stuttgart* **2014**, *46* (11), 1481-1486.
66. Nicolaou, K. C.; Estrada, A. A.; Zak, M.; Lee, S. H.; Safina, B. S., A mild and selective method for the hydrolysis of esters with trimethyltin hydroxide. *Angew Chem Int Edit* **2005**, *44* (9), 1378-1382.
67. Moore, R. E.; Tius, M. A.; Barrow, R. A.; Liang, J.; Corbett, T. H.; Valeriotte, F. A.; Hemscheidt, T. K. Isolation, characterization, and synthesis of new cryptophycin compounds as anticancer agents. WO9640184A1, 1996.
68. Wagner, M. M.; Paul, D. C.; Shih, C.; Jordan, M. A.; Wilson, L.; Williams, D. C., In vitro pharmacology of cryptophycin 52 (LY355703) in human tumor cell lines. *Cancer chemotherapy and pharmacology* **1999**, *43* (2), 115-125.
69. de Montellano, P. R. O., Hydrocarbon Hydroxylation by Cytochrome P450 Enzymes. *Chem Rev* **2010**, *110* (2), 932-948.
70. Meunier, B.; de Visser, S. P.; Shaik, S., Mechanism of oxidation reactions catalyzed by cytochrome P450 enzymes. *Chem Rev* **2004**, *104* (9), 3947-3980.
71. Barrow, R. A.; Hemscheidt, T.; Liang, J.; Paik, S.; Moore, R. E.; Tius, M. A., Total Synthesis of Cryptophycins - Revision of the Structures of Cryptophycin-a and Cryptophycin-C. *J Am Chem Soc* **1995**, *117* (9), 2479-2490.
72. Hoard, D. W.; Moher, E. D.; Martinelli, M. J.; Norman, B. H., Synthesis of cryptophycin 52 using the Shi epoxidation. *Org Lett* **2002**, *4* (10), 1813-5.
73. Pousset, C.; Haddad, M.; Larcheveque, M., Diastereocontrolled synthesis of unit A of cryptophycin. *Tetrahedron* **2001**, *57* (33), 7163-7167.

Chapter 3

Structural Studies and Mechanistic Insights into the Cryptophycin Thioesterase

3.1 Background on Thioesterase Structure and Function

3.1.1 Overall Structural Features of Thioesterases

The promising data from our *in vitro* biochemical assays prompted us to investigate the structural and mechanistic features that impart the broad scope flexibility seen with the CrpTE. Type 1 thioesterases belong to a larger family of α/β hydrolases, which also includes proteases, esterases, and lipases.¹ Unlike other PKS or NRPS domains, thioesterases generally contain very low sequence identity within the family (<30%), making it difficult to predict the type of chemistry these will catalyze. All known structures show that TEs contain a similar β - α - β motif that displays a central β sheet (with either seven or eight strands with seven being more common for Type 1 thioesterases while eight is more frequently seen in other hydrolases, **Figure 3.1**). The active site serine is located between the fifth β strand and N terminus of α helix 3 as a part of a characteristic Gly-xx-Ser-xx-Gly motif, known as the “nucleophilic elbow”. Currently, there are a handful of known macrocyclizing PKS and NRPS TEs which have shed light on the innate differences in

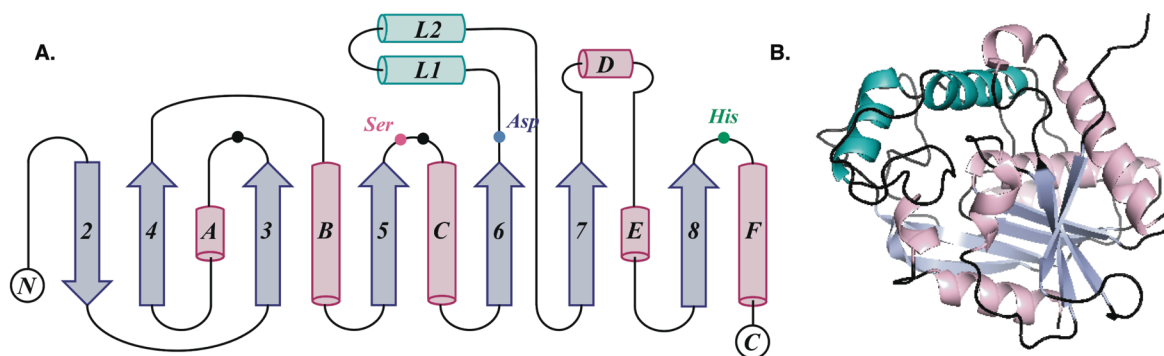


Figure 3.1 General thioesterase structure diagrams. (A) General topology schematic of a Type 1 TE highlighting the active site catalytic triad residues as well as the oxanion participants shown in black circles (B) 3D representation of the aflatoxin TE (pdb 3ILS) highlighting active site residues, the central β sheet, and the lid region.

structure between the two.²⁻¹⁵ Sequence alignments have previously shown that the most structural diversity in TEs lies within two α helices (although three are not uncommon) in the region between β 6 and β 7 known as the lid region (**Figure 3.1, A**). This usually consists of two α helices that can range from 25 to 80 amino acids in length has been hypothesized to play a major role in selectivity.¹⁶ The cryptophycins are made by a mixed PKS/NRPS system with the thioesterase being appended to the terminal NRPS domain. Despite some rather detailed studies on both PKS and NRPS TEs, there have yet to be any on macrocyclizing TE's from mixed systems begging the question, will this display structural features more similar to PKS TEs, NRPS TEs or will it contain some of both?

3.1.2 Structural Insights into PKS Derived TEs

Studies on the PKS TEs in the erythromycin (DEBS) and pikromycin (Pik) pathways revealed unusual features seen in this subtype of hydrolases that are not present in other members of this family. There are two N terminal dimerization helices as well as a surprisingly large and wide active site, shaped as a channel that spans the entire protein. This channel is lined with a mixture of conserved hydrophobic residues as well as a few non-conserved hydrophilic ones, that differ between these proteins and likely play a vital role in the catalytic mechanism.¹⁵ A mixture of docking studies on the DEBS TE as well as crystal structures with a substrate mimic affinity probes show a complex interplay of a few distinct hydrogen bonding interactions as well as significant hydrophobic packing and likely inherent substrate structural features necessary for productive cyclization.^{11-12, 15} This has been corroborated through a mixture of synthetic substrates and docking studies that have shed light on some of the necessary structural features as well as demonstrated the proteins tolerance for non-essential elements with the formulation of new macrocyclic products.^{15, 17}

3.1.3 Structural Insights into NRPS Derived TEs

NRPS TE's have also benefited from structural and biochemical characterization. In the NRPS derived tyrocidine and daptomycin TE systems, solid phase peptide synthesis was utilized to formulate a suite of unnatural chain elongation intermediates that furnished novel macrocyclic analogues with varying biological activities.¹⁸⁻²⁰ The substrate tolerance seen in these TEs has been attributed to a hydrogen bond network that enables substrate preorganization. Thus, the TE in this case, was hypothesized to exert minimal influence except on the amino acid being employed

as the intramolecular nucleophile, which appears to be critical for productive catalysis.²¹ This is further supported by structural studies on the NRPS TEs from the surfactin and fengycin biosynthetic pathways. These TE's possess a large, bowl shaped active site, in contrast to the tunnel seen in PKS TEs. The bowl is lined with predominantly nonpolar and aromatic amino acids, with specific interactions occurring primarily at the hydroxyl containing C-terminus of the linear NRPS substrate.^{10, 14} These compelling studies continue to shed light on the complex mechanism employed in these different systems. Further investigations into PKS, NRPS, and PKS/NRPS hybrid TEs are necessary to expand our understanding of the factors that govern macrocyclization on a broad scale.

Extensive screening in the Sherman/Smith labs over the past 10 years have demonstrated the CrpTE is resistant to crystal packing and has yet to garner any traction, fostering the need for design and formulation of alternate constructs with potentially better crystal packing interfaces. In conjunction with Dr. John Luz at Eli Lilly, we pursued a two-pronged approach to obtain crystals. The first focuses on the identification, cloning, and expression of the initial set of enzyme mutants to help promote crystal packing. The second involved a strategy of trapping native substrates in the active site, which will hopefully facilitate protein ordering, as well as provide important insights regarding substrate binding and orientation.

3.2 Optimization of the CrpTE for Structural Characterization

3.2.1 Rational Construct Design of variant CrpTEs

In accordance with our first approach and in collaboration with Dr. John Luz (Eli Lilly), we identified a series of potential regions for protein engineering. Utilizing the Surface Entropy Reduction prediction (SERp) server developed by the University of California at Los Angeles two surface cysteines, as well as six predicted surface residues were identified as problematic. This server predicts tertiary structure from primary sequence data and utilizes that to identify regions of charged or hydrophilic amino acids that may be interfering with packing, and ultimately crystal formation. Utilizing this knowledge, three separate expression constructs were designed: the first included mutations of the two surface cysteines (C145S and C226S, **Table 3.1** DHS7150) to serines, the second contained the two surface cysteine residue mutations plus the first four mutations of charged residues less polar ones that were found adjacent to one another (E61G,

DHS #	plus 7	minus 5	minus 10	1 (E61G)	2 (K66S)	3 (E70A)	4 (K77A)	5 (S94C)	6 (C145S)	7 (K195G)	8 (K219A)	9 (C226S)	10a/b (H265)	TB Media
7150									X			X		>100 mg/L
7151				X	X	X	X		X			X		82 mg/L
7152				X	X	X	X		X	X	X	X		85 mg/L
7153	X													>100 mg/L
7154		X												95 mg/L
7155			X											70 mg/L
7156	X								X			X		>100 mg/L
7157		X							X			X		85 mg/L
7158	X			X	X	X	X		X			X		Not Expressed
7159		X		X	X	X	X		X			X		Not Expressed
7160								X						>100 mg/L
7161								X					X	>100 mg/L
7162								X						>100 mg/L
7163	X							X					X	>100 mg/L
7164		X						X					X	65 mg/L
7165			X					X					X	65 mg/L

Table 3.1 Schematic and table of mutant constructs of Crp TE generated. Corresponding expression yields are also denoted.

K66S, E70A, and K77A, **Table 3.1** DHS7151), and the third containing mutations to all six of the problematic residues (K195G and K219A, **Table 3.1** DHS7152).

The cryptophycin thioesterase is natively attached to an upstream peptidyl carrier protein on the terminal NRPS module by a linker region. Analysis of the protein sequence using BLAST and AntiSMASH (a secondary metabolite analysis and prediction server) as well as the Phyre2 secondary structure server revealed disordered region at the *N*-terminus of the originally cloned CrpTE, which was excised in the middle of the initial linker. In hopes of developing a construct with better crystallization properties, variants that included the entire linker region, half the linker region, and none of the linker region were designed. All three constructs were made by quick change mutagenesis and consisted of a seven amino acid addition (**Table 3.1** DHS 7153) to the amino terminus of the original clone, a five amino acid truncation (**Table 3.1**, DHS 7154), and a ten amino acid truncation (**Table 3.1**, DHS 7155). The addition is predicted to add secondary structure lending credence to this variant and the truncations would remove the disordered regions in two portions in case of deleterious effects. Combining some of these mutations produced four other constructs that could be utilized as well.

3.2.2 Variant CrpTE Protein Expression and Purification

With the new constructs in hand, we investigated expression and purification of these protein that would be amenable to crystallization screens. Proteins were initially screened on 3 mL cultures for overexpression and solubility. Luckily, all of the constructs had significant overexpression bands seen in supernatant with minimal aggregates in the pellet. All six initial constructs (DHS7151 – 7155) were then grown on large scale, 3L batches in TB. Purification of 1L the mutant proteins in HEPES buffer without glycerol (glycerol is known to cause active site acylation with this protein) and with varying concentrations of imidazole proved effective. The first chromatographic step included nickel affinity chromatography which produced between 70

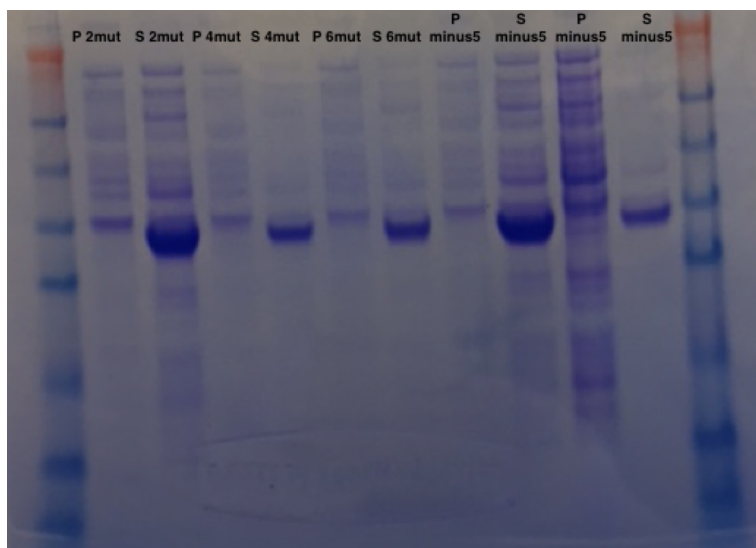


Figure 3.2 Gel of initial expression tests for mutant CrpTEs. These were run on 3 mL volumes and show over expression in the soluble fraction and minimal insoluble protein in the pellet.

and 105 mg of protein for each of the constructs (**Table 1**). Following purification, cleavage with TEV protease and subsequent size exclusion chromatography led to sufficiently pure protein for initial crystallization screening. All the CrpTE variants were tested for activity prior to crystal screen and each showed minimal difference in turnover of substrates.

With these proteins in hand, we in collaboration with Dr. Janet Smith's Lab at the University of Michigan began crystallization screens. Size exclusion chromatography (SEC) of some of the mutant proteins used for setting trays revealed significant differences in monomeric and dimeric protein populations, with the original construct being 3:1 monomer to dimer. PKS TE's are known to be dimers (as their entire modules are dimers) however, NRPS's are thought to

be monomers. Previous biochemical and structural work has briefly touched on the subject with slightly differing results. In the lipopeptide forming surfactin TE, dimerization was seen through the β sheet in the crystal structure, however this was not observed via SEC, causing them to conclude this was an artifact of crystallization.¹⁴ In contrast, the fengycin TE structure showed only monomers, however the SEC showed some tendency for dimerization.¹⁰ Our results have shown that different constructs lengths show different propensities for dimerization. The constructs containing shorter lengths at the amino terminus show interesting results, with the both constructs (DHS7154 – 7155) having significantly higher ratios of monomer to dimer than the initial one (greater than 10:1 vs 3:1). All the SEM mutant constructs as well as the plus 7 amino acid (DHS7150 – 7153) show similar dispersion of monomer and dimer (around 3:1) as the original construct (**Figure 3.3**). These were all separated via SEC and incubated overnight at 4 °C to determine if either the monomers or dimers would re-equilibrate to their original dispersion. Reinjection of all the monomeric forms as well as the three dimeric forms produced in higher quantity showed that neither the monomer or dimer fractions of any of the constructs showed re-equilibration, and that they were stable in their initially adopted state.

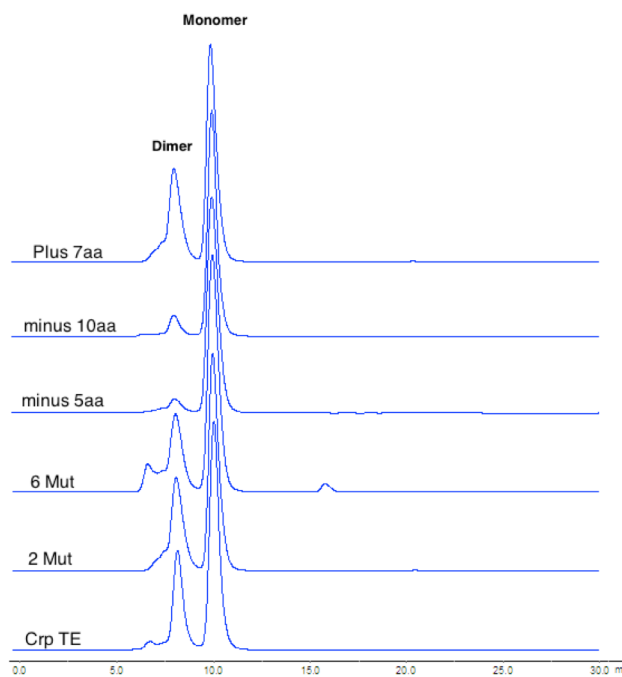


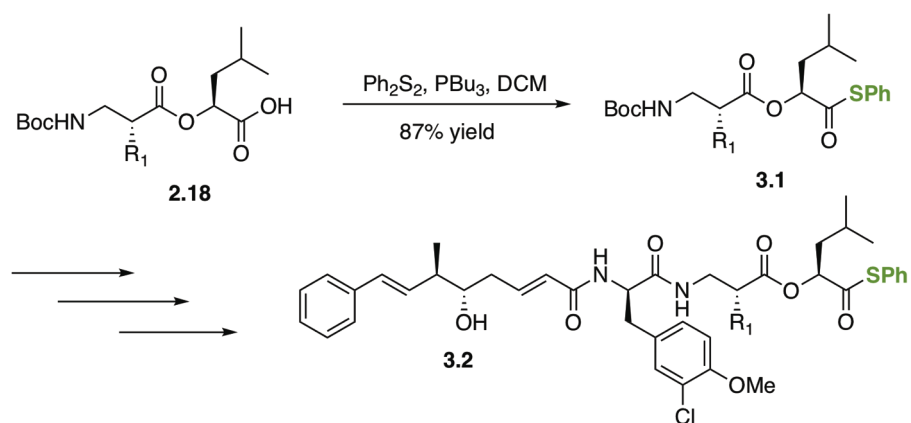
Figure 3.3 Size exclusion results for the different CrpTE constructs. These show that the minus 5 amino acid and minus 10 amino acid variants have a lower propensity for dimerization.

With the different constructs expressed and separated into their monomer and dimer constituents, initial screening trays were set at high concentration (greater than 30 mg/mL) using Qiagen classics I and II kits. These initial screens produced 2 small crystal hits from two different mutant TEs, DHS 7156 and 7158 (minus 5aa) with the underlying factor in each hit being that they are the monomer population and the addition of magnesium chloride. With these promising initial results, countless refinement screens were run, however to date none have produced viable crystals for x-ray diffraction.

3.2.3 Engineering the CrpTE from a Hydrolase to an Acyl Transferase

Our second approach focused on trapping substrates in the CrpTE active site. This approach served two purposes, first often proteins are too flexible to crystalize unless substrate is present as it can help effectively lock the protein into its catalytic conformation and second obtaining a crystal structure with the full length chain elongation intermediate has not been accomplished to date and would provide a wealth of information about the selectivity and catalytic mechanism employed by these proteins. In order to accomplish this, we utilized a strategy previously reported for FAS that effectively changing the enzymes function from a hydrolase to an acyltransferase via two active site mutations.²² The first mutation was to the active site serine to cysteine (S94C, DHS 7160), which would serve as a more effective nucleophile for acylation. The second is to remove the active site histidine (H265) which is responsible for coordination of both the intramolecular hydroxyl group as well as water, which is necessary to abrogate hydrolytic or intramolecular offloading. The S94C as well as two separate histidine 265 mutants (H265N and H265Q) were constructed via quick change mutagenesis, in the hopes that one would be stable (**Table 3.1**, DHS 7161 – 7162) as often active site mutations are deleterious to protein folding. Upon expression and purification of these two variants using the same procedure as the previous constructs produced highly soluble, stable protein much to our surprise as this has not been the case with active site mutations in PKS TEs.

With both double mutant CrpTE proteins in hand, they were assessed for substrate occupancy via QTOF-MS with the N-acetyl cysteamine substrate described previously (**Scheme 2.4, 2.28a**). Initial screens aimed at identifying conditions for effective acylation. High pH buffers (tris pH9/10) were investigated along with temperatures ranging from 4 °C to 37 °C, and substrate to protein ratios from 2:1 to 20:1. Each of these were checked initially at three time points, by flash



Scheme 3.1 Synthesis of thiophenol containing substrate.

freezing prior to assessment on the TOF. These initial screens produced no detectable acylation of the active site for either protein. After exhausting possible buffer and temperature conditions, we decided to investigate a more active substrate, bearing a thiophenol in place of the N-acetyl cysteamine (**Scheme 3.1**). This was generated utilizing a similar synthetic scheme as described in Chapter 2. Unit AB was formulated in an analogous manner to the SNAc containing substrate. Thiophenol containing unit CD was formulated by the benzyl deprotection of **2.19** with H_2/Pd followed by thiophenylation using tributyl phosphine and diphenyl disulfide. This was then Boc deprotected, coupled to unit AB, and desilate as described in **Chapter 2** to produce substrate **3.2**.

With this new, more active substrate, buffer, temperature, and times were again assayed in order to determine the optimal acylation procedure. Results indicated that higher temperatures (30 or 37 °C), high pH buffer (Tris pH = 9) for short times (30 min to 1 hour) were optimal, however slow hydrolysis was still seen upon overnight incubation at 4 °C. Continued screening of temperatures and buffer conditions, indicated it was the higher pH buffers necessary for acylation that was responsible for the aberrant hydrolysis. Quenching of the reactions using a 10% formic acid solution, produced an acylated protein that was stable for 24 hours upon 4 °C storage. In hopes of eliminating the formic acid quench, a quick acylation time (30 min to 1 hour) in pH 9 Tris buffer at 37 °C followed by subsequent buffer exchange back to pH 7 HEPES and storage at 4 °C, produced a substrate bound enzyme that was again stable for more than 24 hours. Subsequent size exclusion chromatography produced protein for crystal screening. Again, the Qiagen classics I and II screening kits were utilized, but did not produce any significant crystals.

3.3 Evaluation of the Cryptophycin Thioesterase as a Candidate for Solution Phase Structure

3.3.1 Background Information on Solution Phase (NMR) Structural Determination

With the discovery of mostly monomeric CrpTE as well as the knowledge that it does not re-equilibrate to dimer, and the lack of crystallization hits in the crystal screens, we began to look for alternative methods for structural characterization. With the advent of super conducting, high field strength magnets, user friendly control software, and multi-frequency detection channels nuclear magnetic resonance (NMR) can be utilized to structurally characterize a wide range of

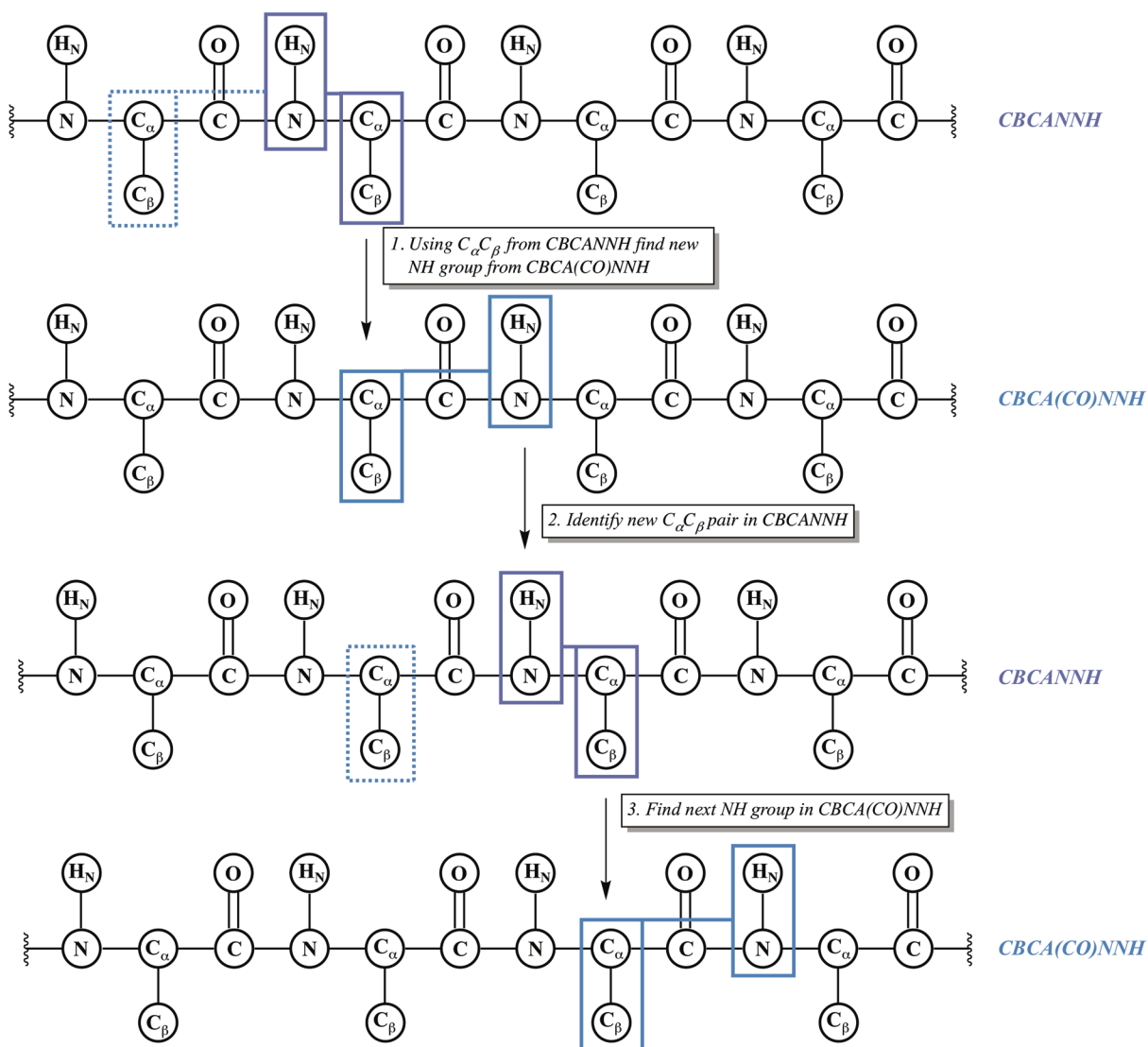


Figure 3.4 General schematic of the workflow involved in assigning carbon and hydrogen signals using standard triple resonance NMR experiments, CBCA(CO)NNH and CBCANNH.

biological entities. This method has the advantage of being able to detect protein structural changes in response to experimental conditions, giving us the ability to titrate in substrates and effectively monitor discrete amino acid shifts as the protein undergoes its catalytic cycle, giving us vital information about the dynamics of TE's.

Smaller proteins (<10 kDa) often lend themselves to assignment based on homonuclear two-dimensional experiments like TOCSY and NOESY, however larger sized proteins are accompanied by exponentially more signals, resulting in crowding that can't be resolved.²³ Further three-dimensional heteronuclear triple-resonance NMR experiments are necessary in these cases to assign the backbone and sidechain shifts. Standard resonance assignments are made through CBCANNH and CBCA(CO)NNH,²⁴⁻²⁶ which gives correlations for each NH group to both the corresponding C α and C β as well as the preceding C α and C β , which allows you to determine

3D NMR Experiments For Assignment of Large Proteins

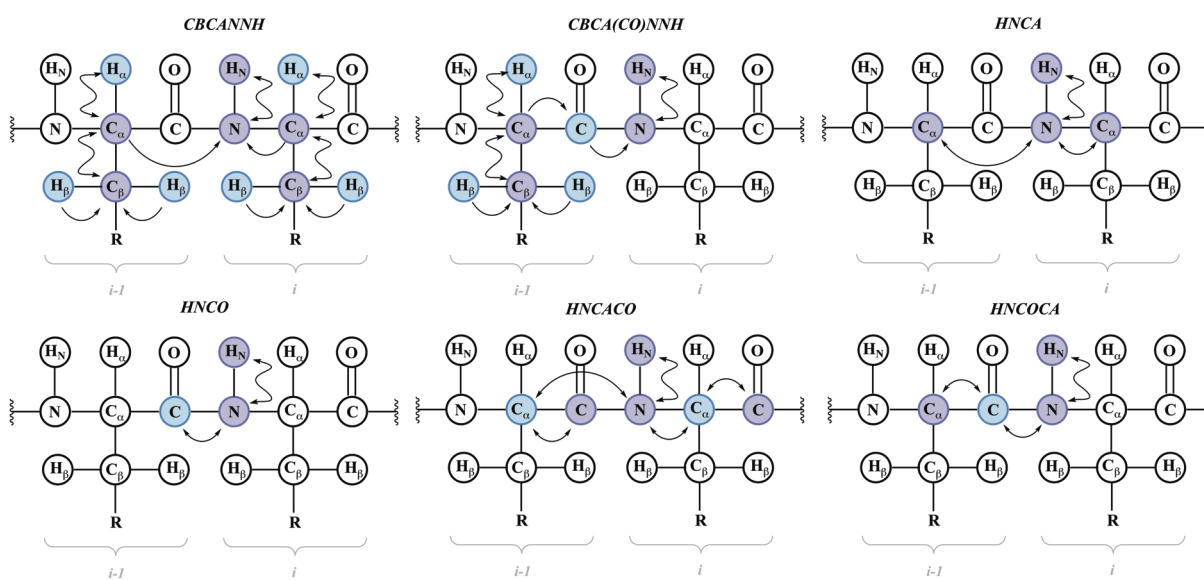


Figure 3.5 Magnetization transfer pathways seen in three-dimensional NMR experiments necessary for the assignment of large proteins: CBCANNH, CBCA(CO)NNH, HNCA, HNCO, HNCACO, and HNCOCA

adjacent amino acid resonances (**Figure 3.4**). Utilizing knowledge of characteristic amino acid frequencies (Alanine, Serine, Threonine, and Glycine contain characteristic resonances) allow you to generate a general sequence idea (ex: Ala-xx-Thr-xx-xx-Ala) and compare that to your known sequence. From here you can identify the portions of the sequence using these known amino acids allowing the assignment of each atom of the polypeptide backbone to a shift in the spectra. In order

to assign the CrpTE, a 35 kDa protein, and ultimately build a structure it is necessary to not only run the previous two experiments, but others to confirm the assignments as well as resolve ambiguous signals. A standard set of three dimensional experiments which allow for the assignment of large proteins may include HNCA, HNCOC, HNCACO, HNCOCA (**Figure 3.5**) all of which require different labeling patterns including ^{13}C , ^{15}N , and ^2H .²⁷ Once the backbone is assigned and the C_α and C_β of each sidechain has been assigned from those initial experiments (**Figure 3.4**) for flowchart on how you can utilize experiments to walk down peptide chain), an HCCH-TOCSY experiment can give the rest of the sidechain assignments, with the help of a separate experiment, HCCONH if these can't be completely resolved. From here J values collected can be used to compute the structure based on the Karplus angles of each atom in the backbone. Sidechain position is assigned in an analogous manner once the backbone has been determined.

3.3.2 Formulation of CrpTE Protein for NMR Experiments

Utilizing the results from the construct optimization, DHS 7154 (minus 5aa) was chosen for structural characterization as it was predominantly monomeric and proved most stable to NMR buffer conditions (sodium phosphate buffer, pH = 6.5). The initial NMR experiment to check for protein folding and stability was a $^1\text{H}/^{15}\text{N}$ HSQC, which required ^{15}N labeled protein. The protein was grown by first inoculating a 5 mL starter culture in LB using freshly transformed B121 (DE3) *E. coli*. This was grown to a high OD_{600} (~6 – 8 hours) and was used to inoculate overnight cultures in M9 media (see SI for recipe) augmented with $^{15}\text{NH}_4\text{Cl}$ and kanamycin (50 $\mu\text{g}/\text{mL}$). The overnight culture was then used to inoculate 1 liter cultures of the M9 (1:100 inoculum) media supplemented with kanamycin (50 $\mu\text{g}/\text{mL}$). This was grown to OD_{600} of 0.5 at 37 °C, cooled to 20 °C and induced with 100 μM IPTG. This was expressed for 18 hours, spun down at 6,000 rpm for 30 min and stored at -78 °C for purification. Frozen cells were purified using Phosphate buffer with varying amounts of imidazole over NiNTA resin, prior to cleavage with TEV protease, and size exclusion chromatography. Buffer exchanging into a pH 6 phosphate buffer yielded protein ready for NMR experiments.

In collaboration with Dr. Vivekanandan Subramanian in UM Biophysics, initial $^1\text{H}/^{15}\text{N}$ HSCQ showed excellent resolution (**Figure 3.6**) and 250 NHs of the 296 total were resolved. In order to start putting together the backbone of the CrpTE, ^{13}C , ^{15}N , and ^2H CrpTE was generated using the same procedure as above, substituting globally ^{13}C labeled glucose and growing in 70%

D₂O. Upon purification and TEV cleavage, this produced 19 mg/L of pure protein which was immediately concentrated to 500 uM and used to run HNCACB, CBCACONH, HNCA, and HNCACO experiments. Utilizing these experiments as well as NMR processing software SPARKY, each of the NHs present in the initial ¹H/¹⁵N HSCQ have been correlated with their respective C_α and C_β. We are currently building the assignments off these correlations which will be used in the future structural characterization.

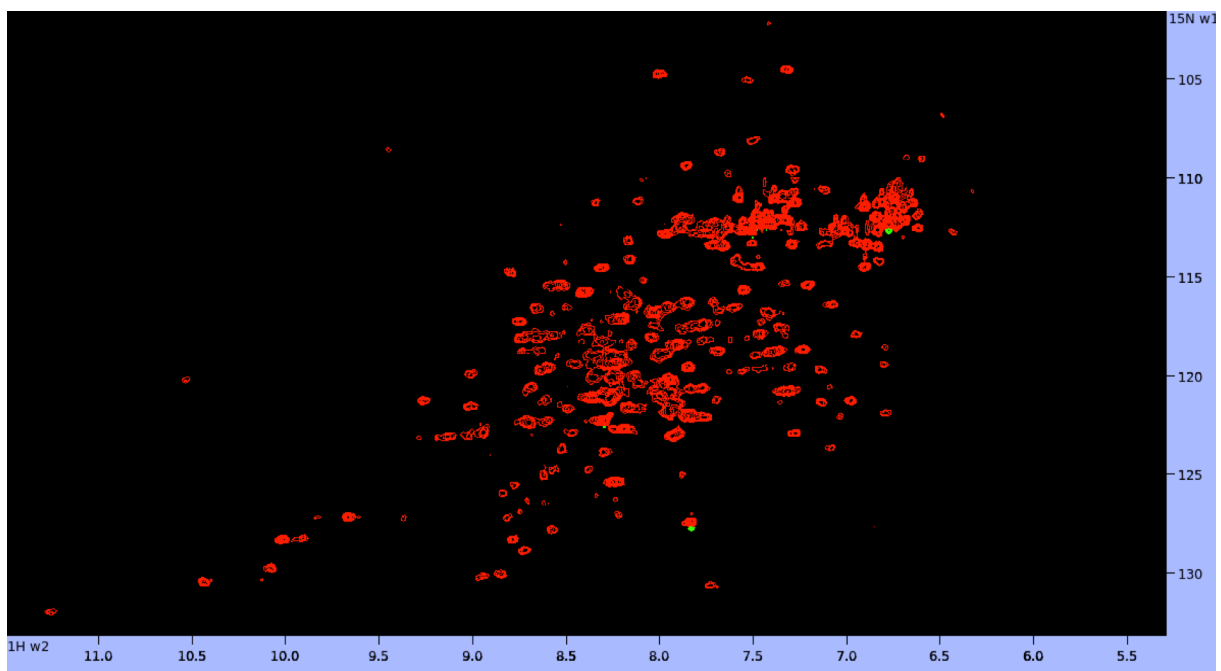


Figure 3.6 ¹⁵N/¹H HSQC spectrum of CrpTE as observed in SPARKY NMR program.

3.4 References

1. Horsman, M. E.; Hari, T. P.; Boddy, C. N., Polyketide synthase and non-ribosomal peptide synthetase thioesterase selectivity: logic gate or a victim of fate? *Nat Prod Rep* **2016**, *33* (2), 183-202.
2. Whicher, J. R.; Florova, G.; Sydor, P. K.; Singh, R.; Alhamadsheh, M.; Challis, G. L.; Reynolds, K. A.; Smith, J. L., Structure and Function of the RedJ Protein, a Thioesterase from the Prodiginine Biosynthetic Pathway in *Streptomyces coelicolor*. *Journal of Biological Chemistry* **2011**, *286* (25), 22558-22569.
3. Liu, Y.; Zheng, T. F.; Bruner, S. D., Structural Basis for Phosphopantetheinyl Carrier Domain Interactions in the Terminal Module of Nonribosomal Peptide Synthetases. *Chem Biol* **2011**, *18* (11), 1482-1488.
4. Gehret, J. J.; Gu, L. C.; Gerwick, W. H.; Wipf, P.; Sherman, D. H.; Smith, J. L., Terminal Alkene Formation by the Thioesterase of Curacin A Biosynthesis STRUCTURE OF A DECARBOXYLATING THIOESTERASE. *Journal of Biological Chemistry* **2011**, *286* (16), 14445-14454.
5. Scaglione, J. B.; Akey, D. L.; Sullivan, R.; Kittendorf, J. D.; Rath, C. M.; Kim, E. S.; Smith, J. L.; Sherman, D. H., Biochemical and Structural Characterization of the Tautomycetin Thioesterase: Analysis of a Stereoselective Polyketide Hydrolase. *Angew Chem Int Edit* **2010**, *49* (33), 5726-5730.
6. Korman, T. P.; Crawford, J. M.; Labonte, J. W.; Newman, A. G.; Wong, J.; Townsend, C. A.; Tsai, S. C., Structure and function of an iterative polyketide synthase thioesterase domain catalyzing Claisen cyclization in aflatoxin biosynthesis. *P Natl Acad Sci USA* **2010**, *107* (14), 6246-6251.
7. Tanovic, A.; Samel, S. A.; Essen, L. O.; Marahiel, M. A., Crystal structure of the termination module of a nonribosomal peptide synthetase. *Science* **2008**, *321* (5889), 659-663.
8. Koglin, A.; Lohr, F.; Bernhard, F.; Rogov, V. V.; Frueh, D. P.; Strieter, E. R.; Mofid, M. R.; Guntert, P.; Wagner, G.; Walsh, C. T.; Marahiel, M. A.; Dotsch, V., Structural basis for the selectivity of the external thioesterase of the surfactin synthetase. *Nature* **2008**, *454* (7206), 907-U68.
9. Frueh, D. P.; Arthanari, H.; Koglin, A.; Vosburg, D. A.; Bennett, A. E.; Walsh, C. T.; Wagner, G., Dynamic thiolation-thioesterase structure of a non-ribosomal peptide synthetase. *Nature* **2008**, *454* (7206), 903-U62.
10. Samel, S. A.; Wagner, B.; Marahiel, M. A.; Essen, L. O., The thioesterase domain of the fengycin biosynthesis cluster: A structural base for the macrocyclization of a non-ribosomal lipopeptide. *J Mol Biol* **2006**, *359* (4), 876-889.
11. Giraldes, J. W.; Akey, D. L.; Kittendorf, J. D.; Sherman, D. H.; Smith, J. L.; Fecik, R. A., Structural and mechanistic insights into polyketide macrolactonization from polyketide-based affinity labels. *Nature Chemical Biology* **2006**, *2* (10), 531-536.
12. Akey, D. L.; Kittendorf, J. D.; Giraldes, J. W.; Fecik, R. A.; Sherman, D. H.; Smith, J. L., Structural basis for macrolactonization by the pikromycin thioesterase. *Nature Chemical Biology* **2006**, *2* (10), 537-542.
13. Tsai, S. C.; Lu, H. X.; Cane, D. E.; Khosla, C.; Stroud, R. M., Insights into channel architecture and substrate specificity from crystal structures of two macrocycle-forming thioesterases of modular polyketide synthases. *Biochemistry-U S* **2002**, *41* (42), 12598-12606.

14. Bruner, S. D.; Weber, T.; Kohli, R. M.; Schwarzer, D.; Marahiel, M. A.; Walsh, C. T.; Stubbs, M. T., Structural basis for the cyclization of the lipopeptide antibiotic surfactin by the thioesterase domain SrfTE. *Structure* **2002**, *10* (3), 301-310.
15. Tsai, S. C.; Miercke, L. J. W.; Krucinski, J.; Gokhale, R.; Chen, J. C. H.; Foster, P. G.; Cane, D. E.; Khosla, C.; Stroud, R. M., Crystal structure of the macrocycle-forming thioesterase domain of the erythromycin polyketide synthase: Versatility from a unique substrate channel. *P Natl Acad Sci USA* **2001**, *98* (26), 14808-14813.
16. Cantu, D. C.; Chen, Y. F.; Reilly, P. J., Thioesterases: A new perspective based on their primary and tertiary structures. *Protein Sci* **2010**, *19* (7), 1281-1295.
17. Pinto, A.; Wang, M.; Horsman, M.; Boddy, C. N., 6-Deoxyerythronolide B Synthase Thioesterase-Catalyzed Macrocyclization Is Highly Stereoselective. *Org Lett* **2012**, *14* (9), 2278-2281.
18. Kopp, F.; Grunewald, J.; Mahlert, C.; Marahiel, M. A., Chemoenzymatic design of acidic lipopeptide hybrids: New insights into the structure-activity relationship of daptomycin and A54145. *Biochemistry-Us* **2006**, *45* (35), 10474-10481.
19. Yeh, E.; Lin, H. N.; Clugston, S. L.; Kohli, R. M.; Walsh, C. T., Enhanced macrocyclizing activity of the thioesterase from tyrocidine synthetase in presence of nonionic detergent. *Chem Biol* **2004**, *11* (11), 1573-1582.
20. Trauger, J. W.; Kohli, R. M.; Mootz, H. D.; Marahiel, M. A.; Walsh, C. T., Peptide cyclization catalysed by the thioesterase domain of tyrocidine synthetase. *Nature* **2000**, *407* (6801), 215-218.
21. Trauger, J. W.; Kohli, R. M.; Walsh, C. T., Cyclization of backbone-substituted peptides catalyzed by the thioesterase domain from the tyrocidine nonribosomal peptide synthetase. *Biochemistry-Us* **2001**, *40* (24), 7092-7098.
22. Witkowski, A.; Witkowska, H. E.; Smith, S., Reengineering the specificity of a serine active-site enzyme. Two active-site mutations convert a hydrolase to a transferase. *The Journal of biological chemistry* **1994**, *269* (1), 379-83.
23. Marion, D., An Introduction to Biological NMR Spectroscopy. *Mol Cell Proteomics* **2013**, *12* (11), 3006-3025.
24. Grzesiek, S.; Bax, A., Amino acid type determination in the sequential assignment procedure of uniformly ¹³C/¹⁵N-enriched proteins. *J Biomol NMR* **1993**, *3* (2), 185-204.
25. Grzesiek, S.; Bax, A., Correlating Backbone Amide and Side-Chain Resonances in Larger Proteins by Multiple Relayed Triple Resonance Nmr. *J Am Chem Soc* **1992**, *114* (16), 6291-6293.
26. Markwick, P. R. L.; Malliavin, T.; Nilges, M., Structural Biology by NMR: Structure, Dynamics, and Interactions. *Plos Comput Biol* **2008**, *4* (9).
27. Kay, L. E.; Ikura, M.; Tschudin, R.; Bax, A., Three-dimensional triple-resonance NMR Spectroscopy of isotopically enriched proteins. 1990. *J Magn Reson* **2011**, *213* (2), 423-41.

Chapter 4

Molecular Interrogation of Polyketide Synthase Modules in the Pikromycin System Using Unnatural Pentaketides

4.1 Background on the Macrolide Antibiotic Pikromycin

4.1.1 Macrolides as Antibiotics

Polyketide antibiotics were originally discovered in 1950 with the isolation of pikromycin, followed closely by the isolation of a second macrolide antibiotic erythromycin, which is still used clinically today.¹⁻² The mechanism of action of these molecules was later determined to be through disruption of protein synthesis by binding to the 50S subunit of the bacterial ribosome.³ More recent work has shown that these likely bind to the peptidyl (P) site and disrupt the peptidyl transfer activity, which joins incoming t-RNA attached amino acids with the growing amino acid chain, ultimately stalling protein synthesis.⁴⁻⁶ It is also thought that these can act as a physical barrier by sitting in the nascent peptide exit channel (NPET).⁷ Although erythromycin was widely successful, its inherent instability causes breakdown products that produce undesirable gastric side effects. This combined with the continued emergence of resistant bacterial strains has led to extensive SAR campaigns for analogues with better biological properties and to combat continually emerging resistance.

Erythromycin is considered a first generation antibiotic and is produced industrially from enhanced strains of *Saccharopolyspora erythraea*. Second generation analogues (**Figure 4.1**)⁸ were developed by semi synthesis from erythromycin in order to combat the pharmacokinetic and pharmacodynamics shortcomings seen in the clinic, which lead to the discovery of the widely used Azithromycin (Z-pac). Third and fourth generation antibiotics have more recently been investigated to help combat one of the major forms of resistance seen in bacteria; macrolide, lincosamides, streptogramin B (MLS_B) resistance. Macrolide antibiotics bind to the 23S RNA portion of the 50S subunit.⁹ Resistance is conferred by either mono or demethylation of the 23S ribosomal RNA by the ERM (erythromycin resistance methylase) family of methyl transferases.¹⁰⁻

¹¹ In the presence of erythromycin (specifically the cladinose sugar appended to C3), the previously

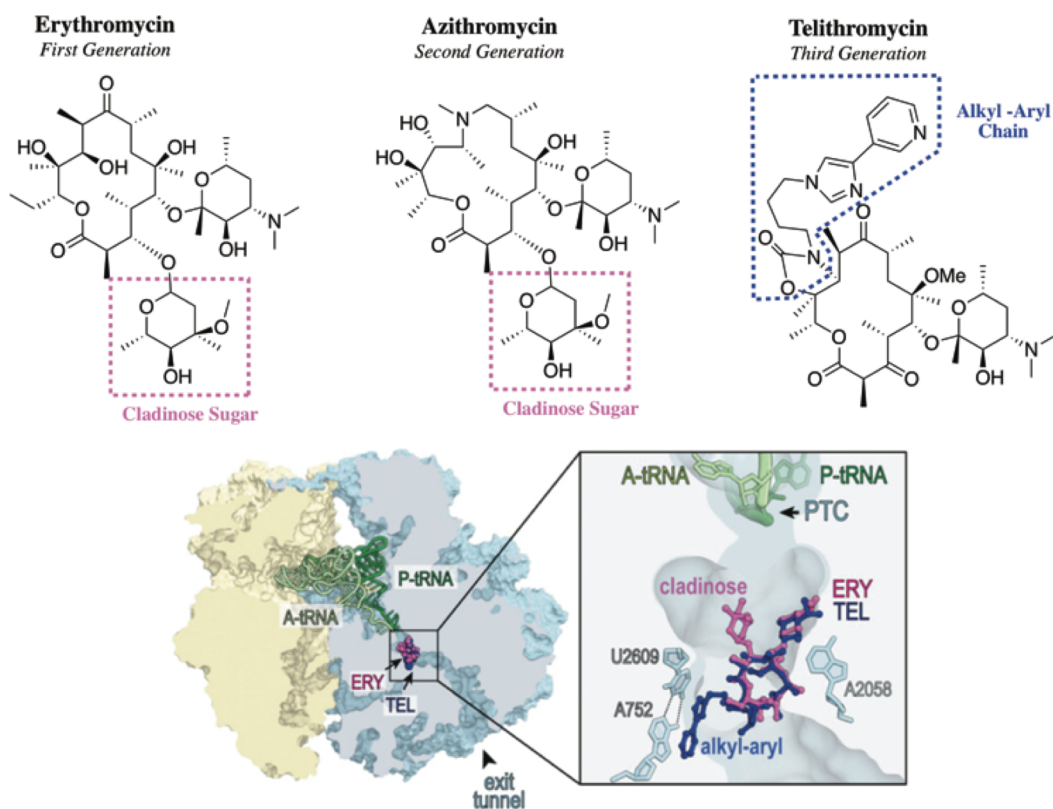


Figure 4.1 Antibiotic generations and their binding site on the ribosome. The MLS inducing cladinose sugar and the alkyl-aryl side chain that confers a second binding region are highlighted in pink and navy.

inaccessible ErmC ribosomal binding site is uncovered and translated, producing the methyl transferase protein that confers resistance. The requirement for the cladinose sugar for this process has led to third generation macrolides known as ketolide antibiotics, which remove the cladinose sugar and oxidize the remaining alcohol to a ketone, inhibiting resistance mechanisms.¹⁰ Addition of the alkyl-aryl side chain at positions 11 and 12 on the Erythromycin core, confers a second binding site on the ribosome and also helps modulate susceptibility in the macrolide resistant strains.

4.1.2 Biosynthesis of Pikromycin

In an effort to facilitate medicinal chemistry efforts necessary for the production of novel antibiotics, the Sherman lab has pursued a detailed understanding of the modular PKS biosynthetic systems responsible for the production of macrolide antibiotics, including pikromycin.¹²⁻¹⁶ Pikromycin, the original member of this family is a natural ketolide antibiotic. Although it is not as potent as the Erythromycin series of antibiotics, its ability to induce MLS

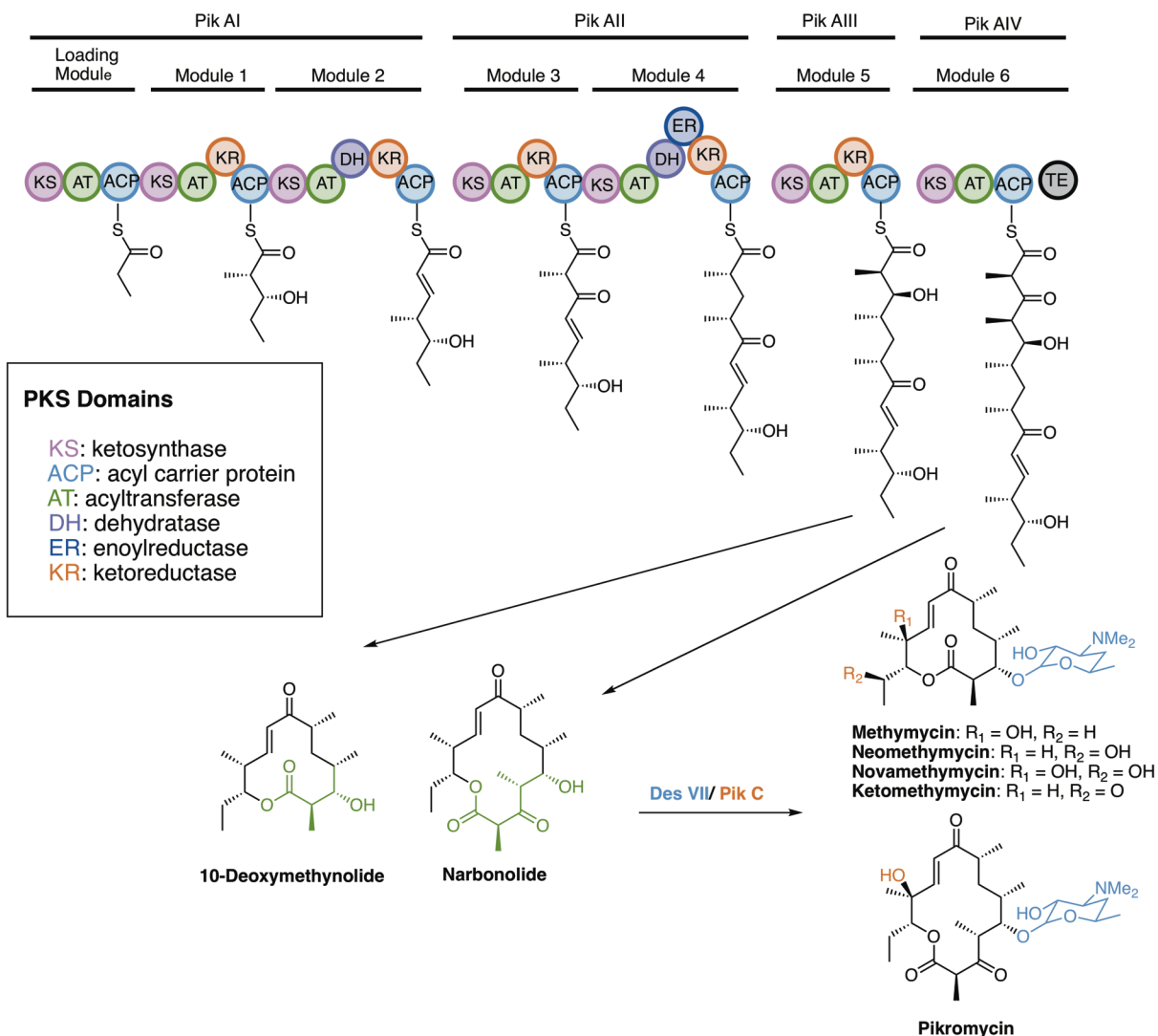


Figure 4.2 Pikromycin biosynthetic pathway for the formation of aglycones 10-Deoxymethynolide (10-DML) and Narbonolide. Further tailoring enzymes for glycosylation and P450 transformations formulate the full macrolide antibiotics.

resistance is greatly diminished. Analogues formulated from this scaffold in efforts to make this macrolide more potent have produced solithromycin which is currently in clinical trials. Pikromycin contains a unique PKS biosynthetic system that it is capable of producing both a 12 membered ring, the methymycin family of natural products as well as the 14 membered pikromycin ring structures (**Figure 4.2**). These can both be glycosylated and oxidized by cytochromes P450 to produce the full macrolide antibiotic (**Figure 4.2**). The inherent flexibility seen within this system makes it uniquely suited for exploration into the use of intact modules for

a biocatalytic syntheses of novel macrolide antibiotics. Utilizing the biosynthetic machinery of macrolide antibiotics to introduce new functionality and alter the core pharmacophore could provide rapid access too novel structures with better pharmacological properties. Bioengineering efforts toward this end have focused on the introduction of non-native and unnatural malonyl derivatives, modification of module domain architecture *in vivo* to produce altered oxidation states, as well as swapping of entire modules with native modules from other systems to produce significant structural modifications.¹⁷ This has met with some success, however generally only trace products are detectable by mass spectrometry and in general this strategy meets with more failure than it does success. In order to further engineer polyketide synthases, a detailed understanding of the key factors involved in producing these must be understood.

4.1.3 Structural Investigations of Polyketide Synthases

Recent structural work on pikromycin modules has provided new insights into the overall architecture of PKS modules and their catalytic mechanism. Historically, crystal structures of excised domains have given us a wealth of information and served as a surrogate for full length module crystals, as to date they have remained elusive. Crystal structures of excised KS-AT from the Curacin and DEBS pathway, initially showed an elongated structure, similar to that of FAS

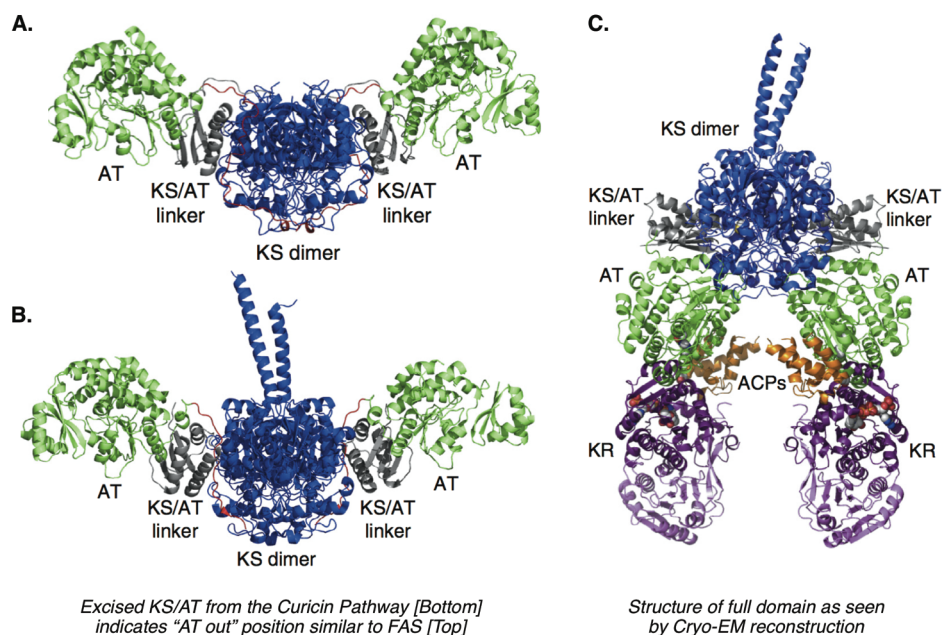


Figure 4.3 Cryo-EM reconstruction of PikAIII. (C) showing the single active site chamber in comparison to the curacin excised module (B) which shows a similar linear structure to FAS (A).

AIITE which were both heterologously expressed and, when combined with the synthetic pentaketides, methyl malonyl and an NADP recycling system, were able to formulate the two aglycones. This was further expanded to produce the active antimicrobial macrolides through biotransformations with engineered strains of *Streptomyces venezuelae* (which natively produce pikromycin) that have had the pikromycin PKS cluster knocked out but are capable of glycosylating and oxidizing macrolactone rings.²³⁻²⁴

In order to probe the selectivity and specificity of these enzymes, unnatural chain elongation intermediates with altered carbon sidechains and stereochemistry on the right half of the pentaketides were formulated in order to interrogate PikAIII-TE.¹² Utilizing this fusion protein alone would hopefully help further narrow down the cause of any processing deficiencies. The results of the altered carbon chains show a clear trend towards less efficient turnover as the modifications become more drastic. The C10 desmethyl (4.5 to 4.12) shows almost wildtype turnover (56%) to its 12 membered macrolactone counterpart however, when you remove the C9

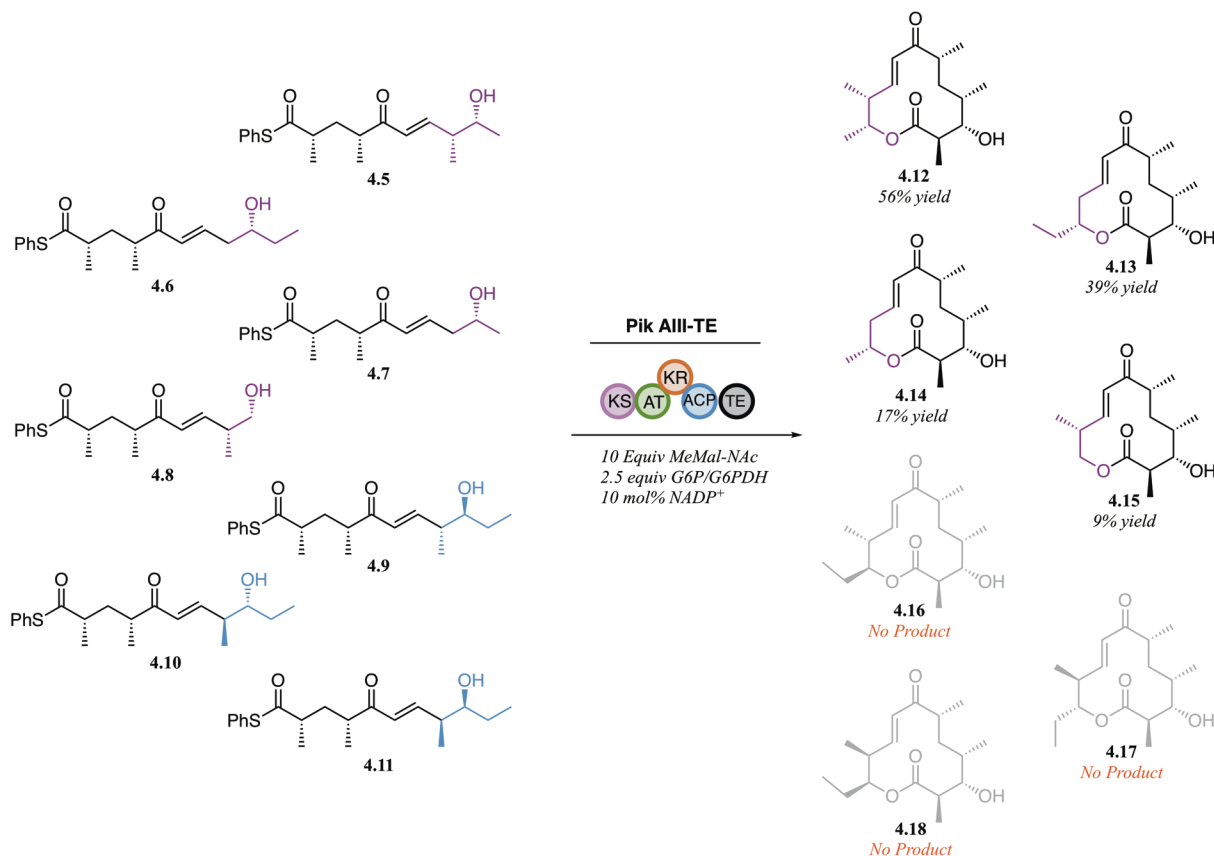


Figure 4.5 Initial right half pentaketides analogues assayed with PikAIII-TE. The different desmethyl analogues show different propensities for extension and cyclization while the epimers showed no turnover to macrolactones.

ethyl group (4.8 to 4.15) you see a significant decrease in macrolactone recovery (9%). Attempts to process substrates with altered stereochemistry at the C8 and C9 position (4.9 – 4.11) produced no macrolactone products, however extended products were isolated and characterized as extended shunt products that included a decarboxylation and a hemiketalization. This suggested that the module was able to process all these substrates to some extent, but that it was the TE that precluded effective production of macrocyclic products. This was further supported through the generation of the Pik hexaketide containing altered stereochemistry and attempts at biocatalytic conversion through the stand alone TE. This produced exclusively hydrolyzed starting material, further demonstrating the profound role the TE plays in macrocycle production.

In an accompanying publication by Dr. Aaron A. Koch, the previous results were further explained and the TE was engineered to partially overcome this effect.¹⁴ Molecular dynamics simulations that showed the PikTE could accommodate the epimerized substrates but that intrinsic substrate organization precluded cyclization. With this knowledge an active site mutation, S148C was made which altered the catalytic mechanism, which was capable of effectively cyclizing the epimerized hexaketide. This was then reincorporated into the PikAIII module and the epimerized pentaketides was again tested. This time, the module was able to formulate 2 corresponding macrolactones, the expected 11-epi-10 DML (4.16, 12% isolated yield) as well as a second ring in which the native KR in PikAIII didn't act on the substrate producing a similar 3-keto-11 epi-10 DML (12% isolated yield). These studies indicate that the modules are capable of processing at least distal chain modifications and continues to highlight that the TE is likely the underlying cause for unproductive formation of macrocyclic products.

4.2 Synthesis of Alternate Pentaketides Chain Elongation Intermediates

In order to continue to probe the flexibility of the terminal PikAIII-TE as well as the PikAIII/PikAIV biosynthetic pathway, a second suite of unnatural pikromycin pentaketides were designed to contain functionality that would not otherwise be present in polyketide synthase products, including heteroatoms in place of carbons, altered side chains, as well as various lengths of the backbone ketide units (Figure 4.6). With these substrates in hand we hoped to assay the ability of our PKS proteins to accept and process them to their corresponding macrolides, or other biproducts and help shed light on the complex factors associated with accepting, extending, and

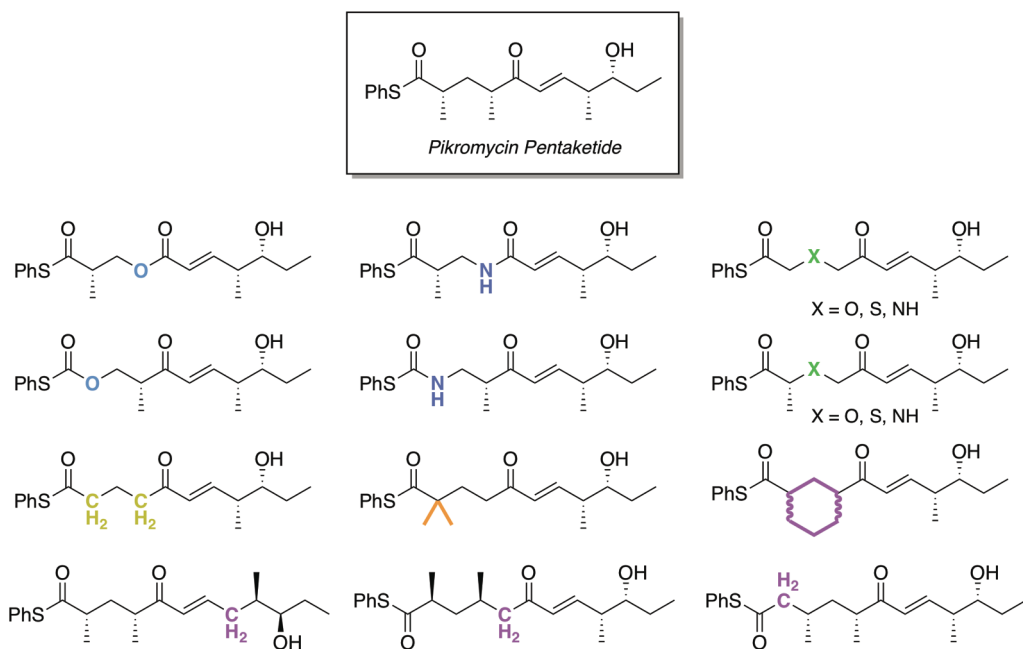


Figure 4.6 Potential unnatural pentaketide analogues. These were designed to contain heteroatoms, unnatural side chains, and altered ketide length

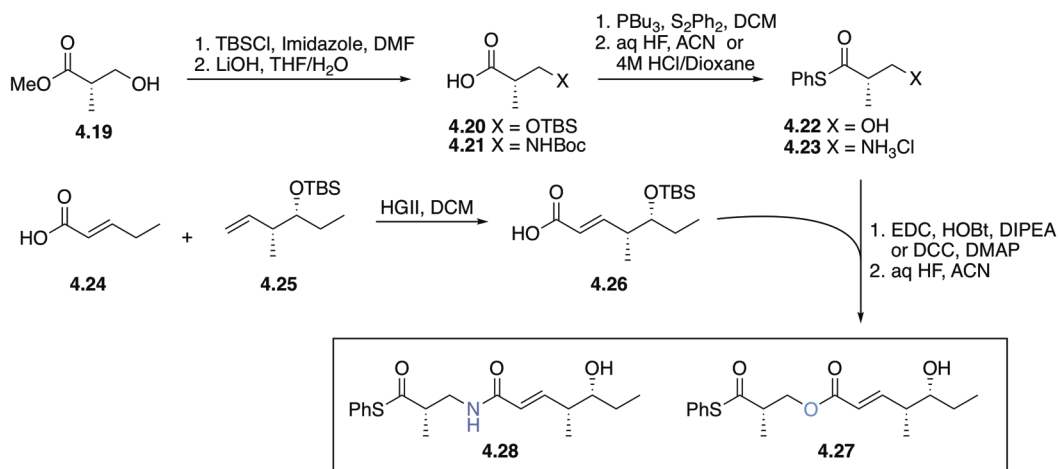
cyclizing polyketide macrolactones, as well as guide structural studies, and ultimate engineering efforts.

4.2.1 Synthesis of Ester and Amide Containing Pentaketides

The first analogues formulated contained an α/β unsaturated ester (**4.27**) and amide (**4.28**) in place of the α/β unsaturated ketone. These were formulated by taking advantage of a peptide coupling strategy. The left portion of both the ester and the amide analogues were synthesized by protecting group manipulation of commercially available (*S*) – Roche ester **4.19** and (*S*)-Boc- β^2 -HomoAla-OH **4.21** followed by thiophenylation of the acid with tributyl phosphine and diphenyl disulfide. The right half was formulated via cross metathesis of 2-pentenoic acid with **4.26** whose synthesis was reported previously.¹³ Subsequent deprotection of the two discrete left halves to produce **4.22** and **4.23** and coupling between these and **4.26** using either HATU or DCC/DMAP produced the desired TBS protected pentaketides. Deprotection with aq. HF produced the desired ester and amide containing pentaketides **4.27** and **4.28**.

4.2.2 Synthesis of Pentaketides containing Varied Alkyl Substituents

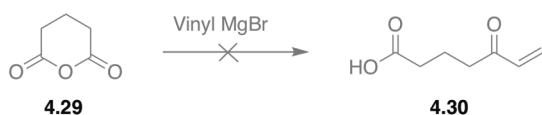
Next we focused on the desmethyl, dimethyl, cyclohexyl, and ether analogues (**4.37** – **4.40**) as we envisioned utilizing a cyclic anhydride ring opening strategy for the formation of all four.



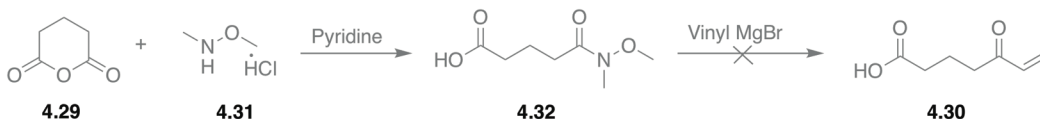
Scheme 4.1 Synthesis of ester and amide containing pentaketides.

Using glutaric anhydride **4.29** as the test platform, conditions for ring opening were investigated. Unfortunately, attempts to open the glutaric anhydride test platform with vinyl magnesium bromide produced either Michael addition polymerization or double addition products (**Scheme 4.2, A**). Although our initial attempts were not successful, the ring opening strategy was still an attractive option for formulating these four analogues, leading us to investigate Weinreb amides. Opening of the anhydride could first be accomplished using N,O-dimethylhydroxylamine hydrochloride (**4.31**) in pyridine and DCM to form the Weinreb amide **4.32**. Attempts to displace

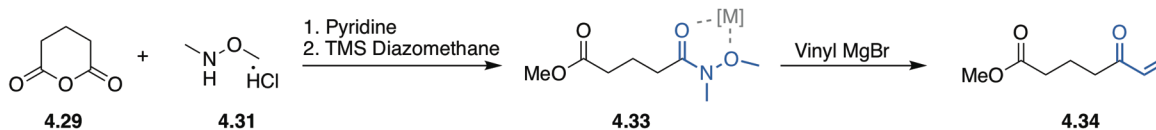
A. Direct Opening of cyclic anhydrides



B. Displacement of Weinreb amide in presence of Acid functionality

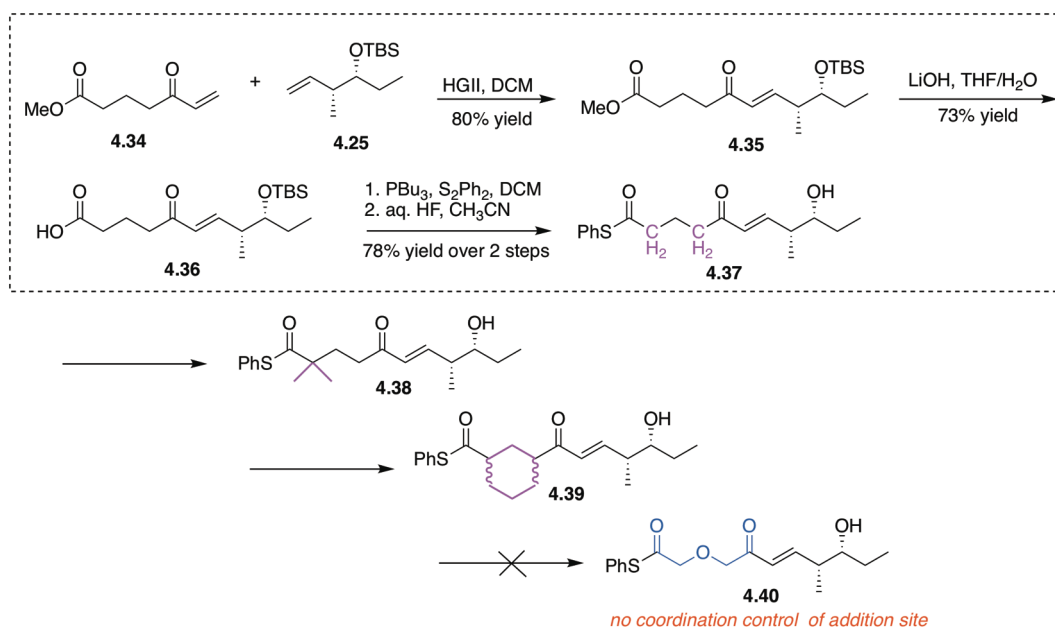


C. Displacement of Weinreb amide in presence of ester functionality



Scheme 4.2 Vinyl magnesium bromide ring opening strategy for analogue formation. First (**A**), second (**B**), and (**C**) third iterations of the cyclic anhydride opening strategy used to formulate altered carbon chain analogues.

the Weinreb amide in the presence of the acid functionality was met with some success although the elevated temperatures necessary to displace the Weinreb again promoted Michael addition and low reaction yields (**Scheme 4.2, B**). In order to mitigate the instability, we hypothesized that protection of the acid as a methyl ester could be used as the Weinreb amide would coordinate the vinyl magnesium bromide well enough to produce predominantly the desired product. This reaction was successful and produced **4.34** in a 62% yield. Subsequent cross metathesis with **4.25** proceeded smoothly, however saponification with LiOH was prone to Michael addition upon the presence of methanol or long reaction times. Thiophenylation and subsequent aq. HF deprotection

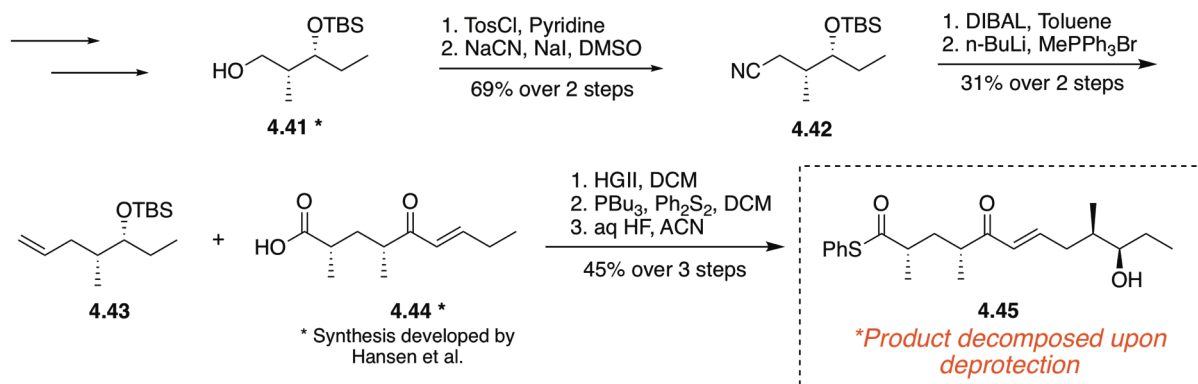


Scheme 4.3 Synthesis of desmethyl, dimethyl and cyclohexyl pentaketide analogues. Desmethyl pentaketides **4.37** as well as the dimethyl pentaketides **4.38** and cyclohexyl pentaketide **4.39** were formulated utilizing the same chemistry. Utilizing the diglycolic anhydride to formulate the ether containing pentaketide **4.40** unfortunately did not produce the corresponding α/β unsaturated ketone.

produced the desired desmethyl pentaketides **4.37**. This strategy was utilized in order to make both the dimethyl and the cyclohexyl (racemic) containing analogues. The dimethyl analogue showed exclusive opening to the less hindered site as expected however unfortunately attempts to utilize the same strategy with a diglycolic anhydride the ether containing Weinreb produced varying products including addition into the methyl ester. This is likely due to the presence of a second five membered ring coordination network that can occur with the ether oxygen into the methyl ester.

4.2.3 Synthesis of Extended Chain Pentaketides

Next we focused our attention on the substrates with altered ketide chain lengths in order to investigate the ability of TEs to formulate odd membered ring sizes. The initial analogue contained a homologation site directly adjacent to the α/β unsaturated ketone. This was chosen as it was easily homologated from the alcohol state of the right half of the pentaketides. After cleavage of the Evans chiral auxiliary to the alcohol **4.41** as reported previously¹³, subsequent tosylation, and cyanide displacement produced **4.42** which was reduced to the aldehyde and subjected to Wittig olefination conditions to produce **4.43**. This was then cross metathesized with **4.44**¹³ to produce the homologated acid product. This was then thiophenylated and deprotected unfortunately, intramolecular Michael addition upon deprotection of the cyclizing alcohol precluded us from testing this substrate directly with our enzymes. Future attempts will be made to add a photocleavable protecting group to this in order to facilitate a single pot deprotection, biocatalytic reaction strategy that has been employed for other unstable substrates.²⁵ Other homologation positions throughout the chain, including closer to the head group as well as prior to the α/β -unsaturated ketone will also be investigated.



Scheme 4.4 Synthetic scheme for the formulation of homologated pentaketides.

4.3 Biochemical Evaluation of Synthesized Pentaketides

With the first set of substrate analogues in hand, analytical enzymatic reactions with the monomodule fusion protein PikAIII-TE, responsible for the production of 12 membered rings as well as the terminal two modules PikAIII/AIV responsible for the production of 14 membered rings were explored. Our previous results with the PikAIII-TE and the PikTE stand-alone proteins

show that the TE is usually the bottleneck to forming unnatural macrolactones, however the effects of this on the 14 membered rings have not been explored.

4.3.1 Evaluation of Pentaketide Analogues with PikAIII-TE

With five new pentaketides analogues in hand we began to assay the PikAIII-TE for its ability to produce new 12 membered rings. PikAIII accepts methyl malonyl as an extender unit which has been synthesized as the SNAc variant. It also contains a KR domain which requires NADPH to complete its reduction. With the high cost of NADPH it is not feasible to use

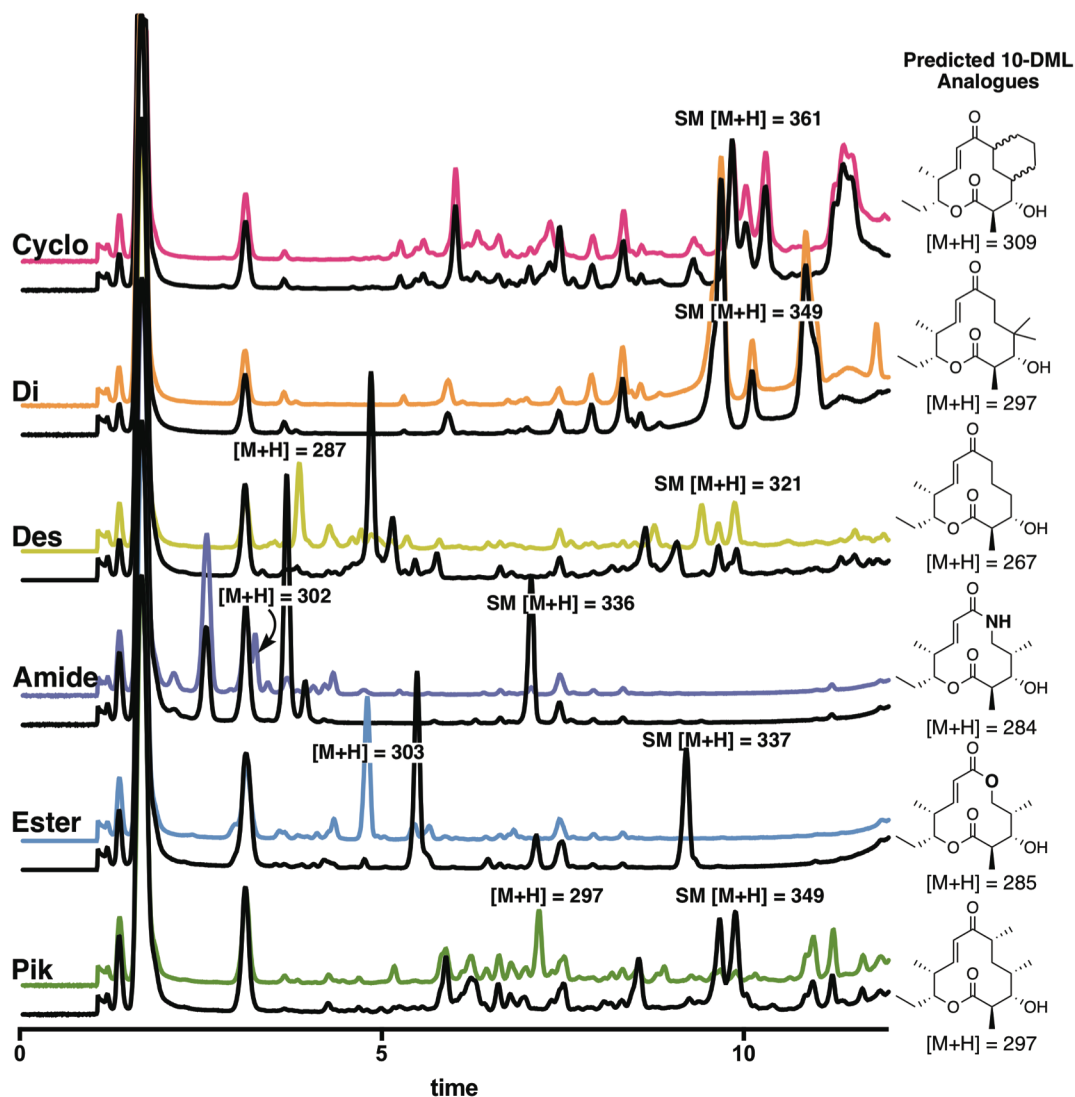


Figure 4.7 Analytical reaction traces with new pentaketides utilizing the PikAIII-TE fusion protein. The no enzyme controls for each being in black and the different enzymatic reactions being denoted in the various colors. [*SM indicates starting material]

stoichiometric equivalents, instead a NADP recycling system which employs glucose-6-phosphate (G6P) and glucose-6-phosphate dehydrogenase (G6PDH) was used.

Analytical reactions on a 50 μL scale were run along with a no enzyme controls to help discern what are enzymatic products versus reactions condition degradation products. Interestingly, the starting materials show different propensities for degradation as is evident when comparing starting material in just buffer versus starting material with the reaction components (see **Chapter 7** for experimental traces). The ester, amide, and desmethyl products appear to show a distinctive $[M+H]$ that is +9 from the starting material mass. It is still unclear what these products are however in the presence of enzyme, they seem to be produced in minimal quantities.

Analysis of the reactions with the PikAIII-TE were initially disappointing (**Figure 4.7**) The native pikromycin pentaketides (**green**) shows a distinctive product peak (whose retention time was verified with an authentic standard), however the five analogues showed no peaks containing either the expected $[M+H]$, $[M+Na]$, or $[M-18]$ peak that are often present when macrolactones are produced. The disappearance of starting material, however indicates that some enzymatic transformation is occurring. Further analysis of the reaction masses led to identification of peak masses that corresponding to an AIII extension, but hydrolysis instead of cyclization in the ester, amide, and desmethyl pentaketides ($[M+H] = 303, 302, 287$, **Figure 4.8**). Water mediated hydrolysis off of the thioesterase is a well-known competing process when it is incapable of cyclization, lending credence to the hypothesis that the thioesterase is often the “bottleneck” for

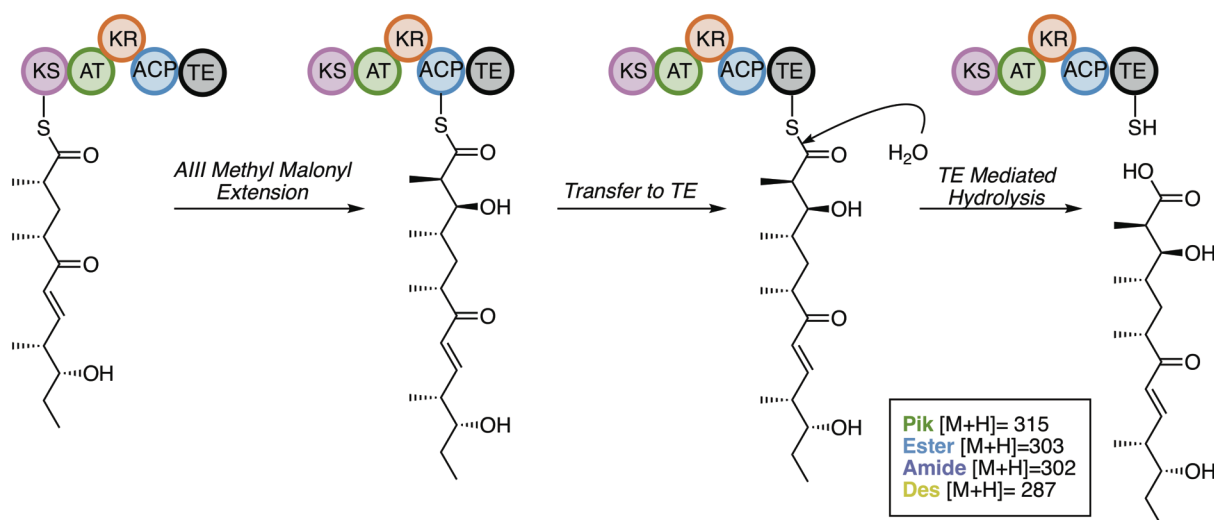


Figure 4.8 Mechanism of hydrolytic byproduct production in PikAIII-TE. Extension of the pentaketides by PikAIII and subsequent TE mediated hydrolysis gives the masses seen in the box for each of the unnatural substrates which correspond to those seen in **Figure 4.7**.

production of novel macrolactones. Analysis of the reactions with the dimethyl and cyclohexyl substituents show minimal, if any consumption of starting material, indicating that the PikAIII is unable to accept these larger substituents. This begins to shed light on the selectivity of PikAIII, which appears to rely heavily on the substituents proximal to the trans-thioesterification site.

4.3.2 Evaluation of Pentaketide Analogues with PikAIII/AIV

Despite to inability of PikAIII-TE to produce macrolactone products, the realization that PikAIII could accept the Ester, Amide, and Desmethyl pentaketides lend us to test them with the PikAIII/AIV system. This would give us insight into whether or not PikAIV would be capable of

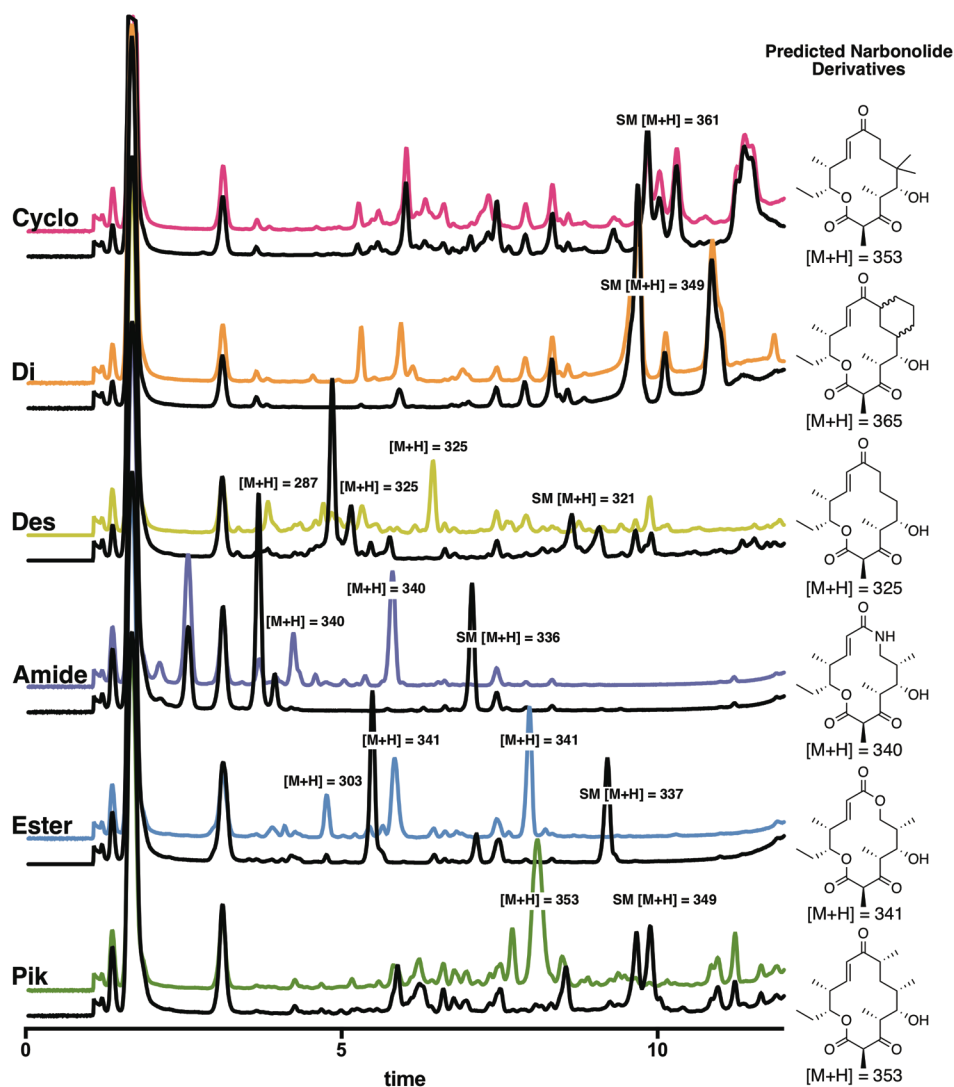


Figure 4.9 Analytical reaction traces with new pentaketides utilizing the PikAIII/AIV coupled system with the no enzyme controls for each being in black and the different enzymatic reactions being denoted in the various colors. [*SM indicates starting material]

accepting and processing them as well as the TE's ability to cyclize 12 versus 14 membered rings. The cyclohexyl and dimethyl analogues were tested as well, with the assumption that they would not be accepted even in the presence of PikAIV. The proteins were expressed and purified as described previously and the fidelity of them was tested using the pikromycin pentaketide. The results were as expected and showed a large peak that was verified to be narbonolide with an authentic standard (**Figure 4.9, Green**).

Analysis of the PikAIII/AIV reactions with the Ester, Amide, and Desmethyl pentaketides proved significantly different from those in the PikAIII-TE reactions. In this case, two peaks with the potential product mass were identified along with some extended, hydrolytic byproduct peaks for. Again, the dimethyl and cyclohexyl showed minimal consumption of starting material.

In order to determine if either of the two peaks corresponding to the product masses were in fact the desired macrolactones, the reactions were run on a 10 mg scale and the products isolated for complete characterization. In each case, the later of the two isobaric peaks was the desired macrolactone isolated in 32% yield, 25% yield and 12% yield for ester, amide, and desmethyl narbonolide derivatives (**Figure 4.10**). Unfortunately, the byproducts were not isolated in large

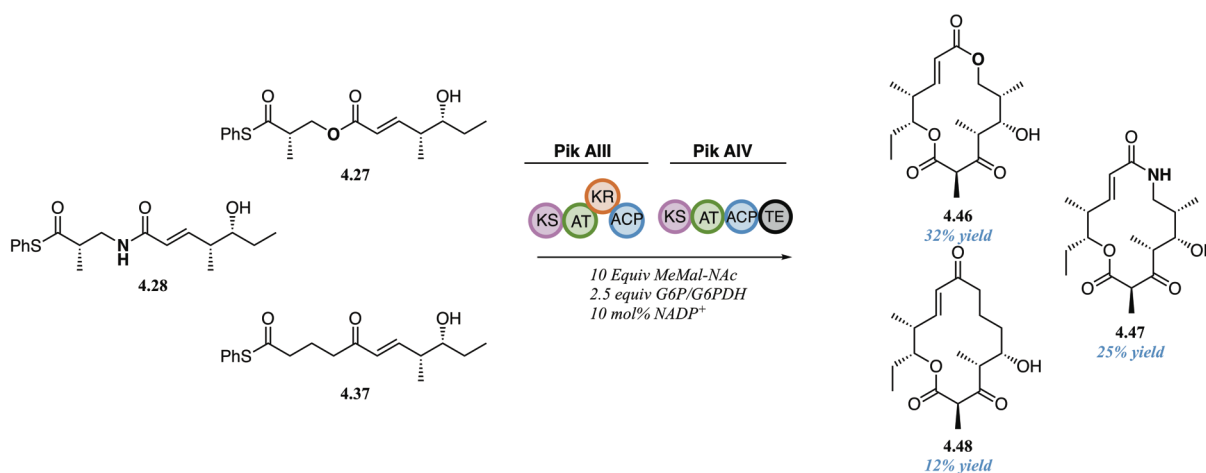


Figure 4.10 Semi-preparative Pik AIII/AIV scale ups of select pentaketides. Utilizing reaction conditions described and 3 μ M of each protein, the corresponding isolation yields were obtained.

enough quantities for full characterization however ongoing efforts to elucidate their structure are underway. Analysis of potential products based on chemical formula derived from the mass, indicates these could be one of a few possibilities. First, although polyketides are usually fairly specific for the stereoisomer they produce, it is possible that with unnatural analogues that alternate ones could be produced. Other potential products that would have the same mass are doubly

extended (PikAIII, PikAIV) hydrolytic products that have either hemiketalized or cyclized off another hydroxyl to produce a six membered macrolactone (**Figure 4.11**). Further characterization

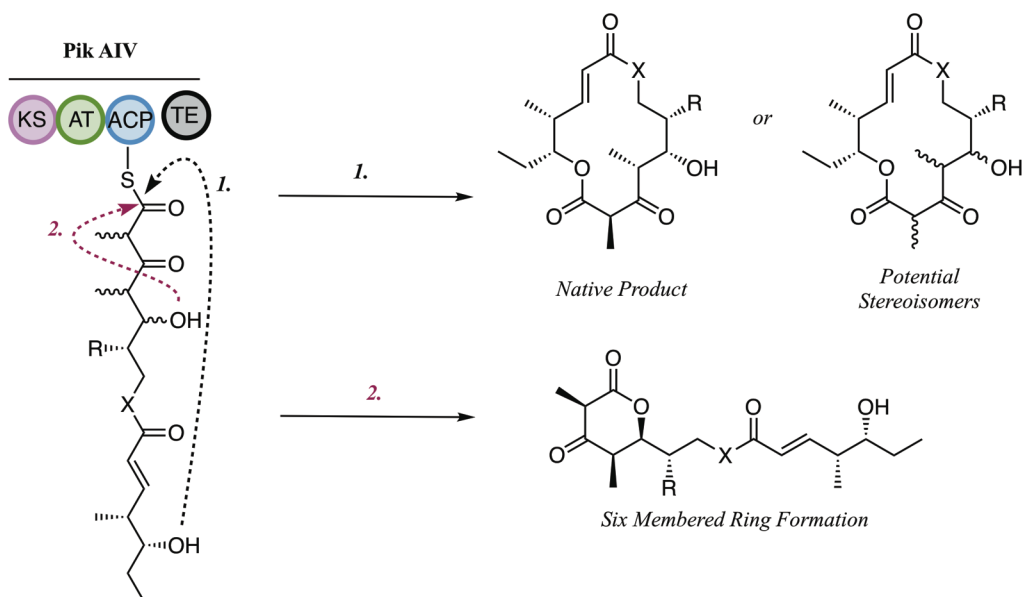


Figure 4.11 Potential isomeric macrolactone products produced by the Pik AIII/AIV system.

will hopefully shed light on these alternate products giving us more insight into the product dispersion.

4.3.3 Evaluation of Pentaketide Analogues with PikAIII-TE S148C Mutant

With our previous publication showing the effectiveness of the PikAIII-TE serine to cysteine mutant for the production of unnatural macrolactones we were cautiously optimistic that this variant may produce better results with the ester, amide, and desmethyl pentaketides. The fidelity of the PikAIII-TE S148C was tested using the pikromycin pentaketides, which shows a similar conversion to the desired product as the native PikAIII-TE (**Figure 4.11, Green**). Unfortunately, with these newly generated analogues, there was still no detection of masses consistent with potential products. What was observed was full conversion to of starting material to a variety of masses which are currently under investigation. For the ester containing pentaketide, the PikAIII-TE showed single extension and hydrolysis peak corresponding to an $[M+H]$ of 319, however in the PikAIII-TE S148C mutant we see conversion to three separate products with $[M+H] = 404, 356,$ and 298 (**Figure 4.11, Blue**), all of which can not be reconciled by any known or proposed byproducts of PKS reactions including dimerization of substrates, hemiketalization, 6

membered ring formation, and decarboxylation of hydrolyzed starting materials. The amide reaction showed production of a single discernable peak with a $[M+H] = 403$ (**Figure 4.11, Purple**), which likely corresponds to the same transformation seen in the analogous mass from the ester reaction. Lastly, the desmethyl reaction shows three new peaks however the actual $[M+H]$ mass is not readily identifiable as there are multiple fragmentation patterns in each peak. The dimethyl and cyclohexyl pentaketides were not run with these mutant proteins, as we have already established that the PikAIII can not accept these substrates making any consumption of starting material likely a TE mediated hydrolytic byproducts that are known to occur with this cysteine containing variant.

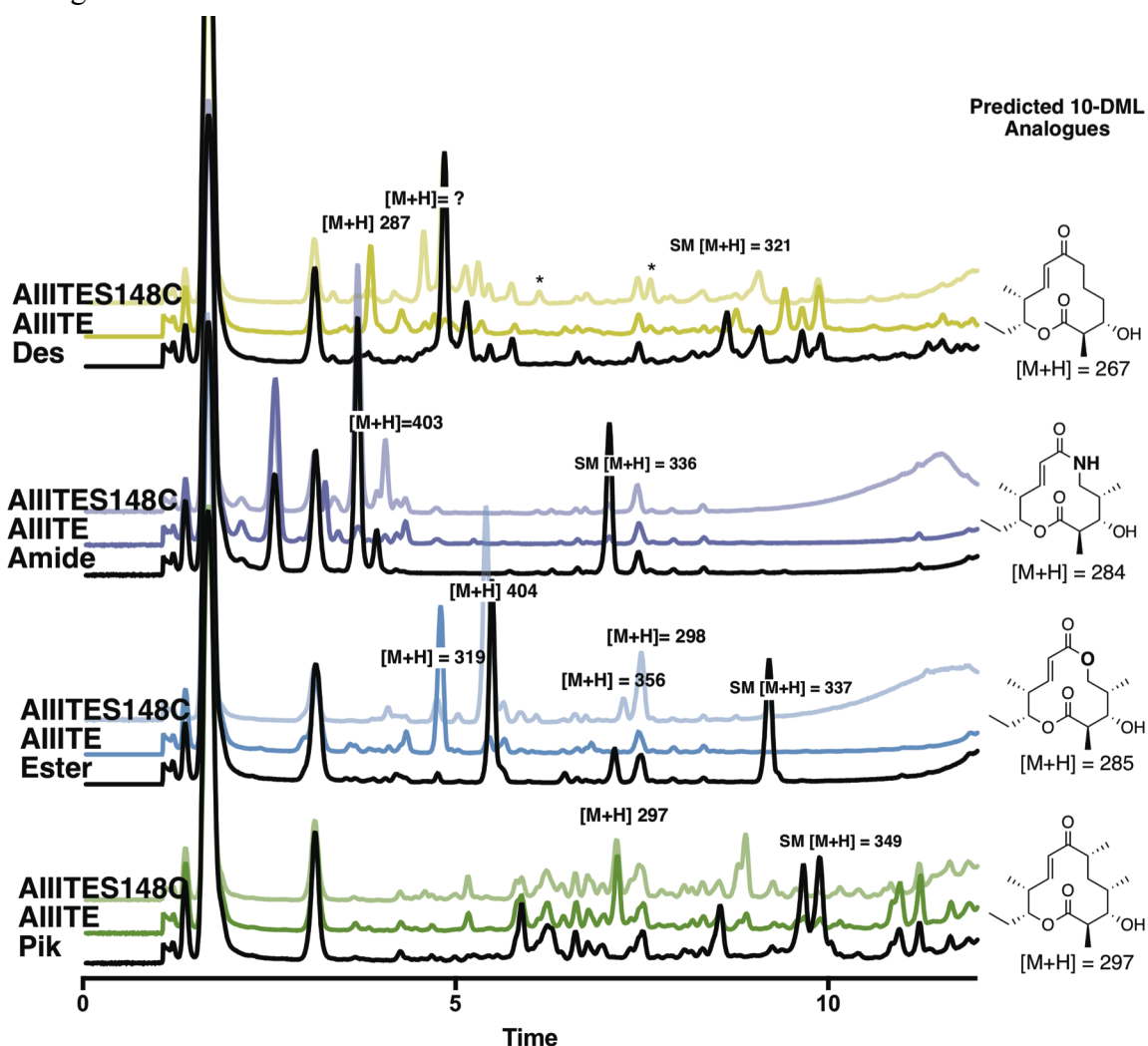


Figure 4.12 Comparison of analytical reactions with Ester, Amide, and Desmethyl Pentaketides against wildtype Pik AIII-TE S148C and Pik AIII-TE S148C. Black denoting the no enzyme control for each with the corresponding traces labeled.

4.4 References

1. Mcguire, J. M.; Bunch, R. L.; Anderson, R. C.; Boaz, H. E.; Flynn, E. H.; Powell, H. M.; Smith, J. W., Ilotycin, a New Antibiotic. *Antibiot Chemother* **1952**, 2 (6), 281-283.
2. Brockmann, H.; Henkel, W., Antibiotica Aus Actinomyceten .6. Pikromycin, Ein Bitter Schmeckendes Antibioticum Aus Actinomyceten. *Chem Ber-Recl* **1951**, 84 (3), 284-288.
3. Knowles, D. J. C.; Foloppe, N.; Matassova, N. B.; Murchie, A. I. H., The bacterial ribosome, a promising focus for structure-based drug design. *Curr Opin Pharmacol* **2002**, 2 (5), 501-506.
4. Poehlsgaard, J.; Douthwaite, S., The bacterial ribosome as a target for antibiotics. *Nature Reviews Microbiology* **2005**, 3 (11), 870-881.
5. Poehlsgaard, J.; Douthwaite, S., The macrolide binding site on the bacterial ribosome. *Curr Drug Targets Infect Disord* **2002**, 2 (1), 67-78.
6. Retsema, J.; Fu, W., Macrolides: structures and microbial targets. *Int J Antimicrob Agents* **2001**, 18 Suppl 1, S3-10.
7. Kannan, K.; Mankin, A. S., Macrolide antibiotics in the ribosome exit tunnel: species-specific binding and action. *Ann Ny Acad Sci* **2011**, 1241, 33-47.
8. Svetlov, M. S.; Vazquez-Laslop, N.; Mankin, A. S., Kinetics of drug-ribosome interactions defines the cidality of macrolide antibiotics. *P Natl Acad Sci USA* **2017**, 114 (52), 13673-13678.
9. Katz, L.; Ashley, G. W., Translation and protein synthesis: Macrolides. *Chem Rev* **2005**, 105 (2), 499-527.
10. Roberts, M. C., Update on macrolide-lincosamide-streptogramin, ketolide, and oxazolidinone resistance genes. *FEMS Microbiol Lett* **2008**, 282 (2), 147-59.
11. Maravic, G., Macrolide resistance based on the Erm-mediated rRNA methylation. *Curr Drug Targets Infect Disord* **2004**, 4 (3), 193-202.
12. Hansen, D. A.; Koch, A. A.; Sherman, D. H., Identification of a Thioesterase Bottleneck in the Pikromycin Pathway through Full-Module Processing of Unnatural Pentaketides. *J Am Chem Soc* **2017**, 139 (38), 13450-13455.
13. Hansen, D. A.; Rath, C. M.; Eisman, E. B.; Narayan, A. R.; Kittendorf, J. D.; Mortison, J. D.; Yoon, Y. J.; Sherman, D. H., Biocatalytic synthesis of pikromycin, methymycin, neomethymycin, novamethymycin, and ketomethymycin. *J Am Chem Soc* **2013**, 135 (30), 11232-8.
14. Koch, A. A.; Hansen, D. A.; Shende, V. V.; Furan, L. R.; Houk, K. N.; Jimenez-Oses, G.; Sherman, D. H., A Single Active Site Mutation in the Pikromycin Thioesterase Generates a More Effective Macrocyclization Catalyst. *J Am Chem Soc* **2017**, 139 (38), 13456-13465.
15. Lowell, A. N.; DeMars, M. D.; Slocum, S. T.; Yu, F. A.; Anand, K.; Chemler, J. A.; Korakavi, N.; Priessnitz, J. K.; Park, S. R.; Koch, A. A.; Schultz, P. J.; Sherman, D. H., Chemoenzymatic Total Synthesis and Structural Diversification of Tylactone-Based Macrolide Antibiotics through Late-Stage Polyketide Assembly, Tailoring, and C-H Functionalization. *J Am Chem Soc* **2017**, 139 (23), 7913-7920.
16. Mortison, J. D.; Kittendorf, J. D.; Sherman, D. H., Synthesis and biochemical analysis of complex chain-elongation intermediates for interrogation of molecular specificity in the erythromycin and pikromycin polyketide synthases. *J Am Chem Soc* **2009**, 131 (43), 15784-93.
17. Weissman, K. J., Genetic engineering of modular PKSs: from combinatorial biosynthesis to synthetic biology. *Nat Prod Rep* **2016**, 33 (2), 203-30.

18. Whicher, J. R.; Smaga, S. S.; Hansen, D. A.; Brown, W. C.; Gerwick, W. H.; Sherman, D. H.; Smith, J. L., Cyanobacterial Polyketide Synthase Docking Domains: A Tool for Engineering Natural Product Biosynthesis. *Chem Biol* **2013**, *20* (11), 1340-1351.
19. Tang, Y. Y.; Kim, C. Y.; Mathews, I. I.; Cane, D. E.; Khosla, C., The 2.7-angstrom crystal structure of a 194-kDa homodimeric fragment of the 6-deoxyerythronolide B synthase. *P Natl Acad Sci USA* **2006**, *103* (30), 11124-11129.
20. Whicher, J. R.; Dutta, S.; Hansen, D. A.; Hale, W. A.; Chemler, J. A.; Dosey, A. M.; Narayan, A. R. H.; Hakansson, K.; Sherman, D. H.; Smith, J. L.; Skiniotis, G., Structural rearrangements of a polyketide synthase module during its catalytic cycle. *Nature* **2014**, *510* (7506), 560-+.
21. Dutta, S.; Whicher, J. R.; Hansen, D. A.; Hale, W. A.; Chemler, J. A.; Congdon, G. R.; Narayan, A. R. H.; Hakansson, K.; Sherman, D. H.; Smith, J. L.; Skiniotis, G., Structure of a modular polyketide synthase. *Nature* **2014**, *510* (7506), 512-+.
22. Smith, J. L.; Skiniotis, G.; Sherman, D. H., Architecture of the polyketide synthase module: surprises from electron cryo-microscopy. *Curr Opin Struct Biol* **2015**, *31*, 9-19.
23. Jung, W. S.; Jeong, S. J.; Park, S. R.; Choi, C. Y.; Park, B. C.; Park, J. W.; Yoon, Y. J., Enhanced heterologous production of desosaminyl macrolides and their hydroxylated derivatives by overexpression of the pikD regulatory gene in *Streptomyces venezuelae*. *Appl Environ Microb* **2008**, *74* (7), 1972-1979.
24. Jung, W. S.; Lee, S. K.; Hong, J. S. J.; Park, S. R.; Jeong, S. J.; Han, A. R.; Sohng, J. K.; Kim, B. G.; Choi, C. Y.; Sherman, D. H.; Yoon, Y. J., Heterologous expression of tylosin polyketide synthase and production of a hybrid bioactive macrolide in *Streptomyces venezuelae*. *Appl Microbiol Biot* **2006**, *72* (4), 763-769.
25. Hansen, D. A.; Koch, A. A.; Sherman, D. H., Substrate Controlled Divergence in Polyketide Synthase Catalysis. *J Am Chem Soc* **2015**, *137* (11), 3735-3738.

Chapter 5

Summary, Discussion, and Future Directions

Polyketides and non-ribosomal peptide synthases natural products are structurally diverse compounds that display a wealth of pharmacological activities. My graduate work has been focused on combining synthetic chemistry and biosynthetic enzymes in order to probe the ability to utilize these enzymes for the chemoenzymatic production of natural products and natural product analogues. The full scope of this work hopes to combine biochemical data on selectivity of biosynthetic enzymes for unnatural substrates with high resolution structural characterization. With a detailed understanding of the selectivity and reaction mechanisms of these enzymes, we can design more general biocatalysts for the production of large libraries of natural products, aiding in not only the drug discovery process, but hopefully the production scale use of chemoenzymatic methods as well. This chapter will summarize the findings of the three projects I worked on for my dissertation as well as discuss continuing and future work towards our ultimate goal of understanding these complex systems well enough to engineer broad scope biocatalysts.

5.1 Biocatalytic Synthesis of Cryptophycin Anticancer Agents

5.1.1 Summary and Discussion of Work Completed

The implementation of a biocatalytic synthesis for the production of cryptophycin anticancer agents has led to two important discoveries including previously unknown structural features that retain pico molar activity and may help modulate toxicity and efficacy as well as important insights into the continued characterization of biosynthetic enzymes. Despite the extensive SAR that was completed for these molecules prior to clinical trials in 2002, a distinct lack of heterocyclic functionality was investigated in unit A, presumably due to the deleterious effects seen with replacing the benzyl group with either a thiophene or furan ring. Despite these failures we saw this as a unique opportunity to not only fill a gap in the SAR of these molecules, but to continue the exploration of a biosynthetic enzyme of interest, the CrpTE. This enzyme has

previously been shown to be flexible to changes in the amino acid portion, however it showed a complete change in selectivity, from productive cyclization to non-productive hydrolysis with the removal of the aryl group.¹ At the time, it remained unclear how alternative starter units would affect the downstream ability of the thioesterase to process these substrates.

Development of a diversifiable synthesis that was amenable to large scale formulation (tens of grams) of the cryptophycin chain elongation intermediate facilitated the production of a library of nine initial heterocyclic unit A analogues. These were assayed with the CrpTE on analytical scale with incredibly promising initial results. All the analogues showed comparable or greater turnover to product. This trend was confirmed upon semi-preparative scale up to 10 mg and isolation of the corresponding macrocycles which proceeded in 49 - 69% in comparison to that of the natural analogues at 49%. The initial hypothesis derived from these observations centered on solubility of the substrate. It is evident from the retention times on the TOF-MS analysis that many of these were more soluble than their benzyl counterpart, however this does not appear to explain all the data presented as a deeper investigation into the concentration dependence on turnover indicated that even well below the solubility threshold, the native substrate never produced turnover numbers higher than 80%. It is currently unclear what factors may produce this interesting result however, utilizing current and future structural studies, described in **Chapter 3** we hope to shed light on this phenomenon.

With our initial nine cryptophycin analogues in hand, we in collaboration with Dr. Frederik Valeriote at the Henry Ford Health Center, investigated the effects on IC₅₀ in HCT 116 human colorectal cancer cells. These results produced three interesting leads with one, the 4-methyl pyrazole being far superior to rest. This compound showed an IC₅₀ of 10 pM in this cell line. In order to do a head to head comparison, cryptophycin 52 (the one used by Eli Lilly for clinical trials) showed an IC₅₀ value of 3.3 pM, indicating our analogue is equipotent. The most interesting discovery with this compound is that it achieves this potency as the styrene derivative. The β epoxy functionality found on all the most potent derivatives previously described indicate that this is necessary for maximum potency, showing between a 100 and 1000-fold difference in potency. This discovery could have important implications for this molecule in the clinic as the epoxide has long been speculated to be partially responsible for the excessive neurotoxicity seen with these compounds. Although this is by far the most interesting compound, the 3-methylpyrazole and the 4-methyl pyrazole also shown picomolar IC₅₀ values, making them also more potent than the

majority of styrene analogues. These all have basic nitrogen's likely placed in similar orientations in chemical space indicating these may be forming a previously unknown interaction upon binding to β tubulin. Further structural work and/or docking studies would be necessary to confirm this.

With the exciting results from the analogues generated by the CrpTE we wanted to expand our chemoenzymatic synthesis to utilizing the CrpE, the P450 responsible for the installation of the β epoxide. Although it was exciting to identify a new analogue with low picomolar activity lacking this group, the majority of the analogues still of interest as warheads for antibody drug conjugates, contain this epoxide functionality, which is notoriously difficult to install. Having an active biocatalyst that can work on a variety of substrates could be of great use in formulating some of these analogues currently. With that we set out to gain active protein and test it for activity with our current analogues. Although these results are not as exciting, with the P450 being able to formulate presumed products for only a few of the analogues, it gives us some information on the current scope of this catalyst. Likely, as the aryl rings are conjugated to the double bond being epoxidized, electronics plays a huge factor in whether or not this can act upon a substrate.

5.1.2 Future Directions

With the discovery of this new, equipotent, styrene analogue continued investigations into its viability as a clinical candidate need to be explored. We are currently working with Dr. Valeriote at the Henry Ford Health Center to run maximum tolerated dose (MTD) studies in order to run a future PK examination of this analogue. It should also be screened more extensively for IC_{50} values in a variety of cancer cell lines, including a more thorough examination of resistant cell lines as that may be where this holds the most promise.

Cryptophycins are currently being extensively analyzed as antibody drug conjugates (ADCs) which could also be an interesting avenue of exploration for this analogue. The methyl pyrazole aryl ring contains a methyl amine functionality which could be replaced or utilized as an alternative linking region for these molecules. Currently, as the cryptophycins don't contain any readily linkable functional groups, a benzyl amine is utilized to facilitate this without deleterious effects. Although many of these ADCs have been made and patented, they have yet to show up in the clinic indicating that they have not been as effective as previously hoped, potentially due to issues with warhead efficacy. Utilizing our analogue, without the epoxide, may show better efficacy and facilitate the continued development of these treatments.

5.2 Structural and Mechanistic Insights into the CrpTE

5.2.1 Summary and Discussion of Work Completed

With the exciting results from **Chapter 2**, our interest in the structural and mechanistic features of the CrpTE led to a collaboration with both Dr. John Lutz at Eli Lilly and Dr. Janet Smith's lab at the University of Michigan in hopes of solving a crystal structure of this fascinating enzyme. After numerous attempts over the past decade, we knew undertaking this again was going to require significant efforts. Utilizing numerous servers and prediction software, we identified a number of regions that could be problematic for crystal packing. Utilizing this knowledge, we designed and constructed numerous mutant CrpTE plasmids. These were all expressed, purified and screened for crystallization. Despite two initial hits, with two separate constructs, numerous counter screens to date, have not produced any viable crystals for x-ray diffraction. Despite this failure, a crucial discovery came during the purification of these mutant proteins which indicated two of the constructs were almost exclusively monomeric, whereas the others showed different dispersions of monomer and dimer as high as 2:1. This discovery facilitated a new collaboration with Dr. Vivekanandan Subramanian in biophysics, with the hopes of being able to utilize NMR to gain a solution phase structure of the CrpTE. Initial experiments looking at the stability, solubility, and tumbling of the CrpTE proved that it was an excellent candidate for further characterization. As this protein is large for the capabilities of NMR, at 35 KD, multiple three-dimensional experiments, containing different ^{15}N , ^{13}C , and ^2H labeling patterns is required in order to gather enough data to unambiguously assign each atom in this protein with its corresponding NMR signal. These proteins have been formulated and the experiments run, with excellent resolution. Although this work has not been complete, the data has been collected and it is a matter of fitting the pieces together in order to complete the assignments.

5.2.2 Future Directions

Once the assignments for the protein have been made, we must utilize the J values acquired from these experiments to build a three-dimensional model of the CrpTE in order to gain a structure. Once this has been completed we will have the unique opportunity to explore the dynamics of this protein using our synthesized substrates. Despite a number of crystal structures to date of type I TEs, there are no NMR structures and none of the crystal structures contain full

length substrate. A few utilized a substrate mimic affinity probes as well as docking/modeling studies in order to gain insight into the binding orientation, however these are only able to speculate about the mechanism of cyclization. Using the NMR we are able to titrate in substrate and visualize the changes in both the protein backbone and sidechains (depending on the labeling pattern). Using these shift perturbations, we should be able to build a model of the changes in pose of this enzyme as it facilitates macrocyclization.

5.2 Molecular Interrogation of Polyketide Synthase Modules in the Pikromycin Biosynthetic Pathway

5.2.1 Summary and Discussion of Work Completed

Engineering of polyketide synthase modules has the ability to produce almost limitless structural modifications, however studies toward this goal have shown that a detailed understanding of these systems and their selectivity will be required to accomplish this. With the successful reconstitution of the PikAIII-TE and PikAIII/AIV modules, we began to focus on formulating “unnatural” pentaketides to interrogate these further and hopefully produce the corresponding macrocycles. In accordance with our goals, five new pentaketides were synthesized and tested with these proteins as well as the PikAIII-TE S148C variant that has previously been shown to facilitate macrolactone production where the wild type failed.

Initial examination of the ester, amide, and desmethyl pentaketides (**4.27**, **4.28**, and **4.37**) with the PikAIII-TE construct indicated that the PikAIII could accept and process these, formulating the extended product, however the TE was not able to cyclize them to macrolactones and only produced hydrolytic byproducts. Running the same assay with the dimethyl and cyclohexyl pentaketides showed no meaningful conversion of starting material by enzymatic conversion indicating these larger groups are unable to be accepted by the PikAIII.

Despite not producing macrolactones, we continued examining these analogues with PikAIII/AIV in order to gain insight into the ability of PikAIV to produce products. The ester, amide, and desmethyl pentaketides again showed consumption of starting material, however with this system, two peaks with the product mass were observed. Scale up reactions of 10 mg were run in hopes of isolating both products, however only the later of the two peaks in all cases (produced

in significantly greater yield) contained significant product for full characterization. These were determined to be 14 membered macrolactones although we only assume the stereochemistry is as expected. Further analysis of these will need to be done in order to confirm the relative stereochemistry is as expected. The other peak corresponding to product mass has not been fully characterized for any of the three products however analysis of mass and hydrogen spectra indicate it may be a six membered macrolactone. Without full characterization this is only speculation and there are other structures that could potentially produce the same mass, however six membered macrolactones do have some precedence. Although it is unknown if this byproduct is TE catalyzed or spontaneous, previous work with triketides have shown that formation of a six membered ring at a rate significantly above a spontaneous are produced in the presence of a TE indicating this is likely a protein mediated process. Testing of the dimethyl and cyclohexyl pentaketides again showed no meaningful consumption of starting material as expected again indicating these are too large for the PikAIII KS to load.

Finally, we tested the PikAIII-TE S148C variant that has previously been shown to facilitate macrolactone production. Analysis of these reactions did not produce peaks that contained a mass consistent with product production. There are a number of produced products, however none are reconcilable with known byproduct pathways. Interestingly both the ester and amide show a peak that corresponds to the same transformation, which is [+ 119] from the product. In the DEBS TE, dimerize substrate has been observed, which could account for the significantly higher mass present here, however no combination of two pentaketides produces this mass (cyclized, dimerized substrate has an $[M+H] = 453$). Further characterization will be necessary to determine what is being produced by this TE variant and may shed light on interesting potential byproducts.

5.2.2 Future Directions

This work is still in the middle stages of completion and requires synthetic work and enzymatic follow up to complete the story and answer some of the questions that have been identified thus far. Full characterization of the products being produced for the ester, amide, and desmethyl substrates with all three proteins is needed to fully understand the limitations of these enzymes as well as continued work on the synthetic substrates that have not been realized in **Figure 4.6**. These studies will continue to shed light on the selectivity of the KS for alternative head groups

as well as the TEs ability to formulate macrolactones with esters/amides in different positions in the ring. Formulation of homologated pentaketides for examination with the PikAIII-TE and PikAIII/AIV may indicate size constraints as well as show that odd membered rings are possible for bacterial TEs (previously these have only been seen in very limited numbers in fungal pathways).

All the newly formulated pentaketides can also be tested with a second reconstituted system, the JuvE5 and JuvE6 from the juvenimycin pathway.² This system natively accepts a hexaktide and produces the core macrolactone (tylactone) of a well-known, veterinary antibiotic tylosin. Recently, our lab has discovered that this system is capable of accepting and processing the pik pentaketide into a 14 membered ring analogous to narbonolide except this one contains for a C3 reduction. Substitution of the native TE with the TE from the DEBS system has shown exceptional turnover to product with isolation yields of 42% (unpublished data). Utilizing the same JuvE5 and JuvE6 fusion protein, we can assay our pentaketides analogues with this system to gain insight into its selectivity.

The next facet of this project will focus on taking the macrolactones produced by this substrate manipulation and utilizing our *Streptomyces venezuelae* biotransformation strains to hopefully construct the corresponding macrolide antibiotics. These can then be tested with a wide range of bacterial pathogens for activity, further establishing this means of antibiotic discovery.

5.4 Contributions to the Understanding of PKS Pathways for use in Combinatorial Biosynthesis

With the continued interest in natural products as drug leads, alternative strategies that reconcile the continued desire for medicinal chemistry efforts with the difficulties in synthesizing these molecules would play a profound role in the drug discovery world. The idea of engineering biosynthetic pathways in a strategy termed combinatorial biosynthesis has long been postulated to be capable of producing almost unlimited structural modifications to natural product scaffolds, facilitating the inexpensive and rapid production of libraries of “unnatural” natural products that can shed light on SAR and impart better drug properties on molecules of interest. Despite some notable examples, this strategy has largely met with failure presumably because we currently only have a limited understanding of the complex factors that govern the selectivity and specificity of

each catalytic domain. In both the cryptophycin pathway and the pikromycin pathway summarized above, we have used a mixture of biochemical analysis with structural interrogation to shed light on different facets of the catalytic cycle that are likely hindering the ability to utilize genetic recombination to formulate new products. Utilizing this knowledge, we envision being able to use mutagenesis both rationally, gained from the structural investigations, and in the form of directed evolution to engineer these proteins to accept and process substrates that are currently out of reach. Once optimized proteins of interest have been identified these can be screened again in an *in vitro* setting as broader scope catalysts with synthetic precursors and/or be reincorporated into the full biosynthetic pathways, pushing the field closer to realizing the vast amounts of products that can potentially be accessed through genetic engineering.

References

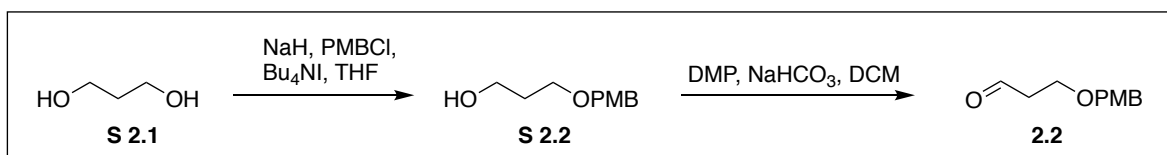
1. Beck, Z. Q.; Aldrich, C. C.; Magarvey, N. A.; Georg, G. I.; Sherman, D. H., Chemoenzymatic synthesis of cryptophycin/arenastatin natural products. *Biochemistry-US* **2005**, *44* (41), 13457-13466.
2. Lowell, A. N.; DeMars, M. D.; Slocum, S. T.; Yu, F. A.; Anand, K.; Chemler, J. A.; Korakavi, N.; Priessnitz, J. K.; Park, S. R.; Koch, A. A.; Schultz, P. J.; Sherman, D. H., Chemoenzymatic Total Synthesis and Structural Diversification of Tylactone-Based Macrolide Antibiotics through Late-Stage Polyketide Assembly, Tailoring, and C-H Functionalization. *J Am Chem Soc* **2017**, *139* (23), 7913-7920.

Chapter 6

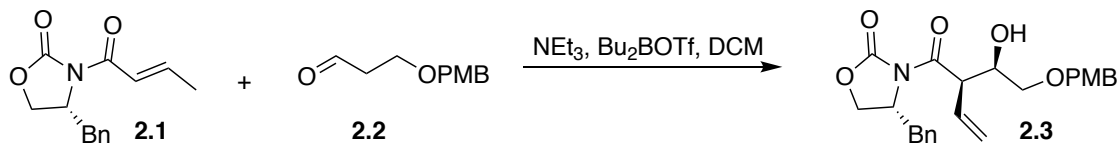
Cryptophycin Experimentals

6.1 Chemical Synthesis of *Seco* Cryptophycin Analogues

6.1.1 Unit A Synthetic Procedures and Characterization

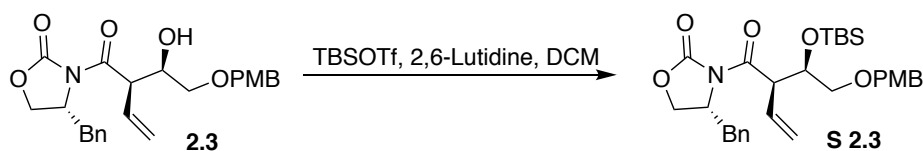


2 was synthesized over two steps from commercially available **S1**, all spectra were in accordance with previous literature.¹⁻²



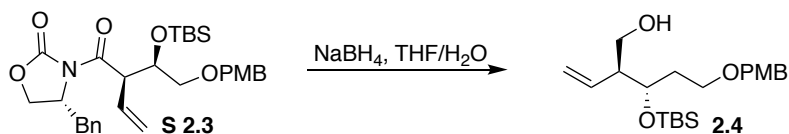
(R)-4-benzyl-3-((2R,3S)-3-hydroxy-5-((4-methoxybenzyl)oxy)-2-vinylpentanoyl)oxazolidin-2-one (2.3). To a flame dried three neck flask under N₂ was added a stirred solution of imide **2.1** (7.5 g, 30.58 mmol, 1 eq) in CH₂Cl₂ (305 mL, 0.1 M) and treated with dibutylboron trifluoromethanesulfonate (1M in DCM, 33.64 mL, 33.64 mmol, 1.1 eq) at -78 °C. After stirring for 5 min, the mixture was treated with Et₃N (6.02 mL, 42.81 mmol, 1.4 eq), then kept for 1 h at -78 °C, and 20 min at 0 °C. The reaction was re-cooled to -78 °C and treated with a solution of the aldehyde **2.2** (8.31 g, 42.81 mmol, 1.4 eq) in CH₂Cl₂ (25 mL). The reaction was kept for 1 h at -78 °C, then warmed to 0 °C for 1 h. The reaction was quenched by addition of pH 7 buffer (30 mL) followed by MeOH (30 mL), keeping temperature > 5 °C. After 5 min, 30% H₂O₂ (30 mL) was added and the mixture stirred for 1 h at 0 °C. Organics were removed under reduced pressure and the remaining aqueous layer was extracted with EtOAc (3 x 100 mL). The organic phase was washed with 1 N HCl, 5% aq NaHCO₃, brine, dried over Na₂SO₄, and concentrated. The crude

product was purified by flash chromatography (33% EtOAc/Hexanes) to give **2.3** (11.98 g, 89% yield) as a clear and colorless oil: $R_f = 0.2$ (33% EtOAc/Hexanes); $^1\text{H NMR}$ (600 MHz, CDCl_3) δ 7.31 (ddd, $J = 7.4, 6.4, 1.3$ Hz, 2H), 7.28 – 7.25 (m, 2H), 7.24 – 7.21 (m, 2H), 7.20 – 7.15 (m, 2H), 6.04 (dddd, $J = 17.6, 10.0, 9.0, 1.1$ Hz, 1H), 5.39 – 5.36 (m, 1H), 5.36 – 5.34 (m, 1H), 4.68 (ddt, $J = 11.4, 6.3, 3.0$ Hz, 1H), 4.58 – 4.51 (m, 1H), 4.42 (s, 2H), 4.25 – 4.19 (m, 1H), 4.18 – 4.11 (m, 2H), 3.78 (d, $J = 1.1$ Hz, 3H), 3.69 – 3.64 (m, 1H), 3.64 – 3.56 (m, 1H), 3.28 – 3.17 (m, 1H), 2.74 (dd, $J = 13.4, 9.5$ Hz, 1H), 1.93 – 1.78 (m, 1H), 1.74 (dt, $J = 14.5, 7.0$ Hz, 1H), 1.55 (s, 2H); $^{13}\text{C NMR}$ (150 MHz, CDCl_3) δ 173.46, 159.19, 152.90, 135.04, 131.67, 130.14, 129.42, 129.30, 128.91, 127.35, 121.00, 113.78, 72.87, 70.54, 67.74, 65.95, 55.25, 55.17, 52.53, 37.58, 33.87; **HRMS** (ESI) calcd for $\text{C}_{25}\text{H}_{29}\text{NO}_6$ [$\text{M}+\text{Na}$] 462.1887, found 462.1885.



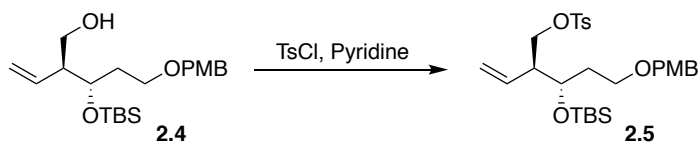
(R)-4-benzyl-3-((2R,3S)-3-((tert-butyldimethylsilyloxy)-5-((4-methoxybenzyloxy)-2-vinylpentanoyl)oxazolidin-2-one)-2-hydroxypropyl)oxazolidin-2-one (S 2.3). To a solution of **3** (17.56 g, 39.9 mmol, 1 eq) and 2,6-lutidine (46.28 mL, 79.9 mmol, 2 eq) in CH_2Cl_2 (135 mL, 0.3 M) was added *tert*-butyldimethylsilyl trifluoromethane sulfonate (11.6 mL, 59.9 mmol, 1.5 eq) and the solution was stirred at rt for 18h. The mixture was quenched with H_2O (100 mL), stirred for 30 min, and the extracted with CH_2Cl_2 (3 x 100 mL). The organic phase was washed with 1 N HCl, sat. aq NaHCO_3 , brine, dried over Na_2SO_4 , and concentrated. The crude product was purified by flash chromatography (20% EtOAc/Hexane) to give **S 2.3** (17.22 g, 78% yield) as a pale yellow oil: $R_f = 0.6$ (33% EtOAc/Hexanes); $^1\text{H NMR}$ (400 MHz, CDCl_3) δ 7.33 – 7.26 (m, 3H), 7.25 (d, $J = 8.8$ Hz, 2H), 7.18 (d, $J = 6.9$ Hz, 2H), 6.85 (d, $J = 8.6$ Hz, 2H), 6.00 (ddd, $J = 9, 9.3, 18.2$ Hz, 1H), 5.27 (d, $J = 10.2$ Hz, 1H), 5.26 (d, $J = 18.1$ Hz, 1H), 4.58 (dd, $J = 6.6$ Hz, 8.8 Hz, 1H), 4.56 – 4.52 (m, 1H), 4.41 (d, $J = 11.4$ Hz, 1H), 4.36 (d, $J = 11.5$ Hz, 1H), 4.21 (td, $J = 5.2$ Hz, 6.4 Hz, 1H), 4.05 (dd, $J = 2$ Hz, 9.2 Hz, 1H), 3.86 (t, $J = 8.2$ Hz, 1H), 3.78 (s, 3H), 3.59 (td, $J = 6.5, 9.2$ Hz, 1H), 3.48 (dt, $J = 6.2, 9.4$ Hz, 1H), 3.23 (dd, $J = 3.0, 13.4$ Hz, 1H), 2.70 (dd, $J = 9.7, 13.4$ Hz, 1H), 1.95 – 1.85 (m, 2H), 0.86 (s, 9H), 0.02 (s, 3H), 0.01 (s, 3H); $^{13}\text{C NMR}$ (100 MHz, CDCl_3) δ 172.62, 159.24, 153.02, 135.58, 134.24, 130.86, 129.68, 129.49, 129.10, 127.48, 127.48, 119.70, 113.86, 72.77,

71.29, 66.03, 65.94, 55.66, 55.48, 53.39, 37.73, 35.47, 26.02, 18.22, -4.23, -4.38; **HRMS** calcd for C₃₁H₄₃NO₆Si [M+Na] 576.2752, found 576.2767



(2*S*,3*S*)-3-((*tert*-butyldimethylsilyloxy)-5-((4-methoxybenzyloxy)-2-vinylpentan-1-ol (2.4).

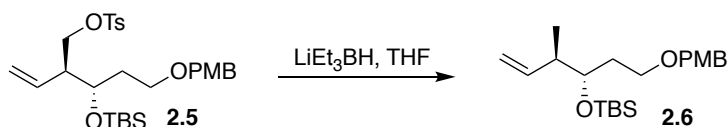
To a stirred solution of **S2.3** (17.22 g, 31.14 mmol, 1 eq) in THF (625 mL, 0.05M) was added a solution of NaBH₄ (5.89 g, 155.7 mmol, 5 eq) in H₂O (240 mL) at 0 °C. The reaction mixture was stirred at 0 °C for 5 min, warmed to rt, and stirred for 5 h. The reaction was quenched by the addition of sat. aq NH₄Cl solution (200 mL) and the mixture stirred at rt for 1 h. The THF was removed under reduced pressure and the aqueous layer was extracted with EtOAc (3 x 75 mL), organics combined, washed with brine, dried over Na₂SO₄, and concentrated. The crude product was purified by flash chromatography (18% EtOAc/Hexanes) to afford **2.4** (10.04 g, 85% yield) as a colorless oil; R_f = 0.25 (20% EtOAc/Hexanes); ¹H NMR (400 MHz, CDCl₃) δ 7.25 (d, *J* = 8.5 Hz, 2H), 6.88 (d, *J* = 8.6 Hz, 2H), 5.71 (ddd, *J* = 17.3, 10.4, 8.6 Hz, 1H), 5.18 (dd, *J* = 10.5, 2.0 Hz, 1H), 5.10 (d, *J* = 17.4 Hz, 1H), 4.43 (d, *J* = 11.5 Hz, 1H), 4.38 (d, *J* = 11.5 Hz, 1H), 3.99 (dd, *J* = 12.7, 3.0 Hz, 0H), 3.80 (s, 3H), 3.75 (dt, *J* = 10.8, 6.6 Hz, 1H), 3.61 (ddd, *J* = 11.0, 7.0, 5.0 Hz, 1H), 3.46 (t, *J* = 6.5 Hz, 2H), 2.50 – 2.35 (m, 1H), 2.15 (t, *J* = 5.7 Hz, 1H), 1.88 – 1.70 (m, 2H), 0.88 (s, 9H), 0.09 (s, 3H), 0.06 (s, 3H); ¹³C NMR (100 MHz, CDCl₃) δ 159.28, 135.60, 130.61, 129.41, 118.67, 113.89, 72.72, 71.06, 66.63, 63.67, 55.43, 51.34, 34.11, 25.98, 18.14, -4



(5*S*,6*S*)-5-(2-((4-methoxybenzyloxy)ethyl)-2,2,3,3,9,9,10,10-octamethyl-6-vinyl-4,8-dioxo-

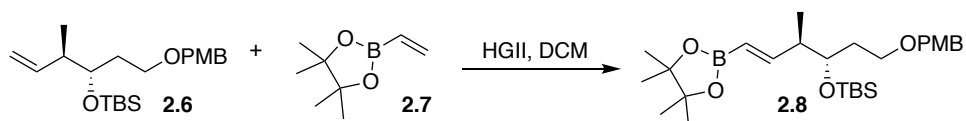
3,9-disilaundecane (2.5).³⁻⁴ To a stirred solution of alcohol (9.81 g, 25.78 mmol, 1 eq) in dry pyridine (250 mL, 0.1 M) was added *p*-toluenesulfonyl chloride (7.37 g, 38.66 mmol, 1.5 eq) at 0 °C. The mixture was warmed to rt and stirred for 4 h prior to re-cooling to 0 °C. The reaction was quenched by the slow addition of 0.5 N HCl (300 mL). The aqueous layer was extracted with diethyl ether (3 x 200 mL), organics combined, washed with 1 M HCl, brine, dried over Na₂SO₄, and concentrated. The residue was purified using a silica plug (18% EtOAc/Hexanes) to afford **2.5**

(11.67 g, 84.6% yield) as a colorless oil: $R_f = 0.4$ (20% EtOAc/Hexanes); $^1\text{H NMR}$ (400 MHz, CDCl_3) δ 7.75 (d, $J = 8.4$ Hz, 2H), 7.30 (d, $J = 8.4$ Hz, 2H), 7.21 (d, $J = 8.4$ Hz, 2H), 6.86 (d, $J = 8.4$ Hz, 2H), 5.58 (ddd, $J = 8.7, 10.3, 17.3$ Hz, 1H), 5.12 (dd, $J = 1.2, 9.2$ Hz, 1H), 5.04 (d, $J = 17.2$ Hz, 1H), 4.39 (d, $J = 11.6$ Hz, 1H), 4.33 (d, $J = 11.6$ Hz, 1H), 4.08 (dd, $J = 6.6, 9.4$ Hz, 1H), 3.94 (dd, $J = 7.4, 9.4$ Hz, 1H), 3.93 – 3.89 (m, 1H), 3.79 (s, 3H), 3.35 (t, $J = 6.4$ Hz, 2H), 2.46 – 2.42 (m, 1H), 2.42 (s, 3H), 1.74 – 1.57 (m, 2H), 0.78 (s, 9H), -0.01 (s, 3H), -0.05 (s, 3H); $^{13}\text{C NMR}$ (100 MHz, CDCl_3) δ 159.30, 144.80, 133.44, 133.15, 130.53, 129.91, 129.39, 128.14, 119.79, 113.92, 72.73, 70.54, 68.83, 66.36, 55.43, 48.61, 34.64, 25.91, 21.77, 18.11, -4.25, -4.69; **HRMS** (ESI) calcd for $\text{C}_{28}\text{H}_{42}\text{O}_6\text{SSi}$ [$\text{M}+\text{H}$] 534.2471, found 534.269.

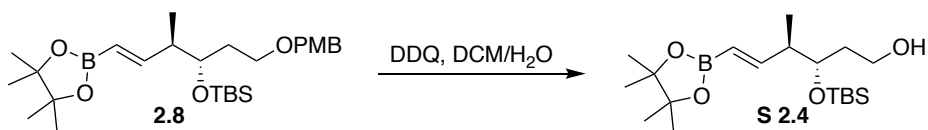


***tert*-butyl(((3*S*,4*R*)-1-((4-methoxybenzyl)oxy)-4-methylhex-5-en-3-yl)oxy)dimethylsilane**

(2.6).⁵ To a flame dried round bottom flask under N_2 was added tosylate **2.5** (3.72 g, 6.96 mmol, 1 eq) in dry THF (70 mL, 0.1 M). The mixture was cooled to 0°C and treated with lithium triethylborohydride (1M in THF, 17.39 mL, 17.39 mmol, 2.5 eq). The reaction was stirred at rt for 2 h, cooled to 0°C , quenched with water (15 mL), 3 N NaOH (15 mL), 30% H_2O_2 (15 mL), and stirred for 30 min. The organics were removed under reduced pressure and the aqueous layer was extracted with EtOAc (3 x 50 mL), the organics were combined, washed with brine, dried over Na_2SO_4 , and concentrated. The crude product was purified by flash chromatography (10% EtOAc/Hexanes) to afford **2.6** (1.87 g, 74% yield) as a clear and colorless oil: $R_f = 0.5$ (10% EtOAc/Hexanes); $^1\text{H NMR}$ (600 MHz, CDCl_3) δ 7.25 (d, $J = 9.0$ Hz, 2H), 6.87 (d, $J = 8.2$ Hz, 2H), 5.85 – 5.66 (m, 1H), 4.43 (d, $J = 11.5$ Hz, 1H), 4.38 (d, $J = 11.5$ Hz, 1H), 3.80 (s, 3H), 3.76 (dt, $J = 8.0, 4.2$ Hz, 1H), 3.52 – 3.43 (m, 2H), 2.29 (td, $J = 7.1, 3.9$ Hz, 1H), 1.75 – 1.60 (m, 3H), 0.99 (d, $J = 6.9$ Hz, 3H), 0.88 (s, 9H), 0.05 (s, 3H), 0.03 (s, 3H); $^{13}\text{C NMR}$ (100 MHz, CDCl_3) δ 159.23, 140.84, 130.85, 129.39, 114.67, 113.87, 72.68, 72.65, 67.24, 55.43, 43.58, 33.36, 26.05, 18.27, 14.68, -4.26, -4.39; **HRMS** (ESI) calcd for $\text{C}_{21}\text{H}_{36}\text{O}_3\text{Si}$ [$\text{M}+\text{H}$] 364.2434, found 364.2439.

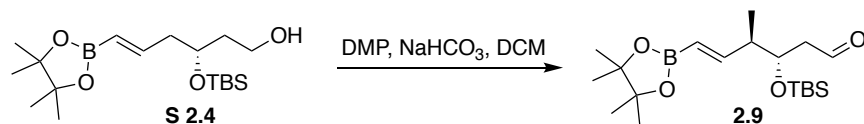


(*tert*-butyl(((3*S*,4*R*,*E*)-1-((4-methoxybenzyl)oxy)-4-methyl-6-(4,4,5,5-tetramethyl-1,3,2-dioxaborolan-2-yl)hex-5-en-3-yl)oxy)dimethylsilane (**2.8**).⁶ A solution of Hoveyda Grubbs II (0.10 g, 0.16 mmol, 0.05 eq) catalyst in dry CH₂Cl₂ (15 mL, 0.2 M) was added to a flame dried two neck flask fitted with reflux condenser under N₂. Olefin **2.6** (1.15 g, 3.15 mmol, 1 eq) was then added to the mixture, followed by vinylboronic acid pinacol ester **2.7** (1.07 mL, 6.31 mmol, 3 eq, passed through silica plug with 10% EtOAc/Hex to remove stabilizer immediately prior to use), and the reaction was heated to reflux for 18 h. The crude reaction was concentrated and purified by flash chromatography (5% EtOAc/Hexanes) to afford **2.8** (1.10 g, 74% yield) as a pale yellow oil: R_f = 0.35 (5% EtOAc/Hexanes); ¹H NMR (400 MHz, CDCl₃) δ 7.25 (d, *J* = 8.1 Hz, 2H), 6.87 (d, *J* = 8.0 Hz, 2H), 6.56 (dd, *J* = 18.1, 6.6 Hz, 1H), 5.43 (d, *J* = 18.1 Hz, 1H), 4.41 (d, *J* = 18.0 Hz, 1H), 4.38 (d, *J* = 17.9 Hz, 1H), 3.87 – 3.75 (m, 1H), 3.80 (d, *J* = 0.8 Hz, 3H), 3.55 – 3.38 (m, 2H), 2.40 (q, *J* = 6.2 Hz, 1H), 1.66 (q, *J* = 6.7 Hz, 2H), 1.26 (s, 12H), 1.00 (d, *J* = 6.9 Hz, 3H), 0.87 (d, *J* = 0.8 Hz, 9H), 0.03 (s, 3H), 0.02 (s, 3H); ¹³C NMR (100 MHz, CDCl₃) δ 159.31, 156.21, 130.88, 129.52, 123.53, 113.96, 83.26, 72.77, 72.45, 67.42, 55.50, 45.53, 32.93, 26.12, 25.06, 24.96, 18.32, 13.32, -4.20, -4.42; HRMS (ESI) calcd for C₂₇H₄₇BO₅Si [M+H] 491.3359, found 491.3350.



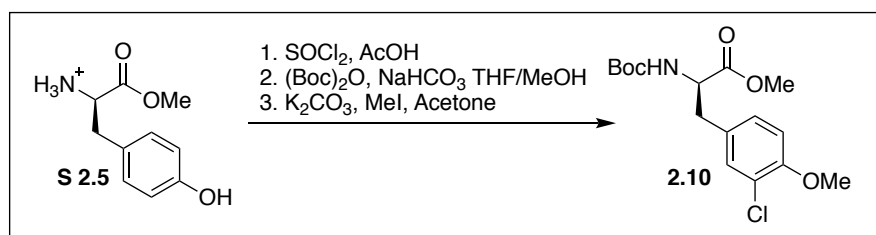
(3*S*,4*R*,*E*)-3-((*tert*-butyldimethylsilyl)oxy)-4-methyl-6-(4,4,5,5-tetramethyl-1,3,2-dioxaborolan-2-yl)hex-5-en-1-ol (**S 2.4**). To a solution of **2.8** (1.90 g, 3.87 mmol, 1 eq) in CH₂Cl₂ (25 mL, 0.15 M) and water (1.49 mL) at rt was added DDQ (1.32 g, 5.81 mmol, 1.5 eq) and the mixture was stirred for 1 h. The reaction was quenched with sat. NaHCO₃ and diluted with water. The aqueous layer was extracted with CH₂Cl₂, the organics were combined, dried over Na₂SO₄, and concentrated. The crude product was purified by flash chromatography (12% EtOAc/Hexanes) to afford **2.8** (1.21 g, 83 % yield) as a colorless oil: R_f = 0.15 (10% EtOAc/Hexanes); ¹H NMR (600 MHz, CDCl₃) δ 6.54 (dd, *J* = 18.1, 6.6 Hz, 1H), 5.46 (dd, *J* = 18.1, 1.5 Hz, 1H), 3.87 (ddd, *J* = 7.9, 5.0, 3.8 Hz, 1H), 3.77 – 3.67 (m, 2H), 2.49 (pdd, *J* = 6.8, 5.0, 1.5 Hz, 1H), 2.03 (t, *J* = 5.4 Hz, 1H), 1.71 – 1.63 (m, 2H), 1.26 (d, *J* = 1.7 Hz, 12H), 1.01 (d, *J* = 6.8 Hz, 3H), 0.89 (s, 9H), 0.08 (s, 3H), 0.07 (s, 3H); ¹³C NMR (150 MHz, CDCl₃) δ 155.72, 123.53, 83.07, 74.24, 60.63,

44.92, 34.15, 25.84, 24.80, 24.71, 17.98, 12.81, -4.41, -4.69; **HRMS** (ESI) calcd for C₁₉H₃₉BO₄Si [M+H] 371.2783, found 371.2778.

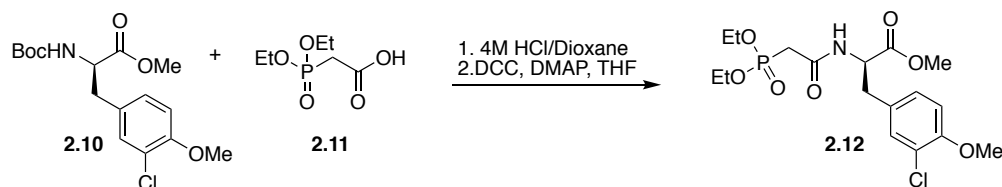


(3*S*,4*R*,*E*)-3-((*tert*-butyldimethylsilyl)oxy)-4-methyl-6-(4,4,5,5-tetramethyl-1,3,2-dioxaborolan-2-yl)hex-5-enal (2.9). To an open round bottom flask was added alcohol **S 2.4** (1.00 g, 4.09 mmol, 1 eq) in CH₂Cl₂ (41 mL, 0.1 M) and treated with NaHCO₃ (1.72 g, 20.45 mmol, 5 eq) and desmartin periodinane (2.082 g, 4.91 mmol, 1.2 eq). The reaction was stirred at rt for 1 hr, quenched with 10% Na₂S₂O₃ solution, and stirred until both layers were clear. The mixture was separated and the aqueous layer extracted with CH₂Cl₂ (3 x 100 mL). The organics were combined, washed with brine, dried over sodium sulfate and concentrated. The crude product was purified by flash chromatography (10% EtOAc/Hexanes) to afford **2.9** (0.768 g, 77% yield) as a colorless oil: R_f = 0.5 (10% EtOAc/Hexanes); ¹H NMR (400 MHz, CDCl₃) δ 9.75 (dd, *J* = 2.1, 1.1 Hz, 1H), 6.50 (dd, *J* = 18.1, 6.6 Hz, 1H), 5.46 (d, *J* = 18.0 Hz, 1H), 4.22 (dt, *J* = 8.1, 4.2 Hz, 1H), 2.54 – 2.42 (m, 2H), 2.41 – 2.33 (m, 1H), 1.25 (s, 12H), 1.01 (dd, *J* = 6.9, 0.9 Hz, 3H), 0.85 (d, *J* = 0.8 Hz, 9H), 0.05 (s, 3H), 0.02 (s, 3H); ¹³C NMR (100 MHz, CDCl₃) δ 202.47, 154.68, 123.53, 83.36, 70.89, 47.17, 45.54, 29.86, 25.92, 24.98, 24.88, 18.16, 13.03, -4.33, -4.56; **HRMS** (ESI) calcd for C₁₉H₃₇BO₄Si [M+H] 368.2554, found 368.250.

6.1.2 Unit AB Synthetic Procedures and Characterization

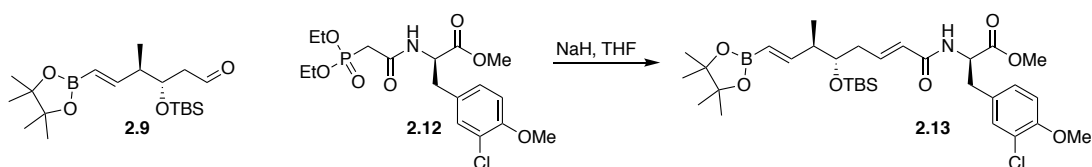


2.10 was synthesized in three steps as previously reported and all spectra were in accordance.⁷



methyl (R)-3-(3-chloro-4-methoxyphenyl)-2-(2-(diethoxyphosphoryl)acetamido)propanoate (2.12). To an open flask was added **2.10** (1.10 g, 3.20 mmol, 1 eq) and 4 M HCl/Dioxane (20 mL). This was stirred for 30 min at rt prior to acid and organics being removed under reduced pressure. The resulting white solid product was used directly.

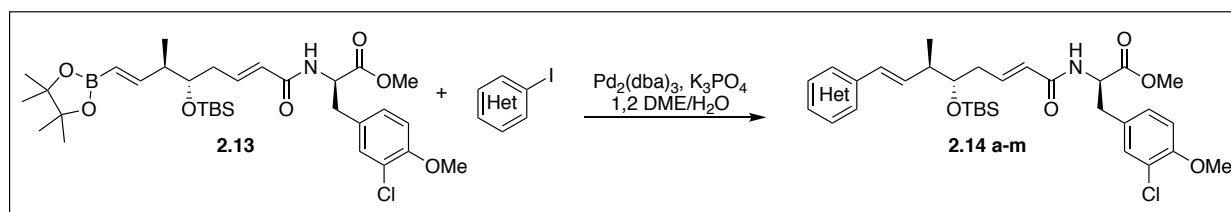
The above, deprotected product was added to a flask under N₂ and suspended in DMF (32 mL, 0.1 M). To this was added 2-(diethoxyphosphoryl)acetic acid **2.11** (0.69 g, 3.52 mmol, 1.1 eq) EDC·HCl (0.73 g, 3.84 mmol, 1.2 eq), HOBt hydrate (0.59 g, 3.84 mmol, 1.2 eq), and DIPEA (1.03 g, 1.40 mL, 8.00 mmol, 2.5 eq) and stirred at rt overnight. The reaction was quenched with half sat. aq NH₄Cl, extracted 3 x 30 mL of DCM, organics combined, washed 2 x 100 mL of sat. aq. NH₄Cl, dried over sodium sulfate, and concentrated. The crude product was purified by flash purification (1-7% MeOH/DCM) to afford **2.12** (0.90 mg, 66.6% yield) as a clear and colorless oil: R_f = 0.2 (2.5% MeOH/DCM); ¹H NMR (600 MHz, CDCl₃) δ 7.16 (d, *J* = 2.2 Hz, 1H), 7.09 (bd, *J* = 7.5 Hz, 1H), 7.04 (dd, *J* = 8.4, 2.2 Hz, 1H), 6.84 (d, *J* = 8.4 Hz, 1H), 4.78 (td, *J* = 7.1, 5.4 Hz, 1H), 4.13 (dt, *J* = 14.9, 7.2 Hz, 1H), 4.06 (dq, *J* = 8.2, 7.1 Hz, 2H), 3.85 (s, 3H), 3.70 (s, 3H), 3.08 (dd, *J* = 14.2, 5.4 Hz, 1H), 2.97 (dd, *J* = 14.2, 6.8 Hz, 1H), 2.85 (d, *J* = 10.7 Hz, 1H), 2.81 (d, *J* = 10.5 Hz, 1H), 1.31 (t, *J* = 7.1 Hz, 3H), 1.27 (t, *J* = 7.1 Hz, 3H); ¹³C NMR (150 MHz, CDCl₃) δ 171.45, 163.95, 163.93, 154.24, 131.09, 129.15, 128.72, 122.48, 112.22, 77.37, 77.16, 76.95, 62.95 (d, *J* = 15.3 Hz), 62.91 (d, *J* = 15.3), 56.25, 53.94, 52.52, 36.88, 35.70, 34.83, 16.48, 16.43, 16.39; HRMS (ESI) calcd for C₁₇H₂₅ClNO₇P [M+H] 421.1057, found 421.1053.



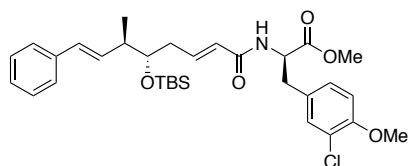
methyl (R)-2-((2E,5S,6R,7E)-5-((tert-butylidimethylsilyl)oxy)-6-methyl-8-(4,4,5,5-tetramethyl-1,3,2-dioxaborolan-2-yl)octa-2,7-dienamido)-3-(3-chloro-4-methoxyphenyl)propanoate (2.13). To a flame dried flask under N₂ was added unit B phosphonate **2.12** (0.63 g, 1.49 mmol, 1 eq) suspended in dry THF (15 mL, 0.1 M). The solution was cooled to 0 °C and NaH (60% suspension in oil, 0.055 g, 1.64 mmol, 1.1 eq) was added slowly. The reaction was stirred for 20 min prior to the dropwise addition of aldehyde **2.9** (0.55g, 1.49 mmol, 1 eq) in THF (5 mL). The reaction was allowed to stir at 0 °C for 1 h and quenched with half sat. NH₄Cl (10 mL). The THF was removed under reduced pressure and the remaining aqueous layer was extracted with DCM (3 x 50 mL), organics

combined, washed with brine, dried over sodium sulfate, and concentrated. The crude product was purified by flash chromatography (6-45% EtOAc/Hexanes) to afford **2.13** (0.545 g, 57.4% yield) as a clear and colorless oil: $R_f = 0.25$ (25% EtOAc/Hexanes); $^1\text{H NMR}$: (400 MHz, CD_3OD) δ 7.21 (d, $J = 2.2$ Hz, 1H), 7.10 (dd, $J = 8.5, 2.2$ Hz, 1H), 6.97 (d, $J = 8.4$ Hz, 1H), 6.75 (dt, $J = 15.2, 7.5$ Hz, 1H), 6.57 (dd, $J = 18.0, 7.7$ Hz, 1H), 5.96 (d, $J = 15.3$ Hz, 1H), 5.38 (d, $J = 18.3$ Hz, 1H), 4.68 (dd, $J = 8.9, 5.5$ Hz, 1H), 3.84 (s, 3H), 3.73 (q, $J = 5.4$ Hz, 1H), 3.70 (s, 3H), 3.11 (dd, $J = 14.0, 5.6$ Hz, 1H), 2.90 (dd, $J = 14.0, 9.0$ Hz, 1H), 2.41 – 2.25 (m, 3H), 1.26 (s, 12H), 1.01 (d, $J = 6.8$ Hz, 3H), 0.89 (s, 9H), 0.06 (s, 3H), 0.03 (s, 3H); $^{13}\text{C NMR}$: (100 MHz, CD_3OD) δ 171.84, 166.53, 155.89, 153.97, 141.84, 130.37, 129.89, 128.26, 124.84, 123.53, 121.75, 111.90, 82.97, 74.64, 55.10, 53.75, 51.28, 45.03, 36.94, 35.85, 25.03, 23.70, 23.65, 17.56, 14.36, -5.44, -5.74; **HRMS** (ESI) calcd for $\text{C}_{32}\text{H}_{51}\text{BClNO}_7\text{Si}$ $[\text{M}+\text{H}]$ 635.3216, found 635.3215.

6.1.3 Heterocyclic Unit AB Analogues



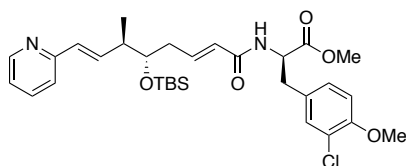
General suzuki coupling procedure: To a long tube was added **2.13** (1 eq), K_3PO_4 (2.5 eq), aryl iodide (2 eq), and $\text{Pd}_2(\text{dba})_3$ (0.05 eq) prior to evacuation and N_2 refill. This was suspended in a mixture 1,2 dichloroethane and water (4:1, 0.1 M) and the reaction was stirred vigorously until reaction completion as assessed by TLC (2 – 12 hours). The reaction was diluted with 0.5 M HCl and CH_2Cl_2 , the aqueous layer was extracted with CH_2Cl_2 (3 x 20 mL). The organics were combined, dried over Na_2SO_4 and purified by flash chromatography system as indicated below.



methyl (R)-2-((2E,5S,6R,7E)-5-((tert-butyldimethylsilyl)oxy)-6-methyl-8-phenylocta-2,7-dienamido)-3-(3-chloro-4-methoxyphenyl)propanoate (2.14a). Reaction was run as per

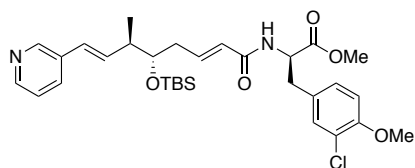
general Suzuki procedure, and purified by flash chromatography system (20 – 50% EtOAc/Hexanes) to afford **23a** (0.086 g, 93% yield) as a pale yellow oil: $R_f = 0.35$ (25% EtOAc/Hexanes); $^1\text{H NMR}$ (400 MHz, CD_3OD) δ 7.33 (d, $J = 7.5$ Hz, 2H), 7.27 (t, $J = 7.6$ Hz,

2H), 7.21 (d, $J = 2.2$ Hz, 1H), 7.18 (t, $J = 7.2$ Hz, 1H), 7.10 (dd, $J = 8.4, 2.2$ Hz, 1H), 6.96 (d, $J = 8.4$ Hz, 1H), 6.78 (dt, $J = 15.2, 7.5$ Hz, 1H), 6.38 (d, $J = 16.0$ Hz, 1H), 6.19 (dd, $J = 16.0, 8.2$ Hz, 1H), 5.96 (d, $J = 15.4$ Hz, 1H), 4.69 (dd, $J = 8.9, 5.6$ Hz, 1H), 3.83 (s, 3H), 3.80 (q, 1H), 3.70 (s, 3H), 3.11 (dd, $J = 14.0, 5.6$ Hz, 1H), 2.90 (dd, $J = 14.0, 9.0$ Hz, 1H), 2.44 (q, $J = 6.5$ Hz, 1H), 2.37 (t, $J = 6.9$ Hz, 2H), 1.11 (d, $J = 6.9$ Hz, 3H), 0.90 (s, 8H), 0.06 (s, 3H), 0.05 (s, 3H); ^{13}C NMR (100 MHz, CD_3OD) 173.28, 168.03, 155.41, 143.50, 139.03, 133.10, 131.82, 131.73, 131.33, 129.67, 129.50, 128.04, 127.06, 126.17, 123.18, 113.33, 76.54, 56.53, 55.15, 52.72, 44.11, 38.62, 37.27, 26.44, 18.98, 16.80, -4.01, -4.32.; HRMS (ESI) calcd for $\text{C}_{32}\text{H}_{44}\text{ClNO}_5\text{Si}$ [$\text{M}+\text{H}$] 586.2750 found 586.2754.



methyl (R)-2-((2E,5S,6R,7E)-5-((tert-butyldimethylsilyl)oxy)-6-methyl-8-(pyridin-2-yl)octa-2,7-dienamido)-3-(3-chloro-4-methoxyphenyl)propanoate (2.14b). Reaction was run as per general Suzuki procedure, and purified by flash chromatography

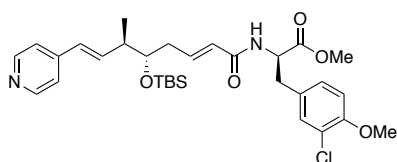
system (Amine Silica, 20 – 50% EtOAc/Hexanes) to afford **2.14b** (0.078 g, 45% yield) as a pale yellow oil: $R_f = 0.35$ (Amine column, 16-60% EtOAc/Hexanes); ^1H NMR (400 MHz, CD_3OD) δ 8.44 (d, $J = 4.0$ Hz, 1H), 7.76 (td, $J = 7.8, 1.8$ Hz, 1H), 7.46 (d, $J = 8.0$ Hz, 1H), 7.28 – 7.18 (m, 1H), 7.21 (d, $J = 2.1$ Hz, 1H), 7.10 (dd, $J = 8.5, 2.2$ Hz, 1H), 6.96 (d, $J = 8.3$ Hz, 1H), 6.77 (dt, $J = 15.3, 7.4$ Hz, 1H), 6.64 (dd, $J = 16.0, 8.2$ Hz, 1H), 6.49 (d, $J = 16.0$ Hz, 1H), 5.98 (d, $J = 15.4$ Hz, 1H), 4.70 (dd, $J = 9.0, 5.5$ Hz, 1H), 3.83 (m, 4H), 3.70 (s, 3H), 3.11 (dd, $J = 14.0, 5.5$ Hz, 1H), 2.90 (dd, $J = 14.0, 9.0$ Hz, 1H), 2.51 (h, $J = 6.8$ Hz, 1H), 2.38 (t, $J = 6.8$ Hz, 2H), 1.14 (d, $J = 6.8$ Hz, 3H), 0.90 (s, 10H). ^{13}C NMR (100 MHz, CD_3OD) δ 173.27, 167.95, 157.17, 155.41, 149.74, 143.24, 139.05, 138.66, 131.83, 131.34, 131.12, 129.70, 126.38, 123.38, 123.17, 122.34, 113.34, 76.26, 56.53, 55.15, 52.73, 44.06, 38.62, 37.31, 26.43, 18.97, 16.47, -4.04, -4.34. HRMS (ESI) calcd for $\text{C}_{31}\text{H}_{43}\text{ClN}_2\text{O}_5\text{Si}$ [$\text{M}+\text{H}$] 587.2703, found 587.2705.



methyl (R)-2-((2E,5S,6R,7E)-5-((tert-butyldimethylsilyl)oxy)-6-methyl-8-(pyridin-3-yl)octa-2,7-dienamido)-3-(3-chloro-4-methoxyphenyl)propanoate (2.14c,d). Reaction was run as per general Suzuki procedure, and purified by flash

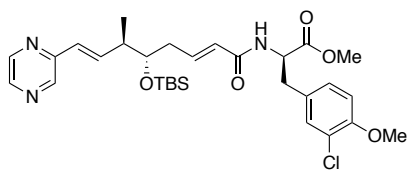
chromatography system (Amine silica, 16-60% EtOAc/Hexanes) to afford **2.14c,d** (0.049 g, 72% yield) as a pale yellow oil: $R_f = 0.15$ (50% EtOAc/Hexanes); ^1H NMR (600 MHz, CD_3OD) δ 8.49

(d, $J = 2.1$ Hz, 1H), 8.35 (dd, $J = 4.9, 1.5$ Hz, 1H), 7.85 (d, $J = 8.0$ Hz, 1H), 7.37 (dd, $J = 8.0, 4.8$ Hz, 1H), 7.21 (d, $J = 2.1$ Hz, 1H), 7.10 (dd, $J = 8.4, 2.2$ Hz, 1H), 6.96 (d, $J = 8.5$ Hz, 1H), 6.78 (dt, $J = 15.2, 7.5$ Hz, 1H), 6.43 (d, $J = 16.1$ Hz, 1H), 6.36 (dd, $J = 16.1, 7.9$ Hz, 1H), 5.97 (dt, $J = 15.3, 1.4$ Hz, 1H), 4.70 (dd, $J = 8.9, 5.6$ Hz, 1H), 3.83 (s, 4H), 3.70 (s, 3H), 3.11 (dd, $J = 14.0, 5.6$ Hz, 1H), 2.91 (dd, $J = 14.0, 9.0$ Hz, 1H), 2.49 (td, $J = 7.2, 4.7$ Hz, 1H), 2.38 (ddd, $J = 7.4, 5.8, 1.4$ Hz, 2H), 1.13 (d, $J = 6.9$ Hz, 3H), 0.90 (s, 9H), 0.06 (s, 3H), 0.05 (s, 3H); ^{13}C NMR (150 MHz, CD_3OD) δ 173.27, 167.97, 155.43, 148.28, 148.13, 143.21, 136.88, 135.48, 134.71, 131.82, 131.35, 129.68, 127.66, 126.31, 125.28, 123.20, 113.39, 76.32, 56.56, 55.15, 52.72, 44.24, 38.69, 37.29, 26.42, 18.96, 16.65, -4.00, -4.34; HRMS (ESI) $\text{C}_{31}\text{H}_{43}\text{ClN}_2\text{O}_5\text{Si}$ $[\text{M}+\text{H}]$ 587.2703, found 587.2702.



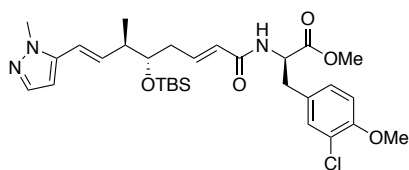
methyl (*R*)-2-((2*E*,5*S*,6*R*,7*E*)-5-((*tert*-butyldimethylsilyl)oxy)-6-methyl-8-(pyridin-4-yl)octa-2,7-dienamido)-3-(3-chloro-4-methoxyphenyl)propanoate (2.14e,f). Reaction was run as per

general Suzuki procedure, and purified by flash chromatography System (Amine Silica, 15 - 55% EtOAc/Hexanes) to afford **2.14e,f** (0.062 g, 71% yield) as a pale yellow oil: $R_f = 0.25$ (50% EtOAc/Hexanes); ^1H NMR (400 MHz, CD_3OD) δ 8.49 (d, $J = 2.2$ Hz, 1H), 8.36 (dd, $J = 4.9, 1.5$ Hz, 1H), 7.85 (dd, $J = 8.0, 2.0$ Hz, 1H), 7.37 (dd, $J = 7.8, 4.8$ Hz, 1H), 7.21 (d, $J = 2.2$ Hz, 1H), 7.10 (dd, $J = 8.4, 2.2$ Hz, 1H), 6.96 (d, $J = 8.4$ Hz, 1H), 6.78 (dt, $J = 15.2, 7.5$ Hz, 1H), 6.44 (d, $J = 16.2$ Hz, 1H), 6.36 (dd, $J = 16.1, 7.6$ Hz, 1H), 5.97 (d, $J = 15.3$ Hz, 1H), 4.69 (dd, $J = 8.9, 5.6$ Hz, 1H), 3.87 – 3.77 (m, 1H), 3.82 (s, 3H), 3.70 (s, 3H), 3.11 (dd, $J = 14.0, 5.5$ Hz, 1H), 2.90 (dd, $J = 14.0, 9.0$ Hz, 1H), 2.56 – 2.44 (m, 1H), 2.38 (t, $J = 6.6$ Hz, 2H), 1.13 (d, $J = 6.8$ Hz, 3H), 0.90 (s, 8H), 0.06 (s, 3H), 0.05 (s, 3H); ^{13}C NMR (150 MHz, CD_3OD) ^{13}C NMR (151 MHz, cd_3od) δ 173.28, 167.96, 155.44, 150.23, 147.68, 143.05, 139.96, 131.83, 131.36, 129.67, 129.19, 126.37, 123.20, 122.32, 113.40, 76.19, 56.56, 55.14, 52.73, 44.24, 38.75, 37.28, 26.41, 18.96, 16.56, -4.02, -4.36; HRMS $\text{C}_{31}\text{H}_{43}\text{ClN}_2\text{O}_5\text{Si}$ $[\text{M}+\text{H}]$ 587.2703, found 587.2699.



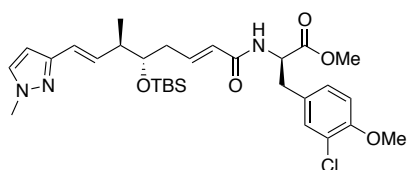
methyl (*R*)-2-((2*E*,5*S*,6*R*,7*E*)-5-((*tert*-butyldimethylsilyl)oxy)-6-methyl-8-(pyrazin-2-yl)octa-2,7-dienamido)-3-(3-chloro-4-methoxyphenyl)propanoate (2.14g). Reaction was run as per general Suzuki procedure, and purified by flash

chromatography system (Amine Silica, 20 – 55% EtOAc/Hexanes) to afford **2.14g** (0.115 g, 65% yield) as a pale yellow oil: $R_f = 0.2$ (50% EtOAc/Hexanes); $^1\text{H NMR}$ (600 MHz, CD_3OD) δ 8.57 (d, $J = 1.5$ Hz, 1H), 8.51 (s, 1H), 8.39 (d, $J = 2.6$ Hz, 1H), 7.21 (d, $J = 2.2$ Hz, 1H), 7.10 (dd, $J = 8.4, 2.2$ Hz, 1H), 6.96 (d, $J = 8.5$ Hz, 1H), 6.90 (dd, $J = 15.9, 8.3$ Hz, 1H), 6.78 (dt, $J = 15.2, 7.5$ Hz, 1H), 6.54 (d, $J = 16.0$ Hz, 1H), 5.98 (d, $J = 15.4$ Hz, 1H), 4.70 (dd, $J = 8.9, 5.5$ Hz, 1H), 3.86 – 3.84 (m, 1H), 3.83 (s, 3H), 3.70 (s, 3H), 3.11 (dd, $J = 14.0, 5.6$ Hz, 1H), 2.91 (dd, $J = 14.0, 9.0$ Hz, 1H), 2.55 (q, $J = 6.9$ Hz, 1H), 2.41 – 2.33 (m, 2H), 1.15 (d, $J = 6.8$ Hz, 3H), 0.89 (s, 9H), 0.06 (s, 3H), 0.05 (s, 3H); $^{13}\text{C NMR}$ (150 MHz, CD_3OD) δ 173.27, 167.93, 155.42, 152.99, 145.49, 143.89, 143.49, 143.07, 141.77, 131.82, 131.34, 129.69, 127.88, 126.41, 123.19, 113.38, 76.20, 56.56, 55.15, 52.73, 44.13, 38.74, 37.30, 26.42, 18.97, 16.46, -4.01, -4.36; **HRMS** (ESI) calcd for $\text{C}_{30}\text{H}_{42}\text{ClN}_3\text{O}_5\text{Si}$ $[\text{M}+\text{H}]$ 588.2655, found 588.2659.



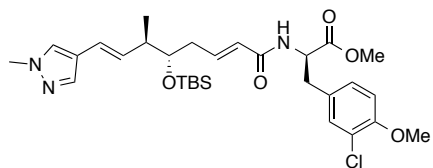
methyl (R)-2-((2E,5S,6R,7E)-5-((tert-butyldimethylsilyl)oxy)-6-methyl-8-(1-methyl-1H-pyrazol-5-yl)octa-2,7-dienamido)-3-(3-chloro-4-methoxyphenyl)propanoate (2.14h). Reaction was run as per general Suzuki procedure, and

purified by flash chromatography system (Amine silica, 20 – 70% EtOAc/Hexanes) to afford **2.14h** (0.044 g, 63% yield) as a pale yellow oil: $R_f = 0.1$ (50% EtOAc/Hexanes); $^1\text{H NMR}$ (600 MHz, CD_3OD) δ 7.32 (d, $J = 2.0$ Hz, 1H), 7.19 (d, $J = 2.2$ Hz, 1H), 7.08 (dd, $J = 8.4, 2.2$ Hz, 1H), 6.95 (d, $J = 8.4$ Hz, 1H), 6.76 (dt, $J = 15.2, 7.5$ Hz, 1H), 6.37 (d, $J = 15.9$ Hz, 1H), 6.32 (d, $J = 2.1$ Hz, 1H), 6.19 (dd, $J = 15.9, 8.3$ Hz, 1H), 5.96 (dt, $J = 15.4, 1.3$ Hz, 1H), 4.68 (dd, $J = 8.9, 5.6$ Hz, 1H), 3.82 (s, 3H), 3.80 (s, 1H), 3.78 (s, 3H), 3.68 (s, 3H), 3.10 (dd, $J = 14.0, 5.6$ Hz, 1H), 2.89 (dd, $J = 14.0, 8.9$ Hz, 1H), 2.46 (s, 1H), 2.36 (t, $J = 6.5$ Hz, 2H), 1.10 (d, $J = 6.9$ Hz, 3H), 0.88 (s, 9H). $^{13}\text{C NMR}$ (150 MHz, CD_3OD) δ 173.28, 167.98, 155.44, 143.09, 142.83, 139.14, 138.52, 131.81, 131.36, 129.67, 126.33, 123.21, 118.11, 113.41, 103.42, 76.23, 56.57, 55.17, 52.72, 44.20, 38.79, 37.28, 36.45, 26.42, 25.03, 18.97, 16.77, -3.99, -4.36; **HRMS** (ESI) calcd for $\text{C}_{30}\text{H}_{44}\text{ClN}_3\text{O}_5\text{Si}$ $[\text{M}+\text{H}]$ 590.2812, found 590.2811.



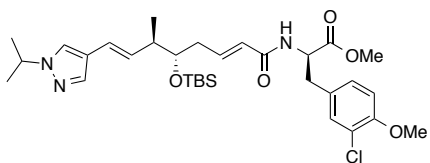
methyl (R)-2-((2E,5S,6R,7E)-5-((tert-butyldimethylsilyl)oxy)-6-methyl-8-(1-methyl-1H-pyrazol-3-yl)octa-2,7-dienamido)-3-(3-chloro-4-methoxyphenyl)propanoate (2.14i). Reaction

was run as per general Suzuki procedure, and purified by flash chromatography (Amine column, 16 - 55% EtOAc/Hexanes) to afford **2.14i** (0.065 g, 70.6% yield) as a pale yellow oil: $R_f = 0.25$ (50% EtOAc/Hexanes); $^1\text{H NMR}$ (600 MHz, CD_3OD) δ 7.46 (d, $J = 2.3$ Hz, 1H), 7.21 (d, $J = 2.2$ Hz, 1H), 7.10 (dd, $J = 8.5, 2.2$ Hz, 1H), 6.96 (d, $J = 8.4$ Hz, 1H), 6.75 (dt, $J = 15.2, 7.5$ Hz, 1H), 6.30 (d, $J = 2.3$ Hz, 1H), 6.17 (dd, $J = 16.2, 8.1$ Hz, 1H), 5.96 (d, $J = 15.4$ Hz, 1H), 4.69 (dd, $J = 9.0, 5.6$ Hz, 1H), 3.84 (s, 3H), 3.83 (s, 3H), 3.78 (q, $J = 5.6$ Hz, 1H), 3.70 (s, 3H), 3.11 (dd, $J = 14.1, 5.6$ Hz, 1H), 2.91 (dd, $J = 14.0, 9.0$ Hz, 1H), 2.42 (p, $J = 6.7$ Hz, 1H), 2.38 – 2.30 (m, 2H), 1.09 (d, $J = 6.8$ Hz, 3H), 0.90 (s, 9H), 0.06 (s, 3H), 0.04 (s, 3H); $^{13}\text{C NMR}$ (150 MHz, CD_3OD) δ 173.29, 167.99, 155.43, 152.12, 143.43, 134.95, 133.03, 131.82, 131.37, 129.71, 126.28, 123.29, 123.22, 113.38, 103.22, 76.44, 56.55, 55.16, 52.71, 43.95, 38.60, 38.52, 37.33, 26.44, 18.98, 16.48, -4.04, -4.32; **HRMS** (ESI) calcd for $\text{C}_{30}\text{H}_{44}\text{ClN}_3\text{O}_5\text{Si}$ $[\text{M}+\text{H}]$ 590.2812, found 590.2809.



methyl (R)-2-((2E,5S,6R,7E)-5-((tert-butyldimethylsilyl)oxy)-6-methyl-8-(1-methyl-1H-pyrazol-4-yl)octa-2,7-dienamido)-3-(3-chloro-4-methoxyphenyl)propanoate

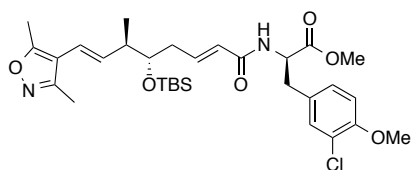
(2.14j,k). Reaction was run as per general Suzuki procedure, and purified by flash chromatography (Amine column, 16 – 60% EtOAc/Hexanes) to afford **2.14j,k** (0.085 g, 92% yield) as a pale yellow oil: $R_f = 0.2$ (50% EtOAc/Hexanes); $^1\text{H NMR}$ (400 MHz, CD_3OD) δ 7.61 (s, 1H), 7.48 (s, 1H), 7.21 (d, $J = 2.2$ Hz, 1H), 7.10 (dd, $J = 8.4, 2.2$ Hz, 1H), 6.96 (d, $J = 8.4$ Hz, 1H), 6.77 (dt, $J = 15.2, 7.5$ Hz, 1H), 6.20 (d, $J = 16.0$ Hz, 1H), 5.95 (d, $J = 15.5$ Hz, 1H), 5.90 (dd, $J = 16.1, 8.1$ Hz, 1H), 4.69 (dd, $J = 8.9, 5.6$ Hz, 1H), 4.46 (p, $J = 6.7$ Hz, 1H), 3.83 (s, 3H), 3.75 (q, $J = 5.5$ Hz, 1H), 3.70 (s, 3H), 3.11 (dd, $J = 14.0, 5.6$ Hz, 1H), 2.91 (dd, $J = 14.0, 8.8$ Hz, 1H), 2.34 (qt, $J = 13.5, 7.1$ Hz, 3H), 1.46 (d, $J = 6.7$ Hz, 6H), 1.07 (d, $J = 6.8$ Hz, 3H), 0.90 (s, 9H), 0.06 (s, 3H), 0.03 (s, 3H); $^{13}\text{C NMR}$ (100 MHz, CD_3OD) δ 173.29, 168.04, 155.42, 143.72, 137.18, 131.83, 131.35, 129.68, 126.09, 126.03, 123.19, 121.88, 121.43, 113.36, 76.65, 56.55, 55.16, 54.99, 52.72, 44.16, 38.27, 37.28, 26.44, 23.07, 18.99, 16.38, -4.04, -4.32; **HRMS** (ESI) calcd for $\text{C}_{30}\text{H}_{44}\text{ClN}_3\text{O}_5\text{Si}$ $[\text{M}+\text{H}]$ 590.2812, found 590.2813.



methyl (R)-2-((2E,5S,6R,7E)-5-((tert-butyldimethylsilyl)oxy)-8-(1-isopropyl-1H-pyrazol-4-yl)-6-methylocta-2,7-dienamido)-3-(3-chloro-4-methoxyphenyl)propanoate

(2.14l). Reaction was run as per general Suzuki procedure,

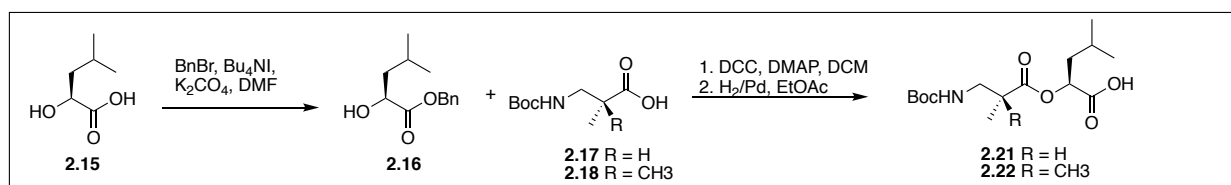
and purified by flash chromatography system (Amine silica, 20 – 50% EtOAc/Hexanes) to afford **2.14l** (0.056 g, 83% yield) as a pale yellow oil: $R_f = 0.35$ (50% EtOAc/Hexanes); $^1\text{H NMR}$ (600 MHz, CD_3OD) δ 7.53 (s, 1H), 7.47 (s, 1H), 7.21 (d, $J = 2.2$ Hz, 1H), 7.10 (dd, $J = 8.4, 2.2$ Hz, 1H), 6.96 (d, $J = 8.4$ Hz, 1H), 6.77 (dt, $J = 15.2, 7.5$ Hz, 1H), 6.18 (d, $J = 16.0$ Hz, 1H), 5.95 (d, $J = 15.4$ Hz, 1H), 5.89 (dd, $J = 16.1, 8.1$ Hz, 1H), 4.69 (dd, $J = 9.0, 5.6$ Hz, 1H), 3.84 (s, 3H), 3.83 (s, 3H), 3.75 (q, $J = 5.5$ Hz, 1H), 3.70 (s, 3H), 3.11 (dd, $J = 14.0, 5.6$ Hz, 1H), 2.90 (dd, $J = 14.0, 9.0$ Hz, 1H), 2.42 – 2.27 (m, 3H), 1.06 (d, $J = 6.9$ Hz, 3H), 0.89 (s, 9H), 0.05 (s, 3H), 0.03 (s, 3H). $^{13}\text{C NMR}$ (150 MHz, CD_3OD) δ 173.29, 168.03, 155.42, 143.67, 137.61, 131.83, 131.58, 131.36, 129.68, 129.33, 126.10, 123.18, 122.45, 121.24, 113.36, 76.60, 56.55, 55.15, 52.72, 44.16, 38.72, 38.32, 37.28, 26.44, 18.98, 16.45, -4.05, -4.31; **HRMS** (ESI) calcd for $\text{C}_{32}\text{H}_{48}\text{ClN}_3\text{O}_5\text{Si}$ [$\text{M}+\text{H}$] 618.3125, found 618.3129.



methyl (*R*)-2-(((2*E*,5*S*,6*R*,7*E*)-5-((*tert*-butyldimethylsilyloxy)-8-(3,5-dimethylisoxazol-4-yl)-6-methylocta-2,7-dienamido)-3-(3-chloro-4-methoxyphenyl)propanoate (2.14m**).** Reaction

was run as per general Suzuki procedure, and purified by flash chromatography system (Amine silica, 10 – 50% EtOAc/Hexanes) to afford **2.14m** (0.057 g, 85% yield) as a pale yellow oil: $R_f = 0.35$ (33% EtOAc/Hexanes); $^1\text{H NMR}$: (400 MHz, CD_3OD) δ 7.20 (d, $J = 2.2$ Hz, 1H), 7.10 (dd, $J = 8.3, 2.2$ Hz, 1H), 6.96 (d, $J = 8.4$ Hz, 1H), 6.76 (dt, $J = 15.2, 7.6$ Hz, 1H), 6.11 (d, $J = 16.3$ Hz, 1H), 5.96 (d, $J = 15.4$ Hz, 1H), 5.90 (dd, $J = 16.4, 8.5$ Hz, 1H), 4.68 (dd, $J = 9.0, 5.5$ Hz, 1H), 3.84 (s, 3H), 3.83 – 3.77 (m, 1H), 3.70 (s, 3H), 3.12 (dd, $J = 14.0, 5.5$ Hz, 1H), 2.90 (dd, $J = 14.0, 9.0$ Hz, 1H), 2.48 – 2.32 (m, 5H), 2.26 (s, 3H), 1.11 (d, $J = 6.9$ Hz, 3H), 0.90 (s, 9H), 0.07 (s, 3H), 0.06 (s, 3H). $^{13}\text{C NMR}$: (100 MHz, CD_3OD) δ 173.27, 167.98, 166.46, 159.59, 155.42, 143.21, 135.80, 131.81, 131.33, 129.67, 126.21, 123.17, 119.01, 114.23, 113.36, 76.35, 56.54, 55.17, 52.73, 44.65, 39.15, 37.26, 26.42, 18.97, 17.68, 11.50, 11.40, -3.95, -4.38; **HRMS** (ESI) calcd for $\text{C}_{31}\text{H}_{45}\text{ClN}_2\text{O}_6\text{Si}$ [$\text{M}+\text{H}$] 605.2808, found 605.2801.

6.1.3 Synthesis of Units CD

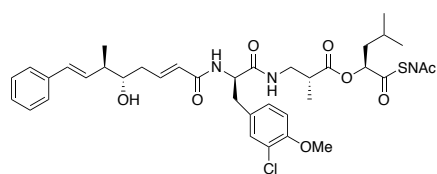


General Peptide Coupling Procedure: Unit A/B (1 eq) was suspended in 1,2 dichloroethane (0.2 M), treated with trimethyl tin hydroxide (4 eq), and heat to 80 °C for 4 hours. The reaction was cooled in a -20 °C freezer for 1 hour, filtered through celite, and concentrated. The crude acid was used directly.

Simultaneously Unit C/D (1.1 eq) was suspended in 4 M HCl/Dioxane (5 mL) and stirred for 1 h, concentrated and used directly.

Unit A/B acid was suspended in DCM, cooled to 0 °C, and treated with HATU (1.1 eq). Simultaneously amine salt of units C/D were suspended in DCM and treated with DIPEA (2.5 eq), cooled to 0 °C and added to Unit A/B. The reaction was allowed to stir overnight, warming to rt. The reaction was diluted with half saturated sodium bicarbonate, the aqueous layer extracted with DCM (3 x 10 mL), organics combined, washed with brine, dried over Na₂SO₄, concentrated and purified as specified below.

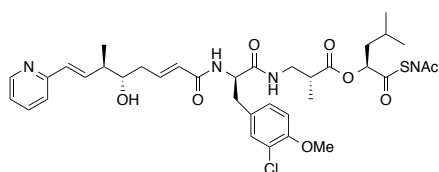
General Deprotection Procedure: The crude coupling product was suspended in acetonitrile (0.1 M) in a polypropylene vial. This was treated with 33% aq. HF (2 eq) and allowed to stir until the reaction was complete, as monitored by TLC. The reaction was quenched by the slow addition of sat. NaHCO₃ until the aqueous layer was basic. The aqueous layer was then extracted with DCM (3 x 10 mL), organics combined, washed with brine, dried over Na₂SO₄, concentrated, and purified as specified.



(S)-1-(((2S,3S,4S)-2-methyl-3-((R)-3-((R)-3-(3-chloro-4-methoxyphenyl)-2-((2E,5S,6R,7E)-5-hydroxy-6-methyl-8-phenylocta-2,7-dienamido)propanamido)-2-methylpropanoate)thio)-4-methyl-1-oxopentan-2-yl **(2.28a).**

Reaction was run as per general coupling procedure, general deprotection procedure, and purified by flash chromatography (1-10% MeOH/DCM) to afford **2.28a** (0.051 g, 42% yield over 3 steps) as a clear and colorless oil: R_f = 0.65 (10% MeOH/DCM). This was then deprotected as per general deprotection procedure and purified by flash chromatography (2 – 15% MeOH/DCM) to afford

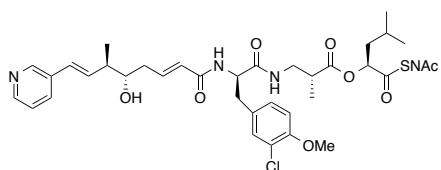
the final product **xx** (xx, xx% yield) as a clear and colorless oil: $R_f = 0.25$ (10% MeOH/DCM); $^1\text{H NMR}$: (600 MHz, CD_3OD) δ 7.37 (d, $J = 7.0$ Hz, 2H), 7.27 (t, $J = 7.9$ Hz, 2H), 7.25 (d, $J = 2.2$ Hz, 1H), 7.18 (t, $J = 7.3$ Hz, 1H), 7.14 (dd, $J = 8.4, 2.2$ Hz, 1H), 6.97 (d, $J = 8.4$ Hz, 1H), 6.81 (dt, $J = 15.1, 7.3$ Hz, 1H), 6.41 (d, $J = 15.9$ Hz, 1H), 6.23 (dd, $J = 15.9, 8.5$ Hz, 1H), 6.01 (d, $J = 15.4$ Hz, 1H), 5.21 (dd, $J = 9.6, 4.0$ Hz, 1H), 4.58 (dd, $J = 8.1, 7.0$ Hz, 1H), 3.83 (s, 3H), 3.65 (dt, $J = 8.7, 4.6$ Hz, 1H), 3.48 (dd, $J = 13.5, 6.6$ Hz, 1H), 3.34 – 3.27 (m, 2H), 3.19 (dd, $J = 13.5, 7.0$ Hz, 1H), 3.06 – 2.97 (m, 3H), 2.85 (dd, $J = 13.7, 8.1$ Hz, 1H), 2.70 (q, $J = 7.0$ Hz, 1H), 2.44 – 2.35 (m, 2H), 2.35 – 2.28 (m, 1H), 1.91 (s, 3H), 1.80 – 1.74 (m, 1H), 1.74 – 1.69 (m, 1H), 1.66 – 1.59 (m, 1H), 1.15 (d, $J = 6.9$ Hz, 3H), 1.10 (d, $J = 7.1$ Hz, 3H), 0.94 (d, $J = 6.5$ Hz, 3H), 0.91 (d, $J = 6.5$ Hz, 3H). $^{13}\text{C NMR}$: (150 MHz, CD_3OD) 200.34, 175.06, 173.49, 173.42, 168.07, 155.40, 143.51, 139.05, 132.50, 132.09, 131.91, 131.50, 129.84, 129.48, 128.05, 127.14, 126.08, 123.20, 113.35, 78.63, 75.34, 56.57, 56.24, 44.21, 42.73, 41.95, 40.57, 39.85, 38.82, 38.07, 28.58, 25.74, 23.48, 22.54, 21.97, 17.53, 14.87; **HRMS** calcd for $\text{C}_{39}\text{H}_{52}\text{ClN}_3\text{O}_8\text{S}$ [$\text{M}+\text{H}$] 758.3236, found 758.3238.



**(S)-1-((2-acetamidoethyl)thio)-4-methyl-1-oxopentan-2-yl
(R)-3-((R)-3-(3-chloro-4-methoxyphenyl)-2-
(2E,5S,6R,7E)-5-hydroxy-6-methyl-8-(pyridin-2-yl)octa-
2,7-dienamido)propanamido)-2-methylpropanoate**

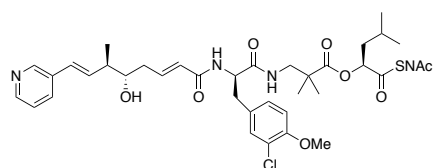
(2.28b). Reaction was run as per general coupling procedure, and purified by flash chromatography (1-10% MeOH/DCM) $R_f = 0.65$ (10% MeOH/DCM). This was then deprotected as per general deprotection procedure and purified by flash chromatography (2 – 15% MeOH/DCM) to afford the final product **2.28b** (0.025 g, 38% yield over 3 steps) as a clear and colorless oil: $R_f = 0.25$ (10% MeOH/DCM); $^1\text{H NMR}$: (600 MHz, CD_3OD) δ 8.44 (d, $J = 4.1$ Hz, 1H), 7.76 (td, $J = 7.7, 1.9$ Hz, 1H), 7.51 (d, $J = 8.1$ Hz, 1H), 7.26 (d, $J = 2.3$ Hz, 1H), 7.25 – 7.22 (m, 1H), 7.14 (dd, $J = 8.4, 2.2$ Hz, 1H), 6.97 (d, $J = 8.4$ Hz, 1H), 6.81 (dt, $J = 15.0, 7.3$ Hz, 1H), 6.67 (dd, $J = 16.0, 8.4$ Hz, 1H), 6.52 (d, $J = 16.0$ Hz, 1H), 6.02 (d, $J = 15.4$ Hz, 1H), 5.21 (dd, $J = 9.5, 4.0$ Hz, 1H), 4.58 (dd, $J = 8.1, 6.9$ Hz, 1H), 3.84 (s, 3H), 3.68 (dt, $J = 8.7, 4.7$ Hz, 1H), 3.48 (dd, $J = 13.5, 6.6$ Hz, 1H), 3.33 – 3.30 (s, 2H), 3.21 (dd, $J = 13.5, 7.0$ Hz, 1H), 3.05 – 2.99 (m, 3H), 2.85 (dd, $J = 13.8, 8.1$ Hz, 1H), 2.71 (q, $J = 7.0$ Hz, 1H), 2.51 – 2.44 (m, 1H), 2.44 – 2.37 (m, 1H), 2.37 – 2.29 (m, 1H), 1.91 (s, 3H), 1.81 – 1.69 (m, 2H), 1.67 – 1.59 (m, 1H), 1.18 (d, $J = 6.9$ Hz, 3H), 1.11 (d, $J = 7.2$ Hz, 3H), 0.95 (d, $J = 6.5$ Hz, 3H), 0.92 (d, $J = 6.5$ Hz, 3H). $^{13}\text{C NMR}$

(150 MHz, CD₃OD) δ 200.34, 175.09, 173.49, 173.42, 168.05, 157.30, 155.43, 149.71, 143.29, 138.74, 138.61, 131.92, 131.56, 131.35, 129.85, 126.27, 123.36, 122.32, 113.42, 111.43, 78.67, 75.12, 56.61, 56.25, 44.08, 42.75, 41.97, 40.60, 39.87, 38.75, 38.09, 28.61, 25.76, 23.46, 22.54, 21.99, 17.10, 14.86; **HRMS** (ESI) calcd for C₃₈H₅₁ClN₄O₈S [M+H] 759.3189, found 759.3184.



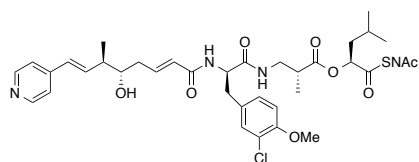
**(S)-1-((2-acetamidoethyl)thio)-4-methyl-1-oxopentan-2-yl
(R)-3-((R)-3-(3-chloro-4-methoxyphenyl)-2-
(2E,5S,6R,7E)-5-hydroxy-6-methyl-8-(pyridin-3-yl)octa-
2,7-dienamido)propanamido)-2-methylpropanoate**

(2.28c). Reaction was run as per general coupling procedure, and purified by flash chromatography (1-10% MeOH/DCM) $R_f = 0.65$ (10% MeOH/DCM). This was then deprotected as per general deprotection procedure and purified by flash chromatography (2 – 15% MeOH/DCM) to afford the final product **2.28c** (0.037, 51% yield over 3 steps) as a clear and colorless oil: $R_f = 0.25$ (10% MeOH/DCM); **¹H NMR** (600 MHz, CD₃OD) δ 8.52 (d, $J = 2.2$ Hz, 1H), 8.36 (dd, $J = 4.9, 1.6$ Hz, 1H), 7.89 (dt, $J = 8.1, 1.9$ Hz, 1H), 7.37 (ddd, $J = 8.0, 4.9, 0.9$ Hz, 1H), 7.26 (d, $J = 2.2$ Hz, 1H), 7.14 (dd, $J = 8.4, 2.3$ Hz, 1H), 6.97 (d, $J = 8.5$ Hz, 1H), 6.81 (dt, $J = 15.2, 7.3$ Hz, 1H), 6.46 (d, $J = 16.1$ Hz, 1H), 6.41 (dd, $J = 16.0, 7.9$ Hz, 1H), 6.02 (d, $J = 15.4$ Hz, 1H), 5.21 (dd, $J = 9.5, 4.0$ Hz, 1H), 4.59 (dd, $J = 8.0, 6.8$ Hz, 1H), 3.84 (s, 3H), 3.67 (dt, $J = 8.0, 4.6$ Hz, 1H), 3.48 (dd, $J = 13.5, 6.6$ Hz, 1H), 3.33 – 3.30 (m, 2H) 3.20 (dd, $J = 13.5, 6.9$ Hz, 1H), 3.03 (td, $J = 6.6, 1.9$ Hz, 3H), 3.04 – 3.00 (m, 1H) 2.85 (dd, $J = 13.7, 8.1$ Hz, 1H) 2.70 (q, $J = 7.0$ Hz, 1H), 2.51 – 2.36 (m, 2H), 2.36 – 2.28 (m, 1H), 1.91 (s, 3H), 1.83 – 1.68 (m, 2H), 1.65 – 1.61 (m, 1H), 1.17 (d, $J = 6.9$ Hz, 3H), 1.10 (d, $J = 7.1$ Hz, 3H), 0.95 (d, $J = 6.5$ Hz, 3H), 0.92 (d, $J = 6.5$ Hz, 3H); **¹³C NMR** (150 MHz, cd3od) δ 200.34, 175.08, 173.48, 173.42, 168.04, 155.42, 148.27, 148.22, 143.30, 136.34, 135.52, 134.79, 131.91, 131.53, 129.85, 127.95, 126.19, 125.24, 123.23, 113.41, 78.66, 75.16, 56.60, 56.24, 49.00, 44.33, 42.75, 41.97, 40.59, 39.86, 38.87, 38.08, 28.60, 25.76, 23.47, 22.54, 21.99, 17.34, 14.86; **HRMS** (ESI) calcd for C₃₈H₅₁ClN₄O₈S [M+H] 759.3189, found 759.3192.



**(S)-1-((2-acetamidoethyl)thio)-4-methyl-1-oxopentan-2-yl
3-((R)-3-(3-chloro-4-methoxyphenyl)-2-((2E,5S,6R,7E)-5-
hydroxy-6-methyl-8-(pyridin-3-yl)octa-2,7-**

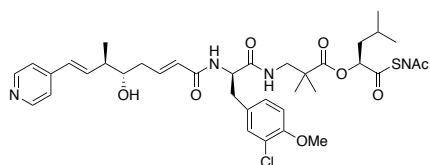
dienamido)propanamido)-2,2-dimethylpropanoate (2.28d). Reaction was run as per general coupling procedure, and purified by flash chromatography (1-10% MeOH/DCM) $R_f = 0.65$ (10% MeOH/DCM). This was then deprotected as per general deprotection procedure and purified by flash chromatography (2 – 15% MeOH/DCM) to afford the final product **2.28d** (0.19, 51% yield over 3 steps) as a clear and colorless oil: $R_f = 0.25$ (10% MeOH/DCM); $^1\text{H NMR}$ (600MHz, CD_3OD) δ 8.52 (d, $J = 2.3$ Hz, 1H), 8.35 (dd, $J = 4.8, 1.6$ Hz, 1H), 7.89 (dt, $J = 8.0, 2.0$ Hz, 1H), 7.74 (t, $J = 6.4$ Hz, 1H), 7.37 (dd, $J = 8.0, 4.9$ Hz, 1H), 7.28 (d, $J = 2.2$ Hz, 1H), 7.15 (dd, $J = 8.4, 2.3$ Hz, 1H), 6.96 (d, $J = 8.5$ Hz, 1H), 6.80 (dt, $J = 15.0, 7.3$ Hz, 1H), 6.46 (d, $J = 16.1$ Hz, 1H), 6.40 (dd, $J = 16.0, 7.9$ Hz, 1H), 6.01 (d, $J = 15.4$ Hz, 1H), 5.20 (dd, $J = 9.5, 3.8$ Hz, 1H), 4.65 (dd, $J = 8.5, 6.5$ Hz, 1H), 3.92 (p, $J = 6.2$ Hz, 2H), 3.83 (s, 3H), 3.66 (dt, $J = 8.7, 4.6$ Hz, 1H), 3.44 – 3.27 (m, 2H), 3.11 – 3.00 (m, 2H), 2.85 (dd, $J = 13.9, 8.5$ Hz, 1H), 2.44 (td, $J = 7.2, 4.3$ Hz, 1H), 2.39 (dt, $J = 13.0, 6.4$ Hz, 1H), 2.32 (dt, $J = 14.9, 7.6$ Hz, 1H), 1.91 (s, 3H), 1.83 – 1.69 (m, 2H), 1.64 (ddd, $J = 13.4, 8.4, 3.9$ Hz, 1H), 1.17 – 1.14 (m, 9H), 0.95 (d, $J = 6.5$ Hz, 3H), 0.92 (d, $J = 6.4$ Hz, 3H). $^{13}\text{C NMR}$ (150 MHz, CD_3OD) δ 200.53, 176.86, 173.76, 173.42, 168.17, 155.38, 148.26, 148.21, 143.36, 136.35, 135.52, 134.80, 131.89, 131.69, 129.82, 127.96, 126.16, 125.25, 123.23, 113.41, 78.81, 75.15, 64.74, 56.61, 56.39, 47.89, 44.69, 44.31, 41.94, 39.86, 38.88, 37.86, 28.73, 25.87, 25.26, 23.49, 23.26, 23.18, 22.59, 21.95, 17.35. **HRMS** (ESI) calcd for $\text{C}_{39}\text{H}_{53}\text{ClN}_4\text{O}_8\text{S}$ $[\text{M}+\text{H}]$ 773.3345, found 773.3353.



**(S)-1-((2-acetamidoethyl)thio)-4-methyl-1-oxopentane-2-yl
(R)-3-((R)-3-(3-chloro-4-methoxyphenyl)-2-((2E,5S,6R,7E)-
5-hydroxy-6-methyl-8-(pyridin-4-yl)octa-2,7-**

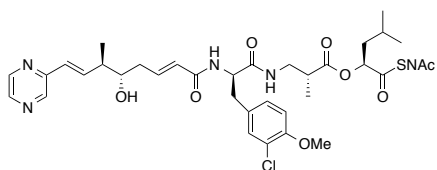
dienamido)propanamido)-2-methylpropanoate (2.28e) Reaction was run as per general coupling procedure, and purified by flash chromatography (1-10% MeOH/DCM) $R_f = 0.65$ (10% MeOH/DCM). This was then deprotected as per general deprotection procedure and purified by flash chromatography (2 – 15% MeOH/DCM) to afford the final product **2.28e** (0.048, 49% yield over 3 steps) as a clear and colorless oil: $R_f = 0.25$ (10% MeOH/DCM); $^1\text{H NMR}$ (599 MHz, Methanol- d_4) δ 8.42 (d, $J = 6.3$ Hz, 1H), 7.40 (d, $J = 6.3$ Hz, 1H), 7.25 (d, $J = 2.2$ Hz, 1H), 7.14 (dd, $J = 8.5, 2.2$ Hz, 1H), 6.97 (d, $J = 8.4$ Hz, 1H), 6.80 (dt, $J = 15.0, 7.3$ Hz, 1H), 6.61 (dd, $J = 16.0, 8.5$ Hz, 1H), 6.44 (d, $J = 15.9$ Hz, 1H), 6.01 (d, $J = 15.4$ Hz, 1H), 5.21 (dd, $J = 9.5, 4.0$ Hz,

1H), 4.58 (dd, $J = 8.1, 6.9$ Hz, 1H), 3.84 (s, 3H), 3.67 (dt, $J = 7.9, 4.7$ Hz, 1H), 3.48 (dd, $J = 13.5, 6.6$ Hz, 1H), 3.20 (dd, $J = 13.5, 7.0$ Hz, 1H), 3.03 (td, $J = 6.7, 1.9$ Hz, 2H), 2.85 (dd, $J = 13.8, 8.1$ Hz, 1H), 2.70 (q, $J = 6.9$ Hz, 1H), 2.51 – 2.42 (m, 1H), 2.42 – 2.25 (m, 2H), 1.91 (s, 3H), 1.82 – 1.68 (m, 2H), 1.63 (ddd, $J = 13.1, 8.1, 4.0$ Hz, 1H), 1.17 (d, $J = 6.8$ Hz, 3H), 1.10 (d, $J = 7.1$ Hz, 3H), 0.94 (d, $J = 6.5$ Hz, 3H), 0.92 (d, $J = 6.5$ Hz, 3H). ^{13}C NMR (150 MHz, CD_3OD) δ 200.34, 175.08, 173.48, 173.42, 168.02, 155.43, 150.20, 147.73, 143.18, 139.50, 131.92, 131.53, 129.84, 129.42, 126.25, 123.24, 122.39, 113.42, 78.67, 75.03, 56.61, 56.23, 44.30, 42.75, 41.97, 40.60, 39.87, 38.90, 38.09, 28.61, 25.76, 23.46, 22.54, 21.99, 17.19, 14.86. HRMS (ESI) calcd for $\text{C}_{38}\text{H}_{51}\text{ClN}_4\text{O}_8\text{S}$ [M+H] 759.3189, found 759.3187.



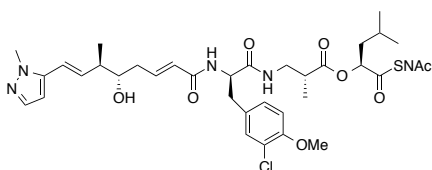
**(S)-1-((2-acetamidoethyl)thio)-4-methyl-1-oxopentan-2-yl
3-((R)-3-(3-chloro-4-methoxyphenyl)-2-((2E,5S,6R,7E)-5-
hydroxy-6-methyl-8-(pyridin-4-yl)octa-2,7-
dienamido)propanamido)-2,2-dimethylpropanoate (2.28f).**

Reaction was run as per general coupling procedure, and purified by flash chromatography (1-10% MeOH/DCM) $R_f = 0.65$ (10% MeOH/DCM). This was then deprotected as per general deprotection procedure and purified by flash chromatography (2 – 15% MeOH/DCM) to afford the final product **2.28f** (0.039, 45% yield over 3 steps) as a clear and colorless oil: $R_f = 0.25$ (10% MeOH/DCM); ^1H NMR (600MHz, CD_3OD) δ 8.41 (d, $J = 6.1$ Hz, 1H), 7.40 (d, $J = 6.1$ Hz, 1H), 7.27 (d, $J = 1.9$ Hz, 1H), 7.15 (dd, $J = 8.5, 2.2$ Hz, 1H), 6.96 (dd, $J = 8.5, 1.0$ Hz, 1H), 6.79 (dt, $J = 14.5, 7.1$ Hz, 1H), 6.61 (dd, $J = 16.0, 8.5$ Hz, 1H), 6.43 (d, $J = 16.0$ Hz, 1H), 6.00 (d, $J = 15.4$ Hz, 1H), 5.20 (dd, $J = 9.5, 3.8$ Hz, 1H), 4.65 (dd, $J = 8.4, 6.6$ Hz, 1H), 3.83 (s, 3H), 3.66 (dt, $J = 8.5, 4.4$ Hz, 1H), 3.40 (d, $J = 13.6$ Hz, 1H), 3.36 (d, $J = 12.9$ Hz, 1H), 3.32 – 3.29 (m, 2H), 3.12 – 2.99 (m, 3H), 2.85 (dd, $J = 14.0, 8.5$ Hz, 1H), 2.51 – 2.42 (m, 1H), 2.41 – 2.34 (m, 1H), 2.35 – 2.27 (m, 1H), 1.90 (s, 3H), 1.81 – 1.68 (m, 2H), 1.68 – 1.60 (m, 1H), 1.16 (s, 6H), 1.15 (d, $J = 5.1$ Hz, 3H), 0.95 (d, $J = 6.5$ Hz, 3H), 0.92 (d, $J = 6.5$ Hz, 3H). ^{13}C NMR (150 MHz, CD_3OD) δ 199.11, 175.43, 172.24, 172.00, 166.71, 153.95, 148.72, 146.35, 141.80, 138.12, 130.47, 130.25, 128.38, 127.99, 124.78, 121.81, 120.98, 112.00, 77.38, 73.59, 55.18, 54.90, 46.35, 43.26, 42.85, 40.51, 38.43, 37.49, 36.43, 27.30, 24.44, 22.06, 21.83, 21.75, 21.16, 20.52, 15.77; $\text{C}_{38}\text{H}_{51}\text{ClN}_4\text{O}_8\text{S}$ [M+H] 759.3189, found 759.3186.



**(S)-1-((2-acetamidoethyl)thio)-4-methyl-1-oxopentan-2-yl
(R)-3-((R)-3-(3-chloro-4-methoxyphenyl)-2-
(2E,5S,6R,7E)-5-hydroxy-6-methyl-8-(pyrazin-2-yl)octa-**

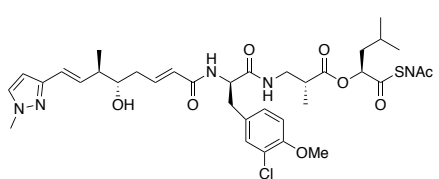
2,7-dienamido)propanamido)-2-methylpropanoate (2.28g). Reaction was run as per general coupling procedure, and purified by flash chromatography (1-10% MeOH/DCM) $R_f = 0.65$ (10% MeOH/DCM). This was then deprotected as per general deprotection procedure and purified by flash chromatography (2 – 15% MeOH/DCM) to afford the final product **2.28g** (xx, xx% yield over 3 steps) as a clear and colorless oil: $R_f = 0.25$ (10% MeOH/DCM); $^1\text{H NMR}$ (400 MHz, CD_3OD) δ 8.62 (s, 1H), 8.51 (s, 1H), 8.39 (d, $J = 2.6$ Hz, 1H), 7.26 (d, $J = 2.0$ Hz, 1H), 7.14 (dd, $J = 8.5, 2.1$ Hz, 1H), 6.97 (d, $J = 8.4$ Hz, 1H), 6.93 (dd, $J = 15.9, 8.5$ Hz, 1H), 6.81 (dt, $J = 14.9, 7.3$ Hz, 1H), 6.57 (d, $J = 16.0$ Hz, 1H), 6.02 (d, $J = 15.4$ Hz, 1H), 5.21 (dd, $J = 9.4, 3.9$ Hz, 1H), 4.58 (t, $J = 7.5$ Hz, 1H), 3.69 (dt, $J = 9.0, 4.7$ Hz, 1H), 3.48 (dd, $J = 13.4, 6.6$ Hz, 1H), 3.37 – 3.24 (m, 2H), 3.20 (dd, $J = 13.5, 7.1$ Hz, 1H), 3.07 – 2.97 (m, 1H), 3.03 (t, $J = 6.8$ Hz, 2H), 2.85 (dd, $J = 13.7, 8.2$ Hz, 1H), 2.70 (apparent q, $J = 6.9$ Hz, 1H), 2.56 – 2.28 (m, 3H), 1.91 (s, 3H), 1.82 – 1.68 (m, 2H), 1.68 – 1.56 (m, 1H), 1.19 (d, $J = 6.8$ Hz, 3H), 1.10 (d, $J = 7.0$ Hz, 3H), 0.95 (d, $J = 6.3$ Hz, 4H), 0.92 (d, $J = 6.3$ Hz, 3H). $^{13}\text{C NMR}$ (151 MHz, cd_3od) δ 200.34, 175.08, 173.47, 173.42, 168.03, 155.42, 153.09, 145.39, 143.89, 143.46, 143.20, 141.38, 131.91, 131.54, 129.86, 128.22, 126.28, 123.24, 113.42, 78.67, 75.01, 56.62, 56.24, 49.00, 44.21, 42.75, 41.97, 40.60, 39.86, 38.80, 38.09, 28.61, 25.76, 23.46, 22.54, 21.99, 16.99, 14.86. **HRMS** (ESI) calcd for $\text{C}_{37}\text{H}_{50}\text{ClN}_5\text{O}_8\text{S}$ $[\text{M}+\text{H}]$ 760.3141, found 760.3143.



**(S)-1-((2-acetamidoethyl)thio)-4-methyl-1-oxopentan-2-yl
(R)-3-((R)-3-(3-chloro-4-methoxyphenyl)-2-
(2E,5S,6R,7E)-5-hydroxy-6-methyl-8-(1-methyl-1H-
pyrazol-5-yl)octa-2,7-dienamido)propanamido)-2-**

methylpropanoate (2.28h). Reaction was run as per general coupling procedure, and purified by flash chromatography (1-10% MeOH/DCM) $R_f = 0.65$ (10% MeOH/DCM). This was then deprotected as per general deprotection procedure and purified by flash chromatography (2 – 15% MeOH/DCM) to afford the final product **2.28h** (xx, xx% yield over 3 steps) as a clear and colorless

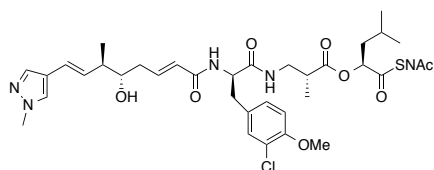
oil: $R_f = 0.25$ (10% MeOH/DCM); $^1\text{H NMR}$ (600 MHz, CD_3OD) δ 7.34 (d, $J = 2.2$ Hz, 1H), 7.25 (d, $J = 2.2$ Hz, 1H), 7.14 (dd, $J = 8.4, 2.2$ Hz, 1H), 6.97 (d, $J = 8.5$ Hz, 1H), 6.81 (dt, $J = 15.0, 7.3$ Hz, 1H), 6.42 (d, $J = 15.9$ Hz, 1H), 6.38 (d, $J = 2.1$ Hz, 1H), 6.25 (dd, $J = 15.9, 8.6$ Hz, 1H), 6.01 (dd, $J = 15.4, 1.5$ Hz, 1H), 5.21 (dd, $J = 9.5, 3.9$ Hz, 1H), 4.58 (dd, $J = 8.1, 7.0$ Hz, 1H), 3.84 (s, 3H), 3.82 (s, 3H), 3.65 (dt, $J = 8.0, 4.6$ Hz, 1H), 3.48 (dd, $J = 13.5, 6.6$ Hz, 1H), 3.33 – 3.30 (m, 2H) 3.20 (dd, $J = 13.5, 7.0$ Hz, 1H), 3.03 (td, $J = 6.6, 1.8$ Hz, 2H), 3.03 – 3.00 (m, 1H) 2.85 (dd, $J = 13.8, 8.1$ Hz, 1H), 2.70 (h, $J = 6.9$ Hz, 1H), 2.50 – 2.36 (m, 2H), 2.36 – 2.28 (m, 1H), 1.91 (s, 3H), 1.82 – 1.68 (m, 2H), 1.63 (ddd, $J = 13.2, 8.1, 3.9$ Hz, 1H), 1.15 (d, $J = 6.9$ Hz, 3H), 1.10 (d, $J = 7.1$ Hz, 3H), 0.95 (d, $J = 6.4$ Hz, 3H), 0.92 (d, $J = 6.5$ Hz, 3H). $^{13}\text{C NMR}$: (150 MHz, CD_3OD) δ 200.35, 175.08, 173.48, 173.44, 168.04, 155.42, 143.25, 142.85, 139.10, 137.95, 131.90, 131.50, 129.85, 126.20, 123.21, 118.41, 113.39, 103.55, 78.65, 75.00, 56.59, 56.25, 44.35, 42.74, 41.97, 40.59, 39.86, 38.87, 38.08, 36.45, 28.59, 25.76, 23.48, 22.54, 21.97, 17.32, 14.86. **HRMS** (ESI) calcd for $\text{C}_{37}\text{H}_{52}\text{ClN}_5\text{O}_8\text{S}$ $[\text{M}+\text{H}]$ 762.3298, found 762.3295.



(S)-1-((2-acetamidoethyl)thio)-4-methyl-1-oxopentan-2-yl (R)-3-((R)-3-(3-chloro-4-methoxyphenyl)-2-((2E,5S,6R,7E)-5-hydroxy-6-methyl-8-(1-methyl-1H-pyrazol-3-yl)octa-2,7-dienamido)propanamido)-2-methylpropanoate (2.28i)

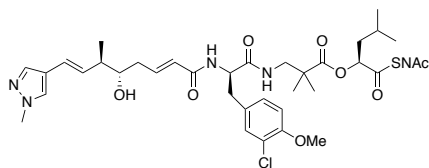
Reaction was run as per general coupling procedure, and purified by flash chromatography (1-10% MeOH/DCM) $R_f = 0.65$ (10% MeOH/DCM). This was then deprotected as per general deprotection procedure and purified by flash chromatography (2 – 15% MeOH/DCM) to afford the final product **2.28i** (0.019, 34% yield over 3 steps) as a clear and colorless oil: $R_f = 0.25$ (10% MeOH/DCM); $^1\text{H NMR}$ (600 MHz, CD_3OD) δ 7.34 (d, $J = 2.2$ Hz, 1H), 7.25 (d, $J = 2.2$ Hz, 1H), 7.14 (dd, $J = 8.5, 2.1$ Hz, 1H), 6.97 (d, $J = 8.5$ Hz, 1H), 6.81 (dt, $J = 15.0, 7.3$ Hz, 1H), 6.42 (d, $J = 15.9$ Hz, 1H), 6.38 (d, $J = 2.1$ Hz, 1H), 6.25 (dd, $J = 15.9, 8.6$ Hz, 1H), 6.01 (dd, $J = 15.4, 1.5$ Hz, 1H), 5.21 (dd, $J = 9.5, 3.9$ Hz, 1H), 4.58 (dd, $J = 8.0, 7.0$ Hz, 1H), 3.84 (s, 3H), 3.82 (s, 3H), 3.65 (dt, $J = 8.0, 4.6$ Hz, 1H), 3.48 (dd, $J = 13.5, 6.6$ Hz, 1H), 3.32 – 3.30 (m, 3H), 3.20 (dd, $J = 13.5, 7.0$ Hz, 1H), 3.05 – 2.98 (m, 3H), 2.85 (dd, $J = 13.8, 8.1$ Hz, 1H), 2.70 (h, $J = 6.9$ Hz, 1H), 2.49 – 2.36 (m, 1H), 2.36 – 2.28 (m, 1H), 1.91 (s, 3H), 1.80 – 1.68 (m, 2H), 1.67 – 1.60 (m, 1H), 1.15 (d, $J = 6.9$ Hz, 3H), 1.10 (d, $J = 7.1$ Hz, 3H), 0.95 (d, $J = 6.4$ Hz, 3H), 0.92 (d, $J = 6.5$ Hz, 3H). $^{13}\text{C NMR}$: (150 MHz, CD_3OD) δ 200.35, 175.08, 173.48, 173.44,

168.04, 155.42, 143.25, 142.85, 139.10, 137.95, 131.90, 131.50, 129.85, 126.19, 123.21, 118.41, 113.39, 103.55, 78.65, 75.00, 56.59, 56.25, 44.35, 42.74, 41.97, 40.59, 39.86, 38.87, 38.08, 36.45, 28.59, 25.76, 23.48, 22.54, 21.97, 17.32, 14.86. **HRMS** (ESI) calcd for C₃₇H₅₂ClN₅O₈S [M+H] 762.3298, found 762.3295.



(S)-1-((2-acetamidoethyl)thio)-4-methyl-1-oxopentan-2-yl (R)-3-((R)-3-(3-chloro-4-methoxyphenyl)-2-((2E,5S,6R,7E)-5-hydroxy-6-methyl-8-(1-methyl-1H-pyrazol-4-yl)octa-2,7-

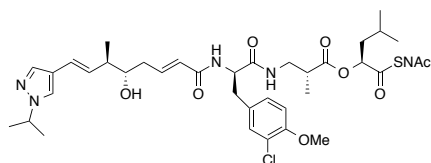
dienamido)propanamido)-2-methylpropanoate (2.28j). Reaction was run as per general coupling procedure, and purified by flash chromatography (1-10% MeOH/DCM) $R_f = 0.65$ (10% MeOH/DCM). This was then deprotected as per general deprotection procedure and purified by flash chromatography (2 – 15% MeOH/DCM) to afford the final product **2.28j** (0.039, 55% yield over 3 steps) as a clear and colorless oil: $R_f = 0.25$ (10% MeOH/DCM); $^1\text{H NMR}$ (600 MHz, CD₃OD) δ 7.54 (s, 1H), 7.50 (s, 1H), 7.25 (d, $J = 2.1$ Hz, 1H), 7.13 (dd, $J = 8.2, 2.1$ Hz, 1H), 6.97 (d, $J = 8.3$ Hz, 1H), 6.80 (dt, $J = 15.0, 7.3$ Hz, 1H), 6.22 (d, $J = 16.0$ Hz, 1H), 6.00 (d, $J = 16.1, 1\text{H}$), 5.94 (dd, $J = 16.0, 8.4$ Hz, 1H), 5.21 (dd, $J = 9.5, 4.0$ Hz, 1H), 4.58 (t, $J = 7.5$ Hz, 1H), 3.84 (s, 3H), 3.84 (s, 3H), 3.60 (dt, $J = 8.5, 4.5$ Hz, 1H), 3.48 (dd, $J = 13.5, 6.6$ Hz, 1H), 3.33-3.30 (m, 2H), 3.20 (dd, $J = 13.5, 6.9$ Hz, 1H), 3.03 (t, $J = 5.8$ Hz, 2H), 3.03 – 3.00 (m, 1H), 2.85 (dd, $J = 13.7, 8.2$ Hz, 1H), 2.70 (q, $J = 7.0$ Hz, 1H), 2.40 – 2.23 (m, 3H), 1.91 (s, 3H), 1.81 – 1.68 (m, 2H), 1.67 – 1.58 (m, 1H), 1.10 (d, $J = 7.0$ Hz, 6H), 0.95 (d, $J = 6.3$ Hz, 3H), 0.92 (d, $J = 6.3$ Hz, 4H). $^{13}\text{C NMR}$ (150 MHz, CD₃OD): **HRMS** (ESI) calcd for C₃₇H₅₂ClN₅O₈S [M+H] 762.3298, found 762.3294.



(S)-1-((2-acetamidoethyl)thio)-4-methyl-1-oxopentan-2-yl 3-((R)-3-(3-chloro-4-methoxyphenyl)-2-((2E,5S,6R,7E)-5-hydroxy-6-methyl-8-(1-methyl-1H-pyrazol-4-yl)octa-2,7-

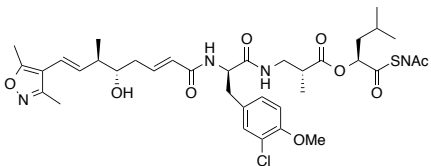
dienamido)propanamido)-2,2-dimethylpropanoate (2.28k). Reaction was run as per general coupling procedure, and purified by flash chromatography (1-10% MeOH/DCM) $R_f = 0.65$ (10% MeOH/DCM). This was then deprotected as per general deprotection procedure and purified by flash chromatography (2 – 15% MeOH/DCM) to afford the final product **2.28k** (0.019, 44% yield over 3 steps) as a clear and colorless oil: $R_f = 0.25$ (10% MeOH/DCM); $^1\text{H NMR}$ (600MHz,

CD₃OD) δ 7.55 (s, 1H), 7.50 (s, 1H), 7.28 (d, J = 2.1 Hz, 1H), 7.15 (dd, J = 8.5, 2.2 Hz, 1H), 6.96 (d, J = 8.5 Hz, 1H), 6.79 (dt, J = 14.9, 7.3 Hz, 1H), 6.21 (d, J = 16.1 Hz, 1H), 5.99 (d, J = 15.4 Hz, 1H), 5.93 (dd, J = 16.0, 8.4 Hz, 1H), 5.20 (dd, J = 9.6, 3.9 Hz, 1H), 4.65 (dd, J = 8.6, 6.5 Hz, 1H), 3.84 (s, 3H), 3.83 (s, 3H), 3.60 (dt, J = 8.8, 4.6 Hz, 1H), 3.44 – 3.32 (m, 2H), 3.12 – 2.98 (m, 3H), 2.85 (dd, J = 13.9, 8.6 Hz, 1H), 2.32 (m, 3H), 1.91 (s, 3H), 1.83 – 1.68 (m, 2H), 1.64 (ddd, J = 12.8, 8.4, 3.8 Hz, 1H), 1.16 (s, 6H), 1.10 (d, J = 6.9 Hz, 3H), 0.96 (d, J = 6.5 Hz, 3H), 0.92 (d, J = 6.5 Hz, 3H). ¹³C NMR (150 MHz, CD₃OD) δ 200.54, 176.85, 173.68, 173.44, 168.22, 155.38, 143.62, 137.71, 131.90, 131.68, 130.86, 129.81, 129.39, 126.00, 123.23, 122.47, 121.60, 113.40, 78.80, 75.37, 56.60, 56.35, 47.77, 44.68, 44.12, 41.94, 39.86, 38.72, 38.67, 37.85, 28.73, 25.87, 23.49, 23.25, 23.17, 22.59, 21.94, 17.40. HRMS (ESI) calcd for C₃₈H₅₄ClN₅O₈S [M+H] xx, found x.



(S)-1-((2-acetamidoethyl)thio)-4-methyl-1-oxopentan-2-yl (R)-3-((R)-3-(3-chloro-4-methoxyphenyl)-2-((2E,5S,6R,7E)-5-hydroxy-8-(1-isopropyl-1H-pyrazol-4-yl)-6-methylocta-2,7-dienamido)propanamido)-2-methylpropanoate (2.281). Reaction was run as per general coupling procedure, and purified by flash chromatography (1-10% MeOH/DCM) R_f = 0.65 (10% MeOH/DCM). This was then deprotected as per general deprotection procedure and purified by flash chromatography (2 – 15% MeOH/DCM) to afford the final product **2.281** (xx, xx% yield over 3 steps) as a clear and colorless oil: R_f = 0.25 (10% MeOH/DCM); ¹H NMR (600 MHz, CD₃OD) δ 7.64 (s, 1H), 7.51 (s, 1H), 7.25 (d, J = 2.2 Hz, 1H), 7.14 (dd, J = 8.4, 2.2 Hz, 1H), 6.97 (d, J = 8.4 Hz, 1H), 6.80 (dt, J = 15.0, 7.3 Hz, 1H), 6.23 (d, J = 16.0 Hz, 1H), 6.00 (d, J = 15.4 Hz, 1H), 5.94 (dd, J = 16.0, 8.5 Hz, 1H), 5.21 (dd, J = 9.5, 4.0 Hz, 1H), 4.58 (t, J = 7.5 Hz, 1H), 4.46 (hept, J = 6.6 Hz, 1H), 3.84 (s, 3H), 3.61 (dt, J = 8.6, 4.5 Hz, 1H), 3.48 (dd, J = 13.5, 6.6 Hz, 1H), 3.33 – 3.30 (m, 2H), 3.20 (dd, J = 13.5, 7.0 Hz, 1H), 3.03 (t, J = 6.6 Hz, 2H), 3.03 – 3.00 (m, 1H), 2.85 (dd, J = 13.8, 8.1 Hz, 1H), 2.70 (h, J = 6.9 Hz, 1H), 2.43 – 2.23 (m, 3H), 1.91 (s, 3H), 1.82 – 1.69 (m, 2H), 1.63 (ddd, J = 13.2, 8.1, 3.9 Hz, 1H), 1.47 (d, J = 6.7 Hz, 6H), 1.11 (d, J = 6.9 Hz, 3H), 1.10 (d, J = 7.1 Hz, 3H), 0.95 (d, J = 6.4 Hz, 3H), 0.92 (d, J = 6.4 Hz, 3H). ¹³C NMR (150 MHz, CD₃OD) δ 200.36, 175.08, 173.49, 173.44, 168.11, 155.42, 143.59, 137.30, 131.92, 131.52, 130.64, 129.85, 126.04 (2), 123.22, 121.90, 121.82, 113.39, 78.65, 75.41, 56.59,

56.24, 54.99, 44.15, 42.74, 41.97, 40.59, 39.86, 38.67, 38.07, 28.59, 25.76, 23.48, 23.08 (2), 22.54, 21.97, 17.44, 14.86. **HRMS** (ESI) calcd for C₃₉H₅₆ClN₅O₈S [M+H] 790.3611, found 790.3608.

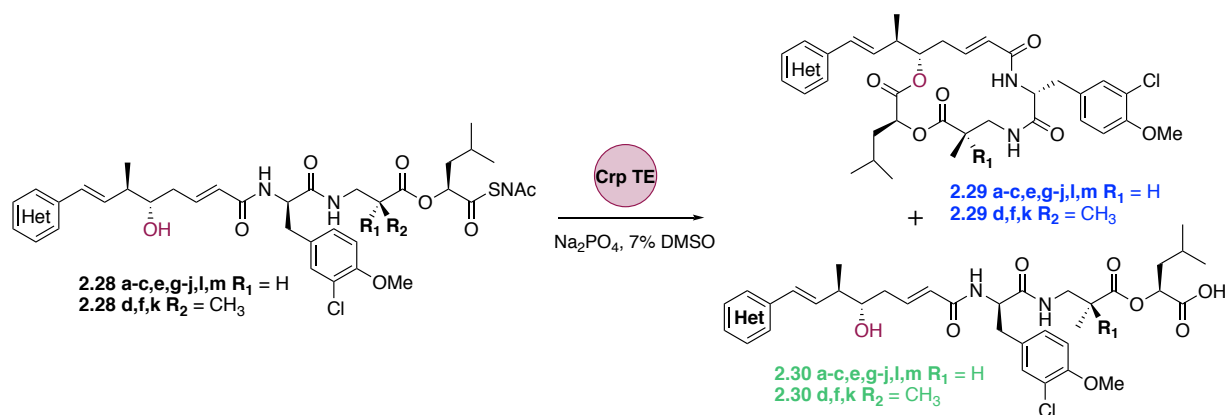


(S)-1-((2-acetamidoethyl)thio)-4-methyl-1-oxopentan-2-yl
(R)-3-((R)-3-(3-chloro-4-methoxyphenyl)-2-((2E,5S,6R,7E)-8-(3,5-dimethylisoxazol-4-yl)-5-hydroxy-

6-methylocta-2,7-dienamido)propanamido)-2-methylpropanoate (2.28m). Reaction was run as per general coupling procedure, and purified by flash chromatography (1-10% MeOH/DCM) $R_f = 0.65$ (10% MeOH/DCM). This was then deprotected as per general deprotection procedure and purified by flash chromatography (2 – 15% MeOH/DCM) to afford the final product **2.28m** (15, 43% yield over 3 steps) as a clear and colorless oil: $R_f = 0.25$ (10% MeOH/DCM); **¹H NMR** (600 MHz, CD₃OD) δ 7.25 (d, $J = 2.1$ Hz, 1H), 7.14 (dd, $J = 8.4, 2.2$ Hz, 1H), 6.97 (d, $J = 8.4$ Hz, 1H), 6.81 (dt, $J = 15.0, 7.3$ Hz, 1H), 6.14 (d, $J = 16.3$ Hz, 1H), 6.01 (d, $J = 15.4$ Hz, 1H), 5.93 (dd, $J = 16.3, 8.5$ Hz, 1H), 5.21 (dd, $J = 9.5, 4.0$ Hz, 1H), 4.57 (t, $J = 7.5$ Hz, 1H), 3.84 (s, 3H), 3.63 (dt, $J = 8.5, 4.7$ Hz, 1H), 3.48 (dd, $J = 13.5, 6.6$ Hz, 1H), 3.33 – 3.30 (m, 2H) 3.20 (dd, $J = 13.5, 7.0$ Hz, 1H), 3.03 (t, $J = 6.8$ Hz, 2H), 3.02 – 2.99 (m, 1H) 2.85 (dd, $J = 13.7, 8.1$ Hz, 1H), 2.70 (h, $J = 7.0$ Hz, 1H), 2.39 (s, 3H), 2.38 – 2.30 (m, 3H), 2.28 (s, 3H), 1.91 (s, 3H), 1.82 – 1.67 (m, 2H), 1.63 (ddd, $J = 12.6, 8.2, 3.9$ Hz, 1H), 1.14 (d, $J = 6.8$ Hz, 3H), 1.10 (d, $J = 7.1$ Hz, 3H), 0.95 (d, $J = 6.4$ Hz, 3H), 0.92 (d, $J = 6.4$ Hz, 3H). **¹³C NMR** (150 MHz, CD₃OD) δ 200.36, 175.08, 173.49, 173.44, 168.04, 166.54, 159.73, 155.42, 143.35, 135.53, 131.90, 131.50, 129.85, 126.13, 123.22, 119.18, 114.25, 113.38, 78.65, 75.09, 56.59, 56.26, 48.57, 44.85, 42.74, 41.97, 40.59, 39.86, 38.94, 38.09, 28.59, 25.76, 23.48, 22.53, 21.97, 17.69, 14.86, 11.47, 11.29. **HRMS** (ESI) calcd for C₃₈H₅₃ClN₄O₉S [M+H] 777.3295, found 777.3293.

6.2 CrpTE Mediated Cyclization Experimentals and Characterization

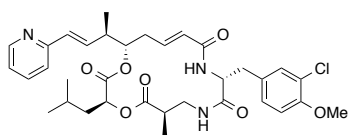
*CrpTE was purified as described in section 6.3



General Analytical CrpTE Cyclization Procedure. Seco cryptophycins **2.28a-m** as a 10 mM solution in DMSO (xx, final conc. 50 μ M) were added to 100 mM sodium phosphate buffer (150 μ L). The reaction medium was supplemented with DMSO to 5 v/v% and CrpTE as a 50 μ M solution in **reaction storage buffer** (see buffer recipes) was added (0.5 μ M final concentration). The reaction was shaken at 120 rpm for 12 hours at 37 °C prior to extraction with 300 μ L of ethyl acetate. 100 μ L of the organic layer was dried into an HPLC vial, taken up in 50 μ L of MeOH and analyzed by Qtof MS, results are summarized in **Figure 2.xx**.

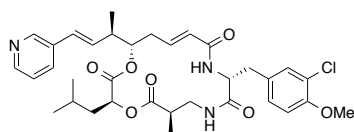
General Semi-Preparative CrpTE Cyclization Procedure. To a 250 mL Erlenmeyer flask was added DMSO (5%), and substrate **2.28a-m** (75 μ M) suspended in DMSO. This was diluted with phosphate buffer (pH = 7.2, 100 mM) and warmed to 30 °C for 20 min prior to treatment with CrpTE enzyme (0.5 μ M). The reaction was allowed to shake at 120 RPM overnight, prior to 1:1 v/v dilution with acetone and chilling to -20 °C in the freezer. The precipitated protein was filtered through celite, washing with acetone, organics removed under reduced pressure, and the remaining aqueous layer was extracted with DCM 3 x 20 mL. The organics were combined, dried over sodium sulfate and concentrated. The reactions were purified using a HydroRP C18 (need dimensions) using a 20 – 80% water/acetonitrile gradient with a flow rate of 3 mL/min.

Heterocyclic Cryptophycin Experimentals



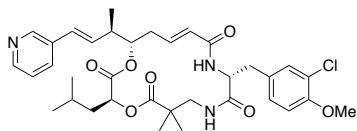
(3*S*,6*R*,10*R*,16*S*,*E*)-10-(3-chloro-4-methoxybenzyl)-3-isobutyl-6-methyl-16-((*R*,*E*)-4-(pyridin-2-yl)but-3-en-2-yl)-1,4-dioxo-8,11-diazacyclohexadec-13-ene-2,5,9,12-tetraone (2.28b). Reaction was

run and purified as general procedure for semi-preparative scale reaction. $^1\text{H NMR}$ (600 MHz, CD_3OD) δ 8.46 (dd, $J = 5.0, 0.9$ Hz, 1H), 7.78 (td, $J = 7.7, 1.8$ Hz, 1H), 7.48 (d, $J = 7.9$ Hz, 1H), 7.28 (d, $J = 2.2$ Hz, 1H), 7.26 (ddd, $J = 7.5, 5.0, 1.1$ Hz, 1H), 7.17 (dd, $J = 8.5, 2.2$ Hz, 1H), 6.98 (d, $J = 8.5$ Hz, 1H), 6.71 (ddd, $J = 15.1, 11.1, 3.9$ Hz, 1H), 6.61 – 6.57 (m, 2H), 5.93 (dd, $J = 15.1, 1.9$ Hz, 1H), 5.09 (ddd, $J = 11.3, 6.9, 1.9$ Hz, 1H), 4.93 (dd, $J = 9.9, 3.6$ Hz, 1H), 4.52 (dd, $J = 11.3, 3.9$ Hz, 1H), 3.84 (s, 3H), 3.58 (dd, $J = 13.8, 3.3$ Hz, 1H), 3.27 (dd, $J = 13.8, 3.0$ Hz, 1H), 3.18 (dd, $J = 14.5, 3.9$ Hz, 1H), 2.80 – 2.73 (m, 2H), 2.73 – 2.65 (m, 2H), 2.39 (dt, $J = 14.5, 11.2$ Hz, 1H), 1.69 – 1.52 (m, 2H), 1.34 (ddd, $J = 14.1, 8.8, 3.6$ Hz, 1H), 1.18 (d, $J = 7.1$ Hz, 6H), 0.74 (d, $J = 6.5$ Hz, 3H), 0.71 (d, $J = 6.6$ Hz, 3H). $^{13}\text{C NMR}$ (151 MHz, CD_3OD) δ 177.53, 174.04, 172.22, 168.33, 156.60, 155.36, 149.99, 143.41, 138.74, 137.58, 132.23, 132.10, 131.49, 129.28, 125.62, 123.71, 123.27, 122.82, 113.50, 78.48, 72.86, 57.35, 56.60, 43.46, 41.19, 40.88, 38.98, 37.99, 36.36, 25.62, 23.20, 21.66, 17.53, 15.06. **HRMS** (ESI) calcd for $\text{C}_{34}\text{H}_{42}\text{ClN}_3\text{O}_7$ [$\text{M}+\text{H}$] 640.2784, found 640.2787.



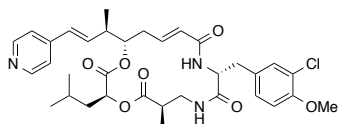
(3S,6R,10R,16S,E)-10-(3-chloro-4-methoxybenzyl)-3-isobutyl-6-methyl-16-((R,E)-4-(pyridin-3-yl)but-3-en-2-yl)-1,4-dioxo-8,11-diazacyclohexadec-13-ene-2,5,9,12-tetraone (2.28c).

Reaction was run and purified as general procedure for semi-preparative scale reaction. $^1\text{H NMR}$ (600 MHz, CD_3OD) δ 8.53 (d, $J = 2.2$ Hz, 1H), 8.38 (dd, $J = 4.8, 1.6$ Hz, 1H), 7.92 (d, $J = 8.0$ Hz, 1H), 7.40 (dd, $J = 8.0, 4.9$ Hz, 1H), 7.28 (d, $J = 2.2$ Hz, 1H), 7.17 (dd, $J = 8.4, 2.2$ Hz, 1H), 6.98 (d, $J = 8.4$ Hz, 1H), 6.71 (ddd, $J = 15.1, 11.2, 3.9$ Hz, 1H), 6.53 (d, $J = 15.9$ Hz, 1H), 6.30 (dd, $J = 15.9, 8.9$ Hz, 1H), 5.93 (dd, $J = 15.2, 1.9$ Hz, 1H), 5.08 (ddd, $J = 11.2, 7.2, 1.9$ Hz, 1H), 4.93 (dd, $J = 9.9, 3.7$ Hz, 1H), 4.52 (dd, $J = 11.2, 3.9$ Hz, 1H), 3.84 (s, 3H), 3.58 (dd, $J = 13.8, 3.3$ Hz, 1H), 3.27 (dd, $J = 13.8, 3.0$ Hz, 1H), 3.18 (dd, $J = 14.5, 3.9$ Hz, 1H), 2.80 – 2.63 (m, 4H), 2.37 (dt, $J = 14.4, 11.1$ Hz, 1H), 1.69 – 1.55 (m, 2H), 1.31 (ddd, $J = 14.1, 8.9, 3.7$ Hz, 1H), 1.19 (d, $J = 3.5$ Hz, 3H), 1.18 (d, $J = 2.9$ Hz, 3H), 0.74 (d, $J = 6.5$ Hz, 3H), 0.70 (d, $J = 6.5$ Hz, 3H). $^{13}\text{C NMR}$ (150 MHz, CD_3OD) δ 180.30, 177.53, 174.03, 172.21, 168.33, 155.36, 148.71, 148.40, 143.42, 135.55, 134.96, 134.86, 132.21, 131.49, 129.28, 128.77, 125.62, 125.40, 113.49, 78.47, 72.80, 57.36, 56.60, 43.75, 41.18, 40.94, 38.97, 37.88, 36.35, 25.60, 23.18, 21.69, 17.50, 15.06. **HRMS** (ESI) calcd for $\text{C}_{34}\text{H}_{42}\text{ClN}_3\text{O}_7$ [$\text{M}+\text{H}$] 640.2784, found 640.2789.



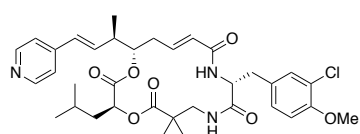
(3*S*,10*R*,16*S*,*E*)-10-(3-chloro-4-methoxybenzyl)-3-isobutyl-6,6-dimethyl-16-((*R,E*)-4-(pyridin-3-yl)but-3-en-2-yl)-1,4-dioxo-8,11-diazacyclohexadec-13-ene-2,5,9,12-tetraone (2.28d).

Reaction was run and purified as general procedure for semi-preparative scale reaction. $^1\text{H NMR}$ (600MHz, CD_3OD) δ 8.53 (s, 1H), 8.38 (d, $J = 4.7$ Hz, 1H), 7.92 (dt, $J = 8.0, 1.9$ Hz, 1H), 7.40 (dd, $J = 8.0, 4.8$ Hz, 1H), 7.28 (d, $J = 2.2$ Hz, 1H), 7.17 (dd, $J = 8.4, 2.2$ Hz, 1H), 6.98 (d, $J = 8.4$ Hz, 1H), 6.72 (ddd, $J = 15.2, 11.2, 3.9$ Hz, 1H), 6.53 (d, $J = 15.9$ Hz, 1H), 6.30 (dd, $J = 16.0, 8.9$ Hz, 1H), 5.92 (dd, $J = 15.1, 1.9$ Hz, 1H), 5.07 (ddd, $J = 11.1, 7.2, 1.8$ Hz, 2H), 4.96 (dd, $J = 9.9, 3.4$ Hz, 1H), 4.51 (dd, $J = 11.3, 3.8$ Hz, 1H), 3.84 (s, 3H), 3.46 (d, $J = 13.6$ Hz, 1H), 3.18 (dd, $J = 14.5, 3.8$ Hz, 1H), 3.08 (d, $J = 13.7$ Hz, 1H), 2.74 (dd, $J = 14.5, 11.4$ Hz, 1H), 2.74 – 2.62 (m, 2H), 2.36 (dt, $J = 14.4, 11.2$ Hz, 1H), 1.66 – 1.55 (m, 2H), 1.37 – 1.26 (m, 3H), 1.20 (s, 3H), 1.16 (s, 3H), 0.74 (d, $J = 6.4$ Hz, 3H), 0.70 (d, $J = 6.4$ Hz, 3H). $^{13}\text{C NMR}$ (150 MHz, CD_3OD) δ 180.03, 178.94, 173.68, 172.01, 168.22, 155.37, 148.71, 148.40, 143.63, 135.55, 134.85, 132.17, 131.46, 129.26, 128.78, 125.43, 123.28, 113.50, 78.43, 72.58, 57.48, 56.60, 47.39, 44.02, 43.75, 40.92, 37.92, 36.48, 31.64, 25.85, 23.32, 23.29, 23.22, 21.65, 17.49. **HRMS** (ESI) calcd for $\text{C}_{35}\text{H}_{44}\text{ClN}_3\text{O}_7$ $[\text{M}+\text{H}]$ 654.2941, found 654.2940.



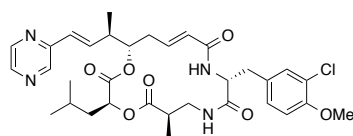
(3*S*,6*R*,10*R*,16*S*,*E*)-10-(3-chloro-4-methoxybenzyl)-3-isobutyl-6-methyl-16-((*R,E*)-4-(pyridin-4-yl)but-3-en-2-yl)-1,4-dioxo-8,11-diazacyclohexadec-13-ene-2,5,9,12-tetraone (2.28e). Reaction was run and purified as general procedure for semi-preparative scale reaction. $^1\text{H NMR}$ (600MHz, CD_3OD) δ 8.43 (d, $J = 6.2$ Hz, 2H), 7.42 (d, $J = 6.3$ Hz, 2H), 7.27 (d, $J = 2.1$ Hz, 1H), 7.15 (dd, $J = 8.5, 2.1$ Hz, 1H), 6.96 (d, $J = 8.4$ Hz, 1H), 6.69 (ddd, $J = 15.1, 11.1, 3.9$ Hz, 1H), 6.50 – 6.47 (m, 2H), 5.91 (dd, $J = 15.2, 1.8$ Hz, 1H), 5.08 (dd, $J = 10.7, 8.3$ Hz, 1H), 4.90 (dd, $J = 9.9, 3.6$ Hz, 1H), 4.51 (dd, $J = 11.2, 3.9$ Hz, 1H), 3.82 (s, 3H), 3.56 (dd, $J = 13.8, 3.3$ Hz, 1H), 3.25 (dd, $J = 13.8, 2.9$ Hz, 1H), 3.16 (dd, $J = 14.5, 3.9$ Hz, 1H), 2.77 – 2.62 (m, 4H), 2.34 (dt, $J = 14.7, 11.2$ Hz, 1H), 1.67 – 1.51 (m, 2H), 1.28 (ddd, $J = 12.9, 8.7, 3.5$ Hz, 1H), 1.17 (d, $J = 2.6$ Hz, 3H), 1.16 (d, $J = 2.0$ Hz, 3H), 0.72 (d, $J = 6.4$ Hz, 3H), 0.68 (d, $J = 6.5$ Hz, 3H). $^{13}\text{C NMR}$ (150 MHz, CD_3OD) δ 177.55, 174.02, 172.17, 168.31, 155.36, 150.42, 147.12, 143.33, 138.63, 132.21, 131.49, 130.23, 129.28, 125.66, 123.27, 122.49,

113.49, 78.35, 72.78, 57.36, 56.60, 43.67, 41.17, 40.91, 38.96, 37.88, 36.35, 25.60, 23.15, 21.66, 17.35, 15.06. **HRMS** (ESI) calcd for C₃₄H₄₂ClN₃O₇ [M+H] 640.2784, found 640.2787.



(3*S*,10*R*,16*S*,*E*)-10-(3-chloro-4-methoxybenzyl)-3-isobutyl-6,6-dimethyl-16-((*R,E*)-4-(pyridin-4-yl)but-3-en-2-yl)-1,4-dioxo-8,11-diazacyclohexadec-13-ene-2,5,9,12-tetraone (2.28f).

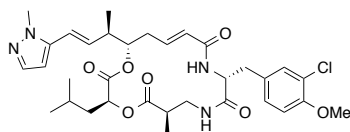
Reaction was run and purified as general procedure for semi-preparative scale reaction. ¹H NMR (600MHz, CD₃OD) δ 8.45 (d, *J* = 5.7 Hz, 2H), 7.44 (d, *J* = 6.3 Hz, 2H), 7.28 (d, *J* = 2.2 Hz, 1H), 7.17 (dd, *J* = 8.4, 2.2 Hz, 1H), 6.98 (d, *J* = 8.5 Hz, 1H), 6.72 (ddd, *J* = 15.1, 11.2, 3.9 Hz, 1H), 6.51 (s, 1H), 6.50 (d, *J* = 4.6 Hz, 1H), 5.92 (dd, *J* = 15.1, 1.9 Hz, 1H), 5.09 (ddd, *J* = 11.3, 7.2, 1.9 Hz, 1H), 4.95 (dd, *J* = 9.9, 3.3 Hz, 1H), 4.51 (dd, *J* = 11.3, 3.7 Hz, 1H), 3.84 (s, 3H), 3.46 (d, *J* = 13.6 Hz, 1H), 3.18 (dd, *J* = 14.6, 3.8 Hz, 1H), 3.08 (d, *J* = 13.6 Hz, 1H), 2.74 (dd, *J* = 14.5, 11.3 Hz, 1H), 2.74 – 2.66 (m, 2H), 2.35 (dt, *J* = 14.5, 11.2 Hz, 1H), 1.67 – 1.54 (m, 2H), 1.37 – 1.24 (m, 1H), 1.19 (s, 3H), 1.16 (s, 3H), 0.74 (d, *J* = 6.3 Hz, 3H), 0.71 (d, *J* = 6.4 Hz, 3H). ¹³C NMR (150 MHz, CD₃OD) δ 177.59, 174.05, 172.32, 168.36, 155.34, 143.63, 137.86, 132.21, 131.48, 130.26, 129.63, 129.28, 125.50, 123.24, 122.46, 121.98, 113.46, 78.68, 72.91, 57.37, 56.58, 43.68, 41.18, 40.87, 38.95, 38.75, 37.84, 36.36, 25.64, 23.18, 21.67, 17.75, 15.07. **HRMS** (ESI) calcd for C₃₅H₄₄ClN₃O₇ [M+H] 654.2941, found 654.2945.



(3*S*,6*R*,10*R*,16*S*,*E*)-10-(3-chloro-4-methoxybenzyl)-3-isobutyl-6-methyl-16-((*R,E*)-4-(pyrazin-2-yl)but-3-en-2-yl)-1,4-dioxo-8,11-diazacyclohexadec-13-ene-2,5,9,12-tetraone (2.28g).

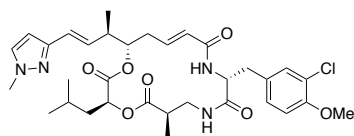
Reaction was run and purified as general procedure for semi-preparative scale reaction. ¹H NMR (600MHz, CD₃OD) δ 8.61 (d, *J* = 1.5 Hz, 1H), 8.54 (dd, *J* = 2.6, 1.5 Hz, 1H), 8.42 (d, *J* = 2.6 Hz, 1H), 7.28 (d, *J* = 2.2 Hz, 1H), 7.17 (dd, *J* = 8.4, 2.2 Hz, 1H), 6.98 (d, *J* = 8.5 Hz, 1H), 6.84 (dd, *J* = 15.7, 8.9 Hz, 1H), 6.71 (ddd, *J* = 15.2, 11.2, 3.9 Hz, 1H), 6.64 (d, *J* = 15.7 Hz, 1H), 5.93 (dd, *J* = 15.1, 1.9 Hz, 1H), 5.11 (ddd, *J* = 11.3, 6.8, 2.0 Hz, 1H), 4.94 (dd, *J* = 9.7, 3.7 Hz, 1H), 4.53 (dd, *J* = 11.2, 3.9 Hz, 1H), 3.84 (s, 3H), 3.58 (dd, *J* = 13.8, 3.4 Hz, 1H), 3.27 (dd, *J* = 13.7, 3.0 Hz, 1H), 3.18 (dd, *J* = 14.5, 3.9 Hz, 1H), 2.81 – 2.72 (m, 3H), 2.69 (ddd, *J* = 12.6, 4.0, 2.0 Hz, 1H), 2.38 (dt, *J* = 14.6, 11.2 Hz, 1H), 1.70 – 1.57 (m, 2H), 1.36 (ddd, *J* = 14.1, 8.7, 3.7 Hz, 1H), 1.19 (d, *J* = 6.9 Hz, 3H), 1.19 (d, *J* = 7.5 Hz, 3H), 0.76 (d, *J* = 6.5 Hz, 3H). ¹³C NMR (150 MHz, CD₃OD) δ

177.53, 174.03, 172.18, 168.32, 155.36, 152.52, 145.69, 144.15, 143.92, 143.33, 140.15, 132.22, 131.48, 129.28, 128.83, 125.65, 123.27, 113.50, 78.45, 72.83, 57.35, 56.60, 43.37, 41.19, 40.91, 38.98, 38.03, 36.35, 25.65, 23.23, 21.74, 17.37, 15.07. **HRMS** (ESI) calcd for [M+H] xx, found xx.



(3*S*,6*R*,10*R*,16*S*,*E*)-10-(3-chloro-4-methoxybenzyl)-3-isobutyl-6-methyl-16-((*R*,*E*)-4-(1-methyl-1*H*-pyrazol-5-yl)but-3-en-2-yl)-1,4-dioxo-8,11-diazacyclohexadec-13-ene-2,5,9,12-tetraone

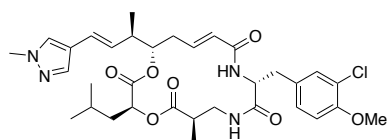
(2.28h). Reaction was run and purified as general procedure for semi-preparative scale reaction. **¹H NMR** (600 MHz, CD₃OD) δ 7.36 (d, *J* = 2.1 Hz, 1H), 7.28 (d, *J* = 2.2 Hz, 1H), 7.17 (dd, *J* = 8.5, 2.2 Hz, 1H), 6.98 (d, *J* = 8.4 Hz, 1H), 6.71 (ddd, *J* = 15.1, 11.2, 3.9 Hz, 1H), 6.52 (d, *J* = 15.8 Hz, 1H), 6.42 (d, *J* = 2.1 Hz, 1H), 6.14 (dd, *J* = 15.8, 9.0 Hz, 1H), 5.93 (dd, *J* = 15.1, 1.9 Hz, 1H), 5.07 (ddd, *J* = 11.3, 6.9, 1.9 Hz, 1H), 4.93 (dd, *J* = 9.8, 3.6 Hz, 1H), 4.52 (dd, *J* = 11.3, 3.9 Hz, 1H), 3.84 (s, 6H), 3.59 (dd, *J* = 13.8, 3.3 Hz, 1H), 3.27 (dd, *J* = 13.8, 3.0 Hz, 1H), 3.18 (dd, *J* = 14.5, 3.9 Hz, 1H), 2.79 – 2.73 (m, 2H), 2.73 – 2.62 (m, 2H), 2.35 (dt, *J* = 14.6, 11.2 Hz, 1H), 1.71 – 1.57 (m, 2H), 1.35 (ddd, *J* = 14.0, 8.6, 3.5 Hz, 1H), 1.19 (d, *J* = 7.4 Hz, 3H), 1.17 (d, *J* = 6.9 Hz, 3H), 0.77 (d, *J* = 6.4 Hz, 6H). **¹³C NMR**: (150 MHz, CD₃OD) δ 177.58, 174.04, 172.22, 168.32, 155.35, 143.40, 142.29, 139.27, 136.81, 132.20, 131.48, 129.28, 125.61, 123.24, 119.18, 113.46, 103.68, 78.39, 72.84, 57.39, 56.58, 43.68, 41.16, 40.96, 38.96, 37.96, 36.51, 36.36, 25.69, 23.25, 21.76, 17.53, 15.08. **HRMS** (ESI) calcd for C₃₃H₄₃ClN₄O₇ [M+H] 643.2893, found 643.2890.



(3*S*,6*R*,10*R*,16*S*,*E*)-10-(3-chloro-4-methoxybenzyl)-3-isobutyl-6-methyl-16-((*R*,*E*)-4-(1-methyl-1*H*-pyrazol-3-yl)but-3-en-2-yl)-1,4-dioxo-8,11-diazacyclohexadec-13-ene-2,5,9,12-tetraone

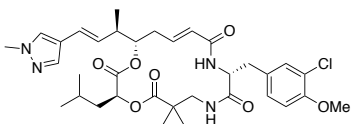
(2.28i). Reaction was run and purified as general procedure for semi-preparative scale reaction. **¹H NMR** (600 MHz, CD₃OD) δ 7.70 (s, 1H), 7.53 (s, 1H), 7.28 (d, *J* = 2.2 Hz, 1H), 7.17 (dd, *J* = 8.4, 2.2 Hz, 1H), 6.98 (d, *J* = 8.5 Hz, 1H), 6.70 (ddd, *J* = 15.1, 11.2, 3.9 Hz, 1H), 6.28 (d, *J* = 15.8 Hz, 1H), 5.92 (dd, *J* = 15.2, 1.9 Hz, 1H), 5.79 (dd, *J* = 15.9, 8.9 Hz, 1H), 4.98 (ddd, *J* = 11.2, 7.5, 2.0 Hz, 1H), 4.91 (dd, *J* = 10.0, 3.5 Hz, 1H), 4.52 (dd, *J* = 11.2, 3.8 Hz, 1H), 4.47 (p, *J* = 6.7 Hz, 1H), 3.84 (s, 3H), 3.58 (dd, *J* = 13.8, 3.3 Hz, 1H), 3.27 (dd, *J* = 13.7, 3.0 Hz, 1H), 3.18 (dd, *J* = 14.5, 3.8 Hz, 1H), 2.79 – 2.71 (m, 2H), 2.71 – 2.63 (m, 1H), 2.50 (h, *J* = 7.2 Hz, 1H), 2.33 (dt, *J* = 14.5,

11.2 Hz, 1H), 1.72 – 1.54 (m, 2H), 1.46 (d, $J = 6.7$ Hz, 6H), 1.37 (ddd, $J = 14.2, 9.0, 3.6$ Hz, 1H), 1.18 (d, $J = 7.4$ Hz, 3H), 1.12 (d, $J = 6.9$ Hz, 3H), 0.77 (d, $J = 6.5$ Hz, 3H), 0.74 (d, $J = 6.6$ Hz, 3H). ^{13}C NMR (150 MHz, CD_3OD) δ 177.60, 174.05, 172.33, 168.37, 155.35, 143.64, 137.40, 132.21, 131.48, 130.12, 129.28, 126.34, 125.51, 123.25, 122.67, 121.38, 113.46, 78.67, 72.93, 57.38, 56.59, 55.07, 43.80, 41.18, 40.87, 38.96, 37.85, 36.37, 25.64, 23.31, 23.09, 21.70, 17.79, 15.07. HRMS (ESI) calcd for $\text{C}_{35}\text{H}_{47}\text{ClN}_4\text{O}_7$ [M+H] 671.3206, found 671.3025.



(3*S*,6*R*,10*R*,16*S*,*E*)-10-(3-chloro-4-methoxybenzyl)-3-isobutyl-6-methyl-16-((*R*,*E*)-4-(1-methyl-1*H*-pyrazol-4-yl)but-3-en-2-yl)-1,4-dioxo-8,11-diazacyclohexadec-13-ene-

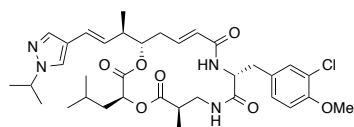
2,5,9,12-tetraone (2.28j). Reaction was run and purified as general procedure for semi-preparative scale reaction. ^1H NMR (600 MHz, CD_3OD) δ 7.61 (s, 1H), 7.51 (s, 1H), 7.28 (d, $J = 2.2$ Hz, 1H), 7.17 (dd, $J = 8.4, 2.2$ Hz, 1H), 6.98 (d, $J = 8.4$ Hz, 1H), 6.70 (ddd, $J = 15.2, 11.2, 3.9$ Hz, 1H), 6.27 (d, $J = 15.9$ Hz, 1H), 5.92 (dd, $J = 15.2, 1.9$ Hz, 1H), 5.80 (dd, $J = 15.9, 8.9$ Hz, 1H), 4.99 (ddd, $J = 11.3, 7.1, 1.9$ Hz, 1H), 4.92 (dd, $J = 10.0, 3.6$ Hz, 1H), 4.52 (dd, $J = 11.3, 3.8$ Hz, 1H), 3.84 (d, $J = 1.8$ Hz, 6H), 3.58 (dd, $J = 13.8, 3.3$ Hz, 1H), 3.27 (dd, $J = 13.8, 2.9$ Hz, 1H), 3.18 (dd, $J = 14.5, 3.8$ Hz, 1H), 2.81 – 2.70 (m, 2H), 2.69 – 2.60 (m, 1H), 2.50 (p, $J = 7.1$ Hz, 1H), 2.33 (dt, $J = 14.5, 11.2$ Hz, 1H), 1.71 – 1.56 (m, 2H), 1.38 (ddd, $J = 13.2, 9.0, 3.6$ Hz, 1H), 1.18 (d, $J = 7.5$ Hz, 3H), 1.11 (d, $J = 6.8$ Hz, 3H), 0.78 (d, $J = 6.5$ Hz, 3H), 0.76 (d, $J = 6.6$ Hz, 3H). ^{13}C NMR (150 MHz, CD_3OD) δ 177.59, 174.05, 172.32, 168.36, 155.34, 143.63, 137.86, 132.21, 131.48, 130.26, 129.63, 129.28, 125.50, 123.24, 122.46, 121.98, 113.46, 78.68, 72.91, 57.37, 56.58, 43.68, 41.18, 40.87, 38.95, 38.75, 37.84, 36.36, 25.64, 23.18, 21.67, 17.75, 15.07. HRMS (ESI) calcd for $\text{C}_{33}\text{H}_{43}\text{ClN}_4\text{O}_7$ [M+H] 643.2893, found 643.2890.



(3*S*,10*R*,16*S*,*E*)-10-(3-chloro-4-methoxybenzyl)-3-isobutyl-6,6-dimethyl-16-((*R*,*E*)-4-(1-methyl-1*H*-pyrazol-4-yl)but-3-en-2-yl)-1,4-dioxo-8,11-diazacyclohexadec-13-ene-2,5,9,12-tetraone

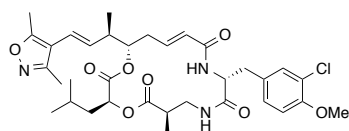
(2.28k). Reaction was run and purified as general procedure for semi-preparative scale reaction. ^1H NMR (600MHz, CD_3OD) 7.60 (s, 1H), 7.51 (s, 1H), 7.27 (d, $J = 2.1$ Hz, 1H), 7.16 (dd, $J = 8.5, 2.2$ Hz, 1H), 6.97 (d, $J = 8.5$ Hz, 1H), 6.70 (ddd, $J = 15.2, 11.2, 3.9$ Hz, 1H), 6.27 (d, $J = 15.9$ Hz, 1H), 5.90 (dd, $J = 15.1, 1.9$ Hz, 1H), 5.79 (dd, $J = 15.9, 8.9$ Hz, 1H), 4.97 (ddd, $J = 11.3, 7.1, 1.6$

Hz, 1H), 4.94 (dd, $J = 9.9, 3.4$ Hz, 1H), 4.50 (dd, $J = 11.4, 3.7$ Hz, 1H), 3.83 (s, 3H), 3.83 (s, 3H), 3.45 (d, $J = 13.6$ Hz, 1H), 3.17 (dd, $J = 14.5, 3.7$ Hz, 1H), 3.07 (d, $J = 13.6$ Hz, 1H), 2.73 (dd, $J = 14.5, 11.4$ Hz, 1H), 2.65 (dt, $J = 14.7, 2.4$ Hz, 1H), 2.50 (h, $J = 7.2$ Hz, 1H), 2.32 (dt, $J = 14.4, 11.2$ Hz, 1H), 1.68 – 1.57 (m, 2H), 1.43 – 1.36 (m, 1H), 1.19 (s, 3H), 1.15 (s, 3H), 1.11 (d, $J = 6.9$ Hz, 3H), 0.77 (t, $J = 6.7$ Hz, 6H). ^{13}C NMR (150 MHz, CD_3OD) δ 178.97, 173.70, 172.12, 168.25, 155.37, 143.83, 137.86, 132.17, 131.46, 130.26, 129.63, 129.26, 125.33, 123.27, 122.48, 121.98, 113.49, 78.65, 72.69, 57.47, 56.59, 47.40, 44.01, 43.68, 40.85, 38.75, 37.88, 36.49, 25.90, 23.32, 23.28, 23.20, 21.64, 17.74. HRMS (ESI) calcd for $\text{C}_{34}\text{H}_{45}\text{ClN}_4\text{O}_7$ [M+H] 643.2893, found 643.2893.



(3*S*,6*R*,10*R*,16*S*,*E*)-10-(3-chloro-4-methoxybenzyl)-3-isobutyl-16-((*R*,*E*)-4-(1-isopropyl-1*H*-pyrazol-4-yl)but-3-en-2-yl)-6-methyl-1,4-dioxo-8,11-diazacyclohexadec-13-ene-2,5,9,12-

tetraone (2.28l). Reaction was run and purified as general procedure for semi-preparative scale reaction. ^1H NMR (600 MHz, CD_3OD) δ 7.70 (s, 1H), 7.53 (s, 1H), 7.28 (d, $J = 2.2$ Hz, 1H), 7.17 (dd, $J = 8.4, 2.2$ Hz, 1H), 6.98 (d, $J = 8.5$ Hz, 1H), 6.70 (ddd, $J = 15.1, 11.2, 3.9$ Hz, 1H), 6.28 (d, $J = 15.8$ Hz, 1H), 5.92 (dd, $J = 15.2, 1.9$ Hz, 1H), 5.79 (dd, $J = 15.9, 8.9$ Hz, 1H), 4.98 (ddd, $J = 11.2, 7.5, 2.0$ Hz, 1H), 4.91 (dd, $J = 10.0, 3.5$ Hz, 1H), 4.52 (dd, $J = 11.2, 3.8$ Hz, 1H), 4.47 (p, $J = 6.7$ Hz, 1H), 3.84 (s, 3H), 3.58 (dd, $J = 13.8, 3.3$ Hz, 1H), 3.27 (dd, $J = 13.7, 3.0$ Hz, 1H), 3.18 (dd, $J = 14.5, 3.8$ Hz, 1H), 2.79 – 2.71 (m, 2H), 2.71 – 2.63 (m, 1H), 2.50 (h, $J = 7.2$ Hz, 1H), 2.33 (dt, $J = 14.5, 11.2$ Hz, 1H), 1.72 – 1.54 (m, 2H), 1.46 (d, $J = 6.7$ Hz, 6H), 1.37 (ddd, $J = 14.2, 9.0, 3.6$ Hz, 1H), 1.18 (d, $J = 7.4$ Hz, 3H), 1.12 (d, $J = 6.9$ Hz, 3H), 0.77 (d, $J = 6.5$ Hz, 3H), 0.74 (d, $J = 6.6$ Hz, 3H). ^{13}C NMR (150 MHz, CD_3OD) δ 177.60, 174.05, 172.33, 168.37, 155.35, 143.64, 137.40, 132.21, 131.48, 130.12, 129.28, 126.34, 125.51, 123.25, 122.67, 121.38, 113.46, 78.67, 72.93, 57.38, 56.59, 55.07, 43.80, 41.18, 40.87, 38.96, 37.85, 36.37, 25.64, 23.31, 23.09, 21.70, 17.79, 15.07. HRMS (ESI) calcd for $\text{C}_{35}\text{H}_{47}\text{ClN}_4\text{O}_7$ [M+H] 671.3206, found 671.3025.



(3*S*,6*R*,10*R*,16*S*,*E*)-10-(3-chloro-4-methoxybenzyl)-16-((*R*,*E*)-4-(3,5-dimethylisoxazol-4-yl)but-3-en-2-yl)-3-isobutyl-6-methyl-1,4-dioxo-8,11-diazacyclohexadec-13-ene-2,5,9,12-

tetraone (2.28m). Reaction was run and purified as general procedure for semi-preparative scale reaction.

¹H NMR (600 MHz, CD₃OD) δ 7.28 (d, *J* = 2.2 Hz, 1H), 7.17 (dd, *J* = 8.4, 2.2 Hz, 1H), 6.98 (d, *J* = 8.4 Hz, 1H), 6.69 (ddd, *J* = 15.1, 11.1, 3.9 Hz, 1H), 6.23 (d, *J* = 16.2 Hz, 1H), 5.93 (dd, *J* = 15.1, 1.9 Hz, 1H), 5.80 (dd, *J* = 16.2, 8.9 Hz, 1H), 5.06 (ddd, *J* = 11.3, 6.7, 1.9 Hz, 1H), 4.93 (dd, *J* = 9.7, 3.8 Hz, 1H), 4.51 (dd, *J* = 11.2, 3.9 Hz, 1H), 3.84 (s, 3H), 3.57 (dd, *J* = 13.7, 3.3 Hz, 1H), 3.27 (dd, *J* = 13.8, 3.0 Hz, 1H), 3.17 (dd, *J* = 14.5, 3.9 Hz, 1H), 2.80 – 2.71 (m, 2H), 2.67 (ddt, *J* = 14.6, 4.0, 2.0 Hz, 1H), 2.58 (dt, *J* = 8.8, 6.6 Hz, 1H), 2.40 (s, 3H), 2.35 (dt, *J* = 14.5, 11.4 Hz, 1H), 2.28 (s, 3H), 1.70 – 1.53 (m, 2H), 1.33 (ddd, *J* = 14.1, 8.7, 3.8 Hz, 1H), 1.18 (d, *J* = 7.4 Hz, 3H), 1.15 (d, *J* = 6.9 Hz, 3H), 0.79 (d, *J* = 3.7 Hz, 3H), 0.78 (d, *J* = 3.8 Hz, 3H). **¹³C NMR** (150 MHz, CD₃OD) δ 177.53, 174.04, 172.23, 168.34, 166.95, 159.53, 155.35, 143.40, 134.36, 132.19, 131.48, 129.29, 125.65, 123.24, 120.19, 113.78, 113.46, 78.53, 72.77, 57.40, 56.58, 44.22, 41.16, 41.02, 38.95, 37.87, 36.35, 25.62, 23.20, 21.77, 17.83, 15.07, 11.55, 11.45. **HRMS** (ESI) calcd for C₃₄H₄₄ClN₃O₈ [M+H] 658.2890, found 658.2893.

6.3 Cryptophycin TE Construct Design (Chapter 3) and Protein Expression

6.3.1 Generation of Mutant Crp TEs

The mutations of CrpTE were generated from a modified pET28b plasmid containing a 8x his tag and a TEV cleavage site in place of the thrombin cleavage site. A quickchange mutagenesis (Stratagene) protocol was utilized for the generation of mutants except the plus 7aa, minus 5aa, and the minus 10aa which utilized the same conditions except only a forward primer was utilize. All new constructs were verified with the UofM Sequencing core.

Mutation	Primer
C145S	5'-GGATAATGCAAAGTGGATAAGCCGAATGGCTGAGGTTATTG-3' 5'-CAATAACCTCAGCCATTTCGGCTTATCCACTTTGCATTATCC-3'
C226S	5'-CCAATCACTTTGTTTAGCGGAGGGAGATAAATC-3' 5'-GATTTATCTCCCTCGCGCTAAACAAAGTGATTGG-3'
E61G	5'-CAAGGTCTTGATGGTGGCACCGAACCTCATAAAAG-3' 5'-CTTTTATGAGGTTGCGGTGCCACCATCAAGACCTTG-3'
K66S	5' GTGGCACCGAACCTCATAGCAGTGTGAAGCAATAGC 3' 5' GCTATTGCTTCAACACTGCTATGAGGTTGCGGTGCCAC 3'
E70A	5'-CATAAAAGTGTGAAGCAATAGCCTCCCAACAC-3' 5'-GTGTTGGGAGGCTATTGCTTCAACACTTTTATG-3'
K77A	5' GCAATAGCCTCCCAACACATTGCGGCAATTCAAACAGTTCAACC 3' 5' GGTTGAACTGTTTGAATTGCCGCAATGTGTTGGGAGGCTATTGC 3'
K195G	5'-GCCTGCTCAAACAGATATCGGCATTGTTGCGTGGTTTATTAC-3' 5'-GTAATAAACCCACGAACAATGCCGATATCTGTTGAGCAGGC-3'
K219A	5'-CCGGAAAAGACTTATGCGACTCCAATCACTTTG-3' 5'-CAAAGTGATTGGAGTCGCATAAGTCTTTTCCGG-3'
Plus 7aa	5' CCAACCGCTAGCGAACGACTAGCACTTCTTGTGGTCCGATTCCGGAGCCGAACCTTTGG 3'
Minus 5aa	5'CCAACCGCTAGCGCCGAACCTTGGTCTCCATTAG 3'
Minus 10aa	5' CCAACCGCTAGCCCATTAGTACCAATTCAATTCAACAAAACG3'
S94C	5' CTTGGCTGGTCATTGCTTTGGCAGTCATG 3' 5' CATGACTGCCAAAGCAATGACCAGCCAAG 3'
H265Q	5' CATATAGTTCCGGGTAATCGTGTTCATGCTGAGTGAG 3' 5' CTCACTCAGCATTGAAACACGATTACCCGGAACCTATATG 3'
H265N	5' CATATAGTTCCGGGTAATCAGGTTTCATGCTGAGTGAGC 3' 5' GCTCACTCAGCATTGAAACCTGATTACCCGGAACCTATATG 3'

Table 6.1 Primers utilized for generation of CrpTE mutants

6.3.2 CrpTE Protein Expression and Purification: Crystallography

Buffers For CrpTE Purification for Reactions and Crystallography

HEPES Lysis: 50 mM HEPES pH 8, 300 mM NaCl, 10 mM imidazole

HEPES Wash: 50 mM HEPES pH 8, 300 mM NaCl, 30 mM imidazole

HEPES Elution: 50 mM HEPES pH 8, 300 mM NaCl, 300 mM imidazole

HEPES Storage: 10 mM HEPES pH 7.5, 150 mM NaCl, 0.2 mM TCEP

Tris Storage: 10 mM Tris pH = 7.5, 100 mM NaCl, 0.2 mM TCEP

General Expression Protocol: Crystallography

Prior to protein production, a starter culture of E. Coli (BAP1) cells were grown by inoculating 10 mL of LB broth supplemented with kanamycin (50 mg/L) from freshly transformed colonies and grown overnight at 37 °C. Following overnight growth, 4 mL/L was used to inoculate a 1L expression culture in TB containing kanamycin (50 mg/L) and grown with shaking at 37 °C until an OD₆₀₀ of 0.8 – 1.2 was reached. At which time the flasks were cooled in an ice bath until an internal temperature of 20 °C was reached (~15 min). The flasks were returned to a 20 °C shaker, induced with 300 uL of IPTG (1M stock solution), and shaken at 200 RPM at 20 °C for a minimum of 18 hours. The cells were harvested by centrifugation (6,000 x g, 25 min, 4 °C). The pellets were frozen in liquid nitrogen and stored at -80 °C until purification.

General Protein Purification Protocol

The frozen cells were suspended in Lysis buffer (7 mL/g cell pellet) and thawed at 4 °C with stirring for 1 hour. Benzenase was added and the solution was sonicated on ice (12 x 10s with 50s rest periods). The resulting cellular lysate was then pelleted by centrifugation (50,000 x g, 30 min, 4 °C) and the supernatant was applied to 5 mL of Ni-NTA resin pre-equilibrated with wash buffer. After binding, the column was washed with 20 column volumes (100 mL) of wash buffer and the protein was subsequently eluted with 15 mL of elution buffer. The eluted fractions were combined, concentrated to 2.5 mL and buffer exchanged into storage (Tris for crystallography, HEPES for enzymatic reactions) buffer using a pre-equilibrated PD-10 column. After elution with 3.5 mL of storage buffer, the fractions were collected and protein concentration determined by absorption at 280 nm.

Enzymatic reactions: The fractions were pooled and diluted to 50 uM with HEPES storage buffer, flash frozen in liquid N₂, and stored at -80 °C until use.

Crystallography: The fractions were pooled and run over an S75 size exclusion column previously equilibrated in Tris storage buffer using an AKTA FPLC system. The populations of monomer and dimer were collected and concentrated to 30 mg/mL concentration or higher and transferred to the Smith Lab for crystallographic screens.

6.3.3 CrpTE Protein Expression and Purification: NMR

*For unlabeled Crp TE, expression was conducted as described above for crystallography

Buffers For CrpTE Purification for NMR experiments

Phosphate Lysis: 100mM NaPO₄ pH 8, 300 mM NaCl, 20 mM imidazole

Phosphate Wash: 100 mM NaPO₄ pH 8, 300 mM NaCl, 50 mM imidazole

Phosphate Elution: 100 mM NaPO₄ pH 8, 300 mM NaCl, 300 mM imidazole

Phosphate Storage: 100 mM NaPO₄ pH 8, 150 mM NaCl

NMR Buffer: 100 mM NaPO₄ pH 6.0, 150 mM NaCl

M9 Salts (1L 5x concentration, no NH₄Cl)

64 g Na₂HPO₄

15 g KH₂PO₄

2.5 gNaCl

1L 100x Trace Elements

5 g EDTA 0.01 g H₃BO₃

0.8 g FeCl₃ 1.6 g MnCl₂

0.05 g ZnCl₂ 0.005 g Ni₂SO₄

0.01 g CuCl₂ 0.005 g Molybdic Acid

0.01 g CoCl₂

Dissolve in 1L water, adjust pH to 7 with NaOH (some precipitation) and sterile filter, store cold

500 mL 1000x vitamins

0.5 g riboflavin

0.5 g niacinamide

0.5 g pyridoxine monohydrate

0.5 g thiamine

Dissolve in 500 mL water, store cold

Minimal Expression Media ¹⁵N, ¹⁵N/¹³C, or ¹⁵N/¹³C/²H (per L)

1 L M9 Salts (200 mL in 800 mL DI H₂O or D₂O)

2 mL 1M MgSO₄

20 mL 20% glucose or 20 mL 20% ¹³C glucose

1 mL Vitamins 100x
10 mL trace elements 100x
1 g $^{15}\text{NH}_4\text{Cl}$
Kanamycin 50 mg/L

Labeled Protein Expression Conditions

Day 1: BL21 (DE3) *E. coli* were transformed with the minus 5aa plasmid

Day 2: Freshly transformed cells were used to inoculate 5 mL of LB containing Kanamycin (50 mg/L) as a pre-culture which was grown to a high OD₆₀₀ (6-8 hours). Overnight cultures were then inoculated in minimal expression media (^{15}N , $^{15}\text{N}/^{13}\text{C}$, or $^{15}\text{N}/^{13}\text{C}/^2\text{H}$) with Kanamycin (50 mg/L) using a 1:100 inoculum. These were grown at 37 °C overnight.

Day 3: 1L minimal expression media ^{15}N main cultures were inoculated with overnight culture (1:100 inoculum, 10 mL per liter culture). These were grown at 37 °C until OD₆₀₀ 0.4 – 0.6 was reached, at which time the cells were cooled to 20 °C for 1 h and induced with 100 μL IPTG (1M). The cultures were allowed to express for 18 h prior to harvesting (6,000 x g, 25 min), flash freezing in liquid N₂, and storage at -80 °C.

General Purification Protocol for NMR

The frozen cells were suspended in Lysis buffer (7 mL/g cell pellet) and thawed at 4 °C with stirring for 1 hour. Benzenase was added and the solution was sonicated on ice (12 x 10s with 50s rest periods). The resulting cellular lysate was then pelleted by centrifugation (50,000 x g, 30 min, 4 °C) and the supernatant was applied to 5 mL of Ni-NTA resin pre-equilibrated with wash buffer. After binding, the column was washed with 20 column volumes (100 mL) of wash buffer and the protein was subsequently eluted with 15 mL of elution buffer. The eluted fractions were combined, concentrated to 2.5 mL and buffer exchanged into storage buffer using a pre-equilibrated PD-10 column. After elution with 3.5 mL of storage buffer, the fractions were collected and protein concentration determined by absorption at 280 nm. These were then flash frozen and stored until NMR experiments were to be run.

Prior to NMR experiments, proteins were thawed, and run over an S75 size exclusion column previously equilibrated in NMR buffer using an AKTA FPLC system. The dimer was excluded and monomeric protein was concentrated to 500 mM (protein would precipitate upon freezing in

this buffer so done directly before). This was then spiked with D₂O and loaded into a shigemi NMR tube for analysis.

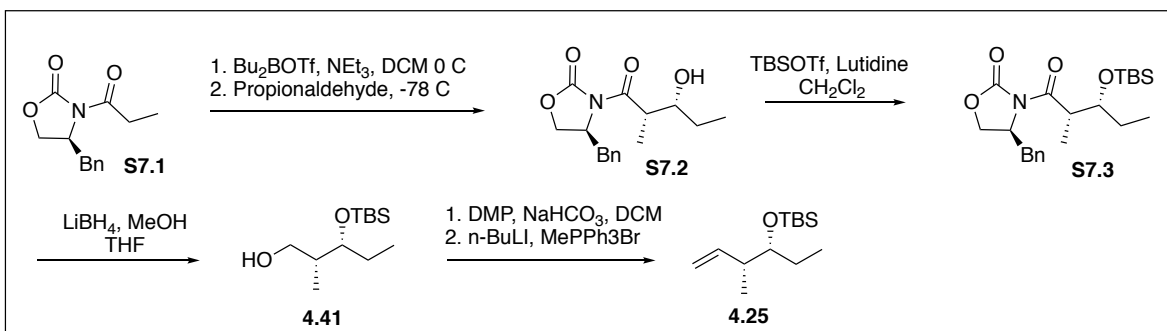
6.4 References

1. Villadsen, J. S.; Stephansen, H. M.; Maolanon, A. R.; Harris, P.; Olsen, C. A., Total Synthesis and Full Histone Deacetylase Inhibitory Profiling of Azumamides A-E as Well as beta(2)- epi-Azumamide E and beta(3)-epi-Azumamide E. *Journal of medicinal chemistry* **2013**, *56* (16), 6512-6520.
2. Dieckmann, M.; Menche, D., Stereoselective Synthesis of 1,3-anti Diols by an Ipc-Mediated Domino Aldol-Coupling/Reduction Sequence. *Org Lett* **2013**, *15* (1), 228-231.
3. Phukan, P.; Bauer, M.; Maier, M. E., Facile generation of alkenes and dienes from tosylates. *Synthesis-Stuttgart* **2003**, (9), 1324-1328.
4. Kotoku, N.; Kato, T.; Narumi, F.; Ohtani, E.; Kamada, S.; Aoki, S.; Okada, N.; Nakagawa, S.; Kobayashi, M., Synthesis of 15,20-triamide analogue with polar substituent on the phenyl ring of arenastatin A, an extremely potent cytotoxic spongean depsipeptide. *Bioorgan Med Chem* **2006**, *14* (22), 7446-7457.
5. Krishnamurthy, S., Rapid Reduction of Alkyl Tosylates with Lithium Triethylborohydride - Convenient and Advantageous Procedure for Deoxygenation of Simple and Hindered Alcohols - Comparison of Various Hydride Reagents. *J Organomet Chem* **1978**, *156* (1), 171-181.
6. Morrill, C.; Grubbs, R. H., Synthesis of functionalized vinyl boronates via ruthenium-catalyzed olefin cross-metathesis and subsequent conversion to vinyl halides. *J Org Chem* **2003**, *68* (15), 6031-6034.
7. McCubbin, J. A.; Maddess, M. L.; Lautens, M., Total synthesis of cryptophycin analogues via a scaffold approach. *Org Lett* **2006**, *8* (14), 2993-6.
8. Ghosh, A. K.; Swanson, L., Enantioselective synthesis of (+)-cryptophycin 52 (LY355703), a potent antimitotic antitumor agent. *J Org Chem* **2003**, *68* (25), 9823-6.
9. Ghosh, A. K.; Bischoff, A., Asymmetric syntheses of potent antitumor macrolides cryptophycin B and arenastatin A. *Eur J Org Chem* **2004**, (10), 2131-2141.
10. Beck, Z. Q.; Aldrich, C. C.; Magarvey, N. A.; Georg, G. I.; Sherman, D. H., Chemoenzymatic synthesis of cryptophycin/arenastatin natural products. *Biochemistry-US* **2005**, *44* (41), 13457-13466.

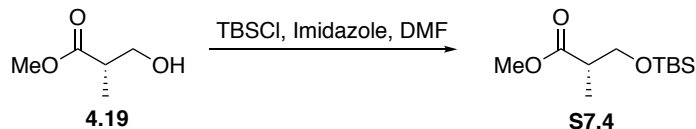
Chapter 7

Polyketide Synthase Experimentals

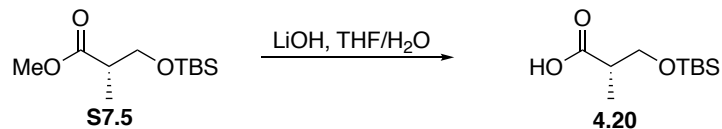
7.1 New Pentaketide Synthetic Procedures and Characterization



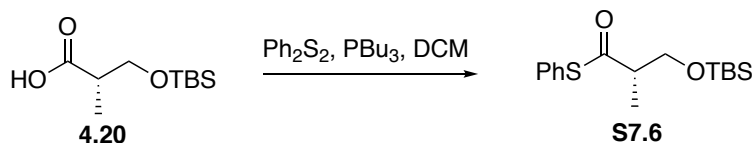
*Synthesis previously developed by Hansen et. al.¹



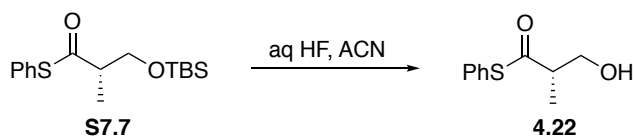
methyl (S)-3-((tert-butyldimethylsilyl)oxy)-2-methylpropanoate (S7.4): To a stirred solution of (S)-Roche ester and imidazole in DMF was added TBSCl and the reaction was stirred at rt overnight. The reaction was diluted with 0.5N HCl and the organics separated, extracted with ethyl acetate (3 x 50 mL), organics combined, washed with sat. NH₄Cl, dried over Na₂SO₄, and concentrated. The crude product was purified by flash chromatography system (2 – 20% Ethyl Acetate/Hexanes) to afford xx (4.12 g, 70% yield) as a colorless oil: $R_f = 0.7$ (10% Ethyl Acetate/Hexanes); ¹H NMR (600 MHz, CDCl₃) δ 3.76 (dd, $J = 9.7, 6.9$ Hz, 1H), 3.66 (d, $J = 1.3$ Hz, 3H), 3.64 (dd, $J = 9.7, 6.0$ Hz, 1H), 2.64 (h, $J = 7.0$ Hz, 1H), 1.12 (d, $J = 7.0$ Hz, 3H), 0.86 (d, $J = 1.8$ Hz, 9H), 0.02 (s, 3H), 0.02 (s, 3H). **HRMS** (ESI) calcd for C₁₁H₂₄O₃Si [M+H] 233.1568, found 233.1571.



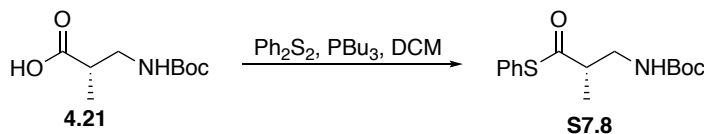
(S)-3-((tert-butyldimethylsilyloxy)-2-methylpropanoic acid (4.20): S7.5 (1 eq, 4.30 mmol, 1.0 g) was suspended in a 4:1 mixture of THF/H₂O (43 mL, 0.1M) and treated with LiOH (4 eq, 17.21 mmol, 0.412 g) and stirred for 4 hours. The reaction was quenched with 1 M HCl (50 mL) and the organics removed under reduced pressure. The aqueous layer was extracted with ethyl acetate (3 x 50 mL), organics combined, washed with brine, dried over Na₂SO₄, and concentrated. The crude product was purified by flash chromatography system (10 – 30% Ethyl Acetate/Hexanes + 1% AcOH) to afford **4.20** (0.81 g, 87% yield) as a clear and colorless oil: R_f = 0.4 (20% Ethyl Acetate/Hexanes); ¹H NMR (600 MHz, CDCl₃) δ 3.79 – 3.66 (m, 2H), 2.65 (td, *J* = 7.2, 6.0 Hz, 1H), 1.17 (d, *J* = 7.1 Hz, 3H), 0.89 (d, *J* = 0.9 Hz, 9H), 0.07 (d, *J* = 1.4 Hz, 6H). ¹³C NMR (15 MHz, CDCl₃) δ 179.21, 64.85, 41.59, 25.71, 18.14, 13.00, -5.55, -5.57. HRMS (ESI) calcd for C₁₀H₂₂O₃Si [M+H] 219.1411, found 219.1419.



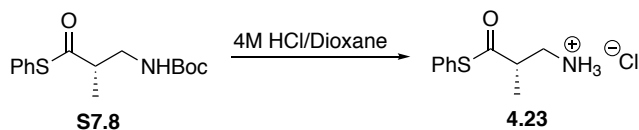
S-phenyl (S)-3-((tert-butyldimethylsilyloxy)-2-methylpropanethioate (S7.6): To a 25 mL flask was added **4.20** (1 eq, 0.92 mmol, 0.20 g) and Ph₂S₂ (1.1 eq, 1.01 mmol, 0.22 g) in CH₂Cl₂ (9.2 mL, 0.1M) and cooled to 0 °C. PBU₃ (distilled, 1.1 eq, 1.01 mmol, 250 uL) was added slowly, the reaction was stirred for 10 min before it was quenched with sat. NaHCO₃. The organics were separated, extracted with CH₂Cl₂ (3 x 20 mL), dried over sodium sulfate, and concentrated. The crude product was purified by flash chromatography system (2 – 40% Ethyl Acetate/Hexanes) to afford **S7.6** (225 mg, 77% yield) as a clear and colorless oil: R_f = 0.25 (25% Ethyl Acetate/Hexanes); ¹H NMR (400 MHz, CDCl₃) δ 7.40 (s, 5H), 3.87 (dd, *J* = 9.9, 7.2 Hz, 1H), 3.66 (dd, *J* = 10.0, 5.9 Hz, 1H), 2.97 (q, *J* = 6.7, 6.2 Hz, 1H), 1.21 (d, *J* = 7.0 Hz, 3H), 0.90 (d, *J* = 1.2 Hz, 9H), 0.06 (s, 3H), 0.06 (s, 3H). ¹³C NMR (150 MHz, CDCl₃) δ 199.98, 134.42, 129.17, 129.06, 127.90, 65.37, 51.06, 25.80, 18.22, 13.98, -5.50. HRMS (ESI) calcd for C₁₆H₂₆O₂SSi [M+H] 311.1496, found 311.1497.



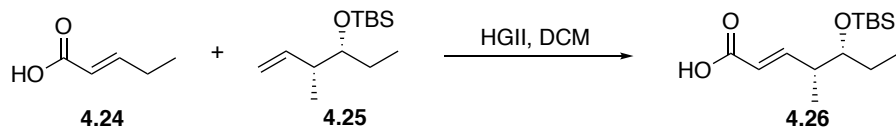
S-phenyl (S)-3-hydroxy-2-methylpropanethioate (4.22): To an open 20 mL polyethylene vial was added **S7.7** in CH₃CN (4 mL, 1M) and aq. HF (48%, 1 mL). The reaction was monitored by TLC and upon completion it was diluted with CH₂Cl₂ (5 mL) and carefully quenched with sat. NaHCO₃ (until pH was acidic). The aqueous layer was extracted with CH₂Cl₂ (3 x 10 mL), organics combined, dried over Na₂SO₄, and concentrated. The crude product was purified by flash chromatography system (20 – 60% Ethyl Acetate/Hexanes) to afford **4.22** (0.72 g, 87%) as a clear and colorless oil: R_f = (0.25) (25% Ethyl Acetate/Hexanes); ¹H NMR (600 MHz, CDCl₃) δ 7.41 (s, 5H), 3.81 (dd, *J* = 11.2, 7.3 Hz, 1H), 3.73 (dd, *J* = 11.3, 4.4 Hz, 1H), 2.99 (pd, *J* = 7.1, 4.5 Hz, 1H), 1.28 (d, *J* = 7.2 Hz, 3H). ¹³C NMR (150 MHz, CDCl₃) δ 201.53, 134.54, 129.49, 129.21, 127.16, 64.69, 50.30, 14.32. HRMS (ESI) calcd for C₁₀H₁₂O₂S [M+H] 197.0631, found xx.



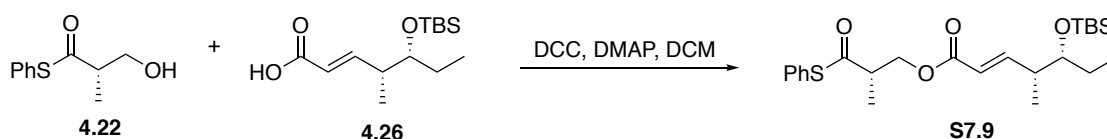
S-phenyl (S)-3-((tert-butoxycarbonyl)amino)-2-methylpropanethioate (S7.8): To a 25 mL flask was added xx (1 eq, 0.98 mmol, 0.20 g) and Ph₂S₂ (1.1 eq, 1.01 mmol, 0.236 g) in CH₂Cl₂ (9.8 mL, 0.1M) and cooled to 0 °C. PBU₃ (distilled, 1.1 eq, 1.01 mmol, 270 uL) was added slowly, the reaction was stirred for 10 min before it was quenched with sat. NaHCO₃. The organics were separated, extracted with CH₂Cl₂ (3 x 20 mL), dried over sodium sulfate, and concentrated. The crude product was purified by flash chromatography system (2 – 40% Ethyl Acetate/Hexanes) to afford xx (225 mg, 77% yield) as a clear and colorless oil: R_f = 0.25 (25% Ethyl Acetate/Hexanes); ¹H NMR (400 MHz, CDCl₃) δ 7.42 (s, 5H), 4.88 (s, 1H), 3.43 – 3.23 (m, 2H), 3.11 – 2.97 (m, 1H), 1.44 (s, 9H), 1.28 (d, *J* = 7.1 Hz, 3H). ¹³C NMR (150 MHz, CDCl₃) δ 201.15, 155.90, 134.48, 129.45, 129.19, 127.27, 79.44, 48.33, 43.20, 28.35, 15.51. HRMS (ESI) calcd for C₁₅H₂₁NO₃S [M+H] 296.1315, found 296.1311.



***S*-phenyl (*S*)-3-amino-2-methylpropanethioate HCl (4.23):** To a 4 dram vial with S4.3 was added 5 mL of 4M HCl/Dioxane, and the mixture was stirred for 30 min, concentrated and used directly.

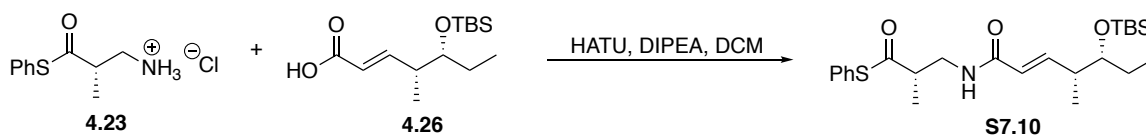


(4*R*,5*R*,*E*)-5-((*tert*-butyldimethylsilyloxy)-4-methylhept-2-enoic acid (4.26): To a long tube under N₂ was added Hoveyda Grubbs II (0.03 eq, 0.03 mmol, 0.019 g), 2-pentenoic acid (1 eq, 1.0 mmol, 0.10 g), and **4.25** (4 eq, 4.0 mmol, 0.913 g) in DCM (2 mL, 0.5 M). This was allowed to reflux for 12 h, cooled, the solvent was removed under reduced pressure and purified directly by flash chromatography (1 – 25% Ethyl Acetate/Hexane + 1% AcOH) to afford **4.26** (0.231 g, 88% yield) as a white solid: R_f = 0.4 (20% Ethyl Acetate/Hexanes); ¹H NMR (600 MHz, CDCl₃) δ 7.11 (dd, *J* = 15.8, 7.4 Hz, 1H), 5.80 (d, *J* = 15.8 Hz, 1H), 3.55 (q, *J* = 5.5 Hz, 1H), 2.49 (dq, *J* = 13.0, 7.0 Hz, 1H), 1.48 (ddd, *J* = 13.2, 7.2, 5.5 Hz, 1H), 1.38 (dp, *J* = 14.1, 7.2 Hz, 1H), 1.03 (d, *J* = 6.8 Hz, 3H), 0.88 (s, 9H), 0.86 (t, *J* = 7.4 Hz, 3H), 0.03 (s, 3H), 0.03 (s, 3H). ¹³C NMR (150 MHz, CDCl₃) δ 171.63, 155.04, 119.92, 76.20, 41.37, 26.82, 25.84, 18.09, 13.88, 9.64, -4.38, -4.56. **HRMS** (ESI) calcd for C₁₄H₂₈O₃Si [M-H] 271.1755, found 271.1759.

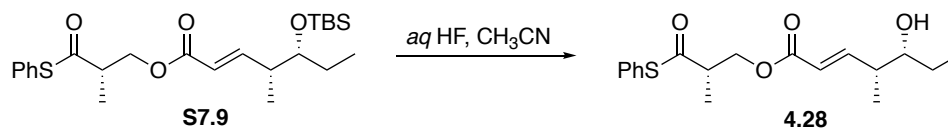


(*S*)-2-methyl-3-oxo-3-(phenylthio)propyl(4*R*,5*R*,*E*)-5-((*tert*-butyldimethylsilyloxy)-4-methylhept-2-enoate (S7.9): To an open flask was added **4.22** (1 eq, 0.31 mmol, 0.060 g) and **4.26** (1 eq, 0.31 mmol, 0.083 g) suspended in CH₂Cl₂ (3.1 mL, 0.1M). The mixture was treated with DCC (1.2 eq, 0.37 mmol, 0.072 g) and DMAP (0.1 eq, 0.03 mmol, 0.004 g) and stirred at rt overnight. The reaction was filtered through celite and concentrated. The crude product was purified by flash chromatography system (2 – 40% Ethyl Acetate/Hexanes) to afford **S7.9** (43 mg, 33% yield): R_f = 0.6 (10% Ethyl Acetate/Hexanes); ¹H NMR (600 MHz, CDCl₃) δ 7.40 (d, *J* =

0.6 Hz, 5H), 7.04 (dd, $J = 15.8, 7.4$ Hz, 1H), 5.81 (dd, $J = 15.8, 1.3$ Hz, 1H), 4.34 (dd, $J = 11.1, 7.8$ Hz, 1H), 4.24 (dd, $J = 11.0, 5.6$ Hz, 1H), 3.54 (dt, $J = 6.5, 5.1$ Hz, 1H), 3.15 (pd, $J = 7.1, 5.4$ Hz, 1H), 2.52 – 2.43 (m, 1H), 1.46 (dtd, $J = 14.8, 7.4, 5.2$ Hz, 1H), 1.38 (dp, $J = 14.2, 7.3$ Hz, 1H), 1.29 (d, $J = 7.0$ Hz, 3H), 1.02 (d, $J = 6.8$ Hz, 3H), 0.88 (s, 9H), 0.85 (t, $J = 7.4$ Hz, 3H), 0.03 (s, 3H), 0.02 (s, 3H). $^{13}\text{C NMR}$ (150 MHz, CDCl_3) δ 198.85, 166.20, 152.97, 134.41, 129.40, 129.15, 127.30, 120.11, 76.28, 65.23, 47.37, 41.32, 26.81, 25.86, 18.10, 14.51, 14.04, 9.62, -4.38, -4.50. **HRMS** (ESI) calcd for $\text{C}_{24}\text{H}_{38}\text{O}_4\text{SSi}$ [$\text{M}+\text{H}$] 451.2333, found 451.2334.

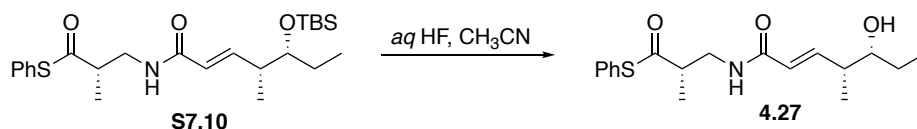


S-phenyl (S)-3-((4R,5R,E)-5-((tert-butyldimethylsilyloxy)-4-methylhept-2-enamido)-2-methylpropanethioate (S7.10): To an open flask was added acid **4.26** suspended in CH_2Cl_2 (2 mL, 0.1M) and treated with HATU (1.2 eq, 0.24 mmol, 0.093 g). Deprotected amine was suspended in DCM (0.5 mL) and DIPEA (2.5 eq, 0.51 mmol, 88 μL) and the mixture was added to the acid portion and stirred at rt overnight. The reaction was diluted with water and extracted with DCM (3 x 20 mL), organics combined, dried over Na_2SO_4 , and concentrated. The crude product was purified by flash chromatography system (8 – 40% Ethyl Acetate/Hexanes) to afford **S7.10** (58 mg, 66% yield) as a colorless oil: $R_f = 0.4$ (20% Ethyl Acetate/Hexanes); $^1\text{H NMR}$ (600 MHz, CDCl_3) δ 7.41 (tq, $J = 7.0, 3.7, 2.9$ Hz, 5H), 6.83 (dd, $J = 15.4, 7.4$ Hz, 1H), 5.84 (s, 1H), 5.69 (dd, $J = 15.5, 1.3$ Hz, 1H), 3.60 (ddd, $J = 13.8, 6.4, 4.2$ Hz, 1H), 3.51 (q, $J = 5.5$ Hz, 1H), 3.46 (ddd, $J = 13.9, 8.0, 6.0$ Hz, 1H), 3.10 (pd, $J = 7.3, 4.1$ Hz, 1H), 2.53 – 2.30 (m, 1H), 1.46 (ddd, $J = 14.1, 7.4, 5.3$ Hz, 1H), 1.39 (tq, $J = 14.1, 7.2, 6.4$ Hz, 1H), 1.31 (d, $J = 7.2$ Hz, 3H), 0.99 (d, $J = 6.8$ Hz, 3H), 0.87 (s, 9H), 0.84 (t, $J = 7.4$ Hz, 3H), 0.02 (s, 3H), 0.02 (s, 3H). $^{13}\text{C NMR}$ (150 MHz, CDCl_3) δ 201.77, 166.04, 147.86, 134.49, 129.53, 129.22, 127.14, 122.74, 76.34, 47.94, 41.67, 41.00, 26.84, 25.88, 18.12, 15.82, 14.43, 9.47, -4.38, -4.45. **HRMS** (ESI) calcd for $\text{C}_{24}\text{H}_{39}\text{NO}_3\text{SSi}$ [$\text{M}+\text{H}$] 450.2493, found 450.2493.

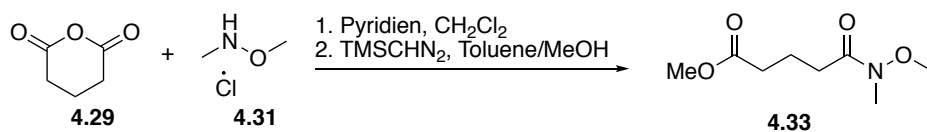


(S)-2-methyl-3-oxo-3-(phenylthio)propyl (4R,5R,E)-5-hydroxy-4-methylhept-2-enoate (4.28): The TBS protected **S7.9** was suspended in 1 mL of CH_3CN in a polyethylene vial and

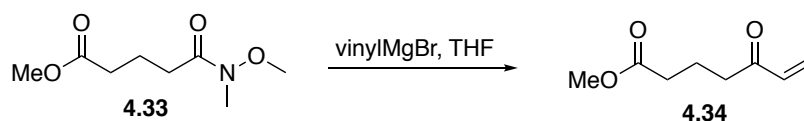
treated with aq. HF (48%, 250 μ L). The reaction was monitored by TLC and upon completion it was diluted with CH_2Cl_2 (5 mL) and carefully quenched with sat. NaHCO_3 (until pH was acidic). The aqueous layer was extracted with CH_2Cl_2 (3 x 10 mL), organics combined, dried over Na_2SO_4 , and concentrated. The crude product was purified by flash chromatography system (12 – 40% Ethyl Acetate/Hexanes) to afford **4.28** (0.035 g, 82% yield) as a clear and colorless oil: $R_f = 0.6$ (33% Ethyl Acetate/Hexanes); $^1\text{H NMR}$ (600 MHz, CDCl_3) δ 7.40 (s, 5H), 6.98 (dd, $J = 15.8$, 7.8 Hz, 1H), 5.87 (dd, $J = 15.7$, 1.3 Hz, 1H), 4.33 (dd, $J = 11.0$, 7.9 Hz, 1H), 4.25 (dd, $J = 11.0$, 5.6 Hz, 1H), 3.48 (h, $J = 4.3$ Hz, 1H), 3.21 – 3.06 (m, 1H), 2.49 – 2.35 (m, 1H), 1.55 – 1.48 (m, 1H), 1.41 – 1.33 (m, 1H), 1.29 (d, $J = 7.0$ Hz, 3H), 1.09 (d, $J = 6.8$ Hz, 3H), 0.95 (t, $J = 7.4$ Hz, 3H). $^{13}\text{C NMR}$ (150 MHz, CDCl_3) δ 198.88, 166.04, 152.00, 129.45, 129.19, 127.23, 120.90, 75.85, 65.35, 47.33, 42.23, 27.37, 14.50, 13.96, 10.22. **HRMS** (ESI) calcd for $\text{C}_{18}\text{H}_{24}\text{O}_4\text{S}$ $[\text{M}+\text{H}]$ 337.1468, found 337.1466.



S-phenyl (S)-3-((4R,5R,E)-5-hydroxy-4-methylhept-2-enamido)-2-methylpropanethioate (4.27): The TBS protected xx was suspended in 1 mL of CH_3CN in a polyethylene vial and treated with aq. HF (48%, 250 μ L). The reaction was monitored by TLC and upon completion it was diluted with CH_2Cl_2 (5 mL) and carefully quenched with sat. NaHCO_3 (until pH was acidic). The aqueous layer was extracted with CH_2Cl_2 (3 x 10 mL), organics combined, dried over Na_2SO_4 , and concentrated. The crude product was purified by flash chromatography system (20 – 60% Ethyl Acetate/Hexanes) to afford **4.27** (0.045 g, 85% yield) as a clear and colorless oil: $R_f = 0.55$ (50% Ethyl Acetate/Hexanes); $^1\text{H NMR}$ (600 MHz, CDCl_3) δ 7.40 (dq, $J = 7.5$, 4.1 Hz, 5H), 6.80 (dd, $J = 15.4$, 7.8 Hz, 1H), 6.01 (t, $J = 6.3$ Hz, 1H), 5.76 (dd, $J = 15.4$, 1.3 Hz, 1H), 3.57 (ddd, $J = 13.8$, 6.4, 4.3 Hz, 1H), 3.49 – 3.39 (m, 2H), 3.09 (pd, $J = 7.3$, 4.2 Hz, 1H), 2.38 (hept, $J = 6.3$ Hz, 1H), 1.51 (dq, $J = 14.9$, 7.5, 3.8 Hz, 1H), 1.43 – 1.32 (m, 1H), 1.30 (d, $J = 7.2$ Hz, 3H), 1.05 (d, $J = 6.8$ Hz, 3H), 0.93 (t, $J = 7.4$ Hz, 3H). $^{13}\text{C NMR}$ (150 MHz, CDCl_3) δ 201.75, 165.95, 147.14, 134.49, 129.56, 129.24, 127.08, 123.52, 75.87, 47.87, 41.93, 41.73, 27.25, 15.82, 13.99, 10.30. **HRMS** (ESI) calcd for $\text{C}_{18}\text{H}_{25}\text{NO}_3\text{S}$ $[\text{M}+\text{H}]$ 336.1628, found 336.1622.

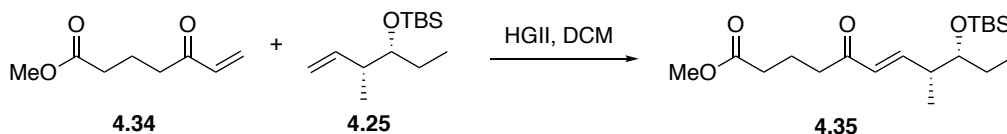


methyl 5-(methoxy(methyl)amino)-5-oxopentanoate (4.33): A solution of glutaric anhydride (1 eq, 42.82 mmol, 5.0 g) and N,O-dimethylhydroxylamine hydrochloride (1 eq, 43.82 mmol, 4.27 g) in CH₂Cl₂ (0.4M, 110 mL) was cooled to 0 °C and treated dropwise with pyridine (2.2 eq, 96.41 mmol, 7.78 mL). The resulting solution was warmed to rt and stirred overnight. The reaction was then concentrated under reduced pressure. The crude product was dissolved in 4:1 Toluene/MeOH (15 mL) and treated dropwise with TMS diazomethane (2M in diethyl ether, 10 mL). Upon persistence of yellow color, the reaction was quenched with a 10% Acetic Acid in CH₂Cl₂. This was concentrated under reduced pressure and the crude product was purified by flash chromatography system (30 – 80% Ethyl Acetate/Hexanes) to afford xx (6.05 g, 80% yield); ¹H NMR (400 MHz, CDCl₃) δ 3.66 (d, *J* = 0.8 Hz, 3H), 3.66 (s, 3H), 3.16 (s, 3H), 2.48 (t, *J* = 7.3 Hz, 2H), 2.39 (t, *J* = 7.2 Hz, 2H), 1.95 (p, *J* = 7.3 Hz, 2H). ¹³C NMR (100 MHz, CDCl₃) δ 173.69, xx 61.19, 51.51, 33.22, 30.82, 19.76. HRMS (ESI) calcd for C₈H₁₅NO₄ [M+H] 190.1074, found 190.1070.

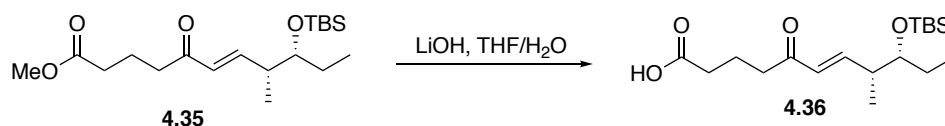


methyl 5-oxohept-6-enoate (4.34): To a flame dried 25 mL flask under N₂ was added 4.33 (1 eq, 1.32 mmol, 0.25 g) in dry THF (0.2 M, 6.5 mL) and the mixture was cooled to 0 °C. Vinyl Magnesium Bromide (0.8 M THF, freshly titrated, 1.2 eq, 1.98 mL) was added slowly and the reaction was allowed to stir at 0 °C for 30 min. The reaction was quenched with half 0.5 N HCl (10 mL) and the aqueous layer was extracted with CH₂Cl₂ (3x20 mL), organics combined, dried over Na₂SO₄, and concentrated. The crude product was purified by flash chromatography system (10 – 50% Ethyl Acetate/Hexanes) to afford **4.34** (105 mg, 51% yield) as a clear and colorless oil (being careful not to pull this off on a high vacuum as it is volatile): R_f = 0.3 (25% Ethyl Acetate/Hexanes); ¹H NMR (400 MHz, CDCl₃) δ 6.34 (dd, *J* = 17.7, 10.4 Hz, 1H), 6.22 (dd, *J* = 17.7, 1.3 Hz, 1H), 5.84 (dd, *J* = 10.4, 1.3 Hz, 1H), 3.67 (s, 3H), 2.67 (t, *J* = 7.2 Hz, 2H), 2.37 (t, *J* = 7.2 Hz, 2H), 1.95 (p, *J* = 7.2 Hz, 2H). ¹³C NMR (101 MHz, CDCl₃) δ 199.87, 173.60, 136.42,

128.26, 51.56, 38.33, 33.00, 18.96. ^{13}C NMR (100 MHz, CDCl_3) δ 199.87, 173.60, 136.42, 128.26, 51.56, 38.33, 33.00, 18.96. HRMS (ESI) calcd for $\text{C}_8\text{H}_{12}\text{O}_3$ [M+H] 157.0862, found 157.0866.

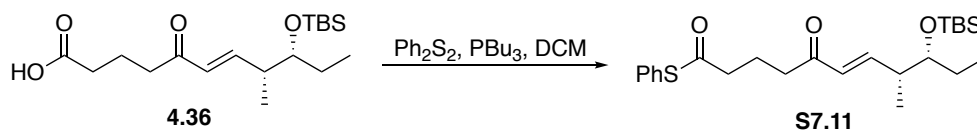


methyl (8*R*,9*R*,*E*)-9-((*tert*-butyldimethylsilyl)oxy)-8-methyl-5-oxoundec-6-enoate (4.35): To a long tube under N_2 was added Hoveyda Grubbs II (0.03 eq, 0.02 mmol, 0.012 g), ester **4.34** (1 eq, 0.58 mmol, 0.09 g), and **4.25** (4 eq, 1.73 mmol, 0.395g) in DCM (2 mL, 0.5 M). This was allowed to reflux for 12 h, cooled, the solvent was removed under reduced pressure and purified directly by flash chromatography (1 – 15% Ethyl Acetate/Hexane) to afford **4.35** (0.152 g, 74% yield) as a colorless oil: $R_f = 0.25$ (10% Ethyl Acetate/Hexanes); ^1H NMR (600 MHz, CDCl_3) δ 6.86 (dd, $J = 16.1, 7.3$ Hz, 1H), 6.05 (dd, $J = 16.1, 1.3$ Hz, 1H), 3.65 (s, 3H), 3.54 (q, $J = 5.4$ Hz, 1H), 2.60 (t, $J = 7.2$ Hz, 2H), 2.46 (dq, $J = 13.2, 6.5$ Hz, 1H), 2.35 (t, $J = 7.3$ Hz, 2H), 1.93 (p, $J = 7.2$ Hz, 2H), 1.47 (ddd, $J = 13.2, 7.5, 5.6$ Hz, 1H), 1.35 (dp, $J = 14.2, 7.2$ Hz, 1H), 1.01 (d, $J = 6.8$ Hz, 3H), 0.88 (s, 9H), 0.85 (t, $J = 7.5$ Hz, 3H), 0.03 (s, 3H), 0.01 (s, 3H). ^{13}C NMR (150 MHz, CDCl_3) δ 195.67, 169.71, 146.41, 125.61, 72.38, 47.58, 37.46, 34.66, 29.19, 22.83, 21.94, 15.24, 14.16, 10.12, 5.71, -8.31, -8.43. HRMS (ESI) calcd for $\text{C}_{19}\text{H}_{36}\text{O}_4\text{Si}$ [M+H] 357.2456, found xx.

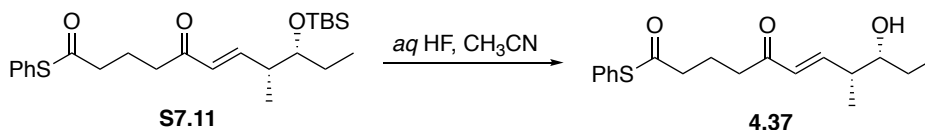


(8*R*,9*R*,*E*)-9-((*tert*-butyldimethylsilyl)oxy)-8-methyl-5-oxoundec-6-enoic acid (4.36): **4.35** (1 eq, 0.30 mmol, 0.106 g) was suspended in a 4:1 mixture of THF/ H_2O (43 mL, 0.1M) and treated with LiOH (3 eq, 0.89 mmol, 0.037 g) and stirred for 4 hours. The reaction was quenched with 1 M HCl (50 mL) and the organics removed under reduced pressure. The aqueous layer was extracted with ethyl acetate (3 x 50 mL), organics combined, washed with brine, dried over Na_2SO_4 , and concentrated. The crude product was purified by flash chromatography system (10 – 40% Ethyl Acetate/Hexanes + 1% AcOH) to afford **4.36** (89 mg, 87% yield) as a clear and colorless oil: $R_f = 0.15$ (25% Ethyl Acetate/Hexane) ^1H NMR (600 MHz, CDCl_3) δ 6.87 (dd, $J = 16.1, 7.3$ Hz, 1H), 6.06 (dd, $J = 16.1, 1.3$ Hz, 1H), 3.55 (q, $J = 5.5$ Hz, 1H), 2.63 (t, $J = 7.2$ Hz, 2H), 2.47 (dp, $J = 13.1, 6.3$ Hz, 1H), 2.41 (t, $J = 7.2$ Hz, 2H), 2.16 (d, $J = 0.7$ Hz, 3H), 1.98 – 1.87

(m, 2H), 1.47 (ddd, $J = 13.3, 7.4, 5.5$ Hz, 1H), 1.35 (dp, $J = 14.1, 7.2$ Hz, 1H), 1.01 (d, $J = 6.8$ Hz, 3H), 0.88 (s, 9H), 0.85 (t, $J = 7.4$ Hz, 3H), 0.03 (s, 2H), 0.01 (s, 3H). ^{13}C NMR (150 MHz, CDCl_3) δ 195.64, 174.68, 146.63, 125.56, 72.37, 37.47, 34.51, 29.03, 28.95, 26.98, 22.84, 22.84, 14.94, 14.15, 10.13, 5.73, -8.30, -8.50. **HRMS** (ESI) calcd for $\text{C}_{18}\text{H}_{34}\text{O}_4\text{Si}$ $[\text{M}+\text{H}]$ 343.2299, found 343.2292.

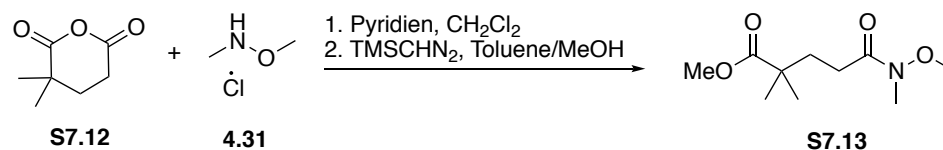


S-phenyl (8R,9R,E)-9-((tert-butyldimethylsilyl)oxy)-8-methyl-5-oxoundec-6-enethioate (S7.11): To a 25 mL flask was added **4.36** (1 eq, 0.37 mmol, 0.126 g) and Ph_2S_2 (1.1 eq, 0.4 mmol, 0.088 g) in CH_2Cl_2 (4 mL, 0.1M) and cooled to 0 °C. PBU_3 (distilled, 1.1 eq, 0.40 mmol, 100 μL) was added slowly, the reaction was stirred for 10 min before it was quenched with sat. NaHCO_3 . The organics were separated, extracted with CH_2Cl_2 (3 x 20 mL), dried over sodium sulfate, and concentrated. The crude product was purified by flash chromatography system (0 – 10% Ethyl Acetate/Hexanes) to afford **S7.11** (0.042 g, 82% yield) as a clear and colorless oil: $R_f = 0.6$ (10% Ethyl Acetate/Hexanes).

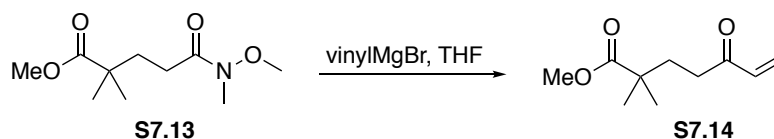


S-phenyl (8R,9R,E)-9-hydroxy-8-methyl-5-oxoundec-6-enethioate (4.37): The TBS protected **S7.11** was suspended in 1 mL of CH_3CN in a polyethylene vial and treated with aq. HF (48%, 250 μL). The reaction was monitored by TLC and upon completion it was diluted with CH_2Cl_2 (5 mL) and carefully quenched with sat. NaHCO_3 (until pH was acidic). The aqueous layer was extracted with CH_2Cl_2 (3 x 10 mL), organics combined, dried over Na_2SO_4 , and concentrated. The crude product was purified by flash chromatography system (12 – 40% Ethyl Acetate/Hexanes) to afford **4.37** (0.036, 92%) as a clear and colorless oil: $R_f = 0.3$ (33% Ethyl Acetate/Hexanes); ^1H NMR (600 MHz, CDCl_3) δ 7.40 (s, 5H), 6.82 (dd, $J = 16.0, 7.7$ Hz, 1H), 6.11 (dd, $J = 16.0, 1.2$ Hz, 1H), 3.49 (dq, $J = 9.1, 4.8$ Hz, 1H), 2.72 (t, $J = 7.1$ Hz, 2H), 2.66 (t, $J = 7.1$ Hz, 2H), 2.42 (h, $J = 6.8, 6.3$ Hz, 1H), 2.01 (p, $J = 7.1$ Hz, 2H), 1.57 – 1.48 (m, 2H), 1.38 (ddt, $J = 16.1, 14.5, 7.4$ Hz, 1H), 1.08 (d, $J = 6.8$ Hz, 3H), 0.95 (t, $J = 7.4$ Hz, 3H). ^{13}C NMR (150 MHz, CDCl_3) δ 199.27, 197.22,

149.42, 134.44, 129.93, 129.38, 129.17, 127.62, 75.90, 42.50, 42.28, 38.65, 27.40, 19.67, 13.91, 10.25. **HRMS** (ESI) calcd for C₁₈H₂₄O₃S [M+H] 321.1519, found 321.1516.

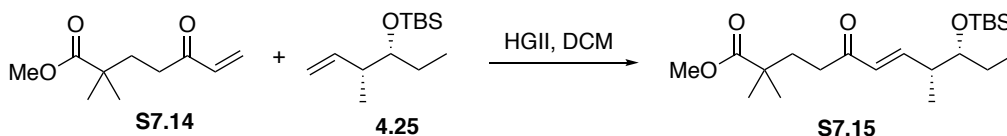


methyl 5-(methoxy(methyl)amino)-2,2-dimethyl-5-oxopentanoate (S7.13): A solution of dimethyl glutaric anhydride (1 eq, 7.03 mmol, 1.0 g) and N,O-dimethylhydroxylamine hydrochloride (1 eq, 7.03 mmol, 1.0 g) in CH₂Cl₂ (0.4M, 17 mL) was cooled to 0 °C and treated dropwise with pyridine (2.2 eq, 15.48 mmol, 1.25 mL). The resulting solution was warmed to rt and stirred overnight. The reaction was then concentrated under reduced pressure. The crude product was dissolved in 4:1 Toluene/MeOH (15 mL) and treated dropwise with TMS diazomethane (2M in diethyl ether, 3 mL). Upon persistence of yellow color, the reaction was quenched with a 10% Acetic Acid in CH₂Cl₂. This was concentrated under reduced pressure and the crude product was purified by flash chromatography system (30 – 70% Ethyl Acetate/Hexanes) to afford **S7.13** (1.36 g, 90% yield) as a clear and colorless oil: R_f = 0.65 (50% Ethyl Acetate/Hexanes); ¹H NMR (600 MHz, CDCl₃) δ 3.66 (s, 3H), 3.65 (s, 3H), 3.15 (s, 3H), 2.36 (t, J = 8.4 Hz, 2H), 1.93 – 1.80 (m, 2H), 1.19 (s, 6H). ¹³C NMR (150 MHz, CDCl₃) δ 177.91, 174.02, 61.18, 51.75, 41.77, 34.97, 27.73, 25.08. **HRMS** (ESI) calcd for C₁₀H₁₉NO₄ [M+H] 218.1387, found 218.1288.

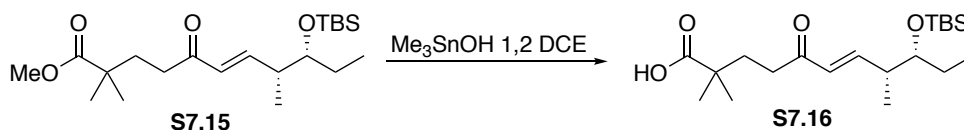


methyl 2,2-dimethyl-5-oxohept-6-enoate (S7.14): To a flame dried 25 mL flask under N₂ was added **S7.13** (1 eq, 0.81 mmol, 0.175 g) in dry THF (0.2 M, 4 mL) and the mixture was cooled to 0 °C. Vinyl Magnesium Bromide (0.8 M THF, freshly titrated, 1.2 eq, 1.21 mL) was added slowly and the reaction was allowed to stir at 0 °C for 30 min. The reaction was quenched with half 0.5 N HCl (10 mL) and the aqueous layer was extracted with CH₂Cl₂ (3x20 mL), organics combined, dried over Na₂SO₄, and concentrated. The crude product was purified by flash chromatography system (5 – 50% Ethyl Acetate/Hexanes) to afford **S7.14** (90 mg, 62% yield) as a clear and

colorless oil (being careful not to pull this off on a high vacuum as it is volatile): $R_f = 0.5$ (25% Ethyl Acetate/Hexanes); $^1\text{H NMR}$ (600 MHz, CDCl_3) δ 6.32 (dd, $J = 17.9, 10.4$ Hz, 1H), 6.21 (d, $J = 17.7$ Hz, 1H), 5.81 (d, $J = 10.6$ Hz, 1H), 3.65 (d, $J = 0.8$ Hz, 3H), 2.57 – 2.51 (m, 2H), 1.87 – 1.82 (m, 2H), 1.18 (s, 6H). $^{13}\text{C NMR}$ (150 MHz, CDCl_3) δ 200.14, 177.84, 136.33, 128.18, 51.81, 41.67, 35.44, 34.12, 25.16. **HRMS** (ESI) calcd for $\text{C}_{10}\text{H}_{16}\text{O}_3$ $[\text{M}+\text{H}]$ 185.1172, found 185.1172.

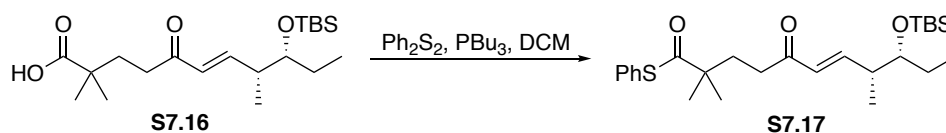


methyl (8R,9R,E)-9-((tert-butyl(dimethyl)silyloxy)-2,2,8-trimethyl-5-oxoundec-6-enoate (S7.15): To a long tube under N_2 was added Hoveyda Grubbs II (0.03 eq, 0.01 mmol, 0.009 g), ester **S7.14** (1 eq, 0.49 mmol, 0.09 g), and **4.25** (3 eq, 1.47 mmol, 0.335 g) in DCM (2 mL, 0.5 M). This was allowed to reflux for 12 h, cooled, the solvent was removed under reduced pressure and purified directly by flash chromatography (0 – 15% Ethyl Acetate/Hexane) to afford **S7.15** (0.102 g, 53% yield) as a colorless oil: $R_f = 0.25$ (10% Ethyl Acetate/Hexanes); $^1\text{H NMR}$ (600 MHz, CDCl_3) δ 6.85 (dd, $J = 16.1, 7.3$ Hz, 1H), 6.05 (d, $J = 16.0$ Hz, 1H), 3.65 (s, 3H), 3.54 (q, $J = 5.5$ Hz, 1H), 2.52 – 2.46 (m, 2H), 2.50 – 2.42 (m, 1H), 1.87 – 1.80 (m, 2H), 1.52 – 1.41 (m, 1H), 1.41 – 1.30 (m, 1H), 1.18 (s, 6H), 1.01 (d, $J = 6.8$ Hz, 3H), 0.88 (s, 9H), 0.85 (t, $J = 7.4$ Hz, 3H), 0.03 (s, 3H), 0.02 (s, 3H). $^{13}\text{C NMR}$ (150 MHz, CDCl_3) δ 199.90, 177.90, 150.25, 129.48, 76.32, 51.78, 41.68, 41.37, 35.63, 34.31, 26.78, 25.84, 25.14, 18.10, 14.05, 9.66, -4.33, -4.52. **HRMS** (ESI) calcd for $\text{C}_{21}\text{H}_{40}\text{O}_4\text{Si}$ $[\text{M}+\text{H}]$ 385.2769, found xx.

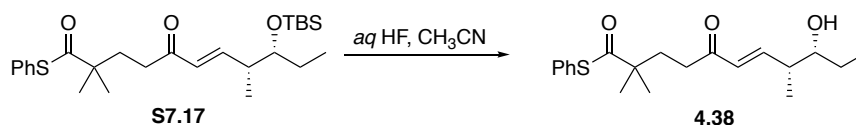


(8R,9R,E)-9-((tert-butyl(dimethyl)silyloxy)-2,2,8-trimethyl-5-oxoundec-6-enoic acid (S7.16): Ester **S7.15** (1 eq, 0.25 mmol, 0.095 g) was dissolved in 1,2 dichloroethane (2.4 mL, 0.1M) and after the addition of trimethyltin hydroxide (10 eq, 2.55 mmol, 0.304 g), the mixture was heated to 70 °C, and monitored by TLC until completion (~4 h). After completion, the reaction was cooled and concentrated. The residue was taken up in ethyl acetate (20 mL) and washed with 1N HCl (20 mL), brine (20 mL), dried over Na_2SO_4 , and concentrated. The crude concentrate was purified by flash chromatography system (5 – 50% Ethyl Acetate/Hexanes + 1% acetic acid) to afford **S7.16**

(75 mg, 83% yield): $R_f = 0.1$ (10% Ethyl Acetate/Hexanes + 1% AcOH); $^1\text{H NMR}$ (400 MHz, CDCl_3) δ 6.88 (dd, $J = 16.2, 7.3$ Hz, 1H), 6.07 (d, $J = 16.1$ Hz, 1H), 3.56 (q, $J = 5.6$ Hz, 1H), 2.62 – 2.53 (m, 2H), 2.46 (dt, $J = 13.6, 6.1$ Hz, 2H), 1.92 – 1.82 (m, 2H), 1.54 – 1.41 (m, 1H), 1.45 – 1.29 (m, 1H), 1.24 – 1.20 (m, 6H), 1.02 (d, $J = 6.8$ Hz, 3H), 0.89 (d, $J = 0.9$ Hz, 9H), 0.85 (d, $J = 7.4$ Hz, 3H), 0.04 (s, 3H), 0.03 (s, 3H). **HRMS** (ESI) calcd for $\text{C}_{20}\text{H}_{38}\text{O}_4\text{Si}$ [$\text{M}+\text{H}$] 371.2612, found 371.2610.

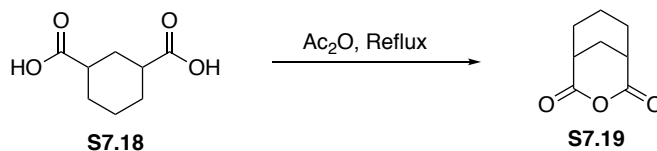


S-phenyl (8R,9R,E)-9-((tert-butyldimethylsilyl)oxy)-2,2,8-trimethyl-5-oxoundec-6-enethioate (S7.17): To a 25 mL flask was added **S7.16** (1 eq, 0.09 mmol, 0.035 g) and Ph_2S_2 (1.1 eq, 0.1 mmol, 0.023 g) in CH_2Cl_2 (1 mL, 0.1M) and cooled to 0 °C. PBu_3 (distilled, 1.1 eq, 0.10 mmol, 30 μL) was added slowly, the reaction was stirred for 10 min before it was quenched with sat. NaHCO_3 . The organics were separated, extracted with CH_2Cl_2 (3 x 20 mL), dried over sodium sulfate, and concentrated. The crude product was purified by flash chromatography system (0 – 10% Ethyl Acetate/Hexanes) to afford **S7.17** as a mixture of product and thiophenol byproducts: $R_f = 0.6$ (10% Ethyl Acetate/Hexanes). This was inseparable from thiophenol byproducts and was carried through to deprotection.

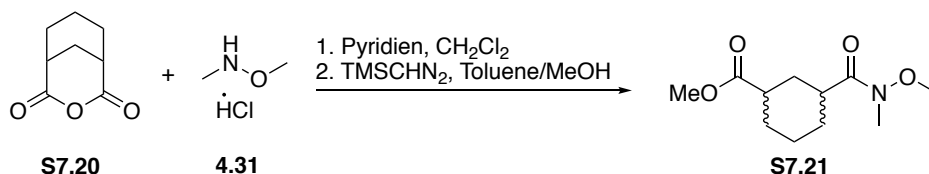


S-phenyl (8R,9R,E)-9-hydroxy-2,2,8-trimethyl-5-oxoundec-6-enethioate (4.38): The TBS protected **S7.17** was suspended in 1 mL of CH_3CN in a polyethylene vial and treated with aq. HF (48%, 250 μL). The reaction was monitored by TLC and upon completion it was diluted with CH_2Cl_2 (5 mL) and carefully quenched with sat. NaHCO_3 (until pH was acidic). The aqueous layer was extracted with CH_2Cl_2 (3 x 10 mL), organics combined, dried over Na_2SO_4 , and concentrated. The crude product was purified by flash chromatography system (12 – 40% Ethyl Acetate/Hexanes) to afford **7.38** (0.027 g, 81% yield) as a clear and colorless oil: $R_f = 0.4$ (10% Ethyl Acetate/Hexanes); $^1\text{H NMR}$ (600 MHz, CDCl_3) δ 7.44 – 7.33 (m, 5H), 6.82 (dd, $J = 16.0, 7.7$ Hz, 1H), 6.11 (d, $J = 15.9$ Hz, 1H), 3.49 (dt, $J = 9.0, 4.6$ Hz, 1H), 2.60 – 2.53 (m, 2H), 2.42 (h,

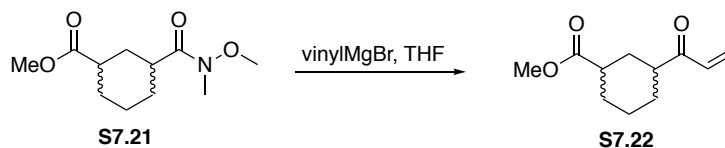
$J = 6.7$ Hz, 1H), 1.99 – 1.94 (m, 2H), 1.55 – 1.47 (m, 1H), 1.42 – 1.33 (m, 1H), 1.32 (s, 6H), 1.07 (d, $J = 6.9$ Hz, 3H), 0.95 (t, $J = 7.4$ Hz, 3H). ^{13}C NMR (151 MHz, CDCl_3) δ 204.03, 199.53, 149.36, 134.92, 129.83, 129.25, 129.12, 127.69, 75.88, 49.64, 42.27, 35.77, 34.74, 27.39, 25.43, 13.87, 10.27. HRMS (ESI) calcd for $\text{C}_{20}\text{H}_{28}\text{O}_3\text{S}$ $[\text{M}+\text{H}]$ 349.1832, found 349.1831.



3-oxabicyclo[3.3.1]nonane-2,4-dione (S7.19): 1,3-cyclohexanedicarboxylic acid (1 eq, 9.70 mmol, 1.67 g) in acetic anhydride (0.5M, 20 mL) was heated to 140 °C and stirred for 10 h. The reaction was cooled and the solvent removed under reduced pressure. The residual white solid was dissolved in CH_2Cl_2 , filtered, and concentrated, yielding **S7.19** (1.27 g, 84% yield). ^1H NMR (600 MHz, CDCl_3) δ 3.06 (d, $J = 3.3$ Hz, 2H), 2.29 – 2.19 (m, 1H), 2.14 – 2.04 (m, 2H), 1.88 – 1.81 (m, 1H), 1.81 – 1.69 (m, 3H), 1.55 – 1.41 (m, 1H). ^{13}C NMR (150 MHz, CDCl_3) δ 169.91, 36.41, 28.56, 27.26, 19.99. HRMS (ESI) calcd for $\text{C}_8\text{H}_{10}\text{O}_3$ $[\text{M}+\text{H}]$ 155.2703, found 155.2705.



methyl 3-(methoxy(methyl)carbamoyl)cyclohexane-1-carboxylate (S7.21): A solution of **S7.20** anhydride (1 eq, 3.24 mmol, 0.5 g) and N,O-dimethylhydroxylamine hydrochloride (1 eq, 3.24 mmol, 0.5 g) in CH_2Cl_2 (0.4M, 8 mL) was cooled to 0 °C and treated dropwise with pyridine (2.2 eq, 7.14 mmol, 0.58 mL). The resulting solution was warmed to rt and stirred overnight. The reaction was then concentrated under reduced pressure. The crude product was dissolved in 4:1 Toluene/MeOH (15 mL) and treated dropwise with TMS diazomethane (2M in diethyl ether, 3 mL). Upon persistence of yellow color, the reaction was quenched with a 10% Acetic Acid in CH_2Cl_2 . This was concentrated under reduced pressure and the crude product was purified by flash chromatography system (30 – 70% Ethyl Acetate/Hexanes) to afford **S7.21** (0.66 g, 89% yield) as a clear and colorless oil: $R_f = 0.65$ (50% Ethyl Acetate/Hexanes);

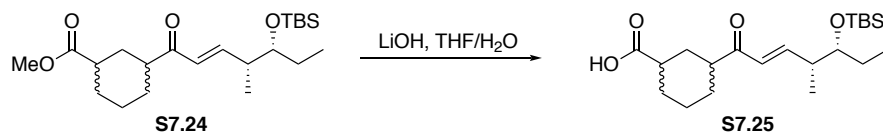


methyl 3-acryloylcyclohexane-1-carboxylate (S7.22): To a flame dried 25 mL flask under N₂ was added **S7.21** (1 eq, 0.65 mmol, 0.150 g) in dry THF (0.2 M, 6 mL) and the mixture was cooled to 0 °C. Vinyl Magnesium Bromide (0.8 M THF, freshly titrated, 1.2 eq, 0.92 mL) was added slowly and the reaction was allowed to stir at 0 °C for 30 min. The reaction was quenched with half 0.5 N HCl (10 mL) and the aqueous layer was extracted with CH₂Cl₂ (3x20 mL), organics combined, dried over Na₂SO₄, and concentrated. The crude product was purified by flash chromatography system (5 – 50% Ethyl Acetate/Hexanes) to afford **S7.22** (65 mg, 51% yield) as a clear and colorless oil (being careful not to pull this off on a high vacuum as it is volatile): R_f = 0.5 (20% Ethyl Acetate/Hexanes); ¹H NMR (600 MHz, CD₃COCD₃) δ 6.49 (dd, *J* = 17.5, 10.6 Hz, 1H), 6.27 (dd, *J* = 17.5, 1.4 Hz, 1H), 5.81 (dd, *J* = 10.6, 1.4 Hz, 1H), 2.84 (tt, *J* = 12.1, 3.2 Hz, 1H), 2.43 (tt, *J* = 12.4, 3.6 Hz, 1H), 2.07 – 2.01 (m, 2H), 1.96 (dtt, *J* = 14.9, 3.5, 1.9 Hz, 1H), 1.91 – 1.83 (m, 2H), 1.50 – 1.37 (m, 2H), 1.31 (tdd, *J* = 13.2, 12.3, 3.5 Hz, 1H), 1.26 – 1.16 (m, 1H). ¹³C NMR (150 MHz, CD₃COCD₃) δ 201.32, 174.91, 135.05, 127.35, 50.77, 46.43, 42.10, 30.50, 28.46, 27.93, 24.67. HRMS (ESI) calcd for C₁₁H₁₆O₃ [M+H] 197.1172, found 197.1179.



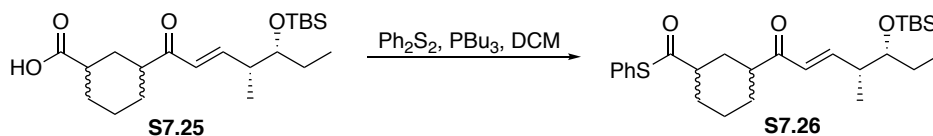
methyl 3-((4*R*,5*R*,*E*)-5-((*tert*-butyldimethylsilyloxy)-4-methylhept-2-enoyl)cyclohexane-1-carboxylate (S7.24): To a long tube under N₂ was added Hoveyda Grubbs II (0.03 eq, 0.01 mmol, 0.006 g), ester **S7.23** (1 eq, 0.31 mmol, 0.060 g), and **4.25** (3 eq, 1.22 mmol, 0.279 g) in DCM (2 mL, 0.5 M). This was allowed to reflux for 12 h, cooled, the solvent was removed under reduced pressure and purified directly by flash chromatography (0 – 15% Ethyl Acetate/Hexane) to afford **S7.24** (0.099 g, 82% yield) as a colorless oil: R_f = 0.2 (10% Ethyl Acetate/Hexanes); ¹H NMR (600 MHz, CD₃COCD₃) δ 6.95 (dd, *J* = 15.9, 7.4 Hz, 1H), 6.23 (dd, *J* = 16.0, 1.4 Hz, 1H), 3.70 (q, *J* = 5.5 Hz, 1H), 3.62 (s, 3H), 2.76 (ttd, *J* = 12.1, 3.4, 1.9 Hz, 1H), 2.59 – 2.49 (m, 1H), 2.41 (ttd, *J* = 12.4, 3.5, 1.3 Hz, 1H), 2.05 – 2.00 (m, 1H), 1.95 (dtd, *J* = 14.4, 3.5, 1.9 Hz, 1H), 1.91 – 1.80 (m, 2H), 1.54 (dtd, *J* = 14.9, 7.4, 5.4 Hz, 1H), 1.48 – 1.36 (m, 3H), 1.31 (qd, *J* = 12.9, 3.5 Hz, 1H),

1.23 (qt, $J = 12.6, 4.2$ Hz, 1H), 1.06 (d, $J = 6.8$ Hz, 3H), 0.92 (s, 9H), 0.89 (t, $J = 7.4$ Hz, 3H), 0.09 (s, 3H), 0.08 (s, 3H). ^{13}C NMR (150 MHz, CD_3COCD_3) δ 200.75, 174.92, 149.45, 127.92, 76.30, 50.75, 46.92, 42.24, 41.15, (30.77 or 30.69), 28.48, (28.17 or 28.09), 26.65, 25.40, 24.75, 17.79, 13.43, 9.06, -5.03, -5.21. HRMS (ESI) calcd for $\text{C}_{22}\text{H}_{40}\text{O}_4\text{Si}$ [M+H] 397.2769, found 397.2772.



3-((4*R*,5*R*,*E*)-5-((*tert*-butyldimethylsilyl)oxy)-4-methylhept-2-enoyl)cyclohexane-1-

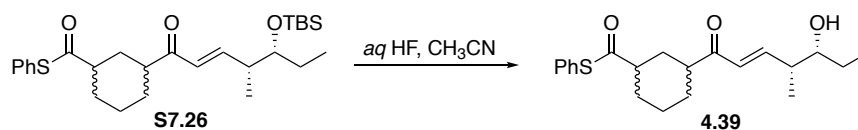
carboxylic acid (S7.25): S7.24 (1 eq, 0.13 mmol, 0.052 g) was suspended in a 4:1 mixture of THF/H₂O (1 mL, 0.1M) and treated with LiOH (3 eq, 0.39 mmol, 0.017 g) and stirred for 4 hours. The reaction was quenched with 1 M HCl (2 mL) and the organics removed under reduced pressure. The aqueous layer was extracted with ethyl acetate (3 x 10 mL), organics combined, washed with brine, dried over Na₂SO₄, and concentrated. The crude product was purified by flash chromatography system (10 – 30% Ethyl Acetate/Hexanes + 1% AcOH) to afford S7.25 (20 mg, 40% yield) as a clear and colorless oil: $R_f = 0.15$ (10% Ethyl Acetate/Hexanes + 1% AcOH); ^1H NMR (400 MHz, CD_3COCD_3) δ 6.96 (dd, $J = 15.9, 7.3$ Hz, 1H), 6.24 (dd, $J = 16.0, 1.4$ Hz, 1H), 3.70 (dt, $J = 6.4, 5.1$ Hz, 1H), 2.77 (tt, $J = 11.8, 2.6$ Hz, 2H), 2.55 (h, $J = 6.7$ Hz, 1H), 2.39 (tt, $J = 12.2, 4.0$ Hz, 1H), 2.12 – 1.95 (m, 1H), 1.94 – 1.81 (m, 2H), 1.62 – 1.17 (m, 6H), 1.06 (d, $J = 6.8$ Hz, 3H), 0.92 (s, 9H), 0.90 (t, $J = 7.5$ Hz, 7H), 0.08 (s, 3H), 0.08 (s, 3H). HRMS (ESI) calcd for $\text{C}_{21}\text{H}_{38}\text{O}_4\text{Si}$ [M+H] 383.2612, found 383.2612.



S-phenyl 3-((4*R*,5*R*,*E*)-5-((*tert*-butyldimethylsilyl)oxy)-4-methylhept-2-enoyl)cyclohexane-1-

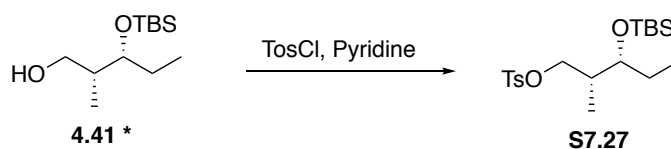
carbothioate (S7.26): To a 25 mL flask was added xx (1 eq, 0.05 mmol, 0.018 g) and Ph₂S₂ (1.1 eq, 0.05 mmol, 0.011 g) in CH₂Cl₂ (1 mL, 0.1M) and cooled to 0 °C. PBU₃ (distilled, 1.1 eq, 0.05 mmol, 15 uL) was added slowly, the reaction was stirred for 10 min before it was quenched with sat. NaHCO₃. The organics were separated, extracted with CH₂Cl₂ (3 x 10 mL), dried over sodium sulfate, and concentrated. The crude product was purified by flash chromatography system (0 – 10% Ethyl Acetate/Hexanes) to afford S7.26 as a mixture of product and thiophenol byproducts:

$R_f = 0.6$ (10% Ethyl Acetate/Hexanes). This was inseparable from thiophenol byproducts and was carried through to deprotection.



***S*-phenyl 3-((4*R*,5*R*,*E*)-5-hydroxy-4-methylhept-2-enyl)cyclohexane-1-carbothioate (4.39):**

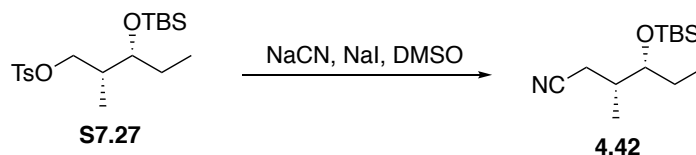
The TBS protected **S7.26** was suspended in 1 mL of CH_3CN in a polyethylene vial and treated with aq. HF (48%, 250 μL). The reaction was monitored by TLC and upon completion it was diluted with CH_2Cl_2 (5 mL) and carefully quenched with sat. NaHCO_3 (until pH was acidic). The aqueous layer was extracted with CH_2Cl_2 (3 x 10 mL), organics combined, dried over Na_2SO_4 , and concentrated. The crude product was purified by flash chromatography system (5 – 25% Ethyl Acetate/Hexanes) to afford **4.39** (0.09 g, 74% yield) as a clear and colorless oil: $R_f = 0.4$; $^1\text{H NMR}$ (400 MHz, CD_3COCD_3) δ 7.49 – 7.37 (m, 5H), 6.94 (dd, $J = 15.9, 8.0$ Hz, 1H), 6.23 (dd, $J = 15.9, 1.2$ Hz, 1H), 3.69 (d, $J = 5.7$ Hz, 1H), 3.45 (td, $J = 9.1, 5.5$ Hz, 1H), 2.87 (tt, $J = 12.1, 3.3$ Hz, 1H), 2.80 – 2.75 (m, 1H), 2.50 – 2.35 (m, 1H), 2.11 (d, $J = 14.1$ Hz, 1H), 1.99 – 1.83 (m, 2H), 1.61 – 1.17 (m, 7H), 1.09 (d, $J = 6.8$ Hz, 3H), 0.94 (t, $J = 7.4$ Hz, 3H). **HRMS** (ESI) calcd for $\text{C}_{21}\text{H}_{28}\text{O}_3\text{S}$ [M+H] 361.1832, found 361.1833.



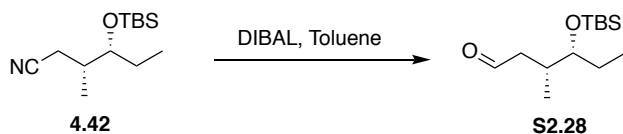
(2*R*,3*R*)-3-((*tert*-butyldimethylsilyl)oxy)-2-methylpentyl 4-methylbenzenesulfonate (S7.27):

To a stirred solution of alcohol (1 eq, 3.44 mmol, 0.80 g) in pyridine (100 eq, 28 mL) was added *p*-toluenesulfonyl chloride (1.3 eq, 4.47 mmol, 0.85 g) at 0 $^\circ\text{C}$. The reaction was warmed to rt and stirred for 3 h, the reaction was quenching with sat. NH_4Cl (30 mL) and concentrated under reduced pressure. The remaining oil was diluted with water and Ethyl Acetate and the aqueous layer was extracted (3 x 30 mL), organics combined, dried over Na_2SO_4 and concentrated. The crude product was purified by flash chromatography system (2 – 15% hexane/Ethyl Acetate) to afford **S7.27** (1.13g, 85% yield) as a pale yellow oil: $R_f = 0.7$ (10% Ethyl Acetate/Hexanes); $^1\text{H NMR}$ (400 MHz, CDCl_3) δ 7.78 (d, $J = 8.2$ Hz, 2H), 7.33 (d, $J = 8.0$ Hz, 2H), 4.00 (dd, $J = 9.2,$

6.3 Hz, 1H), 3.84 (dd, $J = 9.2, 7.4$ Hz, 1H), 3.57 (td, $J = 6.7, 3.0$ Hz, 1H), 2.44 (s, 3H), 1.93 (qd, $J = 6.8, 3.0$ Hz, 1H), 1.50 – 1.28 (m, 2H), 0.82 (d, $J = 7.0$ Hz, 4H), 0.80 (s, 9H), 0.77 (d, $J = 7.5$ Hz, 3H), -0.00 (s, 3H), -0.06 (s, 3H). $^{13}\text{C NMR}$ (100 MHz, CDCl_3) δ 144.58, 133.11, 129.76, 127.92, 73.21, 73.05, 36.88, 26.60, 25.77, 21.60, 17.98, 10.41, 10.08, -4.20, -4.87. **HRMS** (ESI) calcd for $\text{C}_{19}\text{H}_{34}\text{O}_4\text{SSi}$ [$\text{M}+\text{H}$] 387.2020, found 387.2022.

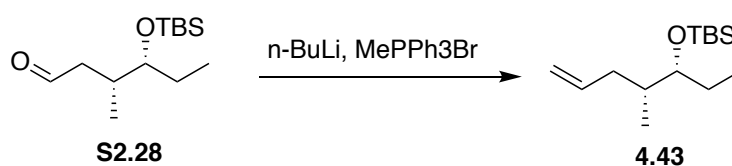


(3*R*,4*R*)-4-((*tert*-butyldimethylsilyloxy)-3-methylhexanenitrile (4.42): To a flame dried flask under N_2 was added tosylate (1 eq, 2.92 mmol, 1.13 g) in anhydrous DMSO (20 mL) and treated with a solution of NaCN (4 eq, 11.69 mmol, 0.573) in DMSO (10 mL). The reaction was then heated to 60 °C for 12h. Upon completion of the reaction, it was cooled, diluted with water and the aqueous layer extracted with Et_2O (3 x 25 mL). The organics were combined, dried over Na_2SO_4 , concentrated under reduced pressure and purified by flash purification system (0 – 10% Ethyl Acetate/Hexanes) to afford **4.42** (577 mg, 81%) as a clear and colorless oil: $R_f = 0.75$ (10% Ethyl Acetate/Hexanes); $^1\text{H NMR}$ (600 MHz, CDCl_3) δ 3.59 (td, $J = 6.5, 3.2$ Hz, 1H), 2.43 (dd, $J = 16.6, 6.3$ Hz, 1H), 2.20 (dd, $J = 16.7, 8.3$ Hz, 1H), 2.05 – 1.95 (m, 1H), 1.52 – 1.34 (m, 2H), 1.00 (d, $J = 6.9$ Hz, 3H), 0.89 (s, 9H), 0.86 (t, $J = 7.5$ Hz, 3H), 0.07 (d, $J = 1.2$ Hz, 6H). $^{13}\text{C NMR}$ (150 MHz, CDCl_3) δ 75.10, 35.05, 26.07, 25.81, 20.81, 18.05, 13.52, 10.06, -4.23, -4.68. **HRMS** (ESI) calcd for $\text{C}_{13}\text{H}_{27}\text{NOSi}$ [$\text{M}+\text{H}$] 242.1935, found 242.1929.

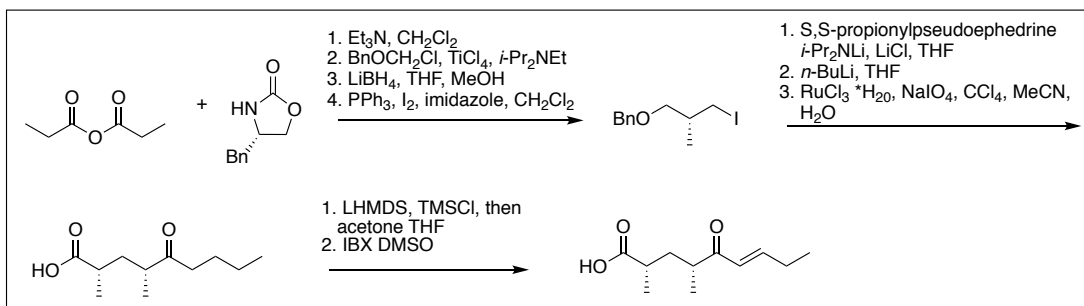


(2*S*,3*R*)-3-((*tert*-butyldimethylsilyloxy)-2-methylpentanal (S2.28): To a flame dried flask under N_2 was added **4.42** (1 eq, 0.83 mmol, 0.201 g) in toluene (0.2 M, 4.2 mL) and cooled to -78 °C. A solution of DIBAL (2M in Hexanes, 1.05 eq, 0.87 mL) was added and the reaction was stirred at -78 °C for 4 h. The solution was then warmed to 0 °C and poured into a mixture of potassium sodium tartrate (20 mL) and Et_2O (20 mL) followed by stirring for 1 h until the phases became almost clear. The aqueous layer was extracted with Et_2O (3 x 40 mL), organics combined,

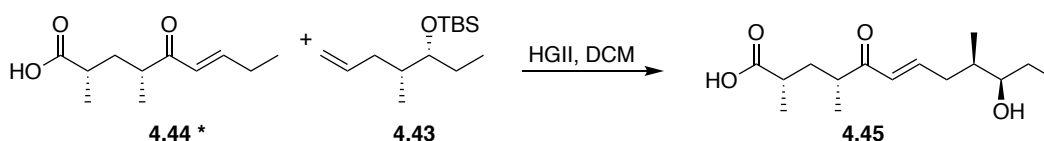
dried over sodium sulfate and concentrated. The crude product was purified by flash chromatography system (0 – 5% Ether/Pentane) to afford **S2.28** (126 mg, 62% yield) as a clear and colorless oil: $R_f = 0.5$ (5% Ethyl Acetate/Hexanes). $^1\text{H NMR}$ (400 MHz, CDCl_3) δ 9.49 (t, $J = 1.9$ Hz, 1H), 3.35 (td, $J = 6.7, 3.5$ Hz, 1H), 2.31 (dd, $J = 16.7, 4.9$ Hz, 1H), 2.21 – 2.03 (m, 1H), 1.88 (ddd, $J = 16.6, 8.5, 2.1$ Hz, 1H), 1.37 – 1.21 (m, $J = 6.6$ Hz, 2H), 1.00 (s, 9H), 0.83 (t, $J = 7.4$ Hz, 3H), 0.78 (d, $J = 6.9$ Hz, 3H), 0.05 (s, 3H), 0.03 (s, 3H). $^{13}\text{C NMR}$ (100 MHz, CDCl_3) δ 200.42, 127.85, 127.62, 76.50, 46.89, 32.34, 25.81, 18.02, 14.41, 10.29, -4.51, -4.64. **HRMS** (ESI) calcd for $\text{C}_{13}\text{H}_{28}\text{O}_2\text{Si}$ [M+H] 245.1932, found xx.



tert-butyl dimethyl(((3*R*,4*R*)-4-methylhept-6-en-3-yl)oxy)silane (4.43): To a flame dried flask under N_2 was added MePPh_3Br (1.1 eq, 1.53 mmol, 0.55 g) and suspended in anhydrous THF (0.2 M, 10 mL) and cooled to 0°C . To this $n\text{-BuLi}$ was added dropwise (the solution turned orange as the precipitant disappeared) and the reaction was allowed to warm to room temperature and stirred for a minimum of 1h. The flask was then re-cooled to -78°C and a solution of aldehyde xx (1 eq, 1.39 mmol, 0.34 g) in THF (5 mL) was added dropwise to the prepared ylide. The solution was stirred at -78°C for 30 min, warmed to 0°C and stirred for an additional 30 min at 0°C . The reaction was quenched with half sat. NH_4Cl and extracted with pentane (3x 40 mL), dried over Na_2SO_4 and concentrated. The crude product was purified by flash chromatography (0 – 5% Diethyl Ether/Pentane) to afford **4.43** (204 mg, 60% yield) as a clear and colorless oil: $R_f = 0.9$ (5% Ethyl Acetate/Hexanes): $^1\text{H NMR}$ (400 MHz, CDCl_3) δ 5.78 (dddd, $J = 16.9, 10.2, 7.7, 6.5$ Hz, 1H), 5.00 (d, $J = 15.1$ Hz, 2H), 4.97 (d, $J = 6.9$ Hz, 1H), 3.47 (td, $J = 6.2, 3.5$ Hz, 1H), 2.24 (ddd, $J = 12.4, 8.7, 4.6$ Hz, 1H), 1.88 – 1.75 (m, 1H), 1.68 – 1.57 (m, 1H), 1.53 – 1.32 (m, 2H), 0.89 (s, 9H), 0.87 (d, $J = 12.5$ Hz, 3H), 0.87 – 0.79 (m, 3H), 0.04 (s, 3H), 0.03 (s, 3H). $^{13}\text{C NMR}$ (100 MHz, CDCl_3) δ 138.34, 115.24, 76.81, 37.34, 37.15, 26.18, 25.93, 18.16, 13.89, 10.26, -4.19, -4.49. **HRMS** (ESI) calcd for $\text{C}_{14}\text{H}_{30}\text{OSi}$ [M+H] 243.2139, found 243.2131.



*Synthesis previously described by Hansen et al.¹



(2*S*,4*R*,9*R*,10*R*,*E*)-10-((*tert*-butyldimethylsilyl)oxy)-2,4,9-trimethyl-5-oxododec-6-enoic acid

(4.45): To a long tube under N₂ was added Hoveyda Grubbs II (0.03 eq, 0.01 mmol, 0.006 g), Acid **4.44** (1 eq, 0.31 mmol, 0.060 g), and **4.43** (3 eq, 1.22 mmol, 0.279 g) in DCM (2 mL, 0.5 M). This was allowed to reflux for 12 h, cooled, the solvent was removed under reduced pressure and purified directly by flash chromatography (0 – 15% Ethyl Acetate/Hexane) to afford **4.45** (0.099 g, 82% yield) as a colorless oil: *R_f* = 0.2 (10% Ethyl Acetate/Hexanes); ¹H NMR (600 MHz, CD₃COCD₃) δ 6.91 (ddd, *J* = 15.8, 7.8, 6.9 Hz, 1H), 6.20 (dt, *J* = 15.8, 1.5 Hz, 1H), 3.59 (td, *J* = 6.3, 3.4 Hz, 1H), 2.92 (dt, *J* = 14.2, 6.9 Hz, 1H), 2.51 – 2.39 (m, 2H), 2.09 – 2.05 (m, 1H), 1.87 – 1.75 (m, 1H), 1.51 (ddd, *J* = 13.4, 7.5, 6.0 Hz, 1H), 1.45 (tt, *J* = 14.1, 7.2 Hz, 1H), 1.32 (ddd, *J* = 13.8, 7.8, 6.2 Hz, 1H), 1.13 (d, *J* = 7.0 Hz, 3H), 1.06 (d, *J* = 6.8 Hz, 3H), 0.91 (s, 9H), 0.88 (t, *J* = 7.3 Hz, 3H), 0.87 (d, *J* = 7.0 Hz, 3H), 0.08 (s, 3H), 0.07 (s, 3H). ¹³C NMR (150 MHz, CD₃COCD₃) δ 201.58, 146.34, 129.91, 76.61, 40.82, 37.02, 36.72, 36.65, 35.59, 25.98, 25.42, 17.81, 17.06, 15.80, 13.47, 9.63, -4.91, -5.15. HRMS (ESI) calcd for C₁₅H₂₆O₄ [M+H] 271.1904, found 271.1900.

7.2 Pikromycin PKS Expression and Purification Protocols

The cloning and expression of Pik AIII, Pik AIV, and Pik AIIITE as well as Pik AIIITE S148C have been reported previously as well as Juv E4 and Juv E5. Buffers used for all purifications include:

Buffers:

[Lysis] – HEPES (50 mM), NaCl (300 mM), imidazole (10 mM), glycerol (10% v/v), pH 8

[Wash] – HEPES (50 mM), NaCl (300 mM), imidazole (30 mM), glycerol (10% v/v), pH 8

[Elution] – HEPES (50 mM), NaCl (300 mM), imidazole (300 mM), glycerol (10% v/v), pH 8

[Storage] – HEPES (50 mM), NaCl (150 mM), glycerol (20% v/v), pH 7.2

[Reaction Buffer] – Sodium Phosphate (800 mM), NaCl (150 mM), pH 7.2

Bap1 pRARE cells were freshly transformed with the desired plasmid and grown overnight on LB agar plates supplemented with 50 ug/mL Kanamycin overnight at 37 °C. Multiple colonies were picked and grown in 15 mL of LB with kanamycin (50 ug/mL), and grown overnight at 37 °C. The following morning, TB media (Kan 50 mg/L) were then inoculated with 4 mL of overnight culture and grown at 37 °C until OD₆₀₀ reached 1.0. These were then flash cooled in ice baths for ~15 min until the internal temperature hit 20 °C, at which time the flasks were returned to a 20 °C shaker, and induced with IPTG (300 uL of 1 M solution) and shaken at 180 RPM at 20 °C for 18 h. The cells were then pelleted at 6500 rpm (4 °C) for 30 min, and flash frozen for future purification.

Frozen overexpression cultures were suspended in 5 mL of lysis buffer per gram of pellet and aloud to thaw at 4 °C with stirring. Cells were treated with 8 units/mL of benzonase and aloud to stir for 20 min prior to sonication (6 x 10s with 50 s rest periods). Cellular debris was pelleted by centrifugation (55,000 x g, 25 min, 4 °C) and the supernatant was passed through a 0.45 uM filter and applied to the top of 5 mL of Ni-NTA resin, pre-equilibrated with wash buffer. This was allowed to gravity flow through, washed with 50 mL of wash buffer, and eluted with 15 mL of elution buffer. Fractions containing protein were assessed via their 280 nm absorbance and were concentrated using a 30 kDa centrifugal filter until volume reached 2.5 mL. These were then desalted on a storage buffer equilibrated PD-10 column, the concentration adjusted to 50 uM, and flash frozen in liquid nitrogen prior to storage in the -80 °C.

7.2.1 Enzymatic Reaction Experimental Procedures

General Analytical Enzymatic Reactions

All Enzymatic reactions were performed at 50 uL volumes. To a PCR tube was added 12.5 uL reaction buffer, 26 uL water, NADP (50 mM, 0.5 uL), glucose-6-phosphate (500 mM, 1 uL), and glucose-6-phosphate dehydrogenase (100 miliunits/uL, 1 uL) which was allowed to sit at room temperature for 10 min. To this was added MeMal (500 mM, 2 uL), AIII (50 uM, 3 uL), AIV (50 uM, 3 uL) and substrate in DMSO (50 mM, 1 uL). These were aloud to stand at rt for 2.5 hours. The reactions were quenched by the addition of 150 uL Methanol and clarified by centrifugation (17,000 x g 20 min, 4 °C). The supernatant was then loaded into an HPLC vial and analyzed via TOF-MS [Gradient from 20% - 100% Acetonitrile over 12 minutes.

General Semi-Preparative Enzymatic Conditions

To a 50 mL falcon tube was added phosphate buffer, water, NADP, glucose-6-phosphate, and glucose-6-phosphate dehydrogenase which was allowed to incubated at room temperature for 10 min. To this was added Methyl Malonyl, desired PKS protein (AIIITE or AIII/AIV), and substrate prior to incubation at room temperature for 2.5 hours. The reaction was quenched by pouring into cold acetone (3x) and incubating at – 20 °C for 1 hour, filtered through celite, and the organics removed. The remaining aqueous layer was extracted with methylene chloride (3 x 20 mL) and concentrated. The remaining residue was purified by reverse phase HPLC.

7.3 New Macrolactone Characterization

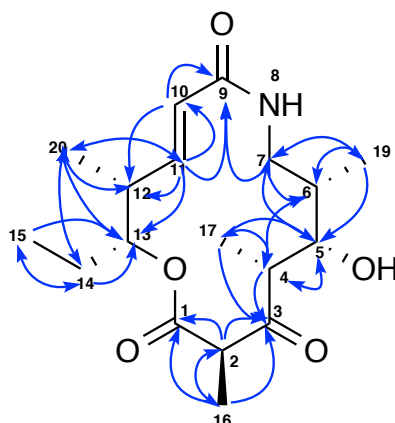


Figure 7.1 HMBC correlations for amide narbonolide as blue arrows.

Position	H	C	COSY	HMBC
1		170.99		
2	3.78 (q, J = 7.1 Hz, 1H)	48.17	16	1, 3, 16
3		205.66		
4	2.55 (p, J = 7.0 Hz, 1H)	50.29	5, 17	3, 5, 6, 17
5	3.49 (m, 1H)	72.24	4,6	7, 4
6	1.76 (tq, J = 7.1, 3.7 Hz, 1H)	37.32	5, 7', 19	
7	3.29 (dt, J = 14.0, 7.1 Hz, 1H)	40.34	6, 7'',8	9,6,19
	3.35 (m, 1H)		7',8	5
8	6.98 (s, 1H)		7',7''	
9		168.02		
10	5.97 (dd, J = 16.1, 1.9 Hz, 1H)	123.91	11	9,12
11	6.67 (dd, J = 16.2, 4.2 Hz, 1H)	146.26	10, 12	9,10,13,12,20
12	2.77 (m, 1H)	38.23	11, 13,20	
13	5.09 (ddd, J = 9.3, 4.6, 2.6 Hz, 1H)	77.66	12, 14', 14''	
14	1.64 1.64 (ddt, J = 14.1, 7.3, 5.0 Hz, 1H)	24.82	13, 15	15
	1.71 (ddt, J = 14.9, 9.8, 7.4 Hz, 1H)		13, 15	13,15
15	0.90 (d, J = 7.1 Hz, 3H)	9.92	14', 14''	14',14''
16	1.25 (d, J = 7.0 Hz, 3H)	14.45	2	1,2,3
17	1.06 (d, J = 7.0 Hz, 3H)	12.16	4	3,4,5
18				
19	0.94 (d, J = 7.1 Hz, 3H)	17.17	6	5,6,7
20	1.09 (d, J = 6.9 Hz, 3H)	8.93	12	11,12,13,14

Table 7.1 Amide narbonolide assignments and correlations.

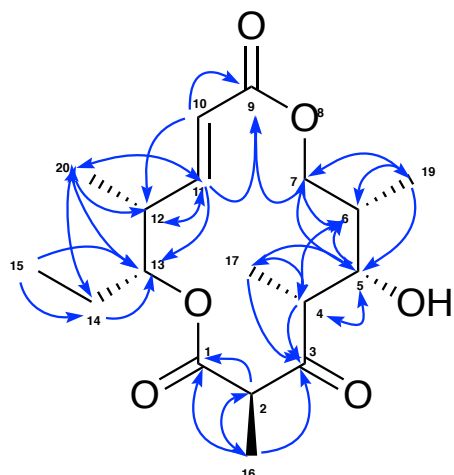
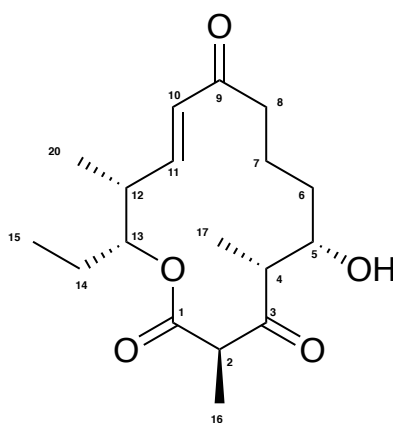


Figure 7.2 HMBC correlations for ester narbonolide as blue arrows.

Position	H	C	COSY	HMBC
1		171.55		
2	3.3 (q, $J = 7.1$ Hz, 1H)	49.51	16	1, 16
3		204.74		
4	2.45 – 2.35 (m, 1H)	50.98	5, 17	3, 5, 17
5	3.91 (t, $J = 5.5$ Hz, 1H)	70.96	4, 6	4, 6, 7
6	1.83 – 1.76 (m, 1H)	36.48	5, 7, 19	
7	4.06 (dd, $J = 10.9, 5.3$ Hz, 1H)	65.19	6, 7''	9, 5, 6, 19
	4.44 (dd, $J = 10.9, 3.3$ Hz, 1H)		6, 7'	9, 6, 19
8				
9		165.67		
10	5.71 (dd, $J = 15.9, 1.4$ Hz, 1H)	121.53	11	9, 12
11	6.86 (dd, $J = 15.9, 6.7$ Hz, 1H)	150.73	10, 12	9, 12, 13, 20
12	1.87 – 1.81 (m, 1H)	38.51	11, 13, 20	11
13	4.79 (ddd, $J = 9.5, 4.4, 2.9$ Hz, 1H)	77.53	12, 14	
14	0.91 (ddd, $J = 14.3, 6.9, 4.5$ Hz, 1H)	24.61	13, 14'', 15	
	1.26 – 1.17 (m, 1H)		13, 14', 15	13
15	0.52 (t, $J = 7.4$ Hz, 3H)	9.73	14	13, 14
16	1.23 (d, $J = 7.1$ Hz, 3H)	14.33	2	1, 2, 3
17	1.03 (d, $J = 6.9$ Hz, 3H)	10.24	4	3, 4, 5
18				
19	0.72 (d, $J = 7.2$ Hz, 3H)	15.61	6	5, 6, 7
20	0.67 (d, $J = 6.5$ Hz, 3H)	9.86	12	11, 12, 13

Table 7.2 Ester narbonolide assignments and correlations.



** Tentative assignments, will confirm upon secondary scale up with HMBC*

Figure 7.3 Desmethyl narbonolide structure.

Position	H	C	COSY	HMBC
1		170.1		
2	3.15 (q, $J = 7.3$ Hz, 1H)	51.9		
3		208.81		
4	2.26 – 2.16 (m, 1H)	39.01	5, 17	
5	3.71 (dt, $J = 8.7, 4.3$ Hz, 1H)	69.03	4, 6	
6	1.39 – 1.31 (m, 1H)	31.88	5, 7	
7	1.71 (ddt, $J = 18.6, 13.6, 4.0$ Hz, 2H)	21.85	6, 8	
8	2.03 (dt, $J = 13.3, 5.5$ Hz, 1H)	36.83	7, 8''	
	2.57 (ddd, $J = 13.5, 10.0, 5.4$ Hz, 1H)		7, 8'	
9		199.89		
10	5.97 (dd, $J = 16.0, 1.5$ Hz, 1H)	131.9	11	
11	6.50 (dd, $J = 16.0, 7.0$ Hz, 1H)	146.59	10, 12	
12	2.26 – 2.16 (m, 1H)	51.4	11, 20, 13	
13	4.83 (dt, $J = 10.1, 3.6$ Hz, 1H)	77.91	12, 14	
14	1.06 (ddd, $J = 14.3, 7.2, 3.9$ Hz, 1H)	22.68	15	
	1.20 (ddd, $J = 14.6, 10.0, 7.3$ Hz, 1H)		13, 15	
15	0.63 (d, $J = 6.9$ Hz, 3H)	10.14	14	
16	1.15 (d, $J = 7.2$ Hz, 3H)	12.92	2	
17	0.92 (d, $J = 7.0$ Hz, 3H)	10.69	4	
18	OH Not Seen			
19				
20	0.60 (d, $J = 7.3$ Hz, 3H)	12.33	12	

Table 7.3 Desmethyl narbonolide assignments and correlations.

7.4 References

1. Hansen, D. A.; Rath, C. M.; Eisman, E. B.; Narayan, A. R.; Kittendorf, J. D.; Mortison, J. D.; Yoon, Y. J.; Sherman, D. H., Biocatalytic synthesis of pikromycin, methymycin, neomethymycin, novamethymycin, and ketomethymycin. *J Am Chem Soc* **2013**, *135* (30), 11232-8.